Covalent microcontact printing

of biomolecules

Dorota I. Rożkiewicz

Members of the Committee:

Chairman:	Prof. Dr. Ir. D. H. A. Blank	University of Twente, The Netherlands
Promotor:	Prof. Dr. Ir. D. N. Reinhoudt	University of Twente, The Netherlands
Assistant-promotor:	Prof. Dr. B. J. Ravoo	University of Twente, The Netherlands
Members:	Prof. Dr. T. Carell	Ludwig-Maximilians University Munich, Germany
	Prof. Dr. L. de Cola	University of Münster, Germany
	Prof. Dr. J. Herek	University of Twente, The Netherlands
	Prof. Dr. R. Marchelli	University of Parma, Italy
	Dr. H. Schönherr	University of Twente, The Netherlands

COVALENT MICROCONTACT PRINTING
OF BIOMOLECULES

PROEFSCHRIFT

ter verkrijging van
de graad van doctor aan de Universiteit Twente,
op gezag van de rector magnificus,
prof. dr. W.H.M. Zijm,
volgens besluit van het College voor Promoties
in het openbaar te verdedigen
op donderdag 18 oktober 2007 om 15.00 uur

door

Dorota Idalia Rożkiewicz

geboren op 24 juli 1978
te Gdańsk, Polen

Dit proefschrift is goedgekeurd door:

Promotor: Prof. Dr. Ir. D. N. Reinhoudt

Assistent-promotor: Prof. Dr. B. J. Ravoo

Mojej mamie, tacie i siostrze

Contents

Contents

Contents

Chapter 1

General introduction

Micropatterning, the fabrication of micrometer-scale structures on a substrate, is one of the most important disciplines in modern science and technology. Micropatterned substrates contain an array of features usually different in dimension and chemical composition. The micropatterns can be fabricated by many techniques such as photolithography,[1-3] beam lithography,[4] soft lithography[5-7] (microcontact printing, replica molding, microtransfer molding, micromolding in capillaries, solvent-assisted micromolding), nanoimprint lithography,[8] scanning probe lithography,[9-12] inkjet printing,[13] organic vapor jet printing,[14, 15] nanopipettes[16-19] and many others. These techniques differ in processing, technology and facilities, duration of time and price. Nowadays patterning methods are very important since many sectors of industry such as information technology or semiconductor industry rely on them. For instance, photolithography plays a main role in microelectronics, optoelectronics, information technology, chip fabrication and others. Although photolithography has many advantages, this technique is rather expensive, limited to feature size, can not be introduced to non-planar surfaces, is not applicable to many materials and has almost no control over the chemistry of the generated features. Soft lithography, in particular microcontact printing (μCP), where molecules are applied as ink to the surface of a stamp and transferred to a substrate by printing, will not replace photolithography but can offer a superior addition to the patterning techniques. The strength of microcontact printing is in its simplicity, reproducibility, use of wide range of substrates materials, low cost, and in replication rather than fabrication of features. This method does not need special conditions to be conducted; usually it is carried out in ambient laboratory environment. The application of microcontact printing is not only limited to simple transfer of molecules. It was shown that microcontact printing can be used as a method for surface synthesis under poly(dimethylsiloxane) (PDMS) stamp confinement.[20-23] The stamp by itself can be used as a pattern of organized features of PDMS solid film that can be transferred from the PDMS stamp to a substrate[24,25] (decal-transfer lithography[26,27] and light stamping lithography[28,29]). Many methods have been developed to modify the surface of

the stamp to make it more compatible with hydrophilic molecules but also several other materials have been used to replace commonly used PDMS.[13,30-32]

Microcontact printing has been extensively used to position proteins, oligonucleotides, antibodies, and carbohydrates on the surface.[33-35] Immobilization of biomolecules is very important in fields like microarray technology, proteomics, biosensor development, implant technology, contact lens technology, cell adhesion studies, microfluidic systems and others. Substrates with patterned biomolecules can find application in medical diagnostics, analytical chemistry, studies of cells on the surface, tissue engineering, implantable devices, and engineering of DNA, proteins or carbohydrates.

Methods for attachment of biomolecules have been studied in order to understand their function in living systems. When the bio-patterned substrates are used in clinical diagnostics, they have to meet a high degree of reproducibility, reliability and quality in order to become a standard tool and provide the best data and process control. Numerous factors can contribute to the quality of such substrates like for instance sample source, the quality of the substrate itself, and the technique of its coating. In addition, the chemistry used for the immobilization of biomolecules, probe labeling, and the method for patterning or spotting should be carefully chosen. A key focus in attachment and patterning of biomolecules is the ability to immobilize them in their native conformation while preserving active sites for functional studies.

With the completion of the Human Genome Project, DNA microarrays are developing rapidly into an important means for high-throughput identification and quantification of genetic information. Techniques to improve the immobilization and density of oligonucleotides quality of the pattern/spot and the substrate, increase the number of spots per slide are still growing. Because of the fundamental differences between DNA and protein, however, protein microarray technology is in early stage of its development. In contrast to DNA, which is stable and unreactive, proteins can lose their activity when immobilized on the surface. Carbohydrates have an important function in fundamental biological processes. They play central role in cancer metastasis and mediating immune response. Carbohydrates microarrays can find practical utility in the investigation of their interactions with other molecules.

This thesis describes several applications of microcontact printing as the simplest method for fabrication of micrometer patterns of (bio)molecules but also as a tool used in nanoscale synthesis on the surface within the patterned area.

Chapter 2 describes a literature overview of methods for the immobilization of biomolecules on planar substrates and techniques used to pattern them. Special attention is

dedicated to covalent immobilization of biomolecules and microcontact printing of biomolecules.

Chapter 3 is focused on reversible imine formation on the surface presented in two different methods: by reaction from solution and via direct microcontact printing. The reversibility of this system can offer the dynamic immobilization of molecules containing aldehyde or amine groups. The substrates can be recycled and used again for the immobilization. The reversibility of this system is explored in Chapter 4 where a dynamic covalent bond is broken and reformed again while the PPI dendritic molecules move over an aldehyde gradient surface. The imine chemistry is further explored in Chapter 5 to pattern cytophilic protein on surfaces. This protein contains a RGD sequence which can interact with cells to improve their spreading and adhesion. When the protein is patterned on the surface it can serve as a template for the cell attachment.

In Chapter 6 a modification of microcontact printing stamps with amine dendrimers is introduced in order to transfer and deliver oligonucleotides to the surface. The DNA pattern is characterized by high uniformity, high density and availability for hybridization with the complementary strand. Similarly atomic microscopy tips were modified with dendrimers in order to transport and deliver DNA and position them on the surface within nanometer scale patterns using dip-pen nanolithography (DPN).

Chapter 7 illustrates the use of microcontact printing as a method for direct synthesis on the surface. Here, the 1,3-dipolar cycloaddition, (Sharpless "click" chemistry) was conducted between the ink, containing an alkyne unit, and the azide functionalized surface, without a catalyst. Chapter 8 expands this subject to the immobilization of oligonucleotides containing acetylene units in their structure on azide-functionalized surfaces by microcontact printing.

Chapter 9 introduces a new method for the direct transfer of (bio)molecules encapsulated within a matrix using DPN. Presented method has the potential to be a universal technique with high loading capacity of ink for the patterning of biomolecules in the nanometer regime.

1.1. References

[1] R. R. Dammel, F. M. Houlihan, R. Sakamuri, D. Rentkiewicz, A. Romano, *Polym. Mater. Sci. Eng.* **2004**, *90*, 283.

[2] K. Ronse, P. De Bisschop, A. M. Goethals, J. Hermans, R. Jonckheere, S. Light, U. Okoroanyanwu, R. Wasto, D. McAfferty, J. Invaldi, et al., *Microeletron. Eng.* **2004**, 5, 73.

[3] H. Wu, T. W. Odom, G. M. Whitesides, *Anal. Chem.* **2002**, *74*, 3267.

[4] A. A. Tseng, K. Chen, C. D. Chen, K. J. Ma, *IEEE Trans. Electron. Packag. Manuf.* **2003**, *26*, 141.

[5] Y. Xia, G. M. Whitesides, *Angew. Chem. Int. Ed.* ***1998**, 37*, 550.

[6]   J. C. Love, L. A. Estroff, J. K. Kriebel, R. G. Nuzzo, G. M. Whitesides, *Chem. Rev.* **2005**, *105*, 1103.

[7]   B. D. Gates, Q. Xu, M. Stewart, D. Ryan, C. G. Willson, G. M. Whitesides, *Chem. Rev.* **2005**, *105*, 1171.

[8]   S. Y. Chou, P. R. Krauss, P. J. Renstorm, *Appl. Phys. Lett.* **1995**, *67*, 3114.

[9]   D. M. Eigler, E. K. Schweizer, *Nature* **1990**, *344*, 524.

[10]   M. F. Crommie, C. P. Lutz, D. M. Eigler, *Science* **1993**, *262*, 218.

[11]   K. B. Lee, K. S. Park, C. A. Mirkin, J. C. Smith, M. Mrksich, *Science* **2002**, *295*, 1702.

[12]   L. M. Demers, D. S. Ginger, S. J. Park, Z. Li, S. W. Chung, C. A. Mirkin, *Science* **2002**, *296*, 1836.

[13]   Y. Xia, G. M. Whitesides, *Angew. Chem. Int. Ed.* **1998**, *37*, 550.

[14]   M. Shtein, P. Peumans, J. B. Benziger, S. R. Forrest, *Adv. Mater.* **2004**, *16*, 1615.

[15]   M. Shtein, P. Peumans, J. B. Benziger, S. R. Forrest, *J. Appl. Phys.* **2004**, *96*, 4500.

[16]   K. T. Rodolfa, A. Bruckbauer, D. Zhou, Y. E. Korchev, D. Klenerman, *Angew. Chem. Int. Ed.* **2005**, *44*, 6854.

[17]   A. Bruckbauer, L. Ying, A. M. Rothery, D. Zhou, A. I. Shevchuk, C. Abell, Y. E. Korchev, D. Klenerman, *J. Am. Chem. Soc.* **2002**, *124*, 8810.

[18]   A. Bruckbauer, D. Zhou, D.-J. Kang, Y. E. Korchev, C. Abell, D. Klenerman, *J. Am. Chem. Soc.* **2004**, *126*, 6508.

[19]   K. T. Rodolfa, A. Bruckbauer, D. Zhou, A. I. Schevchuk, Y. E. Korchev, D. Klenerman, *Nano Lett.* **2006**, *6*, 252.

[20]   J. Lahiri, E. Ostuni, G. M. Whitesides, *Langmuir* **1999**, *15*, 2055.

[21]   K. B. Lee, D. J. Kim, Z. W. Lee, S. I. Woo, I. S. Choi, *Langmuir* **2004**, *20*, 2531.

[22]   J. H. Hyun, H. W. Ma, P. Banerjee, J. Cole, K. Gonsalves, A. Chilkoti, *Langmuir* **2002**, *18*, 2975.

[23]   T. P. Sullivan, M. L. van Poll, P. Y. W. Dankers, W. T. S. Huck, *Angew. Chem. Int. Ed.* **2004**, *43*, 4190.

[24]   Y.-L. Loo, R. L. Willett, K. W. Baldwind, J. A. Rogers, *J. Am. Chem. Soc.* **2002**, *124*, 7654.

[25]   Y.-L. Loo, R. L. Willett, K. W. Baldwind, J. A. Rogers, *Appl. Phys. Lett.* **2002**, *81*, 562.

[26]   W. R. Childs, R. G. Nuzzo, *J. Am. Chem. Soc.* **2002**, *124*, 13583.

[27]   W. R. Childs, R. G. Nuzzo, *Adv. Mater.* **2004**, *16*, 1323.

[28]   K. S. Park, E. K. Seo, Y. R. Do, K. Kim, M. M. Sung, *J. Am. Chem. Soc.* **2006**, *128*, 858.

[29]   T. W. Odom, V. R. Thalladi, J. C. Love, G. M. Whitesides, *J. Am. Chem. Soc.* **2002**, *124*, 12112.

[30]   C. Donzel, M. Geissler, A. Bernard, H. Wolf, B. Michel, J. Hilborn, E. Delamarche, *Adv. Mater.* **2001**, *13*, 1164.

[31]   A. P. Quist, E. Pavlovic, S. Oscarsson, *Anal. Biochem. Chem.* **2005**, *381*, 591.

[32]   T. W. Odom, J. C. Love, D. B. Wolfe, K. E. Paul, G. M. Whitesides, *Langmuir* **2002**, *18*, 5314.

[33]   A. Bernard, J. P. Renault, B. Michel, H. R. Bosshard, E. Delamarche, *Adv. Mater.* **2000**, *12*, 1067.

[34]   S. A. Lange, V. Benes, D. P. Kern, J. K. H. Hober, A. Bernard, *Anal. Chem.* **2004**, *76*, 1641.

[35]   E. Delamarche, C. Donzel, F. S. Kamounah, H. Wolf, M. Geissler, R. Stutz, P. Schmid-Winkel, B. Michel, H. J. Mathieu, K. Schaumburg, *Langmuir* **2003**, *19*, 8749.

Chapter 2

Soft lithography and surface engineering for biomolecule immobilization

This Chapter presents a general overview of a wide range of chemical methods for the immobilization of biomolecules on surfaces. The overview includes modern techniques of surface patterning and modification such as new approaches for microcontact printing, patterning through microchannels and microwells or parallel dip-pen nanolithography. The focus is on nucleic acids, proteins and carbohydrates since these biologically active compounds are currently the most often used in microarrays applications and research.

2.1. Introduction

Biochips and bioplatforms that aim at simultaneous analysis of thousands of oligonucleotides,[1] antibodies/antigens, proteins,[2] carbohydrates,[3] drug-like molecules,[4] cells,[5] tissues[6] and other have attracted a lot of attention for the last ten years. Currently, there is a high demand for methods to produce substrates for biomolecule immobilization that simultaneously provide a high probe loading density, maintain biological activity, and are easy to prepare and use. The development of an ultimate method for biomolecule immobilization will reduce the differences in chip production or increase the reproducible comparison between chips fabricated by many companies.

Surface chemistry is one of the keys to successful development of reliable microarrays and bioplatforms. Surfaces must be designed and prepared to optimize the immobilization of probe biomolecules and also should resist non-specific binding of target species. In terms of immobilization method, the chemical and biochemical difference between different classes of biomolecules has to be taken into account. For any given probe molecule, there is likely to be an optimal surface immobilization technique which will allow for attachment at the highest possible concentration and with preservation of required activity. The biomolecules of interest can be broadly grouped into proteins (antibodies, enzymes, receptors), nucleic acids (DNA, RNA, PNA), carbohydrates and glycoconjugates, lipids, small molecules (e.g. metabolites, peptides, hormones) and other biomolecules. For instance, proteins are chemically and structurally much more complex and heterogeneous than nucleic acids, and they can easily lose their structure and biochemical activity due to denaturation, dehydration or oxidation. The detection of proteins by antibody-antigen interactions is characterized by a broad range of specificity and affinity while the hybridization of two DNA strands is limited by complementarity of two strands and a few other physical parameters like T_m or ionic strength.[7] For the reason that DNA is uniformly negatively charged, the spontaneous adsorption to the substrate is much easier to exclude in comparison with protein adsorption due to electrostatic, van der Waals and Lewis acid-base forces, hydrophobic interactions as well as conformational changes.[8] The immobilization of the biomolecules should be conducted in such a manner that the background signal is minimal. Achieving a low degree of unspecific binding is a very important factor for the quality of the microarray, signal intensity, and quantification of binding events. Another important factor that should be taken into consideration when designing a bioplatform is lateral interaction that can affect the density of surface-bound biomolecules. These interactions can result from either a) electrostatic repulsion between molecules with like charges, or b) dipole-dipole interactions, which can be repulsive or attractive, depending on the

position and ordering of molecules on the surface. Taking into account above mentioned issues, the surface chemistry must be carefully tailored depending on the application of each biochip.

The final performance of the immobilized biomolecules is strongly dependent upon a number of parameters related to the immobilization process. These include: (i) the chemical and physical properties of the surface, since they can influence nonspecific binding of target and non-target molecules; (ii) the distance between the immobilized biomolecules and the solid surface and the orientation of the immobilized molecules; (iii) the density of the biomolecules on the surface which can limit its sensitivity; and (iv) the chemical composition and structure of the biomolecule. Overall, it is complex to predict or model all effects of the above interactions and the behavior of biomolecule adsorption on a particular surface.
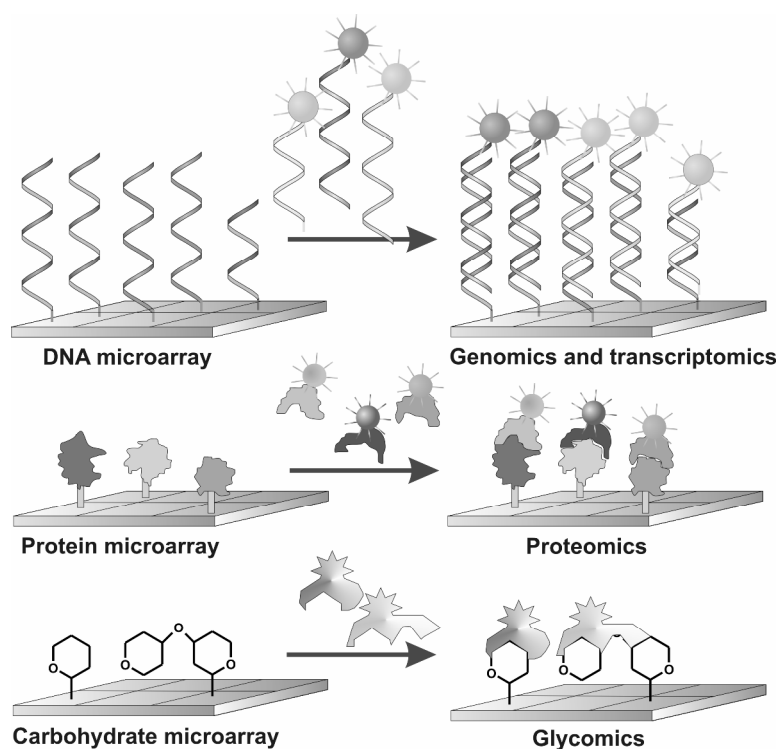
Figure 2-1. Immobilization of biomolecules in microarray format for studies of biological processes. (Picture adopted from the reference [9]).

The surface and type of selected immobilization method will affect the bioactivity, the concentration, and the target-binding ability of bound probe molecules. Gold and glass substrates are good candidates for the immobilization of biomolecules. Those two types of substrates are in general characterized by chemical homogeneity and stability, ability to control surface properties like wettability, ability to be modified with a wide range of chemical functionalities, reproducibility of the surface modification process, and in case of glass, low

intrinsic fluorescence. Glass substrates are very commonly used for microarrays application due to their chemical resistance against solvents, low fluorescent noise, optical transparence, flat, nonporous surface. In addition they are easy to handle and inexpensive. The immobilization of biomolecules onto gold and/or glass supports involves three general steps: (a) the chemical modification of the biomolecule in such a manner that it can interact with complementary functionalities present on the substrate to form a stable bond; (b) the modification of the support surface with sufficient functional groups to allow specific binding and prevent nonspecific adsorption of the biomolecules; and (c) the use of a transport-delivery system (e.g. a stamp, a tip, or a microfluidic channel) that brings small quantities of the biomaterial to specific positions on the surface.

Specific groups involved in covalent immobilization of biomolecules to the surface are very often introduced into the structure of this molecule, especially in biomolecules like oligonucleotides or carbohydrates. Carboxylic and amino functionalities are the modifications most frequently used, although aldehyde, thiol, oxyamino are useful alternatives. In some cases coupling molecules (cross-linkers) are necessary to increase the affinity (or reactivity) of the interacting groups.

Direct attachment of biomolecules to the surface can introduce a steric constrain to reactivity of the molecule which is not encountered when considering molecules free in a solution. This effect can be minimized if, for example, a spacer is introduced between the biomolecule and the linking group (Figure 2-2). The spacer can be of nearly any desired length and possess a variety of chemical characteristics, i.e. it can be rigid or flexible, hydrophilic or hydrophobic, charged or neutral.[1,10]

Biomolecule

Cross-linker

Surface activating agent
Solid support

Figure 2-2. Schematic representation of the immobilization of a biomolecule on a surface.

Depending on the type of biomolecule, different approaches in attachment to the substrate are preferred. Proteins usually are bound to the surface via amino groups of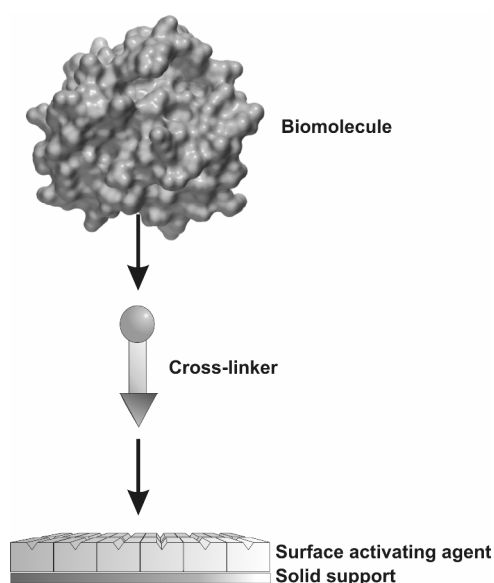 lysines or at the termini of the peptide chain. Antibodies can be bound through thiol groups, with the most reactive of them being positioned either in the hinge region or between light and heavy chains. Alternatively antibodies can be bound via carbohydrate residues of the Fc region and coupled with protein A or G.[7,11] Oligonucleotides can be bound to the surface through the reactive linker introduced into the 5'-terminus of the strand. Chemically modified or unmodified carbohydrates can be attached covalently to functionalized supports or can be nonspecifically and non-covalently immobilized to the underivatized surfaces.[9] Lipids and lipid bilayers can be physisorbed onto hydrophilic surfaces such as mica or amino-modified substrates.

The covalent immobilization of biomolecules seems to be the best method for the attachment since physical adsorption of molecules, although the simplest strategy can be rather uncontrollable. In case of adsorption, the close proximity between the molecules and the surface could have an influence on the reactivity of that molecule. In addition the surface can be susceptible to exchanging adsorbed molecules with others, for example, adsorbed proteins can be exchanged with the proteins from the solution.[12] Covalent attachment of biomolecules to a surface appears to have more advantages. It can be designed in more controlled fashion when the immobilization takes place by exposing the active sites on the surface and binding occurs through specific sites that are distributed elsewhere in the biomolecule. The covalent immobilization could also be random when the binding occurs through the active functional groups that are arbitrarily or widely distributed over the structure of the molecule. Nevertheless, the advantages of covalent immobilization depend strongly on surface chemistry and analytical techniques used for detection.

Another issue in the immobilization of biomolecules on solid supports is spatial control and diversity or loading capacity of different molecules on one substrate. Many techniques have been developed to pattern DNA, proteins, carbohydrates and other biomolecules on the planar substrates. Soft lithography opened the access to simple and cost-effective methods to create patterns of biomolecules by microcontact printing, microfluidic networks and microwells. Dip-pen nanolithography enables to produce sub-micrometer features and when conducted using the multiple-pen array it can result in thousands of features produced simultaneously. Ink-jet technology and contact printing systems have been developed specially for microarray purposes. These massively parallel methods can fabricate thousands of spots of different oligonucleotides or protein on one chip.

In this Chapter methods and aspects of immobilization and patterning of biomolecules are described. The main attention is focused on the covalent immobilization of biomolecules and soft lithography as a universal technique for fabrication of patterns.

2.2. Immobilization of biomolecules on self-assembled monolayers

2.2.1. Activation of glass slides

Glass slides are one of the most popular substrates for the immobilization of biomolecules, since they possess many advantages such as availability, low cost, flatness, rigidity and transparency and possibility of introduction of diverse reactive chemical groups.[13-17] The main method for the functionalization of glass slides for covalent attachment of biomolecules is the reaction between the surface silanols (Si-OH) (obtained after activation of the surface with, for example, "piranha" solution or oxygen plasma) and organofunctional silanes like alkyltrichlorosilanes, trialkoxy(alkyl)silanes or chlorodimethyl alkylsilanes.

The density of active surface groups is an important factor that can influence the immobilization of biomolecules. One example for enhancing surface density with reactive groups on the glass surface is modification with dendrimers or dendritic structures. These nanoscopic polymers are characterized by regular dendritic branching, radial symmetry, ease of control of surface functionality and uniform size.[18] Covalent attachment of dendrimers to a support builds a 3D structure which can consequently yield a higher density of reactive groups and as a result of that a higher density of immobilized molecules. Dendrimer modified substrates were previously used for the attachment of DNA molecules.[19,20] The method was based on modification of glass with aminosilanes and subsequent activation with a homobifunctional linker, such as disuccinimidylglutarate (DSG) or 1,4-phenylenediisothiocyanate (PDITC). The activated amine groups were further reacted with a starburst dendrimer that contains amino groups in the outer sphere (poly(amidoamine) dendrimers, PAMAM). The final step of this functionalization relied on activation and cross-linking of attached dendrimers with a homobifunctional spacer (DGS or PDITC). Alternatively, after attachment of dendrimers to the surface, glutaric anhydride activated with *N*-hydroxysuccinimide can be used. This surface modification yields a thin, chemically reactive polymer film, which is covalently attached to the glass support and can be directly used for the covalent attachment of amino-modified components, such as DNA or peptides (Figure 2-3B).
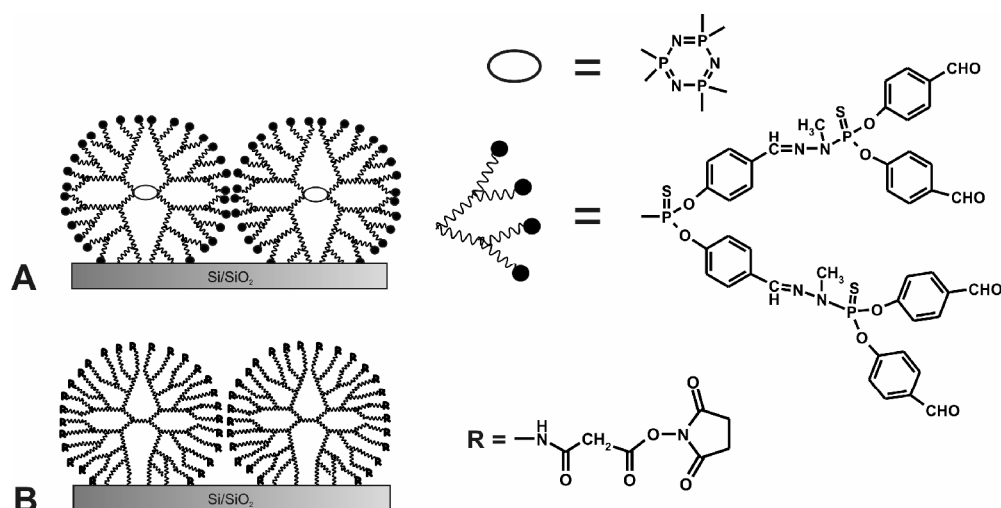
Figure 2-3. Schematic illustration of dendrimer-modified glass support. A) aldehyde-terminated dendrimers attached onto amino-modified glass slides (dendrislides). B) PAMAM dendrimers activated with glutaric anhydride and N-hydroxysuccinimide.

Dendron-modified glass slides were used to obtain controlled spacing between immobilized DNA molecules.[21,22] Aldehyde-functionalized dendrimers were attached covalently to the amino-silanized glass substrates generating a reactive, layer that can bind efficiently amino-functionalized DNA. These "dendrislides" can create high surface coverage with oligonucleotides that can be further hybridized with high yield (Figure 2-3A).[23] Grafting of DNA on such a surface resulted in uniform, homologous and also high density layers. The modification with dendritic molecules can be achieved by either in-situ synthesis or by direct surface attachment of presynthesized branched structures.

Another interesting modification of glass surface was introduced by Beier et al.[24] The group has synthesized a flexible, dendritic linker system that enables covalent immobilization of oligonucleotides and peptide nucleic acids (PNAs) with high loading capacity in a controlled manner. This method facilitates modulation of surface properties with respect to hydrophobicity and charge. The synthesis of the linker system involves a serial application of two reactions: an acylation of surface-bound amine groups with acid chloride (4-nitrophenyl-chloroformate or acryloylchloride) and subsequent reaction with an amine. A bis-amine results in a linker system, while a polyamine produces a dendritic structure (Figure 2-4). Because polyamines possess primary and secondary amine groups, not one unique product is generated in such a reaction but a mixture of compounds.
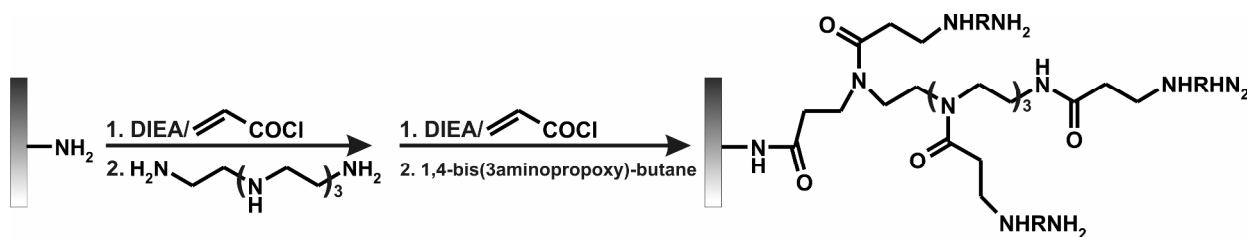
Figure 2-4. Dendritic linker structure synthesized on amino-functionalized substrate. DIEA = diisopropylethylamine.

The density of immobilized proteins was successfully improved when a dendrimer-activated surface was used.[25] Poly(propyleneimine) dendrimers were bound to the Si and glass surface that was modified with 1,1'-carbonyldiimidazole under anhydrous conditions. Due to the high concentration of charged amine groups of dendrimers, this method provides a fine platform for high density protein immobilization.

Another method to increase the number of reactive groups on the surface is modification of the substrates with colloidal silica films. These films are usually spin-coated onto a glass substrate and stabilized by thermal curing.[26] The "three-dimensional", porous, colloidal silica coatings of surfaces exhibit better performance than flat glass substrates in terms of the efficiency of chemical synthesis. Glazer *et al.* showed immobilization of DNA probe arrays onto the substrates modified with colloidal silica films.[27] Subsequent hybridization with the target sequence revealed 20 times higher intensity signal than the one obtained on modified, flat glass. Cambell and coworkers[28] have established that colloidal silica films can be attached to plastic supports and used for immobilization of antibodies with higher protein loading per cm^2 than conventional two-dimensional surfaces.

2.2.2. Activation of metal surfaces with self-assembled monolayers of thiols

Self-assembled monolayers on gold and other metal surfaces have been extensively studied in biosensors applications.[29-31] The thiol-gold chemistry is well-known and is much easier controlled than organosilane chemistry (Figure 2-5).[32-35] On the other hand, the cost involved in the gold-coating process may be one of the obstacles when thinking of applying this method.
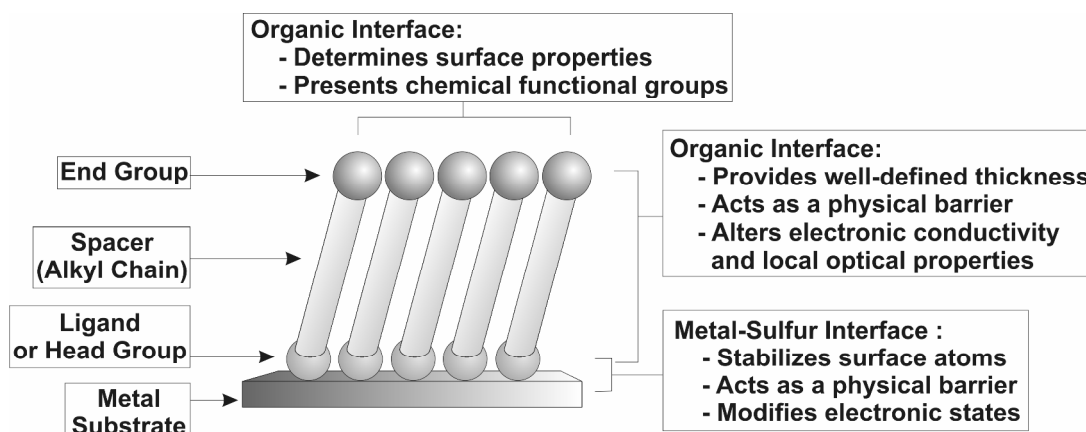
Figure 2-5. Schematic diagram of SAM of alkanethiolates on gold substrate. Picture adopted form the reference [32].

The functionality of the thiol SAM can be tailored by choosing a reactive end group of the thiol (carboxylic, hydroxyl or amine are the most frequently used examples). The biomolecules can be covalently attached to such monolayers in two manners: directly to the gold surface (when possessing linkers with thiol termination or when possessing thiol residues in its structure) or by the reaction with an end group of a thiol SAM. Monolayers can also be introduced as a mixture of usually two components, thiols with different functionalities as end groups (mixed monolayers). This influences the spacing between attachment points for biomolecules and prevents steric hindrance between them, protecting the loss of their full reactivity. Mixed SAMs for the covalent attachment of biomolecules possess utility in minimizing nonspecific binding or affinity of biomolecules to the surface when the thiols with reactive groups are mixed with thiols that can prevent nonspecific absorption (mainly thiols modified with polyethylene glycol, polyvinylpyrrolidone, polyvinyl alcohol chains and others).[36]

Even though gold showed the best properties for the functionalization with self-assembled monolayers, other metal surfaces also have been used for the attachment of biomolecules. Oligonucleotides and proteins have been immobilized onto SAMs on metal substrates such as titanium, aluminum, and silver. [37-40]

2.3. Immobilization of biomolecules on polymeric surfaces

Polymers can be either modified with reactive groups that can bind biomolecules or can be fixed to a solid support in the form of pads to serve as a platform for the immobilization of biomolecules. Polymers such as poly(dimethylsiloxane) (PDMS) or poly(methyl methacrylate) (PMMA)[41] can be good candidates as solid support for the attachment of biologically active molecules. They are optically transparent, can be modified to expose reactive groups on the

surface, and in addition they are good materials for molding, patterning and nanofabrication. PDMS can be activated in oxygen plasma reactor to introduce reactive silanol groups. These groups can be subsequently reacted with organosilanes to obtain a desirable functionality on the surface of polymers to bind specific biomolecules.

Functionalized PMMA has been successfully used as a substrate for the immobilization of proteins[42] and DNA. Fixe *et al.*[41] have shown a reliable method of modification of polymer surface groups yielding amino groups, suitable for immobilization of different types of biomolecules. The polymer was reacted with hexamethylene diamine to obtain an aminated surface for immobilization of DNA in microarrays. (Figure 2-6). An alternative route was proposed by Bulmus *et al.*[43] Amino-modified PMMA can be further reacted with cross-linkers such as glutaraldehyde or sulfo-EMCS to immobilize amino- or sulfhydryl-functionalized biomolecules, respectively.
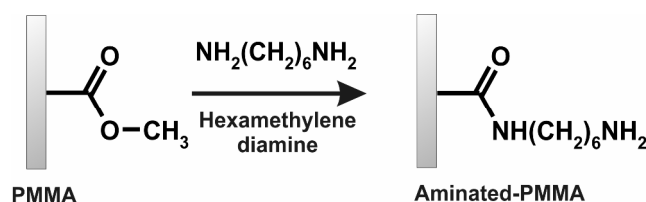
Figure 2-6. Functionalization of poly(methyl methacrylate) substrates for biomolecule immobilization. Direct reaction of polymer with hexamethylene diamine proposed by Fixe *et al.*[41]

Other examples of polymeric surfaces which can serve as good surfaces for the immobilization of biomolecules involve polymers fixed covalently or electrostatically onto rigid, activated supports (mainly glass). Among these polymers are: polyacrylamide, polysaccharides, chitosan or activated dextrans. Theoretically, these kinds of substrates allows the immobilization of a large amount of molecules due to the greatly enhanced surface area of their 3D structure, offering the potential for improved sensitivity compared to planar substrates. Such polymers were successfully used in DNA microarrays application and protein immobilization.

Acrylamide can be photopolymerized onto a substrate functionalized with acrylic groups, for instance glass substrate modified with 3-(triethoxysilylpropyl)acrylamide.[44,45] In the next step, the polymer can be activated with hydrazine or ethylenediamine to generate amino groups on the surface. These amine groups can be further reacted with different cross-linkers to couple appropriate biomolecules.

Chitosan is an amino-modified, natural, non-toxic polysaccharide; it is biodegradable and biocompatible and can be used for covalent binding of biomolecules.[46] Due to its pH responsive properties it can be immobilized onto glass supports.[47] Chitosan is soluble at low

pH, while it becomes insoluble when the pH is raised above its pK$_a$ (~6.3). The amine groups can be reacted covalently with cross-linkers to bind biomolecules such as oligonucleotides or proteins. Due to the presence of ionizable amine groups, chitosan can bind electrostatically other molecules which behave like polyanions, for instance gelatin or collagen, as was reported by Taravel *et al*.[48] Besides biocompatible advantages, chitosan is optically transparent for UV and visible light, can form 3D networks which can offer high binding capacities and in addition is safe, abundant and inexpensive.[49]

Another class of carbohydrates that can be used as substrates for the immobilization of biomolecules is activated dextran. Dextran is a complex, branched polysaccharide made of many glucoses joined into chains of varying lengths. Supports containing that biopolymer were widely used for the immobilization of oligonucleotides.[50,51] Dextran hydroxyl groups can be oxidized to the corresponding aldehyde groups and the polysaccharide can be covalently immobilized onto amino-functionalized supports (Figure 2-7).[51,52] Non-reacted aldehyde groups can be further used for the immobilization of other amino-modified molecules.
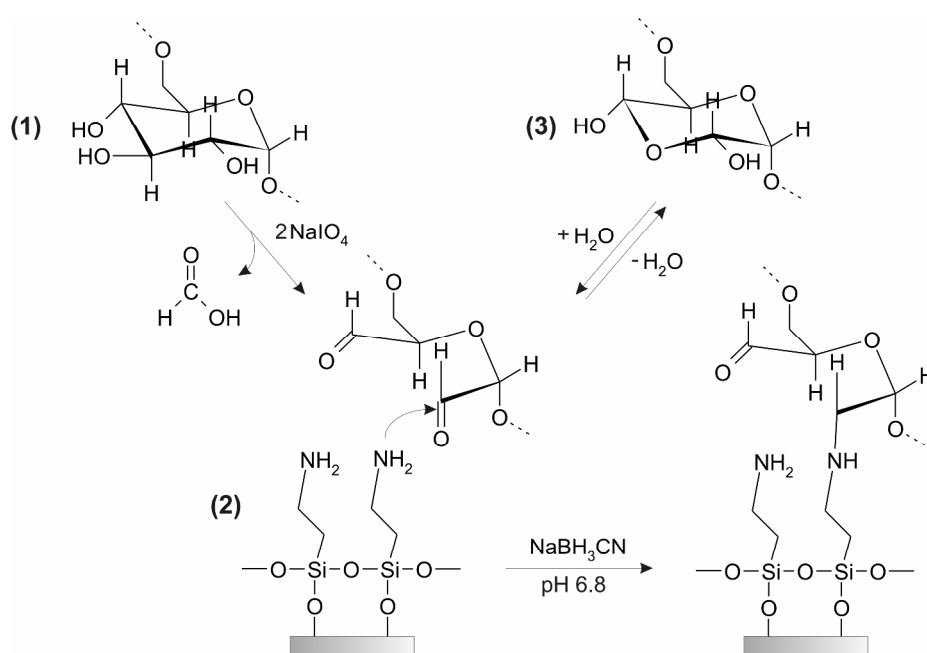
Figure 2-7. Schematic representation of the oxidation of dextran glucopyranoside subunits by NaIO$_4$ with formation of formic acid and subsequent surface immobilization through reductive amination in the presence of NaBH$_3$CN. Illustration adopted form the reference [52].

Alternatively, the hydroxyl groups of dextran can be oxidized and subsequently reacted with aspartic acid to yield a negatively charged polymer. This polymer can be deposited onto positively charged surfaces through electrostatic interactions. To form covalent bonds with biomolecules, the polymer has to be activated by oxidation to obtain aldehyde groups.

Biodegradable polyesters such as poly(L-lactic acid) (PLA) and its various copolymers with D-lactic acid and glycolic acid have been extensively studied as substrates for biomolecule and cell attachment.[53]

2.4. Covalent immobilization of biomolecules

The reactivity of the substrates is determined by the surface functional groups. Immobilization of the biomolecules to the substrates can be performed via several routs. This can be done by a direct attachment of the molecule to the functionalized or non-functionalized surface, or by the employment of a cross-linker (homobifunctional, heterobifunctional or multifunctional) between the functionalized surface and biomolecule.

Generally, the selection of the substrate and the chemistry is very important for the successful immobilization of biomolecules and application of that substrate. Here, the reaction between the biomolecule and the reactive surface groups is described for both types of substrates: silicon oxide/glass and gold.

2.4.1. Surface activation for covalent attachment

Surface activation compounds are bound to the substrate to change the functionality of the substrate. Gold and silicon oxide or glass surfaces can be modified with reactive monolayers such as thiols and alkylsilanes, respectively. These monolayers should bear a functionality that can react with biomolecules via a covalent bond. The monolayers may be modified, by the introduction of reactive groups or non-modified, owning their native reactive groups. The preparation of clean gold or glass surfaces in order to remove any organic surface contaminations that could possibly interfere with subsequent monolayer formation involves cleaning with detergents, strong oxidizers ("piranha" solution, H_2SO_4/H_2O_2, NH_3/H_2O_2), UV-plasma cleaning or sonication.

Very common chemistry involved in binding biomolecules relies on the reaction between epoxide-, aldehyde-, or isothiocyanate-terminated reactive monolayers and amino-modified or amino-containing biomolecules. Examples of such surface reactions are listed in Table 2-1.

Table 2-1. Characteristic surface reactions used to couple biomolecule with the solid supports.

Surface chemistry	Modification of biomolecule	Reference
Si-SiO$_2$/glass-silane-epoxide	aminolink-DNA	Beattie et al.[54], Lamture et al.[55]
Si-SiO$_2$/glass-silane-PDI-PAMAM-PDI	aminolink-DNA	Benters et al.[20]
Si-SiO$_2$/glass-silane-aldehyde	aminolink-DNA	Zammatteo et al.[56]
Si-SiO$_2$/glass-silane-sulfhydryl	disulfide-DNA	Rogers et al.[57]
Si-SiO$_2$/glass-silane-sulfhydryl	maleimide-DNA, maleimide-carbohydrates	Steel et al.[58] Park et al.[9, 59]
Si-SiO$_2$/glass-silane-maleimide	thiol-DNA	Okamoto et al.[60]
Si-SiO$_2$/glass-silane-bromoacetamide	phosphorothiolate-DNA	Pirrung et al.[61]
Si-SiO$_2$/glass-silane-sulfhydryl	acrylamide-DNA	Demers et al.[62]
Si-SiO$_2$/glass-silane-phosphane derivative	azide-carbohydrates	Waldmann et al.[63]
Si-SiO$_2$/glass-silane-bromoacetamide	(internal)phosphorothiolate-DNA	Zhao et al.[64]
Si-SiO$_2$/glass	silanized-DNA	Kumar et al.[65]
gold-thiol/amine-maleimide	thiol-DNA	Corn et al.[66]
gold-thiol/amine-disulfide	thiol-DNA	Corn et al.[67]
gold-thiol/azide	acetylene-DNA	Chidsey et al.[68]
gold-thiol/benzoquinone	cyclopentadiene-carbohydrates	Mrksich et al.[69]
gold-thiol/NHS ester	amino-proteins	Delamarche et al.[70]
gold	thiol-DNA or cysteine-containing peptides or proteins	Demers et al.[62]

Reaction of surface hydroxyl groups with 2,2,2-trifluoroethanesulfonyl chloride (tresyl chloride) yields sulfonate esters functionality which in a subsequent step can be reacted with amino- or mercapto-modified biomolecules for covalent immobilization (Figure 2-8a).[71] Aldehyde modified surfaces can be reacted with amino groups of biomolecule to form imine linkages which can be subsequently reduced to secondary amines by the reaction with sodium borohydride (Figure 2-6b).[72] Disulfide-modified biomolecules can be immobilized onto mercapto-silanized glass supports by a thiol/disulfide exchange reaction (Figure 2-8c).[57] Isothiocyanate functionalized substrates can be used for the immobilization of amino-functionalized molecules (Figure 2-8d) similarly to epoxy-terminated SAMs (Figure 2-8e).[73] Azide-functionalized surfaces can be used to immobilize alkyne-bearing molecules by triazole formation usually using copper(I) catalyst (Figure 2-8g). This chemistry is highly predictable, fast and resistant to side reactions.[68] Active sulfhydryl-functionalized surfaces can be easily reacted with maleimide-modified biomolecules.[67] Biomolecules containing free amino groups can be coupled to a monolayer bearing NHS ester groups on the surface through an amide bond.

The NHS-ester coupling reaction is easy to carry out and proceeds in good yields (Figure 2-8h).[70]
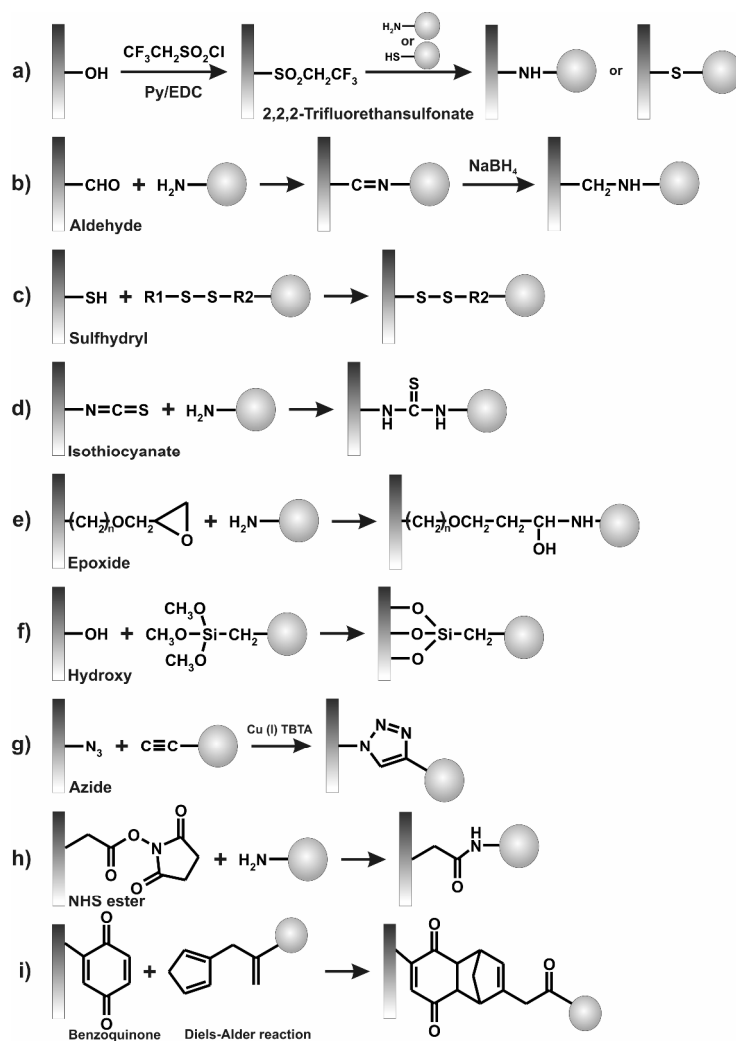
Figure 2-8. Surface activation for direct immobilization of biomolecules.

Silicon substrates can be modified with mercaptopropyltrimethoxysilane (MPTMS) and reacted with biomolecule functionalized with acrylamide groups. The acrylamide moieties react with surface thiol groups by Michael addition forming covalent links between biomolecule and the surface. In terms of using this chemistry to pattern the surface, remaining thiol surface groups can be passivated by the reaction with acrylic acid monomers at pH 10.[62]

Unmodified microscope slides may be used for direct covalent conjugation with an activated, silanized oligonucleotide (Figure 2-8f).[74] The advantage of this system is that the immobilization process is very simple and functionalization of the surface is not necessary.

A clean gold surface can directly react with thiol-containing molecules. Direct immobilization of proteins on gold surfaces can be obtained simply by affinity of cysteine residues in the protein to gold surface resulting in a strong adsorption.[75,76] After immobilization, the

passivation should be proceeded in order to block remaining gold areas. The benefit of that method is that no surface modification is needed in order to attach the molecule.[62] The introduction of a diene-functionality into a protein is a one-step reaction by acylation of the amino group of lysine from the protein and a bifunctional cross-linker which possess a succinimidyl ester on one end and hexadienyl functionality on the other end. This dienyl conjugate can then be immobilized onto maleimide-modified substrate via Diels-Alder cycloaddition. The Diels-Alder reactions was shown to be compatible in the bioconjugation process and immobilization of oligonucleotides and other biomolecules.[77,78] The reaction is highly selective and can be carried out in water with a higher rate than in organic solvents. Another example of the application of Diels-Alder reactions for the immobilization of biomolecules was presented by Mrksich and coworkers.[69] Cyclopentadiene-modified carbohydrates were reacted with a benzoquinone-functionalized monolayer on gold. This reaction was found to be highly efficient and selective for the immobilization of carbohydrates on the surface (Figure 2-8i).

2.4.2. Introduction of homobifunctional cross-linkers on the surface

It is important that after immobilization of biomolecules on the surface, the biomolecule will retain its activity. In order to prevent the loss of the bioactivity, the molecule should be separated from the surface to avoid steric clashes with incoming molecules. One way to do so is to introduce a linker molecule to create a distance between the surface and biomolecule. Homobifunctional surface-activating molecules possess double sided reactive groups to conjugate two equal functional groups between attached biomolecule and the (modified) surface. Usually the homobifunctional cross-linker is first reacted with the surface and then the biomolecule is attached. The requirement for this linker is that it should not connect two neighboring groups on the surface blocking the reactivity for the further attachment of other molecules. The linker should be rigid and chemically stable. The most commonly used homobifunctional cross-linkers are glutaraldehyde, 1,4-butanediol diglycidyl ether, 1,4-phenylene diisothiocyanate, dimetylsuberimidate or terephthaldialdehyde (Figure 2-9).[72]

Amino-modified surfaces can be applied for attachment of molecules that contain free amino groups when the substrate is reacted with a homobifunctional cross-linker like bis(sulfosuccinimidyl)suberate (BS^3, Pierce) in acetate buffer,[79] terephthaldialdehyde, disuccinimidyl carbonate or others (Figure 2-9).

A sulfhydryl-terminated monolayer on gold or on silicon oxide surface can be reacted with 2,2'-dipyridyl disulfate to form disulfide bonds on the surface.[67] These disulfide bonds can then be

used in a thiol-disulfide exchange reaction with free sulfhydryls in order to attach biomolecules, such as thiol-modified DNA or cysteine-containing polypeptides, onto the surface (Figure 2-9j).
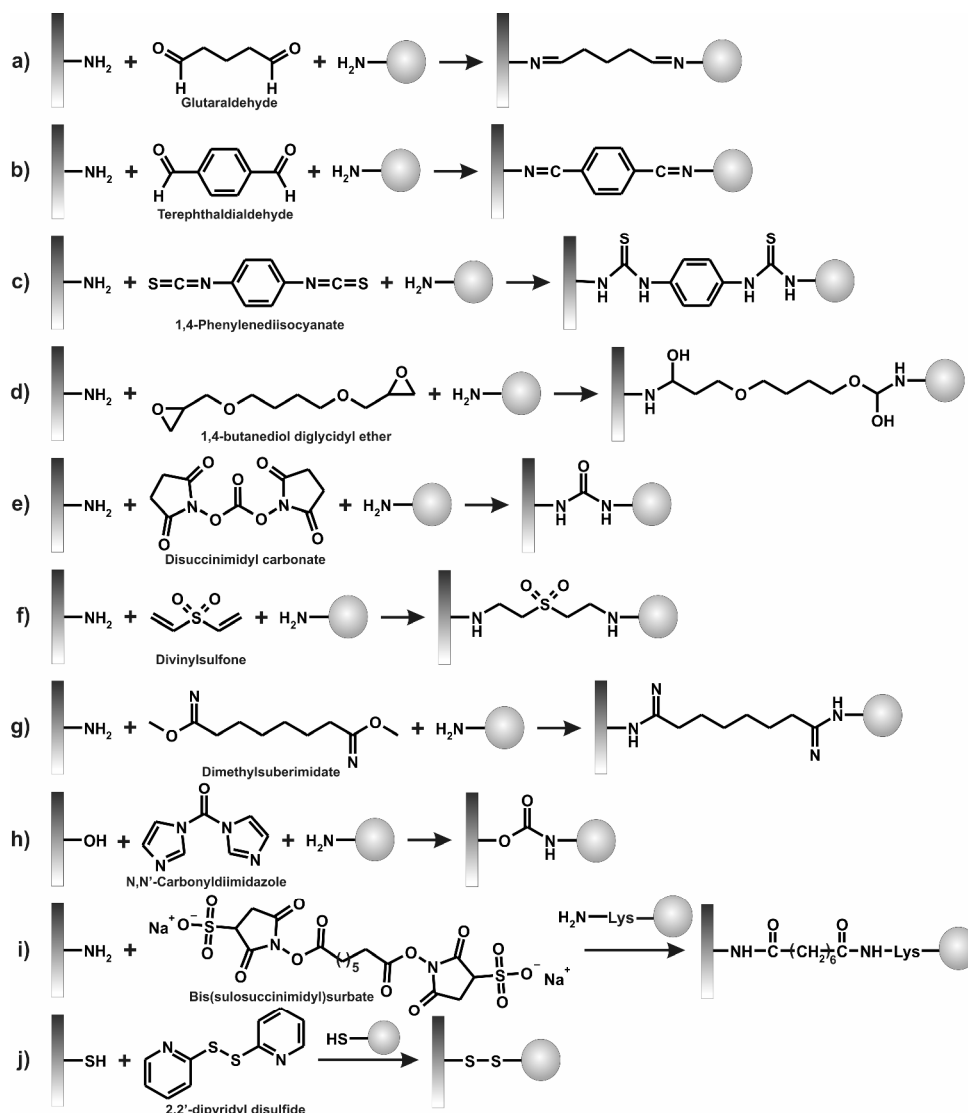
Figure 2-9. Homobifunctional cross-linkers for connecting equal functional groups.

2.4.3. Introduction of heterobifunctional cross-linkers on the surface

Heterobifunctional cross-linkers are employed to couple two different functional groups between the monolayer and the molecule for the subsequent immobilization. The wide range of these cross-linkers and their specific reaction is presented in Figure 2-10. One example where the use of heterobifunctional cross-linkers was applied for immobilization of biomolecules was work of Corn and coworkers where the SSMCC (sulfosuccinimidyl 4-(*N*-maleimidomethyl)cyclohexane-1-carboxylate) linker was applied to link thiol-modified DNA molecules with an amino-functionalized surface.[66]
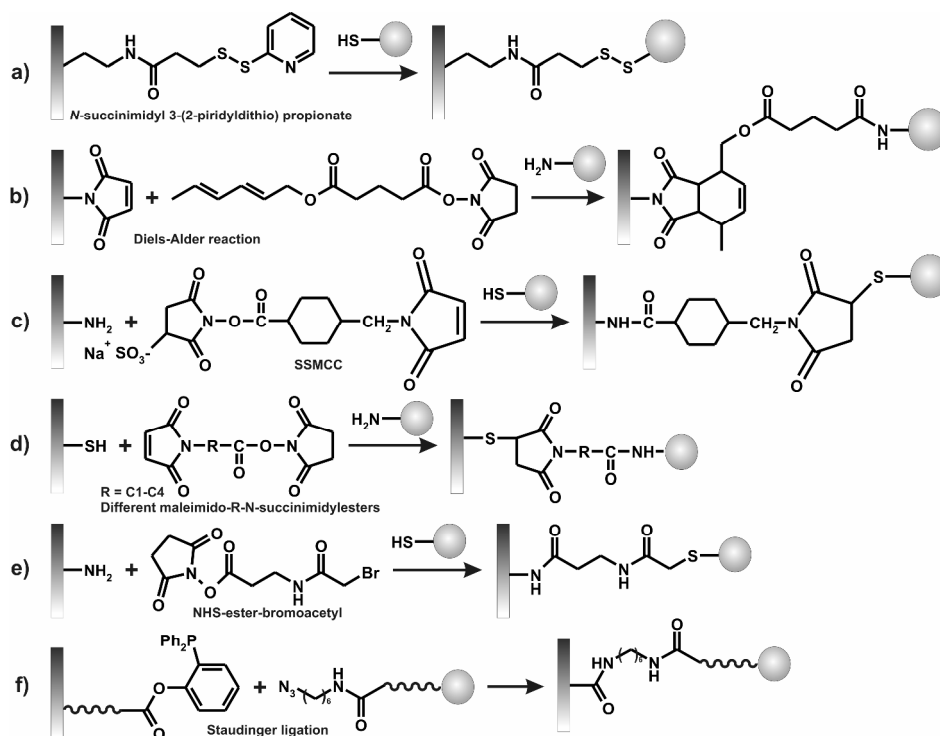
Figure 2-10. Application of heterobifunctional cross-linkers for immobilization of biomolecules.

Mercapto-functionalized surfaces can be modified with a heterobifunctional linker in order to bind amine groups from biomolecules like, for instance, antibodies.[80] Amino-group-containing biomolecules can be bound to that surface via maleimido-R-*N*-succinimidylester, which contains a sulfhydryl reactive maleimide group at one end and an NHS ester at the other end (Figure 2-10h). Similarly, the maleimide-NHS cross-linker can bind mercapto-functionalized biomolecules in reverse orientation on the amino-functionalized surface (Figure 2-10g). Another example of coupling two molecules where one contains an amino functionality, and the other a sulfhydryl can involve succinimdyl 3-(bromoacetamido)propionate. The NHS ester group will bind the linker to amino-functionalized surfaces, exposing bromoacetyl group for the subsequent reaction with a sulfhydryl containing molecule. A useful review about heterobifunctional cross-linkers can be found in reference [81].

An additional advantage of using a NHS-maleimide cross-linker (e. g. aminocaproic acid linker) is that once it is bound to NH_2-surface groups exposing maleimid functionality it can react with diene-modified biomolecules (for instance proteins).[82] Waldmann *et al*. have explored the Staudinger ligation to immobilize azide-containing carbohydrates onto phosphane-derivatized glass slides and fabricate small molecules microarrays (Figure 2-10f).[63] The glass substrate was functionalized with PAMAM dendrimers to increase the number of reactive sites on the surface.

2.5. Surfaces resistant towards proteins and cells

When substrates are specifically patterned with biomolecules (or cells) in a well-defined manner, usually there is a need to make the remaining areas, outside the pattern, resistant to the adhesion of other biomolecules and to exclude non-specific interaction with the background that surrounds the reactive pattern. These modifications are most often used against proteins and cell adhesion and are commonly applied in developing and designing implants, contact lenses and surgery materials, sensors and devices for drug delivery. Proteins adsorb to solid surfaces usually due to hydrogen bonding, hydrophobic and electrostatic interactions. Hydrogen bonds can be formed between hydrophilic groups of the substrate and polar groups of the proteins. Hydrophobic interactions can be induced between hydrophobic surfaces and the hydrophobic regions of the protein, while electrostatic interactions are associated with charged groups on the protein and the solid substrate. When a protein is adsorbed on the surface it can retain its biological activity, but frequently it may denature (unfold) and loose its properties.[83]

Typically, surfaces which show resistance towards proteins are also resistant towards cell adhesion and tissue culture growth.[84-86] There are many surfaces that exhibit resistance to proteins or cells but one of the most important examples are poly(ethylene glycol) (PEG),[87] PEG-derivatized alkanethiols,[88,89] interpenetrated copolymers of PEG,[90-92] multilayers of PEG-functionalized with $SiCl_3$ groups,[93,94] poly(N-acryloylsarcosine methyl ester) films,[95] sulfonate-terminated alkylsilane SAMs,[96-98] alkanethiol SAMs functionalized with tri(propylene sulfoxide),[99] sarcosine-based polypeptide SAMs,[100] elastin-like polypeptide coatings,[101] polyelectrolyte surfaces, phospholipids,[102] phosphorylcholine SAMs,[103] bovine serum albumin (BSA), cellulose acetate,[104] polysaccharides,[85,105] polyacrylamides,[106] agarose,[107] paraffin,[108] fluorocarbon polymers,[109] poly(vinyl alcohol),[110] surfaces exposed to the surfactant Tween 20[111] or Pluronic F68.[112] Some of these surface-modifying agents are described in more details below.

2.5.1. Poly(ethylene glycol) (PEG)-derivatized surfaces

Poly(ethylene glycol) (PEG) grafted on glass or metal surfaces is successful for preventing nonspecific adsorption of proteins and cell adhesion.[92,113,114] A variety of these methods including adsorption, covalent immobilization and cross-linking have been applied in studies on "inert" materials.[87,90-92] It was shown in the past that monolayers which are PEG-terminated showed protein resistant properties.[115] Whitesides and coworkers have studied different SAMs of alkanethiols on Au and Ag surfaces and concluded that the resistance of oligo(ethylene glycol) (OEG)-functionalized alkanethiolate SAMs to adsorption of fibrinogen

from a buffered solution, correlates with the molecular conformation of the OEG moieties.[88,89] They have observed that crystalline helical and amorphous forms of OEG on gold substrates are resistant to adsorption of proteins, while a densely packed "all-trans" form of methoxy-terminated tri(ethylene glycol) present on silver surfaces adsorbs proteins. These observations were compatible with the hypothesis that binding of interfacial water by the OEG moieties is important in their ability to resist protein adsorption.

2.5.2. *Phospholipids and phosphorylcholine SAMs*

Phospholipids are another class of molecules which posses protein resistant properties. In particular phosphorylcholine-derived surfaces have shown improved resistance.[102] Zwitterions having a balanced charge and minimized dipole are excellent candidates as "nonfouling" materials due to their strong hydration capacity via electrostatic interactions. Zwitterionic (oligo)phosphorylcholine (PC) self-assembled monolayers (SAMs) have shown protein resistant properties.[103] Many methods to produce PC-modified surfaces rely on the ability of these molecules to self-assemble just like planar supported lipid bilayers. This can be achieved by vesicle fusion,[116] spin-coating[117] or by Langmuir-Blodgett deposition.[118] The main drawback of this system is its stability. Numerous attempts have been made to improve the binding of the PC-based films including cross-linking the phosphorylcholine chains via diene groups in the alkyl chains,[119] copolymerizing phosphorylcholine methacrylates with other monomers,[120] grafting to plasma-irradiated surfaces,[121] and forming SAMs of phosphorylcholine-terminated alkanethiols onto gold.[122]

2.5.3. *Protein resistant surfaces based on osmolytes*

Surfaces presenting groups derived from certain osmolyte molecules such as self-assembled monolayers based on the kosmotropes are very often show protein-resistant.[123] To the kosmotropes (molecules that exclude themselves from the protein-water interface) belong polyols, betaines,[124,125] taurine, trimethylamine-*N*-oxide, dimethyl acetamide, dimethyl sulfoxide, and hexamethylphosphoramide. Yancey *et al.*[126] and others[123,127] have suggested that it could be beneficial for an osmolyte to be preferentially excluded from the surface of a protein (Figure 2-11). Binding of osmolyte to protein would reduce the activity of the osmolyte in "bulk" solution; the increase in osmotic pressure due to the osmolyte would therefore be smaller than that in the absence of binding. Kane *et al.*[123] have synthesized SAMs which are structurally similar to the osmolytes like betain ($HS(CH_2)_{11}N(CH_3)_2^+CH_2CO_2^-$) and taurine ($HS(CH_2)_{11}N(CH_3)_2^+CH_2CH_2SO_3^-$). After SAMs formation the substrates have been tested for

their resistance towards proteins (fibrinogen and lysozyme). The results showed the connection between protein-resistance, kosmotropicity and biological function as an osmolyte.
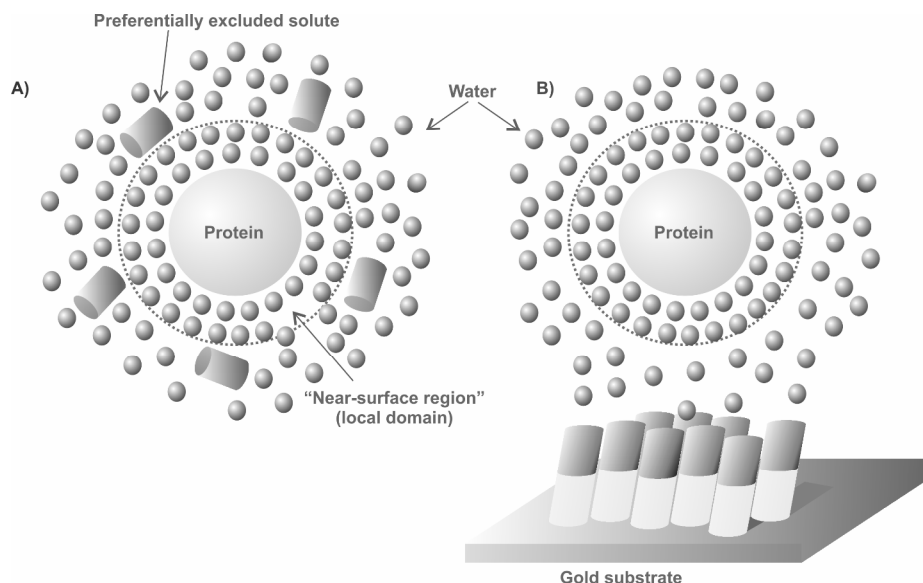
Figure 2-11. Schematic illustration (A) of solute that is completely excluded from the surface of the protein (the local domain),there are no solute-protein contacts, (B) of protein that does not absorb onto a surface, the surface (to which the preferentially excluded solute is attached) is completely excluded from the surface of the protein. Picture adopted from the reference [128].

2.5.4. Bovine serum albumin (BSA)

This protein is commonly used in immunoassays (e.g. ELISA) to block some part of the surface against nonspecific adsorption of other proteins.[129,130] Albumin does not contain any known integrin-binding sequence and this is why it is often used as a cell resistance coating.[131] Patterning BSA on the surface can define areas for attachment or adsorption of a second protein. Immobilization of BSA on the surface can also resist cell adhesion.[132] The coating of BSA was used in patterning using microwells. The interior of wells was covered with ECM protein while the space between the wells was coated with BSA as cell resistant areas. Cells were immobilized only on ECM-modified pattern.[84] The disadvantage of the use of BSA is that this strategy can suffer from problems associated with denaturation of the blocking protein over time or exchange of this protein with others in solution.[133,134]

2.5.5. Polyelectrolyte surfaces

Polyelectrolyte supported multilayers have been shown as a useful, protein- and cell-resistant surfaces. Rubner and coworkers[135] have shown that layer-by-layer, hydrogen-bonded assembly of polyacrylamide and weak polyacids such as poly(acrylic acid) and poly(methacrylic acid) can form a protein and cell resistant coating.[136] These H-bonded multilayers are

hydrogel-like coatings that are capable of a high level of swelling in buffered solutions and are characterized by great stability over time. Similarly, multilayers made of polycation poly(allylamine hydrochlodire) (PAH) and polyanion poly(acrylic acid) (PAA) constructed at pH deposition conditions of 2.0/2.0 were bioinert.[135] These multilayers swell substantially in physiological conditions to present richly hydrated surfaces, resisted towards fibroblast attachment.

2.6. Soft lithography of biomolecules

2.6.1. Microcontact printing – procedure, limitations and applications

Soft lithography[128,137-139] is an emerging method in nanotechnology for micro- and nanofabrication of two- or three-dimensional structures on the surface.[140] This method which was developed by Whitesides and coworkers[128,137-139,141-142] uses elastomeric stamps, molds, and conformable photomasks for creating patterns as small as tens of nanometers on substrates. Depending on the way that molds are used there are different techniques that belong to soft lithography: replica molding (REM), micromolding in capillaries (MIMIC), microtransfer molding (µTM), solvent-assistant microcontact molding (SAMIM) and microcontact printing (µCP).

The great advantage of these techniques lies in the ease and simplicity of their use, which makes it attractive for a wide range of applications. Microcontact printing is one of the simplest methods for fabrication of patterns on a surface. An elastomeric stamp with a chemical ink is contacted with the target substrate and forms a self-assembled monolayer pattern, as in Figure 2-12.
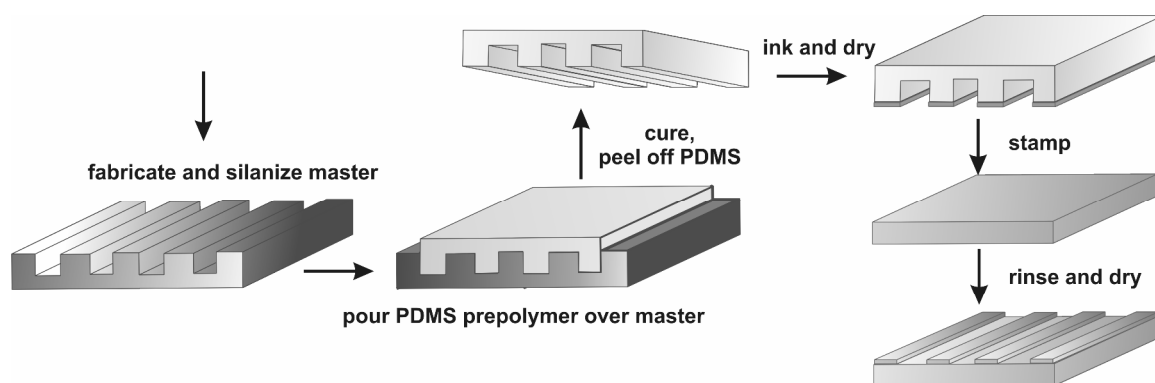

Figure 2-12. Schematic representation of the fabrication of PDMS stamp and process of microcontact printing.

Soft lithography, in particular microcontact printing, relies on the fabrication of a master that is used to produce replicas in an elastomeric polymer. The master can be fabricated by any

technique that is capable of producing well-defined relief structures on a surface. The most commonly used technique for silicon master fabrication is photolithography. Flexible stamps are generated by casting a liquid elastomer, poly(dimethylsiloxane) (PDMS) on the top of the mold and subsequent curing for at least one hour at 60 ˚C. Since the PDMS stamp is flexible, it is important that its pattern is well defined by means of lateral and vertical control of the chemical pattern. The ratio of width to depth of the pattern should be carefully designed so deformations like pairing, buckling or collapsing will be avoided.[143] Another drawback of the PDMS stamps is contamination of low molecular mass unpolymerized alkylsiloxanes coming out from the stamp during the printing process. This problem can be avoided by extraction of the stamp with apolar solvents.[144] Swelling during inking of the stamp can cause pattern enlargement during printing.[145,146] A pattern that is increased in size can also be made by applying too much pressure on the stamp during printing. Furthermore, diffusion of the ink due to the low molecular mass of the ink or too high concentration of the ink, or excess of the ink can affect the quality of the pattern. The diffusion of ink that is bound to the surface non-covalently can also occur.[147] Even though µCP has its limitations in resolution, edge definition and deformation of the stamp as well as diffusion of inks, this technique is still very attractive for printing biomolecules since it is biocompatible and does not influence on damage the molecule. Biomolecules generally have a higher molecular mass which limits diffusion of molecules during the printing process.

The surface of the PDMS stamp can be tailored by depositing other layers e.g. functional silanes, to transfer the ink to the surface with higher yield and better compatibility. The surface chemistry plays important role since it can attract, bind or adhere the ink molecules.[138, 148]

Although µCP was initially used for printing alkylthiols on gold substrates[138] this method was extended to alkylsiloxanes on glass and silicon oxide surfaces which resulted in additional applications in the biotechnology field such as patterned surfaces for local cell immobilizations, fabrication of microarrays or for biosensor and microfluidic purposes.

The scope of ink molecules have been broadened from alkylthiols and alkylsiloxanes to various particles, inorganic inks, organic molecules such as dendrimers,[62] peptides,[149] proteins,[150] or DNA.[151,152]

2.6.2. Microcontact printing of biomolecules on glass and gold surfaces

Transfer of biomolecules from the stamp to the substrate by microcontact printing, generally depends on how the surfaces of the stamp and the substrate are chemically, physically or biochemically modified. The simplest µCP approach for patterning of biomolecules relies on

the direct transfer of the ink molecules, which are adsorbed on the stamp, to a target surface by conformal contact. Nevertheless, depending on the properties of the biomolecule, the surface of the stamp needs to be modified in terms of wettability, charge distribution, introduction of reactive groups etc. Generally biomolecules such as proteins, lipids or oligonucleotides are suitable for µCP due to their large molecular weight which helps in formation of well-defined, high-contrast patterns since the diffusion is limited.

In terms of printing of biomolecules, there are several important factors that have to be taken into consideration. The affinity of the biomolecule to stamp and to substrate must be tailored so that it is higher for the substrate than for the stamp. The binding of the biomolecule should not cause denaturation (if applied, e.g. in case of proteins) therefore should not affect the secondary or tertiary structure that can cause the unfolding of the molecule. The biomolecule should be attached to the substrate in the way that it will expose all the active sites on the surface to the target molecules.

Surface modification of PDMS stamps plays an important role in transfer and printing of biological material. Although the mechanism behind protein transfer by microcontact printing is not totally understood, Tan *et al.* have demonstrated that both stamp and substrate wettability is crucial for biomolecule transport. They showed that a minimum wettability of the substrate is required for successful µCP of proteins, and this minimum wettability can be decreased if the wettability of the stamp is decreased. Their findings also revealed that the mechanism of µCP of protein is different from protein adsorption in the meaning that (i) surfaces that are resistant to protein adsorption in aqueous environment are susceptible to µCP under ambient conditions and (ii) the amount of immobilized proteins and the wettability of the substrate varies gradually for the adsorption process but transitions at a threshold wettability for the µCP process.[153] It was shown in the literature that many proteins (e.g. IgG) readily adsorb to uncharged PDMS surfaces through van der Waals interactions under physiological conditions even though electrostatic interactions can play a more important role at lower ionic strengths on charged surfaces.[154] Applied strategies of pattern formation of proteins or other biomolecules on surfaces relies on: inking of the non-modified stamp with biomolecule solution, incubation, drying the stamp and bringing the stamp into conformal contact with the (modified) substrate.[154,155] Bernard *et al.* pioneered work on direct transfer of proteins from non-modified PDMS stamps to a target glass surface resulting in patterns with high surface coverage (Figure 2-13).[129,156]
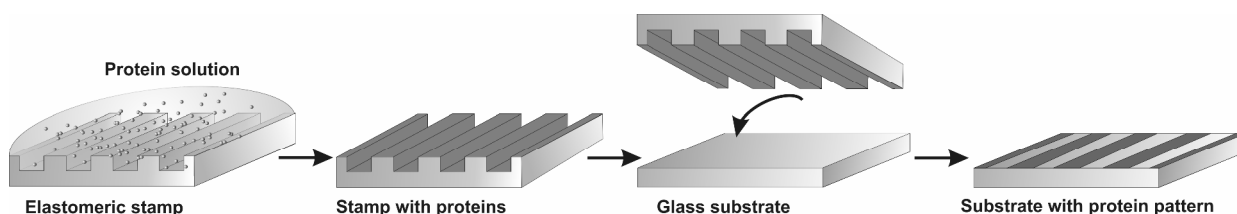
Figure 2-13. Schematic representation of microcontact printing of proteins. First, a protein solution is incubated on the top of an elastomeric stamp. After drying, the stamp is brought into conformal contact with the glass substrate and transfer of proteins occurs only in the places of contact between the stamp and the substrate.[129]

BSA proteins adsorb readily from solution to hydrophobic surfaces including PDMS and can be easily printed on different types of modified surfaces. For instance, Ross *et al.* printed BSA from non-modified PDMS stamp to substrate modified with planar supported lipid bilayer (poly(bis-SorbPC)).[157] The deposition of proteins by μCP was demonstrated on different types of substrates including oxides, metals and polymers.[129,158] The concept of direct microcontact printing of protein onto a glass substrate via non-modified PDMS stamps was further extended to the fabrication of single protein molecules such as antibodies (e.g. IgG) and green fluorescent proteins (GFPs) on glass surface.[158] Gold binding polypeptide is an interesting example of a protein that is applicable in direct μCP on gold surfaces. This protein does not contain cysteine residues which are generally known to form a covalent bond with gold. The binding of this protein is independent of thiol linkages and offers therefore a new way of interaction between the biomolecule and the surface. GBP-EGFP-6His fusion protein was printed directly onto a gold surface in a mixture with BSA, Tween 20, sodium phosphate and NaCl. The protein was immobilized by chemisorption onto the substrate and later applied for high throuput assays of protein-protein as well as DNA-DNA interactions in microfluidic devices.[159] Kwak *et al.* patterned cytochrome C onto gold surfaces using a non-modified PDMS stamp.[160] Since cytochrome C has the ability to transfer an electron, this protein is often used in studies on biomolecular photodiode systems. Cytochrome C was used as an ink to wet the surface of PDMS stamps and the protein arrays were directly transferred from the stamp to a carboxyl-terminated SAM (16-mercaptohexadecanoic acid, MHA) on gold. After successive washing with detergent and water the pattern of protein stayed intact on the surface. Active enzymes were also successfully patterned using SAMs on gold surfaces.[161] Metalloprotein (azurin) was printed on the glass substrate modified with mercaptosilane that allows a site-specific binding of

the protein. The pattern was assessed by immunofluorescent experiments with anti-Az serum.[162]

The hydrophobic nature of the PDMS stamp can be adjusted by oxidation in O_2-plasma, which produces a thin, glassy silicate layer on the stamp. This layer is usually brittle and loses its hydrophilic character unless the stamp is kept under water.[79] Another method for changing the surface properties of the stamp is modification with siloxanes e.g. APTES or poly(ethylene glycol) siloxane. Polylysine was microcontact printed on a clean, non-modified glass surfaces via an oxidized PDMS stamp using electrostatic interactions between the positively charged polypeptide and the negatively charged glass surface.[163]

Other biomolecules that are of interest in microcontact printing are lipids and lipid bilayers. Supported lipid bilayers are very fragile assemblies that are formed by lipids that are organized into two opposing leaflets on hydrophilic surfaces, such as glass or mica substrates. These structures can be also patterned on the surface but the microcontact printing technique slightly differs form the ones that were applied for proteins or DNA. Firstly, the bilayer has to be formed on the oxidized PDMS stamp from the buffer solution by lipid vesicle fusion. Secondly, the printing has to be carried out in water otherwise the bilayer will lose its structure.[164] This method allows efficient and reliable transfer of membrane patches to glass surfaces.

The non-covalent adsorption of proteins by μCP is experimentally simple, and suffers from the disadvantage that the attachment can be reversible by rinsing the pattern with certain buffers and detergents or replaced by other proteins in solution. Moreover, the orientation of the deposited protein is not controlled.

Delamarche *et al.* proposed the use of the stamps modified with poly(ethylene oxide) silanes.[165] The modification was conducted by oxidation of the PDMS stamp and reaction with 3-aminopropyltriethoxysilane to yield an amino-functionalized surface. The next step was the reaction with cross-linker, bis(sulfosuccinimidyl)suberate (BS^3), to bind surface amino groups with PEG chains (Figure 2-14).
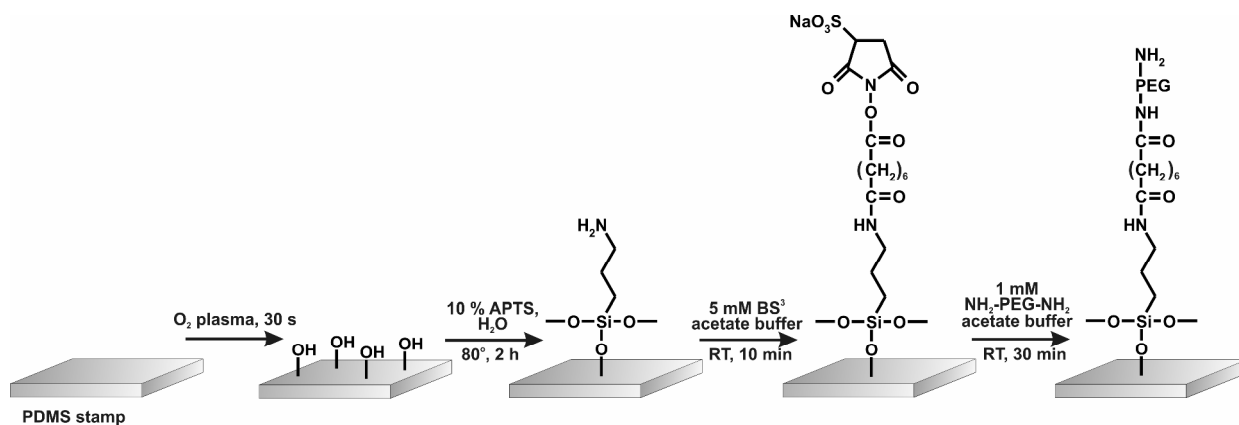
Figure 2-14. Modification of a PDMS stamp for microcontact printing of polar inks. Oxidized PDMS stamp is reacted with 3-aminopropyltriethoxysilane and subsequently with BS³. In the last step the stamp is reacted with poly(ethylene glycol).

When poly(ethylene oxide) silane (PEO) was grafted onto oxidized PDMS stamps it can act as a protein repellent layer. This property was utilized to design a flat stamp with regions that can attract proteins (non-modified PDMS) and regions modified with PEO that have protein-repellent properties. The local modification of native PDMS was conducted by oxidation in O_2-plasma with the application of metal mask (areas that were covered by the mask were not oxidized and not modified). Proteins (IgG) were successfully transferred to the glass substrates and immobilized in well-defined pattern with high accuracy and contrast. When proteins are applied to such a stamp they are directed to the hydrophobic parts of the stamp. A different approach has also been presented. When the PEO-modified stamp (according to procedure mentioned above) is contacted with another flat, dry, non-modified PDMS stamp (inker pad) that was incubated with IgG buffer solution, a homogeneous layer of proteins is transferred to the PEO regions of the other stamp. This stamp can be subsequently contacted with glass substrate and used to pattern IgG proteins.

An additional example where the modification of the stamp surface was an important factor is microcontact printing of DNA molecules.[151] To attract DNA molecules to the stamp, the surface of that stamp was modified with APTES resulting in positively charged amino group functionalization. In that experiment, electrostatic interactions play an important role in transfer and delivery of DNA (considering DNA as a negatively charged polyelectrolyte). A different approach to pattern DNA molecules on the surface was proposed by Xu *et al*. DNA-surfactant molecules were prepared by attaching a hydrophobic alkyl chain to the 3' or 5' end.[152] The hydrophobic tail allows for the appropriate adsorption to the hydrophobic PDMS stamp. This method allows for efficient transfer and delivery of DNA to the surface.

Another way to overcome problems with wettability and compatibility with aqueous solutions of PDMS stamp is simply to use other material for fabrication of the stamp. There are many approaches and many examples have been presented in the literature but two of them were very successful. Agarose stamps introduced by Grzybowski and coworkers[166] are highly suitable as a mold for transferring water soluble biomolecules due their high permeability to water. Multiple stamping is possible without the need for intermediate re-inking of the stamp. Spencer introduced polyolefin plastomers (POPs) as a stamp material for microcontact printing of proteins (fibrinogen and poly-L-lysine-*g*-poly(ethylene glycol).[167] By using POP elastomer a higher resolution of the printed pattern can be achieved and also possible contamination from the stamp (which sometimes can be observed in case of PDMS stamp) does not occur.

Flat PDMS stamps can be substituted for PDMS stamps possessing protruding features.[168] The method was presented by Geissler *et al.* and it showed improved contrast and resolution of pattern. The technique relies on introducing a pattern to the flat stamp by contacting with another PDMS stamp (with features) (Figure 2-15) or by using microfluidic networks or microwells (see Chapter 2.6.5). Subsequently, the patterned flat stamp can be contacted with glass or another substrate to transfer the pattern. This method can be specifically applied for high molecular weight inks.

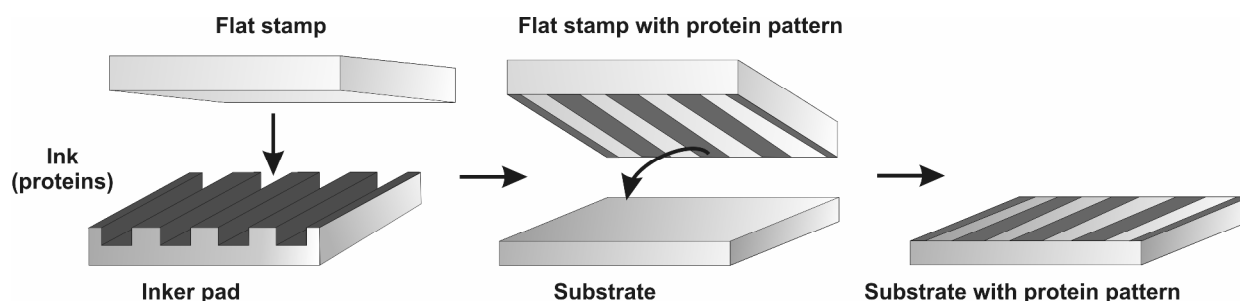Figure 2-15. Modification of flat PDMS stamp for pattern transfer application. (The illustration was adopted from the reference [168]).

2.6.3. Covalent microcontact printing

Microcontact printing was not only used to position (bio)molecules on the surface but also to synthesize them on planar supports.[169-171] Huck *et al.* introduced peptide synthesis by microcontact printing (Figure 2-16).[149]
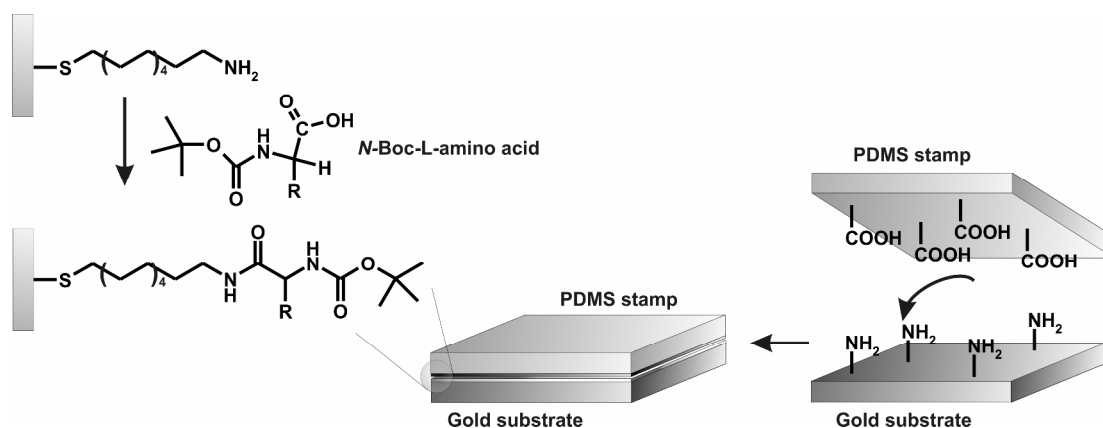
Figure 2-16. Peptide synthesis by microcontact printing. An oxidized PDMS stamp is inked with an *N*-Boc-L-amino acid and pressed into a contact against an amino-functionalized gold substrate to yield new, covalent, amide bond. Boc = tert-butoxycarbonyl.[149]

The authors used an oxidized, hydrophilic PDMS stamp inked with a solution of {2-[2-(Fmoc-amino)ethoxy]ethoxy}acetic acid to activate an amino-functionalized surface. In the second step the elastomeric stamp was inked with Boc-protected amino acid and brought into conformal contact with activated surface to form a covalent amide bond without the use of a catalyst. Similarly 20-mer peptide nucleic acid (PNA) was synthesized by printing commercially available nucleotides in 20 steps by using the same activation cycle. PNA strand was finally hybridized with complementary and non-complementary DNA.[149]

Another example where the PDMS stamp was used as a tool to locally transfer and covalently bind molecules was reported by Wilhelm and Wittstock.[161] Enzyme glucose oxidase (GOx) was mixed together with a coupling agent (EDAC, *N*-(3-dimethylaminopropyl)-*N*-ethylcarbodiimide hydrochloride) in PBS buffer and printed directly onto amino-terminated glass substrate. During contact time the activated enzyme was allowed to react covalently with amino-terminated monolayer on the glass. The activity of immobilized enzyme was confirmed by scanning electrochemical microscopy (SECM) measurements.

Using a pattern of two different types of biomolecules on the surface, it is possible to tailor the surface containing regions that are cell adhesive and cell resistant. Feng *et al*. showed that by covalent µCP of chitosan onto aldehyde-enriched glass surface followed by incubation in BSA solution, the surface will have properties of cell localization and cell growth guidance.[172] Matthews and coworkers[16] used covalent µCP for the attachment of glycosaminoglycan (GAG) polysaccharides and heparin sulfate proteoglycan. The GAG solution was mixed with a reducing agent (NaBH$_3$CN) and used as an ink. The ink was incubated on a non-modified PDMS stamp and printed onto amino-functionalized glass substrate. Similarly, a solution of heparan sulfate

proteoglycans was mixed with heterobifunctional cross-linker (BS^3) and incubated on a hydrophilic oxPDMS stamp. Finally, the stamp was contacted with an APTES modified glass slide to immobilize heparan covalently.

2.6.4. Affinity contact printing

Affinity contact printing (αCP)[168,173,174] relies on inking the surface of the PDMS stamp with antibodies as "capture molecules" which allows subsequent binding of selective proteins from a solution containing mixtures of proteins (Figure 2-17). Affinity stamps were prepared by modification of the PDMS stamp with aminosilanes following the reaction with a homobifunctional cross-linker (BS^3) to produce the activated, hydrophilic surface. This activated stamp was used to couple proteins to small areas using (i) microwells, (ii) microfluidic networks and (iii) μCP. Using one of these methods, a PDMS stamp was patterned with proteins and transferred to another activated PDMS to bind the biomolecules specifically and covalently. Repeating this procedure with a different type of protein, the stamp could be fabricated with multiple components which is valuable for microarray applications. When several types of antigens are immobilized on an activated stamp they can be further exposed to a solution of different antibodies to extract and immobilize a "matching partner". The captured antibodies can be then printed onto a glass substrate forming new microarrays of antibodies.
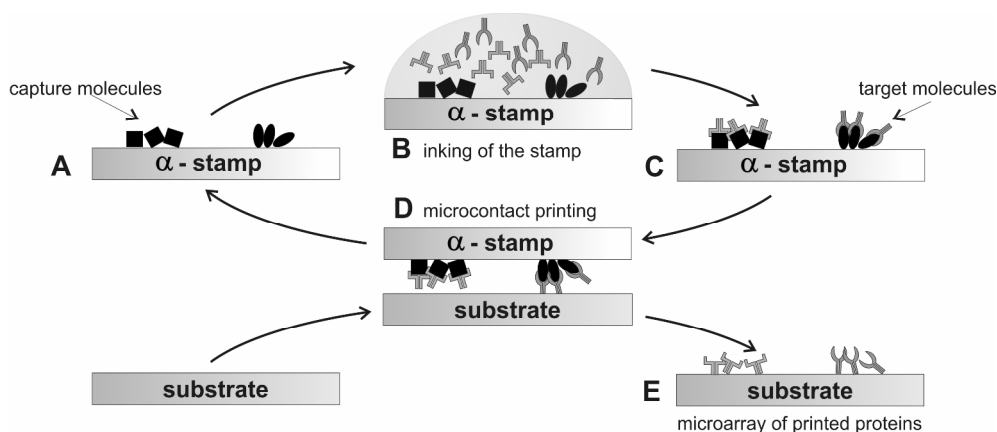
Figure 2-17. Affinity contact printing. Illustration adopted form the reference [173].

A different example of affinity contact printing was shown by Jang *et al*.[175] This multi-step approach relies on modification of a PDMS stamp with aminosilanes and succinic anhydride to introduce carboxylic acid groups on the surface, followed by covalent immobilization of monoclonal antibody to epidermal growth factor receptor (EGFR). The EGFR modified stamp was subsequently incubated with a solution of membrane proteins from cell membrane extracts and crude cell lysates. Finally, the stamp was contacted with the gold substrate that was

modified with an amino-terminated monolayer with nematic liquid crystals (LCs) of 4-cyano-4'-pentylbiphenyl (5CB) through hydrogen bonding. The advantage of that system is that the micrometer-thick film of LCs can assume orientations on the amino-terminated surface which is different from regions of a surface presenting EGFR, providing a facile means to amplify and optically detect the presence of the EGFR on the surface. This method does not require matching pairs of antibodies or fluorescent labels on proteins. Similarly, the group of Abbott used affinity contact printing to immobilize proteins that subsequently can be imaged with liquid crystals.[176] The approach relies on covalent modification of PDMS stamp with biotinylated bovine serum albumin. The BSA-functionalized stamp was inked with anti-biotin IgG and brought into conformal contact with amino-modified gold surface. After stamping, the protein pattern was imaged by placement of liquid crystals on the surface.

2.6.5. Patterning of biomolecules via microchannels and microwells

To overcome the limitation related to microcontact printing like for instance, low surface density of immobilized biomolecules (specially on polymeric surfaces), due to the small amount of reactant absorbed on the stamp, Hyun *et al*. developed a new patterning technique using elastomeric microwells.[177] This method relies on fabrication of hydrophilic μwells in a PDMS stamp. Oxidation of the PDMS stamp, modification of the stamp areas between the wells with hydrophobic monolayers (hexadecanethiol), inking the stamp with protein solution that goes directly into hydrophilic wells avoiding hydrophobic areas, drying the stamp, and printing the pattern onto the target substrate (Figure 2-18). A cell-adhesive peptide was covalently printed on NHS-ester-functionalized poly(ethylene terephthalate) substrates.
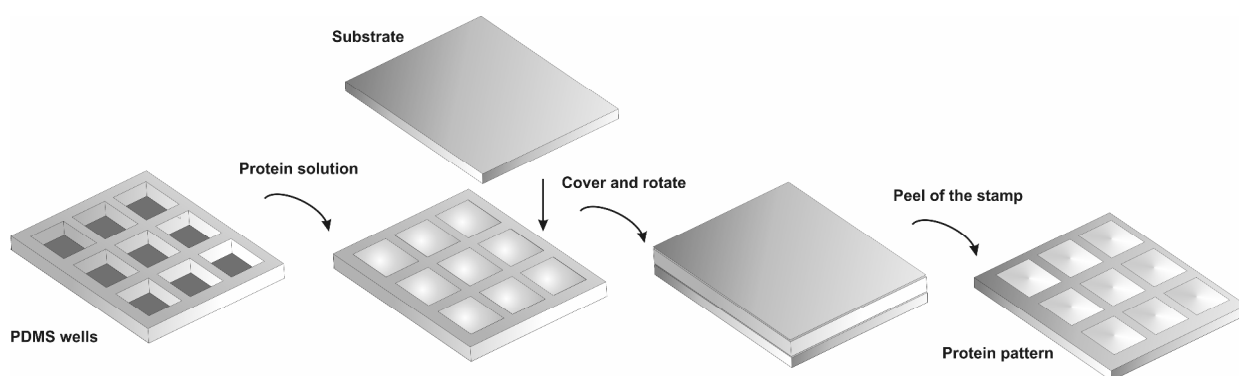
Figure 2-18. Micropatterning of biological molecules on a polymer surface using elastomeric microwells.

Similarly, substrates can be patterned with biomolecules by means of a microfluidic network (μFN).[178] Bernard *et al*. presented patterns of antigen made by flow of solution in a microfluidic network. After a blocking step with BSA, the solution with antibodies was delivered in a second μFN across the pattern of antigens.[179] Binding between antigen and

antibody resulted in a pattern from cross-reacted zones. This method has many advantages like high density parallel patterns that are precise and well defined due to the fact that microfluidic networks have high resolution and high-contrast capabilities.

Microcontact printing of proteins was also combined with microfluidic networks (MFNs) by stamping fluorescently labeled antibodies inside microstructures (independent microchannels) coated with Au and a thiolated poly(ethylene glycol) (HS-PEG).[180] The modified, hydrophilic channels repel proteins from solution but promote their transfer from a stamp during printing. Such patterned channels might find application in miniaturization of fluorescence surface immunoassays for in vitro diagnostics, drug discovery or environmental monitoring. Similarly, Geissler *et al*. used IgGs proteins to locally deposit them from the solution onto planar PDMS by microfluidic networks (µFNs).[168] Subsequently, the PDMS stamp was brought into conformal contact with a clean (non-modified) glass substrate. The proteins were chemisorbed onto this support in a well-defined manner and the pattern had high contrast and resolution. The same protein (IgG) was efficiently microcontact printed when the substrate was more hydrophilic than the PDMS stamp whose surfaces were modified with –CF_3 or –NH_2 functionalities.[153]

Whitesides and coworkers combined microfluidic networks with a PDMS platform to create patterned, gradients of biomolecules on the surface.[181] This method involves a two-step process: (i) formation of gradient of avidin within well-defined patterns by use of microfluidic channels and (ii) specific interaction between the avidin gradient pattern and biotin. Such patterns with a density gradient of immobilized biomolecules may find application in studies on cell development and function.

2.7.   Spotting of biomolecules

In the microarray industry the most commonly used technique to pattern biologically active molecules is ink-jet or contact printing technology. In general, these methods can fabricate biochips of thousands different compounds, which can be analyzed simultaneously. The most commonly spotted biomolecules include oligonucleotides, proteins, peptides and carbohydrates.

Microarray-based platforms have been commonly used in sequencing, single polymorphism (SNP) detection, characterization of protein-DNA interactions, screening antigen-antibody and carbohydrate-protein interactions, detection of biomarkers, in disease proteomics, and others. Various robotic systems deposit biomolecules into an accurately designed grid made of spots with an average size of 100 µm.

2.7.1. Contact printing

Contact printing relies on dispensing pico- or nanoliters of a biomolecule solution from a set of metallic pins which physically contact the substrate onto which the biomolecules should be immobilized (Figure 2-19).
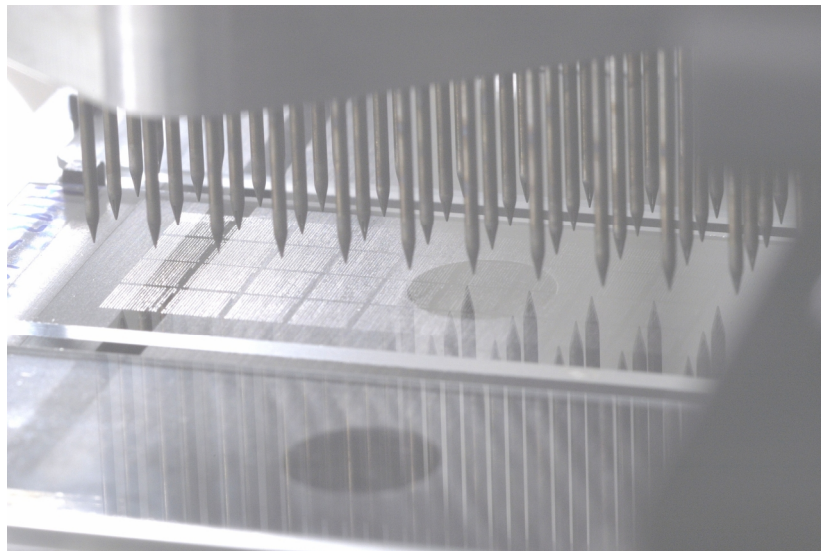
Figure 2-19. Set of pins built within a print head for contact printing in microarrays applications. (Image courtesy of The Netherlands Cancer Institute, W. Brugman).

A defined probe-volume is loaded into the pin cavity via capillary forces. Small drops of biomolecule solution are deposited by surface tapping (Figure 2-20). Pins for contact printing are available in a wide assortment of tip and channel sizes. Tip size determines a spot size and the smaller the tip the smaller is spot. The smallest tip size that is currently commercially available is 50 µm in diameter and can produce spots about 65 µm in diameter with the sample channel size from 0.25 µL to 1.25 µL. Usually the spot size is approximately 30 % larger than the diameter of the tip capillary with the standard sample channel of 0.25 µL. The advantage of this system is that the drop is placed in exactly defined position on the substrate; there are no shifts of the drop which is very often observed in non-contact methods. The disadvantage of this system is that pins while contacting the substrate may damage the coating of the slide.
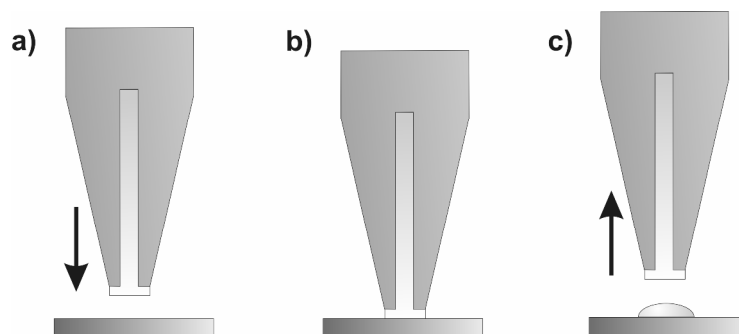
Figure 2-20. Printing mechanism based on surface tension and adhesion. Sample is first loaded into a sample channel by capillary action. The horizontal terminus of the tip ensures that a thin layer of a sample solution is cumulated at the end of the tip. The loaded tip contacts the printing surface depositing a droplet between the substrate and the pin. After the contact time (0.05 s) the pin is retracted, and the droplet is held by strong adhesive forces of the substrate.

2.7.2. Ink-jet printing

Ink-jet printing is a non-contact method; the sample solution is dispensed without direct contact between the print head and the substrate. In modern ink-jet technology a piezoelectric print head is used for printing the arrays. The print head contains a set of nozzles in a linear arrangement controlled by a computer which directs them where to deposit ink, how much to use and which biomolecules to spot. The nozzles can be employed in subsets for printing microarrays of variety of sample types. There many different types of nozzles such as piezoelectric, bubble-generated (thermal printers) or microsolenoid driven. The volume of the dispensed drops is usually of 100 pL, which depending on the buffer and the surface chemistry of the substrate, produces spots of size 90-120 μm in diameter. Ink-jet technology is especially suitable for protein microarrays since proteins are very fragile and this method is less invasive than contact printing. The disadvantage of this method is the accuracy of drop positioning and delivery. Ink-jet methods can be used to print DNA, proteins, cells and other biomolecules.

2.8. Scanning probe lithography of biomolecules on gold and glass/SiO$_2$ surfaces

One of the challenges in the microarray technology is the spot size, spot density on the substrate and miniaturization in the form of nanoarrys that could allow fitting much more genes or proteins on one chip. Diverse methods including dip-pen nanolithography (DPN), nanografting, nanoshaving, focus ion beam lithography have been developed to fabricate nanoscale patterns of biomolecules on the surface. Dip-pen nanolithography is a promising tool that has perspectives to generate massive, parallel biomolecule arrays in nanoscale regime.

2.8.1. Dip-pen nanolithography

Dip-pen nanolithography (DPN) is a scanning-based lithography method[182,183] for fabrication of nanometer-size patterns where the AFM tip is used to transport and deliver ink containing chemical reagents to the target surface (Figure 2-21).[184]

AFM tip

Material transfer

Scan direction

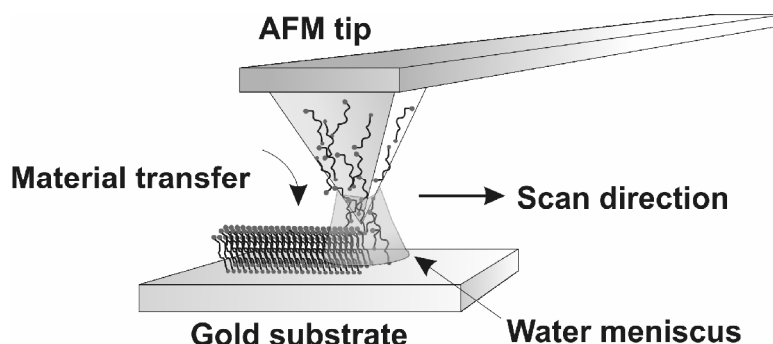**Gold substrate**   **Water meniscus**

Figure 2-21. Dip-pen nanolithography; the ink (thiols) is transferred from the tip to the gold substrate through water meniscus between the tip and the substrate according to the direction of scan.

This technique was initially used to pattern gold surfaces with octadecanethiol (ODT) or 16-mercaptohexadecanoic acid (MHA) and the pattern was used as a etch resists to produce both metal and semiconductor nanostructures. Later the technique was expanded to a variety of inks (i.e. oligonucleotides,[62] proteins,[185,186] silanes,[187,188] colloidal particles[189]) and substrates (polymers, glass, silicon oxide).

The minimal size of the features that can be generated by this method is in the sub-100 nm range. There are many factors like humidity, set-point, tip modification, the chemistry involved in binding between ink and the substrates, chemical purity of ink, tip and the substrate, tip shape and size, properties of ink and the substrate that play an important role in a successful pattern formation by DPN.

Humidity is a critical factor that should be taken into account when DPN is used to pattern biomolecules.[76] For instance, protein patterning was conducted with a relative humidity of 80-90 % at room temperature. Very often these experiments are conducted in glove box or environmental chamber to control the humidity. Another important factor controlling the transport of ink molecules from the tip to the surface is the set-point since large set-points can lead to larger features and contact area.[190] The transport of the ink to the substrate is a complex process that depends on many, above mentioned factors. This transport occurs through the meniscus of water which is condensed between the tip and the surface. The water meniscus seems to influence the transport of the ink strongly and this is the reason why humidity control and water solubility of ink is crucial in successful delivery of molecules.[184]

DPN was applied for fabrication of DNA patterns on gold and silicon oxide surfaces.[62,191] For the successful transfer and delivery of oligonucleotides, the AFM silicon nitride tip was modified with aminosilanes which promotes adhesion of the negatively charged DNA ink to the tip surface. When gold substrates were patterned, thiol-modified DNA was used as an ink. After drawing an array of DNA spots the remaining bare gold area was passivated with hydrophobic octadecanethiol. The same tip inked with 5-acrylamide-modified DNA can be used to pattern silicon oxide substrates activated with mercaptopropyltrimethoxysilane (MPTMS). The acrylamide moieties can react with thiol groups from the substrate by Michael addition to link covalently DNA molecules. After patterning the substrate, the remaining thiols groups can be blocked with acrylic acid monomer. The biological activity of immobilized DNA can be investigated by subsequent hybridization with fluorescently labeled complementary and non-complementary oligonucleotides. Another experiment relied on the employment of the DPN combined with wet etching techniques to generate arrays of gold nanostructures that were functionalized with oligonucleotide.[192] The fabrication of the gold nanostructure arrays was conducted by drawing 16-mercaptohexadecanoic acid patterns by DPN on a gold surface which served as etch-resistant layer, etching the remaining gold areas, passivating exposed silicon oxide areas with octadecyltrimethoxysilane and removing the alkanethiol layer from the remaining gold regions by photooxidiation of the substrate with a UV lamp. The final step involved immobilization of disulfide-modified oligonucleotides

A different approach has been proposed to generate protein patterns by DPN.[76] Since proteins can adsorb spontaneously to the gold surface, the gold AFM cantilever was first protected by the deposition of 11-mercaptoundecylpenta(ethylene glycol)disulfide (PEG-SH) in order to preserve the reflective properties of Au. The subsequent step involved coating of the AFM tip with gold and reaction with thioctic acid to obtain a hydrophilic, carboxylic acid functionalized surface which facilitates protein adsorption. The tip was consequently covered with proteins (lysozyme and rabbit immunoglobin-gamma). The experiment was carried out at 80-90 % relative humidity at room temperature. The writing process was carried out directly on gold surfaces since cysteine residues in proteins possess strong affinity to gold. After patterning the gold regions surrounding the pattern were reacted with PEG-SH to form a protein-resistant layer. A similar experiment was also carried out on modified silicon oxide surface.[190] To transfer successfully antirabbit immunoglobulin G (IgG) and other proteins, the AFM tip was modified with 2-[methoxypoly(ethyleneoxy)propyl]trimethoxysilane (Si-PEG) to make the tip surface hydrophilic and biocompatible (Figure 2-22).
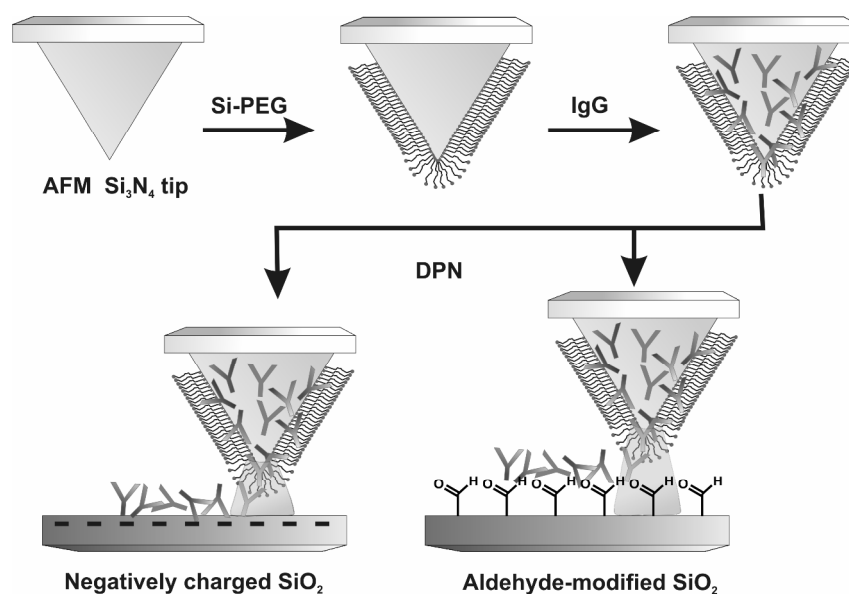
Figure 2-22. Schematic representation of DPN of protein IgG. The pattern formation can be conducted by two methods, using negatively charged SiO_2 or aldehyde-modified SiO_2.[190]

This modification also causes inhibition of protein adsorption, allowing the proteins to be transferred from the tip to the target surface. To immobilize the proteins two surfaces were chosen, negatively charged silicon obtained by treatment with base and aldehyde-terminated silicon. In the first case, the proteins can be attached by electrostatic interactions between the positively charged parts of the protein and the negatively charged surface. In the second case, the proteins can be attached covalently to the aldehyde-modified surface by reaction between amino groups from the lysine residues on α-amines at N termini in the proteins and aldehyde surface groups, resulting in the formation of Schiff bases. To expand the array to multiple components, two different fluorophore-labeled proteins antirabbit IgG and antihuman IgG were deposited on aldehyde-modified silicon oxide surface by DPN in a serial fashion.

Considering the affinity between metal ions (i.e. Zn^{II}, Cu^{II}, Ni^{II}, Co^{II}) and proteins another method to pattern proteins on gold surfaces by DPN was developed.[193] This method utilizes Zn^{II} ions ($Zn(NO_3)_2 \cdot 6H_2O$) that can be coordinated with 16-mercaptohexadecanoic acid (MHA), which can be patterned on gold by AFM tip after passivation of the remaining gold areas with PEG-SH. The zinc-modified features can be subsequently reacted with the desired antibody. Biorecognition properties can be further studied by interaction with other proteins.

More complex biomolecules were used to generate patterns on gold surfaces by DPN. Tabacco mosaic virus (TMV) patterns were fabricated by following method. First, patterns of 16-mercaptohexadecanoic acid on gold were fabricated using DPN.[194] The remaining gold areas were reacted with PEG-SH to minimize nonspecific binding of the virus particles to the unpatterned regions. To bridge the virus particles and patterned carboxylic groups from the

surface, Zn^{2+} ions were added to the substrate and TMV particles were then immobilized. The protein coat of virus has metal-binding groups for Zn^{2+} and other metals and this finding was utilized to immobilize these particles to the patterned surface. The TMV attachment was confirmed by the highly specific reaction with antiserum TMV, which by binding to the virus particles increase the height of each virus.

2.8.2. *Parallel dip-pen nanolithography for immobilization of biologically active molecules*

"Classic" dip-pen nanolithography (DPN), which involves just one tip for writing, is not a high-speed and efficient method in patterning over large, centimeter areas. Parallelization of writing process is an essential issue for enhancing the acceleration of the ink deposition process. The major challenges in performing parallel-probe lithography include the simultaneous engagement of tips to the surface and also fabrication of large arrays of sharp tips, control over tip feedback, introducing wide variety of inks to the array and characterization of drawn features.[195-197]

Fifty-five thousand pens, writing simultaneously at the same time, have been used to draw patterns in the nanometer regime on the substrates (Figure 2-23).[198] This setup can generate 88 million features (dots) with a diameter of 100 ± 20 nm spaced by 400 nm and was used to write patterns of 1-octadecnathiol and 1-mercaptohexadecanoic acid.
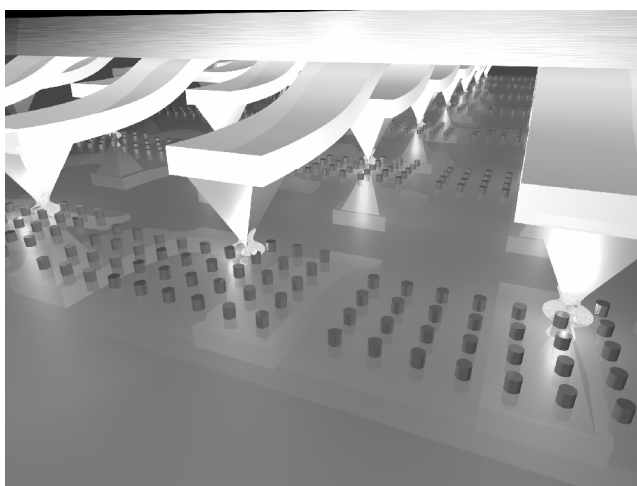
Figure 2-23. Massively parallel DPN with 2D cantilever array. Picture adopted from reference [198] by the permission of Rafael A. Vega.

The array of 55 000 tips was also used to simultaneously generate phospholipids (1,2-dioleoyl-sn-gycero-3-phosphocholine, DOPC) patterns over a surface area of 1 cm^2.[199] Parallel DPN patterning was used in an indirect approach to generate templates on the surface for protein immobilization.[200] Smaller pen arrays were also used to design diverse patterns. A

26-pen array was applied to draw dot features of reactive 11-mercaptoundecanoyyl-*N*-hydroxyysuccinimide ester on a gold surface. After drawing an array of $NHSC_{11}SH$ dots on a gold surface, the substrate was passivated with 11-mercaptoundecyltri(ethylene glycol) and reacted with protein A/G that was selectively immobilized only on the dot areas that were written by DPN through covalent coupling. To extend this method to antibody-based arrays, the substrate with patterns of A/G proteins was reacted with human IgG antibody. The biological activity of that array was presented by the reaction with antigen (*β*-galactosidase and ubiquitin).

2.8.3. Hybrid dip-pen nanolithography

Conventional silicon nitride tips used in dip-pen nanolithography can poorly absorb chemical "inks". This can be detected since during writing process in DPN the spreading out of ink is commonly observed. To enhance the ink absorption to the tip surface two important factors should be considered: (i) tip coating or fabrication of a tip from the material with better absorption than Si_3N_4, and (ii) ink-diffusion from the tip to the surface.

Wang *et al.* have developed a new tip made entirely of poly(dimethylsiloxane) to write efficiently patterns using octadecanethiol ink.[201] This method is called "scanning probe contact printing" (SP-CP) offers the advantages of the microcontact printing and dip-pen nanolithography to generate monolayer features chemisorbed on a gold surface in sub-micron scale. To overcome the limitation related to AFM feedback control and performance due to the non-reflective PDMS material, an improved method of SP-CP was developed.[202] A clean, Si_3N_4 tip was immersed in liquid PDMS in the inkwell to coat the tip with the polymer using an AFM to control the movement of the tip (Figure 2-24).
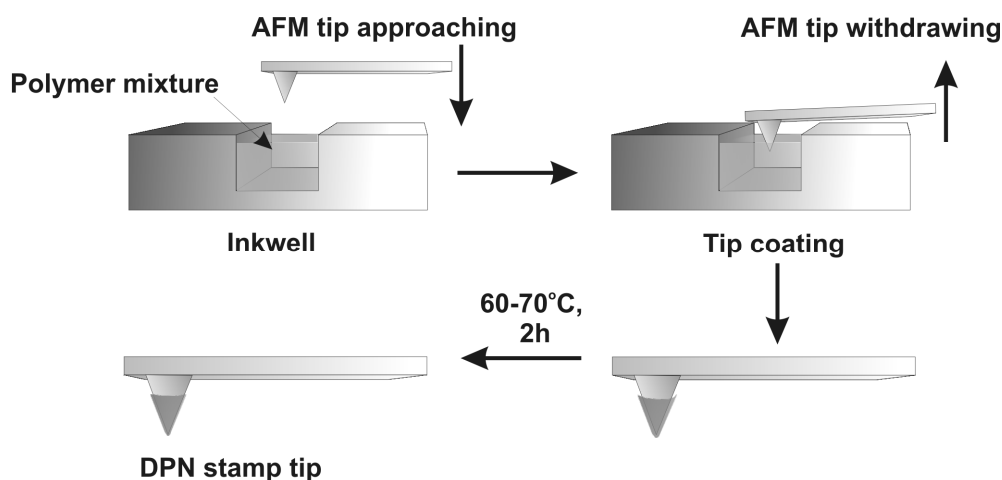

Figure 2-24. Process for fabricating a DPN stamp-tip.[202]

The PDMS coating acts as an ink reservoir that easily absorbs different types of ink. This tip is biocompatible with proteins, oligonucleotides and other biomolecules. Different patterns can be generated including hollow dots and lines, using stamp-tip and the minimum width of the features can reach sub-100 nm. The stamp-tip can serve not only as a tool to create nanopatterns but also to image the generated patterns.

2.9. Concluding remarks

With the increasing interest in DNA and protein microarrays, biosensors, cell-surface studies, implant technology, biocompatibility studies, different systems and strategies for the immobilization and patterning of biomolecules have been developed and some have become well established. A wide diversity of chemical methods for probe immobilization is implemented by different laboratories. Often the choice of the method is a compromise between the effectiveness, cost and technology. In consideration of stability and durability of attached biomolecules certainly, the covalent attachment has to be preferred.

Microcontact printing and its variations is a useful tool in generation of biomolecule patterns. The applications of biomolecular patterns can be found in many areas of (bio)nanotechnology, molecular biology, cell engineering, microarrays and others. The most efficient printing would be achieved when the ink could form covalent bonds with the reactive support and when the stamp would have an array of different molecules introduced so each stamping would results is replication of array of biomolecules and not only one ink. An attractive solution seems to be the combination of microcontact printing with microfluidic systems where many inks can be introduce in parallel to the stamp although the density of channels and the conformal contact with the substrate is limited and can be an obstacle in achieving high diversity of molecules.

The surface synthesis under PDMS stamp confinement opened up the opportunity of conducting the reactions much faster on the surface than in the solution, and preferably without the use of a catalyst.

To decrease the size of the pattern on the surface, dip-pen nanolithography can offer plenty of possibilities. The newest technology from NanoInk Inc. introduced fifty-five thousand tip pens working in parallel which can create 88 million features on 1 cm^2 area. The biggest challenge still remains in this field: to introduce additionally fifty-five thousand different inks to the array of tips.

2.10. References

[1]   C. Heise, F. F. Bier, *Top Curr. Chem.* **2006**, *261*, 1.

[2]   B. Schweitzer, S. F. Kingsmore, *Curr. Opin. Biotechnol.* **2002**, *13*, 14.

[3]   K. R. Love, P. H. Seeberger, *Angew. Chem. Int. Ed.* **2002**, *41*, 3583.

[4]   K. S. Lam, M. Renil, *Curr. Opin. Chem. Biotechnol.* **2002**, *6*, 353.

[5]   R. Z. Wu, S. N. Bailey, D. Sabatini, *Trends Cell Biol.* **2002**, *12*, 485.

[6]   M. S. Fejzo, D. J. Slamon, *Am. J. Pathol.* **2001**, *159*, 1645.

[7]   W. Kusnezow, J. D. Hoheisel, *J. Mol. Recognit.* **2003**, *16*, 165.

[8]   V. V. Hlady, J. Buijs, *Curr. Opin. Biotechnol.* **1996**, *7*, 72.

[9]   I. Shin, S. Park, M.-R. Lee, *Chem. Eur. J.* **2005**, *11*, 2894.

[10]   A. del Campo, I. J. Bruce, *Top Curr. Chem.* **2005**, *260*, 77.

[11]   R. Horejsi, G. Kollenz, F. Dachs, H. M. Tillian, K. Schauenstein, E. Schauenstein, W. Steinschifter, *J. Biochem. Biophys. Meth.* **1997**, *34*, 227.

[12]   V. Ball, P. Huetz, A. Elaissari, J. P. Cazenave, J. C. Voegel, P. Schaaf, *Pro. Natl. Acad. Sci. U.S.A.* **1994**, *91*, 7330.

[13]   P. J. Hergenrother, K. M. Depew, S. L. Schreiber, *J. Am. Chem. Soc.* **2000**, *122*, 7849.

[14]   M. C. Pirrung, C.-Y. Huang, *Bioconjugate Chem.* **1996**, *7*, 317.

[15]   X.-L. Sun, C. L. Stabler, C. S. Cazalis, E. L. Chaikof, *Bioconjugate Chem.* **2006**, *17*, 52.

[16]   A. Peramo, A. Albritton, G. Matthews, *Langmuir* **2006**, *22*, 3228.

[17]   X. Zhao, S. Nampalli, A. J. Serino, S. Kumar, *Nucleic Acids Res.* **2001**, *29*, 955.

[18]   W. Heiser, *Methods in molecular biology. Gene delivery to mammalian cells. Vol. 1. Nonviral gene transfer technique* **2004**.

[19]   R. Benters, C. M. Niemeyer, D. Wöhrle, *ChemBioChem* **2001**, *2*, 686.

[20]   R. Benters, C. M. Niemeyer, D. Drutschmann, D. Blohm, D. Wöhrle, *Nucleic Acids Res.* **2002**, *30*, e10.

[21]   B. J. Hong, V. Sunkara, J. W. Park, *Nucleic Acids Res.* **2005**, *33*, e106.

[22]   B. J. Hong, S. J. Oh, T. O. Youn, S. H. Kwon, J. W. Park, *Langmuir* **2005**, *21*, 4257.

[23]   V. Le Berre, E. Trévisiol, A. Dagkessamanskaia, S. Sokol, A.-M. Caminade, J.-P. Majoral, B. Meunier, J. François, *Nucleic Acids Res.* **2003**, *31*, e88.

[24]   M. Beier, J. D. Hoheisel, *Nucleic Acid Res.* **1999**, *27*, 1970.

[25]   S. Pathak, A. K. Singh, J. R. McElhanon, P. M. Dentinger, *Langmuir* **2004**, *20*, 6075.

[26]   S. Wong, V. Kitaev, G. A. Ozin, *J. Am. Chem. Soc.* **2003**, *50*, 15589.

[27]   M. Glazer, J. Fidanza, G. McGall, C. Frank, *Chem. Mater.* **2001**, *13*, 4773.

[28]   E. Cunningham, C. J. Campbell, *Langmuir* **2003**, *19*, 4509.

[29]   F. Xu, G. Zhen, F. Yu, E. Kuennemann, M. Textor, W. Knoll, *J. Am. Chem. Soc.* **2005**, *127*, 13084.

[30]   J. J. Gooding, V. G. Praig, E. A. H. Hall, *Anal. Chem.* **1998**, *70*, 2396.

[31]   C. Boozer, J. Ladd, S. Chen, Q. Yu, J. Homola, S. Jiang, *Anal. Chem.* **2004**, *76*, 6967.

[32]   J. C. Love, L. A. Estroff, J. K. Kriebel, R. G. Nuzzo, G. M. Whitesides, *Chem. Rev.* **2005**, *105*, 1103.

[33]   J. J. Gooding, F. Mearns, H. Yang, J. Liu, *Electroanalysis* **2003**, *15*, 81.

[34]   H. Schonherr, F. J. B. Kremer, S. Kumar, J. A. Rego, H. Wolf, H. Ringsdorf, M. Jaschke, H.-J. Butt, E. Bamberg, *J. Am. Chem. Soc.* **1996**, *118*, 13051.

[35]   D. K. Schwartz, *Annu. Rev. Phys. Chem.* **2001**, *52*, 107.

[36]   T. P. Sullivan, W. T. S. Huck, *Eur. J. Org. Chem.* **2003**, 17.

[37]   K. M. Pertays, G. E. Thompson, M. R. Alexander, *Surf. Interface Anal.* **2004**, *36*, 1361.

[38]   A. Nanci, J. D. Wuest, L. Peru, P. Brunet, V. Sharma, S. Zalzal, M. D. McKee, *J. Biomed. Mater. Res.* **1998**, *40*, 324.

[39]   A. Klinger, D. Steinberg, D. Kohavi, M. N. Sela, *J. Biomed. Mater. Res.* **1997**, *36*, 387.

[40]   J. P. Lee, Y. J. Jang, M. M. Sung, *Adv. Funct. Mater.* **2003**, *13*, 873.

[41]   F. Fixe, M. Dufva, P. Telleman, C. B. V. Christensen, *Nucleic Acids Res.* **2004**, *32*, e9.

[42]   A. C. Henry, T. J. Tutt, M. Galloway, Y. Y. Davidson, C. S. McWhorter, S. A. Soper, R. L. McCarley, *Anal. Chem.* **2000**, *75*, 5331.

[43]   V. Bulmus, H. Ayhan, E. Piskin, *Chem. Eng. J.* **1997**, *65*, 71.

[44]   E. N. Timofeev, S. V. Kochetkova, A. D. Mirzabekov, V. L. Florentiev, *Nucleic Acids Res.* **1996**, *24*.

[45]   L. Goldstein, A. Niv, *Appl. Biochem. Biotechnol.* **1993**, *42*, 19.

[46]   A. Lauto, M. Ohebshalom, M. Esposito, J. Mingin, P. S. Li, D. Felsen, M. Goldstein, D. P. Poppas, *Biomaterials* **2001**, *22*, 1869.

[47]   H. M. Yi, L. Q. Wu, J. J. Summer, J. B. Gillespie, G. F. Payne, W. E. Bentley, *Biotech. Bioeng.* **2003**, *83*, 646.

[48]   M. N. Taravel, A. Domard, F. E. Regnier, *Biomaterials* **1993**, *14*, 930.

[49]   A. Lauto, J. Hook, M. Doran, F. Camacho, L. A. Poole-Warren, A. Avalio, L. J. R. Foster, *Lasers Surg. Med.* **2005**, *36*, 193.

[50]   T. R. Gingeras, D. Y. Kwoh, G. R. Davis, *Nucleic Acids Res.* **1987**, *15*, 5373.

[51]   M. Fuentes, C. Mateo, L. Garcia, J. C. Tercero, J. M. Guisan, R. Fernandez-Lafuente, *Biomacromol.* **2004**, *5*, 883.

[52]   D. Miksa, E. R. Irish, D. Chen, R. J. Composto, D. M. Eckmann, *Biomacromol.* **2006**, *7*, 557.

[53]   J. J. Yoon, Y. S. Nam, J. H. Kim, T. G. Park, *Biotech. Bioeng.* **2002**, *78*, 1.

[54]   W. G. Beattie, L. Meng, S. L. Turner, R. S. Varma, D. D. Dao, K. L. Beattie, *Mol. Biotechnol.* **1995**, *4*, 213.

[55]   J. B. Lamture, K. L. Beattie, B. E. Burke, M. D. Eggers, D. J. Ehrlich, R. Fowler, M. A. Hollis, B. B. Kosicki, R. K. Reich, S. R. Smith, et al., *Nucleic Acid Res.* **1994**, *22*, 2121.

[56]   N. Zammatteo, L. Jeanmart, S. Hamels, S. Courtois, P. Loutte, J. Hevesi, J. Remacle, *Anal. Biochem.* **2000**, *280*, 143.

[57]   H.-Y. Rogers, P. Jiang-Baucom, Z.-J. Huang, V. Bogdanov, S. Anderson, M. T. Boyce-Jacino, *Anal. Biochem.* **1999**, *266*, 23.

[58]   A. Steel, M. Torres, J. Hartwell, Y.-Y. Yu, N. Ting, G. Hoke, H. Yang, *Microarray Chip Technology* **2000**, 87.

[59]   S. Park, M.-R. Lee, S.-J. Pyo, I. Shin, *J. Am. Chem. Soc.* **2004**, *126*, 4812.

[60]   T. Okamoto, T. Suzuki, N. Yamamamoto, *Nat. Biotecgnol.* **2000**, *18*, 438.

[61]   M. C. Pirrung, J. D. Davis, A. L. Odenbaugh, *Langmuir* **2000**, *16*, 2185.

[62]   L. M. Demers, D. S. Ginger, S.-J. Park, Z. Li, S.-W. Chung, C. A. Mirkin, *Science* **2002**, *296*, 1836.

[63]   M. Köhn, R. Wacker, C. Peters, H. Schröder, L. Soulere, R. Breinbauer, C. M. Niemeyer, H. Waldmann, *Angew. Chem. Int. Ed.* **2003**, *42*, 5829.

[64]   X. Zhano, S. Nampalli, A. J. Serino, S. Kumar, *Nucleic Acid Res.* **2001**, *29*, 955.

[65]   A. Kumar, O. Larsson, D. Parodi, Z. Liang, *Nucleic Acids Res.* **2000**, *28*, e71.

[66]   J. M. Brockman, A. G. Frutos, R. M. Corn, *J. Am. Chem. Soc.* **1999**, *121*, 8044.

[67] E. A. Smith, M. J. Wanat, Y. Cheng, S. V. P. Barreirs, A. G. Frutos, R. M. Corn, *Langmuir* **2001**, *17*, 2502.

[68] N. K. Devaraj, G. P. Miller, W. Ebina, B. Kakaradov, J. P. Collman, E. T. Kool, C. E. D. Chidsey, *J. Am. Chem. Soc.* **2005**, *127*, 8600.

[69] B. T. Houseman, M. Mirksich, *Chem. Biol.* **2002**, *9*, 443.

[70] E. Delamarche, A. Bernard, H. Schmid, A. Bietsch, B. Michel, H. Biebuyck, *J. Am. Chem. Soc.* **1998**, *120*, 500.

[71] P. Kumar, K. C. Gupta, *Bioconjugate Chem.* **2003**, *14*, 507.

[72] D. I. Rożkiewicz, B. J. Ravoo, D. N. Reinhoudt, *Langmuir* **2005**, *21*, 6337.

[73] K. Lindroos, U. Liljedahl, M. Raitio, A. C. Syvänen, *Nucleic Acid Res.* **2001**, *29*, e69.

[74] A. Kumar, O. Larsson, D. Parodi, Z. Liang, *Nucleic Acid Res.* **2000**, *28*, e71.

[75] D. L. Wilson, R. Martin, S. Hong, M. Cronin-Golomb, C. A. Mirkin, D. L. Kaplan, *Pro. Natl. Acad. Sci. U.S.A.* **2001**, *98*, 13660.

[76] K.-B. Lee, J.-H. Lim, C. A. Mirkin, *J. Am. Chem. Soc.* **2003**, *125*, 5588.

[77] G. M. Husar, D. J. Anziano, M. Leuck, D. P. Sebesta, *Nucleosides Nucleic Acids* **2001**, *20*, 559.

[78] H. A. Latham-Timmons, A. Wolter, J. S. Roach, R. Giare, M. Leuck, *Nucleosides Nucleic Acids* **2003**, *22*, 1495.

[79] C. Donzel, M. Geissler, A. Bernard, H. Wolf, B. Michel, J. Hilborn, E. Delamarche, *Adv. Mater.* **2001**, *13*, 1164.

[80] W. Kusnezow, A. Jacob, A. Walijew, F. Diehl, J. D. Hoheisel, *Proteomics* **2003**, *3*, 254.

[81] G. T. Hermanson, *Bioconjugate Techniques* **1996**.

[82] A. D. de Araujo, J. M. Palomo, J. Cramer, M. Köhn, H. Schröder, R. Wacker, C. M. Niemeyer, K. Alexadrov, H. Waldmann, *Angew. Chem. Int. Ed.* **2006**, *45*, 296.

[83] K. Nakanishi, T. Sakiyama, K. Imamura, *J. Biosci. Bioeng.* **2001**, *91*, 233.

[84] E. Ostuni, C. S. Chen, D. E. Ingber, G. M. Whitesides, *Langmuir* **2001**, *17*, 2828.

[85] Y. Y. Luk, M. Kato, M. Mrksich, *Langmuir* **2000**, *16*, 9604.

[86] R. G. Chapman, E. Ostuni, S. Takayama, R. E. Holmlin, L. Yan, G. M. Whitesides, *J. Am. Chem. Soc.* **2000**, *122*, 8303.

[87] W. R. Gombotz, G. H. Wang, T. A. Horbett, A. S. Hoffman, *J. Biomed. Mater. Res.* **1991**, *25*, 1547.

[88] K. L. Prime, G. M. Whitesides, *Science* **1991**, *252*, 1164.

[89] K. L. Prime, G. M. Whitesides, *J. Am. Chem. Soc.* **1993**, *115*, 10714.

[90] P. D. Drumheller, D. I. Elbert, J. A. Hubbell, *Biotech. Bioeng.* **1994**, *43*, 772.

[91] P. D. Drumheller, J. A. Hubbell, *Anal. Biochem.* **1994**, *222*, 380.

[92] P. D. Drumheller, J. A. Hubbell, *J. Biomed. Mater. Res.* **1995**, *29*, 207.

[93] M. Q. Zhang, T. Desai, M. Ferrari, *Biomaterials* **1998**, *19*.

[94] M. Q. Zhang, M. Ferrari, *J. Biomed. Microdecies* **1998**, *1*, 81.

[95] D. O. Teare, W. C. E. Schofield, R. P. Garrod, J. P. S. Badyal, *J. Phys. Chem. B* **2005**, *109*, 20923.

[96] S. K. Bhatia, L. C. Shriver-Lake, K. J. Prior, J. H. Georger, J. M. Calvert, *Anal. Biochem.* **1989**, *178*, 408.

[97] S. K. Bhatia, J. J. Hickman, F. S. Ligler, *J. Am. Chem. Soc.* **1992**, *114*, 4432.

[98] S. K. Bhatia, J. L. Teixeira, M. Anderson, L. C. Shriver-Lake, J. M. Calvert, *Anal. Biochem.* **1993**, *208*, 197.

[99] L. Deng, M. Mrksich, G. M. Whitesides, *J. Am. Chem. Soc.* **1996**, *118*, 5136.

[100] E. Ostuni, R. G. Chapman, M. N. Liang, G. Meluleni, G. Pier, D. R. Ingber, G. M. Whitesides, *Langmuir* **2001**, *17*, 6336.

[101] N. Nath, J. Hyun, H. Ma, A. Chilkoti, *Surf. Sci.* **2004**, *570*, 98.

[102] A. L. Lewis, *Colloids Surf. B* **2000**, *18*, 261.

[103] S. Chen, J. Zheng, L. Li, S. Jiang, *J. Am. Chem. Soc.* **2005**, *127*, 14473.

[104] S. B. Carter, *Nature* **1965**, *208*, 1183.

[105] E. Ostuni, R. G. Chapman, R. E. Holmlin, S. Takayama, G. M. Whitesides, *Langmuir* **2001**, *17*, 5605.

[106] D. L. Huber, R. P. Manginell, M. A. Samara, B. Kim, B. C. Bunker, *Science* **2003**, *301*, 352.

[107] J. Ponten, L. Stolt, *Exp. Cell. Res.* **1980**, *129*, 367.

[108] N. G. Maroudas, *Nature* **1973**, *244*, 353.

[109] T. G. Vargo, E. J. Bekos, Y. S. Kim, J. P. Ranieri, R. Bellamkonda, e. al., *J. Biomed. Mater. Res.* **1995**, *29*, 767.

[110] T. Sugawara, T. Matsuda, *J. Biomed. Mater. Res.* **1995**, *29*, 1047.

[111] M. Q. Zhang, M. Ferrari, *Biotechnol. Bioeng.* **1997**, *56*, 618.

[112] J. B. Lhoest, E. Detrait, J. L. Dewez, A. P. van den Bosch, P. Bernard, *J. Biomater. Sci. Polym. Ed.* **1996**, *7*, 1039.

[113] C. S. Chen, M. Mrksich, S. Huang, G. M. Whitesides, D. E. Ingber, *Science* **1997**, *276*, 1425-1428.

[114] R. Singhavi, A. Kumar, G. P. Lopez, G. N. Stephanopoulos, D. I. Wang, G. M. Whitesides, D. E. Ingber, *Science* **1994**, *264*, 696.

[115] P. Harder, M. Grunze, R. Dahint, G. M. Whitesides, P. E. Laibinis, *J. Phys. Chem. B* **1998**, *102*, 426.

[116] K. Glasmastar, C. Larsson, F. Hook, B. Kasemo, *J. Colloid Interface Sci.* **2002**, *246*, 40.

[117] M. Malmsten, *J. Colloid Interface Sci.* **1995**, *172*, 106.

[118] M. Malmsten, *Colloids Surf. A* **1999**, *159*, 77.

[119] E. E. Ross, T. Spratt, S. Liu, L. J. Rozanski, D. F. O'Brien, S. S. Saavedra, *Langmuir* **2003**, *19*, 1766.

[120] K. Ishihara, H. Nomura, M. Mihara, K. Kurita, Y. Iwasaki, N. Nakabayashi, *J. Biomed. Mater. Res.* **1998**, *39*, 323.

[121] G. H. Hsiue, S. D. Lee, P. C. Chang, C. Y. Kao, *J. Biomed. Mater. Res.* **1998**, *42*, 134.

[122] R. E. Holmlin, X. Chen, R. G. Chapman, S. Takayama, G. M. Whitesides, *Langmuir* **2001**, *17*, 2841.

[123] R. S. Kane, P. Deschatelets, G. M. Whitesides, *Langmuir* **2003**, *19*, 2388.

[124] S. L. West, J. P. Salvage, E. J. Lobb, S. P. Armes, N. C. Billingham, A. L. Lewis, G. W. Hanlon, A. W. Lloyd, *Biomaterials* **2004**, *25*, 1195.

[125] H. Kitano, A. Kawasaki, H. Kawasaki, S. Morokoshi, *J. Colloid Interface Sci.* **2005**, *282*, 340.

[126] P. H. Yancey, M. E. Clark, S. C. Hand, R. D. Bowlus, G. N. Somero, *Science* **1982**, *217*, 1214.

[127] S. N. Timasheff, *Adv. Protein Chem.* **1998**, *51*, 355.

[128] R. S. Kane, S. Takayama, E. Ostuni, D. E. Ingber, G. M. Whitesides, *Biomaterials* **1999**, *20*, 2363.

[129] A. Bernard, J. P. Renault, B. Michel, H. R. Bosshard, E. Delamarche, *Adv. Mater.* **2000**, *12*, 1067.

[130] H. D. Inerowicz, S. Howell, F. E. Regnier, R. Reifenberfer, *Langmuir* **2002**, *18*, 5263.

[131] A. Folch, M. Toner, *Annu. Rev. Biomed. Eng.* **2000**, *2*, 227.

[132] R. J. Jackman, D. C. Duffy, O. Cherniavskaya, G. M. Whitesides, *Langmuir* **1999**, *15*, 2973.

[133] M. Mrksich, G. M. Whitesides, *Annu. Rev. Biophys. Biomol. Struct.* **1996**, *25*, 55.

[134] L. Vroman, A. L. Adams, G. C. Fischer, P. C. Munoz, *Blood* **1980**, *55*, 156.

[135] J. D. Mendelsohn, S. Y. Yang, J. A. Hiller, A. I. Hochbaum, M. F. Rubner, *Biomacromol.* **2003**, *4*, 96.

[136] S. Y. Yang, J. D. Mendelsohn, M. F. Rubner, *Biomacromol.* **2003**, *4*, 987.

[137] X.-M. Zhao, Y. Xia, G. M. Whitesides, *J. Mater. Chem* **1997**, *7*, 1069.

[138] Y. Xia, G. M. Whitesides, *Angew. Chem. Int. Ed.* **1998**, *37*, 550.

[139] Y. Xia, G. M. Whitesides, *Annu. Rev. Mater. Sci.* **1998**, *28*, 153.

[140] J. A. Rogers, R. G. Nuzzo, *Materials Today* **2005**, 50.

[141] A. Kumar, H. A. Biebuyck, G. M. Whitesides, *Langmuir* **1994**, *10*, 1498.

[142] J. L. Wilbur, A. Kumar, E. Kim, G. M. Whitesides, *Adv. Mater.* **1994**, *6*, 600.

[143] J. A. Rogers, K. E. Paul, G. M. Whitesides, *J. Vac. Sci. Technol. B* **1998**, *16*, 88.

[144] D. J. Graham, D. D. Price, B. D. Ratner, **2002**, *18*, 1518.

[145] Y. Xia, G. M. Whitesides, *Langmuir* **1997**, *13*, 2059.

[146] J. A. Helmuth, H. Schmid, R. Stutz, A. Stemmer, H. Wolf, *J. Am. Chem. Soc.* **2006**, *128*, 9296.

[147] R. B. Bass, A. W. Lichtenberger, *Appl. Surf. Sci.* **2004**, *226*, 335.

[148] A. P. Quist, E. Pavlovic, S. Oscarsson, *Anal. Biochem. Chem.* **2005**, *381*, 591.

[149] T. P. Sullivan, M. L. van Poll, P. Y. W. Dankers, W. T. S. Huck, *Angew. Chem. Int. Ed.* **2004**, *43*, 4190.

[150] K. E. Schmalenberg, H. M. Buettner, K. E. Uhrich, *Biomaterials* **2004**, *25*, 1851.

[151] S. A. Lange, V. Benes, D. P. Kern, J. K. H. Hober, A. Bernard, *Anal. Chem.* **2004**, *76*, 1641.

[152] C. Xu, P. Taylor, M. Ersoz, P. D. I. Fletcher, V. N. Paunov, *J. Mater. Chem* **2003**, *13*, 1851.

[153] J. L. Tan, J. Tien, C. S. Chen, *Langmuir* **2002**, *18*, 519.

[154] J. R. LaGraff, Q. Chu-LaGraff, *Langmuir* **2006**, *22*, 4685.

[155] D. J. Graber, T. J. Zieziulewicz, D. A. Lawrence, W. Shain, J. N. Turner, *Langmuir* **2003**, *19*, 5431.

[156] A. Bernard, E. Delamarche, H. Schmid, B. Michel, H. R. Bosshard, H. Biebuyck, *Langmuir* **1998**, *14*, 2225.

[157] E. E. Ross, J. R. Joubert, R. J. Wysocki, K. Nebesny, T. Spratt, D. F. O'Brien, S. S. Saavedra, *Biomacromolecules* **2006**, *7*, 1393.

[158] J. P. Renault, A. Bernard, A. Bietsch, B. Michel, H. R. Bosshard, E. Delamarche, M. Kreiter, B. Hecht, U. P. Wild, *J. Phys. Chem. B* **2003**, *107*, 703.

[159] T. J. Park, S. Y. Lee, S. J. Lee, J. P. Park, K. S. Yang, K.-B. Lee, S. Ko, J. B. Park, T. Kim, S. K. Kim, et al., *Anal. Chem.* **2006**, *78*, 7197.

[160] S. K. Kwak, G. S. Lee, D. J. Ahn, J. W. Choi, *Mat. Sci. Eng. C-Bio.* **2004**, *24*, 151.

[161] T. Wilhelm, G. Wittstock, *Langmuir* **2002**, *18*, 9485.

[162] A. Biasco, D. Pisignano, B. Krebs, R. Cingolani, R. Rinaldi, *Synthetic Metlas* **2005**, *153*, 21.

[163] C. D. James, R. C. Davis, L. Kam, H. G. Craighead, M. Isaacson, J. N. Turner, W. Shain, *Langmuir* **1998**, *14*, 741.

[164] J. S. Hovis, S. G. Boxer, *Langmuir* **2001**, *17*, 3400.

[165] E. Delamarche, C. Donzel, F. S. Kamounah, H. Wolf, M. Geissler, R. Stutz, P. Schmid-Winkel, B. Michel, H. J. Mathieu, K. Schaumburg, *Langmuir* **2003**, *19*, 8749.

[166] C. J. Campbell, S. K. Smoukov, K. J. M. Bishop, B. A. Grzybowski, *Langmuir* **2005**, *21*, 2637.

[167] G. Csusc, T. Künzler, K. Feldman, F. Robin, N. D. Spencer, *Langmuir* **2003**, *19*, 6104.

[168] M. Geissler, A. Bernard, A. Bietsch, H. Schmid, B. Michel, E. Delamarche, *J. Am. Chem. Soc.* **2000**, *122*, 6303.

[169] J. Lahiri, E. Ostuni, G. M. Whitesides, *Langmuir* **1999**, *15*, 2055.

[170] K. B. Lee, D. J. Kim, Z. W. Lee, S. I. Woo, I. S. Choi, *Langmuir* **2004**, *20*, 2531.

[171] J. H. Hyun, H. W. Ma, P. Banerjee, J. Cole, K. Gonsalves, A. Chilkoti, *Langmuir* **2002**, *18*, 2975.

[172] J. Feng, C. Gao, B. Wang, J. Shen, *Thin Solid Films* **2004**, *460*, 286.

[173] J. P. Renault, A. Bernard, D. Juncker, B. Michel, H. R. Bosshard, E. Delamarche, *Angew. Chem. Int. Ed.* **2002**, *41*, 2320.

[174] A. Bernard, D. Fitzli, P. Sonderegger, E. Delamarche, B. Michel, H. R. Bosshard, H. Biebuyck, *Nat. Biotecgnol.* **2001**, *19*, 866.

[175] C.-H. Jang, M. L. Tingey, N. L. Korpi, G. J. Wiepz, J. H. Schiller, P. J. Bertics, N. L. Abbott, *J. Am. Chem. Soc.* **2005**, *127*, 8912.

[176] M. L. Tingey, S. Wilyana, S. E. J., N. L. Abbott, *Langmuir* **2004**, *20*, 6818.

[177] J. Hyun, A. Chilkoti, *J. Am. Chem. Soc.* **2001**, *123*, 6943.

[178] A. Papra, A. Bernard, D. Juncker, N. B. Larsen, B. Michel, E. Delamarche, *Langmuir* **2001**, *17*, 4090.

[179] A. Bernard, B. Michel, E. Delamarche, *Anal. Chem.* **2001**, *73*, 8.

[180] J. Foley, H. Schmid, R. Stutz, E. Delamarche, *Langmuir* **2005**, *21*, 11296.

[181] X.-Y. Jiang, Q. Xu, K. W. Dertinger, A. D. Stroock, T. Fu, G. M. Whitesides, *Anal. Chem.* **2005**, *77*, 2338.

[182] D. M. Eigler, E. K. Schweizer, *Nature* **1990**, *344*, 524.

[183] M. F. Crommie, C. P. Lutz, D. M. Eigler, *Science* **1993**, *262*, 218.

[184] (a) M. Jaschke, H.-J. Butt, *Langmuir* **1995**, *11*, 1061.(b) D. S. Ginger, H. Zhang, C. A. Mirkin, *Angew. Chem. Int. Ed.* **2004**, *43*, 30.

[185] A. Noy, A. E. Miller, J. E. Klare, B. L. Weeks, B. W. Woods, J. J. De Yoreo, *Nano. Lett.* **2002**, *2*, 109.

[186] K.-B. Lee, S.-J. Park, C. A. Mirkin, J. C. Smith, M. Mrksich, *Science* **2002**, *295*, 1702.

[187] H. Jung, R. Kulkarni, C. P. Collier, *J. Am. Chem. Soc.* **2003**, *125*, 12096.

[188] D. J. R. Pena, M. P.; Byers, J. M., *Langmuir* **2003**, *19*, 9028.

[189] M. Ben Ali, T. Ondarcuhu, M. Brust, C. Joachim, *Langmuir* **2002**, *18*, 872.

[190] J.-H. Lim, D. S. Ginger, K.-B. Lee, J. Heo, J.-M. Nam, C. A. Mirkin, *Angew. Chem. Int. Ed.* **2003**, *42*, 2309.

[191] S.-W. Chung, D. S. Ginger, M. W. Morales, Z. Zhang, V. Chandrasekhar, M. A. Ratner, C. A. Mirkin, *Small* **2005**, *1*, 64.

[192] H. Zhang, Z. Li, C. A. Mirkin, *Adv. Mater.* **2002**, *20*, 1472.

[193] R. A. Vega, D. Maspoch, C. K.-F. Shen, J. J. Kakkassery, B. J. Chen, R. A. Lamb, C. A. Mirkin, *ChemBioChem* **2006**, *7*, 1653.

[194] R. A. Vega, D. Maspoch, K. Salaita, C. A. Mirkin, *Angew. Chem. Int. Ed.* **2005**, *44*, 6013.

[195] K. Salaita, S. W. Lee, X. Wang, L. Huang, T. M. Dellinger, C. Liu, C. A. Mirkin, *Small* **2005**, *1*, 940.

[196] S. W. Lee, R. G. Sanedrin, B.-K. Oh, C. A. Mirkin, *Adv. Mater.* **2005**, *17*, 2749.

[197] S. Hong, C. A. Mirkin, *Science* **2000**, *288*, 1808.

[198] K. Salaita, Y. Wang, J. Fragala, R. A. Vega, C. Liu, C. A. Mirkin, *Angew. Chem. Int. Ed.* **2006**, *45*, 7220.

[199] S. Lenhert, P. Sun, Y. Wang, H. Fuchs, C. A. Mirkin, *Small* **2007**, *3*, 71.

[200] S. W. Lee, B.-K. Oh, R. G. Sanedrin, K. Salaita, T. Fujigaya, C. A. Mirkin, *Adv. Mater.* **2006**, *18*, 1133.

[201] X. Wang, K. S. Ryu, D. A. Bullen, J. Zou, H. Zhang, C. A. Mirkin, C. Liu, *Langmuir* **2003**, *19*, 8951.

[202] H. Zhang, R. Elghanian, N. A. Amro, S. Disawal, R. Eby, *Nano. Lett.* **2004**, *4*, 1649.

Chapter 3

Reversible covalent patterning of gold and silicon oxide surfaces[*]

This Chapter describes the generation of reversible patterns on gold and silicon oxide surfaces via the formation of reversible covalent bonds. The reactions of (patterned) self-assembled monolayers (SAMs) of 11-amino-1-undecanethiol (11-AUT) with propanal, pentanal, decanal or terephthaldialdehyde result in well-organized imine monolayers. These imine monolayers can be regenerated to the 11-AUT monolayer by hydrolysis at pH 3. The (patterned) monolayers were characterized by atomic force microscopy (AFM), Fourier transform infrared spectroscopy (FTIR), X-ray photoelectron spectroscopy (XPS), contact angle and electrochemical measurements. Imines can also be formed by microcontact printing (μCP) of amines on terephtaldialdehyde-terminated substrates. Lucifer yellow ethylenediamine was employed as a fluorescent amine-containing marker to visualize the reversible covalent patterning on a terephtaldialdehyde-terminated glass surface by confocal microscopy. These experiments demonstrate that with reversible covalent chemistry it is possible to print and erase chemical patterns on surfaces repeatedly.

3.1. Introduction

Self-assembled monolayers (SAMs) find increasing use as platforms where a two-dimensional chemical pattern is expressed and amplified into a three-dimensional functional structure.[1-3] Chemical diversity of functional groups on a surface can direct the attachment of macromolecules,[4-8] nanoparticles,[9,10] proteins and DNA,[11-15] liposomes,[16] or cells.[17-19] Microcontact printing (μCP) of absorbate molecules on a substrate can pattern the surface with functional groups at sub-100 nm resolution.[20, 21]

Homogeneous as well as patterned SAMs have been modified by covalent chemistry to tune surface properties by the introduction of functional groups.[2,22] The advantage of covalent chemistry for the modification of SAMs and the immobilization of molecules and nanoparticles on SAMs is the broad scope of available reactions and the stability of the covalent link. On the other hand, our group has recently introduced "molecular printboards" that can be modified via non-covalent host-guest interactions.[23-25] A molecular printboard is a chemisorbed monolayer of host molecules that acts as a template onto which guest molecules can be immobilized. Molecular printboards can serve to position guest molecules on the host surface by μCP ("supramolecular microcontact printing").[24] The advantage of non-covalent, supramolecular chemistry is the potential to immobilize molecules and particles with tunable binding strength through multivalent interaction. Under appropriate conditions, the (multivalent) non-covalent bond can be either stable or readily reversible. This was illustrated in our demonstration of supramolecular μCP, where patterns based on host-guest interactions can be printed and erased.[24]

A method for repeatedly "printing" and "erasing" a pattern on a substrate using a *reversible covalent* reaction is described here. The aim is to demonstrate that reversible covalent chemistry can combine the advantages of covalent chemistry (i.e. wide scope of reactions and stable immobilization) and non-covalent chemistry (i.e. "write and erase" under appropriate conditions). Several examples of potentially reversible covalent reactions on surfaces, like disulfide exchange,[13] protection and deprotection of amine and hydroxyl terminated SAMs,[26] and imine formation[27] have been reported in the literature. However, there are no reports on reversible covalent patterning of SAMs.

In this Chapter the reversible formation of imines from amines and aldehydes, on gold and silicon oxide surfaces is demonstrated. Imine formation on the surface has numerous other advantages: it is simple and selective, it does not require sophisticated reaction conditions, it can be carried out in mild, physiological environments and it is biocompatible. Amine-terminated substrates are a good platform for the reversible immobilization of any molecule with an

aldehyde group (e.g. carbohydrates, steroids, drugs, and certain metabolic intermediates). On the other hand there are many other molecules that contain primary amino groups (peptides, proteins, dendrimers, aminosugars, hormones, alkaloids, antibiotics, steroids, drugs) which may be coupled to an aldehyde-terminated surface by imine formation (see Chapter 4, 5 and 6).
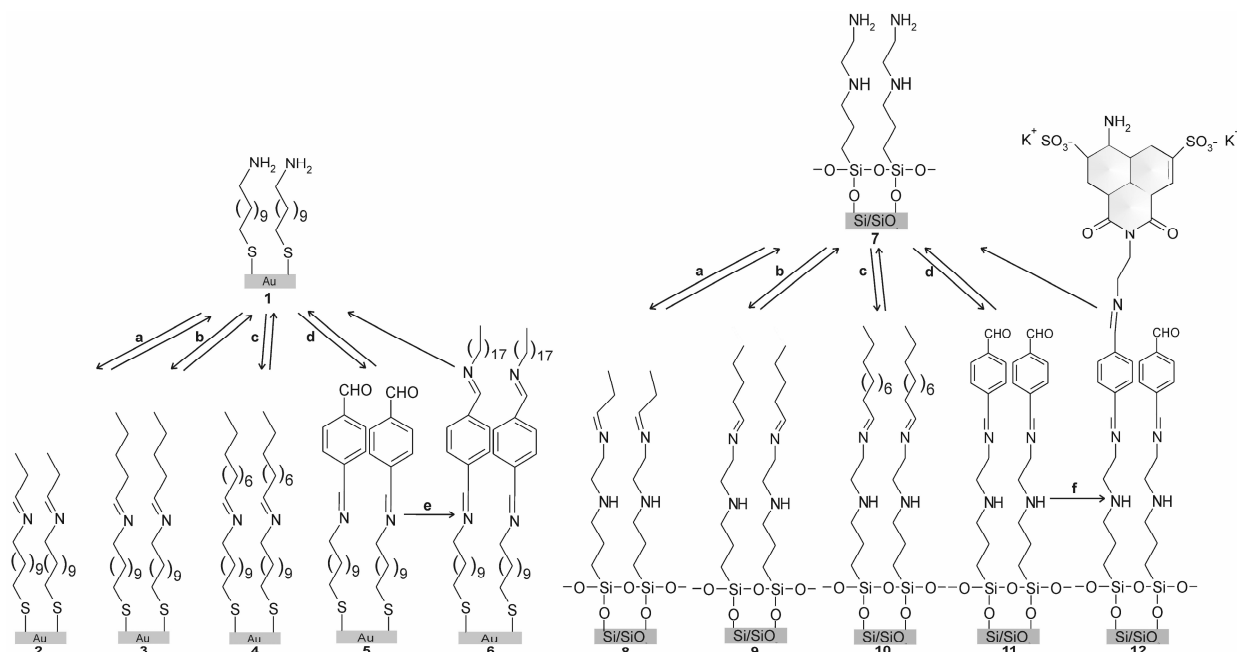

Figure 3-1. Schematic representation of the procedure for imine formation on gold (**1-6**) and silicon oxide (**7-12**) substrates (a) propanal, (b) pentanal, (c) decanal, (d) terephthaldialdehyde, (e) octadecylamine, (f) lucifer yellow. All reactions are reversible under acid-catalyzed hydrolysis (aqueous solution of acetic acid, pH 3).

Imine formation on gold and silicon oxide surfaces is a multistep process. First, a gold or silicon oxide substrate is functionalized with an amino-terminated monolayer (Figure 3-1, SAMs **1**, **7**) to provide a reactive substrate. The amine SAMs (**1**, **7**) are converted into imine SAMs by reaction with propanal (**2**, **8**), pentanal (**3**, **9**), decanal (**4**, **10**) and terephthaldialdehyde (**5**, **11**) that switches the functionality from a terminal amino group to an aldehyde end group. In the latter case the aldehyde end groups may subsequently be reacted with octadecylamine (ODA) (**6**), or with fluorescent lucifer yellow (**12**). All these reactions are reversible under acid catalyzed hydrolysis with acetic acid solution at pH 3. Moreover, imine formation can occur on SAMs patterned by μCP or directly by μCP of amines on aldehyde SAMs.

3.2. Formation and hydrolysis of imines on the surface

The formation of amine-terminated SAMs was the first step in creating imine derivatized SAMs (Figure 3-1). The primary amine group in SAMs of 11-AUT on gold (Figure 3-1, substrate **1**) or TMSPEDA on silicon oxide (Figure 3-1, substrate **7**) can be reacted with propanal (**2**, **8**), pentanal (**3**, **9**), decanal (**4**, **10**) or terephthaldialdehyde (**5**, **11**). Reaction of terephthaldialdehyde with the amine SAMs resulted in formation of aldehyde-terminated SAMs, which can be further reacted with ODA (**6**) or fluorescent lucifer yellow (**12**).

SAM	θ_{adv} [deg]	θ_{rec} [deg]	θ_{adv} [deg]	θ_{rec} [deg]	C/N (XPS)	C/N (calcd)	Capacitance [$\mu F/cm^2$]
	Before hydrolysis		After hydrolysis				
1	62±2	50±2	n. a.	n. a.	10.6±0.7	11	3.17
2	77±2	62±2	60±2	46±2	13.9±0.4	14	3.04
3	94±2	80±2	65±2	51±2	16.2±0.6	16	2.56
4	101±2	86±2	68±2	54±2	17.6±0.3	21	2.27
5	68±2	55±2	59±2	43±2	18.3±0.3	19	n. d.
6	98±2	86±2	60±2	45±2	16.5±0.6	18.5	n. d.
7	57±2	45±2	n. a.	n. a.	2.6±0.4	2.5	n. d.
8	74±2	62±2	55±2	42±2	3.0±0.3	4.0	n. d.
9	91±2	78±2	55±2	42±2	7.0±0.4	5.0	n. d.
10	98±2	84±2	54±2	41±2	5.8±0.6	7.5	n. d.
11	65±2	54±2	52±2	40±2	5.8±0.3	6.5	n. d.

n. a. – not applicable, n. d. – not determined
θ_{adv} – advancing water contact angle, θ_{rec} – receding water contact angle

Table 3-1. Water contact angle before and after hydrolysis, atomic ratios of elements C, N from XPS, and capacitance of amine and imine monolayers on gold and silicon oxide surfaces.

Water contact angles after amine monolayer formation and imine formation are shown in Table 3-1. It is clear that the water contact angles increase with the length of the aldehyde alkyl chain and approach the values for monolayers of alkanethiols (θ_{adv}= 112±3 ° for octadecanethiol (ODT) on gold).[1]

The C/N ratios from XPS measurements for all amine and imine SAMs are in agreement with the molecular composition, with the exception of **4**, **6**, **10**. These long chain imines have slightly lower C/N ratio than expected, indicating an extensive but incomplete conversion of aldehyde and amine into imines. Figure 3-2 shows the high-resolution XPS spectra of the C 1s region.

The peaks of amino-terminated and imine **2**, **3**, **4** monolayers are present at 285 eV and it is clear that the concentration of carbon increases with the length of the alkyl chain in the imines.
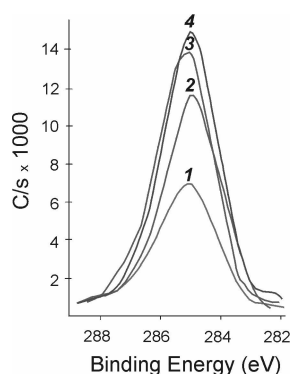

Figure 3-2. X-ray photoelectron spectra of the C 1s region for NH_2-terminated SAM **1**, and imine monolayers **2**, **3**, **4**.

FT-IRRAS spectra are presented in Figure 3-3. The spectrum of 11-AUT on gold (Figure 3-3, **1**) contains one broad band centered at 3320 cm^{-1} and two bands at 2924 cm^{-1} and 2847 cm^{-1} that can be assigned to the stretching mode of the amino group (and possibly some adsorbed water) and to the symmetric CH_2 and asymmetric CH_2 vibrations, respectively. The presence of these three peaks clearly indicates the formation of an amino-terminated SAM on the gold surface. After exposure of the 11-AUT SAM to terephthaldialdehyde, several changes are observed in the spectra (Figure 3-3, **5**). The broad peak of the amino group disappeared, indicating complete reaction on the surface. Furthermore, several new bands appear: imine C=N stretching vibration at 1645 cm^{-1} and a band at 1705 cm^{-1} assigned to the C=O stretching vibration of the second aldehyde group attached to the aromatic ring. Bands at 2927 cm^{-1} and 2854 cm^{-1} indicate CH_2 symmetric and asymmetric stretching vibrations respectively. Weak peaks at approximately 1606 and 1560 cm^{-1} could be assigned to the aromatic ring stretching vibrations. The presence of these characteristic imine and aldehyde bands and the absence of the bands assigned to the amine group provides strong evidence that terephthaldialdehyde was attached covalently via an imine bond, leaving reactive aldehyde groups on the surface. The imine peak is also clearly visible at 1645 cm^{-1} in the spectra of monolayer **4** (imine of 11-AUT and decylaldehyde). Here, two additional peaks responsible for asymmetric and symmetric stretching vibrations of the methyl group at 2966 cm^{-1} and 2877 cm^{-1} are observed. After acid catalyzed hydrolysis of **5** to **1** (Figure 3-3, **1***) no imine peaks or methyl peaks were found. In fact, the spectrum of **1*** is nearly identical to the spectrum of **1**.
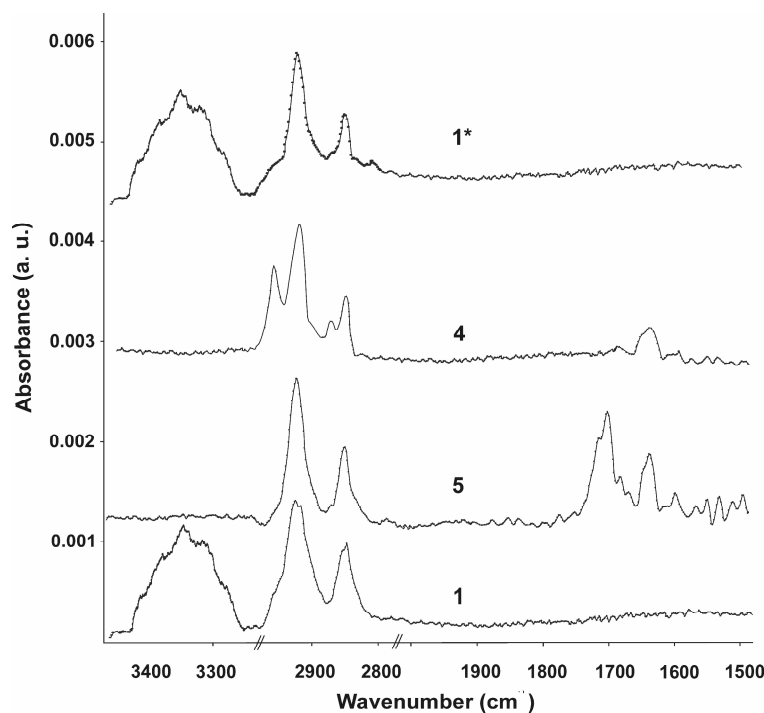
Figure 3-3. FT-IRRAS spectra of imine (**5**, **4**), amine (**1**), and recycled amine (**1***) monolayers.

From heterogeneous electron transfer measurements the abundance and distribution of defects in monolayers on gold can be determined. All SAMs (substrates **1**-**4**) block the current quite well. The shape of cyclic voltammograms suggests that there are very few pinholes defects present in the imine monolayers. From the voltammograms it can also be observed that there is a trend when longer alkyl imines SAMs block the current more effectively than shorter ones. The values of the capacitances of monolayers **1**-**4** are listed in Table 3-1. From those measurements it can be concluded that the monolayers are not as well packed as for example a 1-decanethiol monolayer ($C_{SAM} = 1.24(\pm0.05)\ \mu F\ cm^{-2}$).[1]

Acid catalyzed hydrolysis of imine was monitored by the contact angle with water (Figure 3-4). The reaction was carried out at 40 °C, 60 °C or 100 °C for a period of time ranging up to 8 hours. Imine **2** shows the fastest hydrolysis which is expected because the access of water to the imine bond is the most easy. All reactive SAMs of imines can be hydrolyzed using aqueous acetic acid solution at pH 3 (conditions for hydrolysis are presented in "Experimental section"). Hydrolysis of these imines is much faster at higher temperatures. As a control experiment imine **2** monolayer was immersed in water at pH 7 at 20 °C or 40 °C for 2 days. The contact angle showed that no significant hydrolysis took place. Hence, the imine SAMs are stable in water but sensitive to acidic aqueous solution.
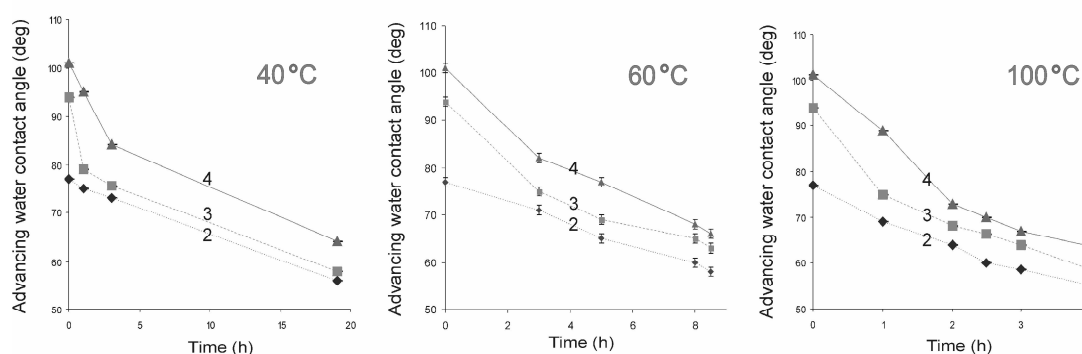
Figure 3-4. Advancing water contact angles after hydrolysis of imines **2**, **3**, **4** at 40 °C, 60 °C and 100 °C and pH 3.

3.3. Patterning of SAMs by imine formation

Further evidence for reversible imine formation and hydrolysis was obtained from surface patterning by µCP. Two methods were applied to obtain imine patterns: (1) indirectly, by printing a reference pattern of ODT and 11-AUT and forming imines from the solution on the 11-AUT area of the substrate and (2) directly, by printing ODA onto aldehyde-terminated SAM **5**. In the first, indirect patterning protocol, ODT was microcontact printed in dots on a gold surface (Figure 3-5A). Subsequently, the remaining bare gold areas were filled with 11-AUT (Figure 3-5B) and the 11-AUT areas were reacted with decanal (Figure 3-5C). Finally the imines were hydrolyzed to give 11-AUT/ODT-pattern (Figure 3-5D, equivalent to Figure 3-5B). Note the contrast reversal between (A) and (B) and the increased contrast from (B) to (C). This "molecular ruler" experiment demonstrates that imine patterns can be printed and erased on the gold surface.
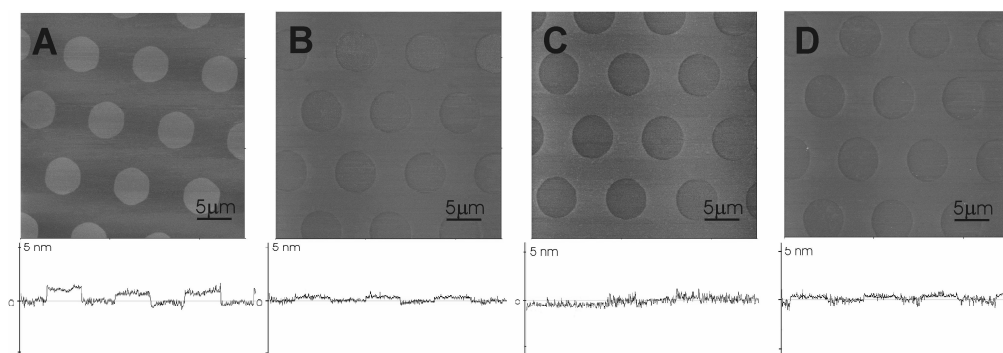

Figure 3-5. Contact mode AFM height images of imine formation on the gold substrate. (A) ODT dots on the gold substrate. (B) ODT dots surrounded by 11-AUT. (C) ODT dots surrounded by imine **4** resulting from 11-AUT that was reacted with decanal. (D) ODT dots surrounded by 11-AUT after acid catalyzed hydrolysis at pH 3 of imine **4**.

In the second, direct patterning protocol, ODA was microcontact printed using a poly(styrene-*b*-(ethylene-*co*-butylene)-*b*-styrene) (SEBS) stamp[17] onto aldehyde-terminated SAM **5**. The ink concentration was 1 mM and the contact time was 1 min. The surface was imaged with AFM before printing (Figure 3-6A, B), after printing (Figure 3-6C, D) and after acid catalyzed hydrolysis (Figure 3-6E, F). The contrast (visible in height, 6C, but especially in friction mode, 6D) confirms the formation of an imine pattern on the surface. In a control experiment the SEBS stamp without ink was brought into contact with an aldehyde-terminated SAM **5** for 1 min. No pattern was observed on the surface.
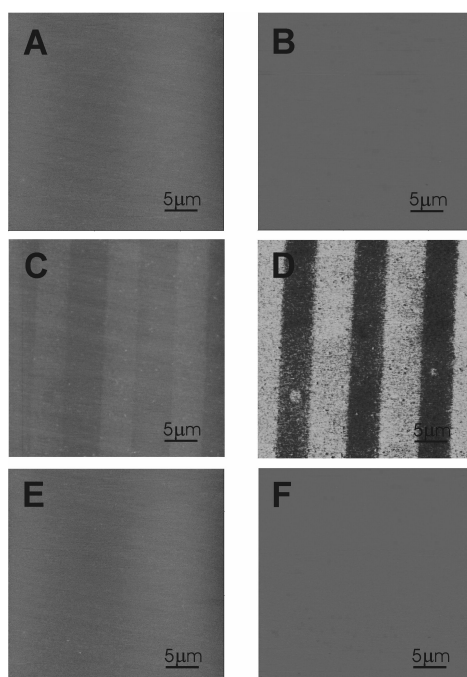

Figure 3-6. AFM height (all left images) and friction (right images) of ODA printed on aldehyde-terminated gold substrate **5**. (A, B) Aldehyde-terminated gold substrate **5** before printing. (C, D) Imine patterns after printing of ODA. (E, F) Removal of imine patterns after acid catalyzed hydrolysis.

3.4.   Printing and erasing patterns of fluorescent molecules

In order to visualize the patterns and quantify the formation of immobilized imines, a reversible and recyclable covalent patterning method of aldehyde substrate **11** with the fluorescent amine lucifer yellow was developed. As described above, an indirect and a direct patterning approach was used. In the indirect patterning protocol, octadecyltrichlorosilane (ODS) patterns were microcontact printed on a silicon oxide surface.[28] Aldehyde-terminated monolayer **11** was deposited in between the ODS lines and reacted with fluorescent molecules *via* the imine bond. The fluorescent patterns were visible in a confocal microscope (Figure 3-7A). This fluorescent pattern was hydrolyzed with an acetic acid solution at pH 3 (Figure 3-7B),

recycled and reacted again with lucifer yellow (Figure 3-7C). These patterns were also hydrolyzed and a third cycle of the same reactions was carried out. In order to once more confirm imine formation on the surface, the patterned imine SAM (Figure 3-7A and -7C) were exposed to a reducing agent, sodium borohydride in ethanol, which converts imines into secondary amines. The presence of generated secondary amines was confirmed by reaction with aqueous acetic acid solution (which hydrolyzes imines but not amines) as confirmed by confocal microscopy (Figure 3-7D).
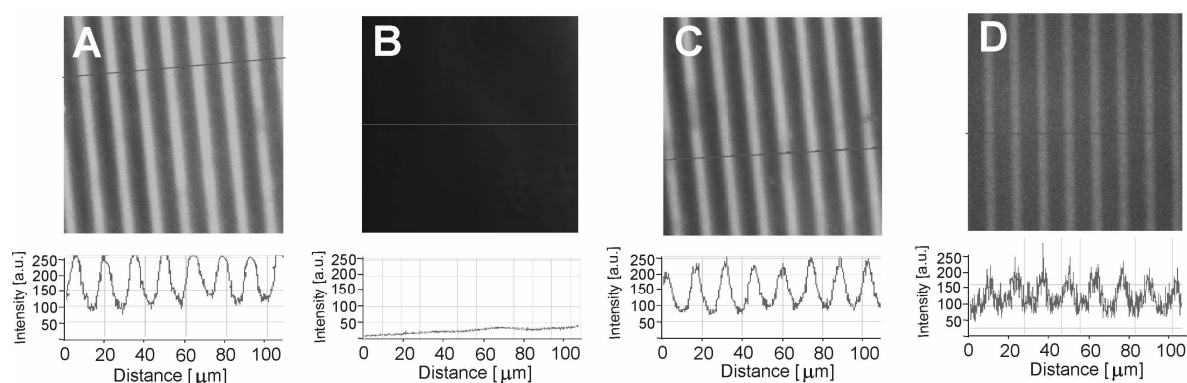

Figure 3-7. Confocal microscopy (scale 110 x 110 μm^2) of imine patterns formed through reaction between lucifer yellow (from solution) and aldehyde-terminated SAM **11** patterned through μCP on glass slides. (A) Image of imine pattern, (B) after acid catalyzed hydrolysis, (C) recycled monolayer (after third cycle of reactions), (D) after reduction with sodium borohydride and subsequent acid catalyzed hydrolysis.

In the direct patterning protocol, the reactant lucifer yellow was microcontact printed with an oxidized PDMS (oxPDMS) stamp directly onto aldehyde substrate **11** (Figure 3-8F). The printing time was 1 min. Fluorescent patterns could be removed from the surface through acid catalyzed hydrolysis (not shown).

Figure 3-8 illustrates the relation between conversion and reaction time for the reaction from the solution (the concentration of the solution of lucifer yellow was 1 mM, identical to the ink solution in the above experiment) and *via* direct microcontact printing. Pre-patterned glass slides were immersed in lucifer yellow solution for 5 min, 15 min, 30 min, 1 h, or 2 h. The fluorescence intensity increases with increasing reaction time (Figure 3-8A-E). From the intensity profile it can be concluded that to have a high degree of immobilization of lucifer yellow only 1 min of contact time is required in direct patterning by μCP while to obtain the same degree of immobilization at least 1 h of the reaction in solution is necessary. This

spectacular rate enhancement is characteristic for nanoscale confinement of the reagents between stamp and substrate.[29]
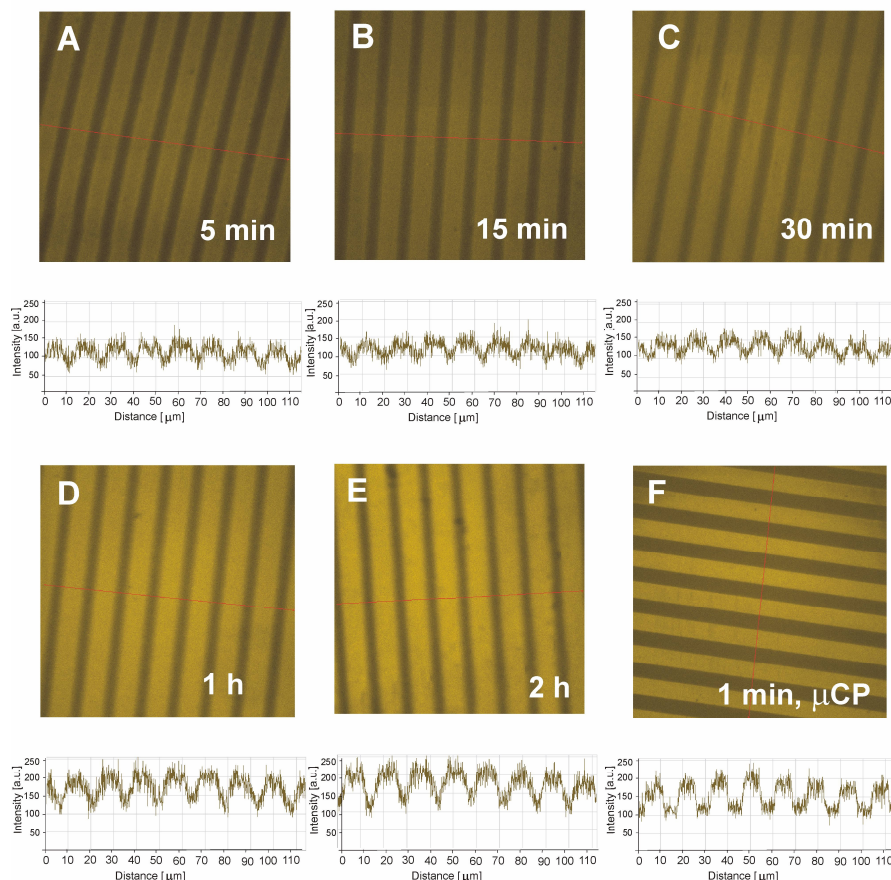

Figure 3-8. Confocal microscopy (scale 110 x 110 μm^2) of patterns obtained from reaction between lucifer yellow and patterned ODS/**12** SAMs, A) after 5 min of reaction time, B) 15 min, C) 30 min, D) 1 h, E) 2 h, F) after 1 min contact time of direct μCP of lucifer yellow on aldehyde-terminated SAM **11**.

3.5. Conclusions

Consistent experimental evidence that imine SAMs can be formed by reaction of an amine SAM with an aldehyde from solution or by reaction of an aldehyde SAM with an amine from the solution have been provided. Also, two methods for the reversible patterning of gold and silicon oxide surfaces via imine chemistry have been shown. The first is the reaction of patterned amino-terminated SAMs with aldehydes. The second approach is to microcontact print amines on aldehyde-terminated SAMs. These patterns are stable in water but erased by acid catalyzed hydrolysis. With lucifer yellow as a fluorescent marker, these patterned substrates could be recycled and used again for imine formation with no loss of resolution. Formation of imines on the surface has advantages over numerous other reversible systems because it does not require harsh conditions or sophisticated catalysts and it does not need

special, expensive facilities. The patterns can be quickly generated, removed and regenerated. "Microcontact chemistry"- chemistry in the contact region between a stamp and a SAM substrate - is a versatile tool to create chemical surface patterns and arrays.

3.6.   Experimental section

Materials. The following materials and chemicals were used as received: 11-aminoundecanethiol (11-AUT, Dojindo Laboratories), octadecanethiol 98% (ODT, Acros), propanal 99+% (Acros), pentanal 98% (Acros), decanal 95% (Acros), terephthaldialdehyde 99% (Aldrich), poly(dimethylsiloxane) (PDMS) (Dow Corning), N-[3-(trimetoxysilyl)propyl]ethylenediamine (TMSPEDA) 97% (Aldrich), octadecyltrichlorosilane 95% (ODS, Acros), *N*-(2-aminoethyl)-4-amino-3,6- disulfo-1,8-naphthalimide, dipotassium salt (lucifer yellow ethylenediamine,) (Molecular Probes), $NaBH_4$ (Aldrich). All solvents were HPLC grade, and all other reagents were analytical grade. Other solvents or reagents were purchased from either Aldrich or Sigma.

Monolayer formation. Gold substrates. Gold substrates were obtained from Ssens BV (Hengelo, The Netherlands) as a layer of 20 nm gold on titanium (2 nm) on silicon. Before use, the substrates were treated with piranha solution for 15 s (concentrated H_2SO_4 and 33% aqueous H_2O_2 in a 3:1 ratio) *(Warning! Piranha solution should be handled with caution: it has been reported to detonate unexpectedly.)*, rinsed with water (MilliQ) and ethanol. Self-assembled monolayers were prepared by immersing the freshly cleaned gold substrates in a 1 mM ethanolic solution of 11-AUT at room temperature for 14 h. The SAMs were rinsed with ethanol, triethylamine/ethanol (1:1) to ensure all amines were deprotonated, and dried under a stream of nitrogen**.**

Silicon substrates. Si(100), p-doped 2 x 2 cm silicon substrates and microscope glass slides were used for monolayer preparation. Prior to monolayer formation, the substrates were oxidized by immersion in boiling piranha for 30 min, rinsed with copious amount of MilliQ water, and dried under a stream of nitrogen. The wafers treated in this way are rich in hydroxyls at the oxide surface and suitable for silanization. Substrates were exposed to a 0.1 vol. % TMSPEDA in dry toluene (freshly distilled over sodium) for 1h. Following monolayer formation, the substrates were rinsed with toluene to remove any excess of silanes and subsequently dried in a stream of nitrogen.

Imine formation on gold and silicon substrates. Amine-terminated substrates were reacted with propanal, pentanal, and decanal (1 mM solution in ethanol) respectively, for 3 h. After the imine formation, the substrates were removed, sonicated in ethanol for 30 s, rinsed with ethanol and dried with nitrogen. Amine-terminated surfaces (11-AUT on gold or TMSPEDA on silicon oxide) were also reacted with terephthaldialdehyde 1 mM aqueous solution for 30 min to obtain aldehyde-terminated SAM. Subsequently the substrates were removed from the solution, rinsed with copious volume of MilliQ water and dried under stream of nitrogen.

Patterning of gold substrates. PDMS stamps were prepared according to published procedures.[20,30] The stamp was inked with a solution of ODT (1 mM) in ethanol for 1 min, dried under stream of nitrogen and placed on the clean gold surface. After 1 min contact time the stamp was lifted off and the substrate washed vigorously with ethanol. The remaining bare gold areas were filled by exposing the sample to ethanolic solution of 11-AUT (1 mM) for 1 h. The substrate was rinsed with ethanol, dried with nitrogen and placed in 1 mM solution of decanal in ethanol for 3 h. After reaction time the substrate was rinsed with ethanol and dried with nitrogen.

Printing amines on aldehyde-terminated gold substrate. Aldehyde-terminated monolayer on gold substrate was prepared according to method presented above. Here we used a SEBS stamp,[31] which showed better results than a PDMS stamp to print ODA. The stamp was immersed in 1 mM ethanolic solution of ODA for 1 min, blown dry with N_2 and brought into conformal contact with aldehyde-terminated gold substrate for 1 min. After that time the stamp was removed and the substrate was rinsed vigorously with ethanol and dried with nitrogen. The pattern was removed by acid catalyzed hydrolysis in aqueous acetic acid solution (pH 3) for 1 h at room temperature. After hydrolysis the substrate was rinsed well with water and ethanol, sonicated in ethanol for 5 min, rinsed again with ethanol and dried with nitrogen.

Preparation of patterned substrates for confocal microscopy. A PDMS stamp was inked with a solution of an ODS (1 mM) in toluene, dried under a stream of nitrogen, and placed on freshly cleaned silicon substrate for 1 min. After that time the stamp was lifted off and the substrate washed with toluene, and immersed for 30 min in 1 mM solution of TMSPEDA in toluene. The substrate was rinsed vigorously with toluene, dried with nitrogen and placed in 1 mM aqueous solution of terephthaldialdehyde for 30 min. Subsequently the substrate was

washed with water and immersed in 0.1 mM aqueous solution of lucifer yellow for 1 h. Finally, the substrate was sonicated in water for 5 min.

Printing amines on aldehyde-terminated glass slides. Aldehyde-terminated glass slides were prepared according to procedures mentioned above. PDMS stamps were oxidized in UV/ozone reactor for 1 h, placed in water to maintain hydrophilic properties of the stamp and subsequently immersed in 1 mM aq. solution of lucifer yellow for 1 min. Before printing the stamp was blown dry in a stream of nitrogen. The stamp was brought into conformal contact with the substrate for 1 min. After that time the stamp was removed and the substrate rinsed with copious volume of water, blown dry with N_2 and imaged with laser scanning confocal microscope. Subsequently the pattern was removed by acid catalyzed hydrolysis in aqueous acetic acid solution (pH 3) for 1 h at room temperature. After hydrolysis the substrate was rinsed well with MilliQ water, sonicated in water for 5 min, rinsed with water and ethanol and dried with nitrogen.

Hydrolysis of imines. Silicon or gold substrates coated with imine SAMs were immersed in aqueous acetic acid solution (pH 3) for certain reaction times and temperatures depending on imine properties.

Reduction of imines on the surface. Imine patterns on the glass slides were obtained according to procedures presented above and immersed for 1 h in 0.25 M ethanolic solution of sodium borohydride at room temperature. After reaction the substrates were rinsed vigorously with ethanol and dried with nitrogen.

Instrumentation. *Contact angle measurements.* Contact angles were measured on a Krüss G10 goniometer, equipped with a CCD camera. Advancing and receding contact angles (θ_a and θ_r) were determined automatically during growth and shrinkage of the droplet by a drop shape analysis. MilliQ water (18.4 MΩ cm) as a probe liquid. Both angles (advancing and receding) were measured on at least three different locations on each sample.

FT-IRRAS. Polarized FT-IRRAS spectra of 1024 scans at 8 cm^{-1} were obtained using a BioRad FTS-60A spectrometer with a liquid nitrogen-cooled cryogenic mercury cadmium telluride detector and RAS accessory (BIO-RAD).

Atomic force microscopy (AFM) imaging. AFM measurements were carried out with a digital multimode Nanoscope III (Digital Instruments, Santa Barbara, CA, USA) scanning force

microscope in contact mode, with 512 x 512 data acquisitions, using V-shaped Si_3N_4 AFM tips (Nanoprobes, Digital Instruments) with a nominal spring constant of 0.32 N/m. The scan angle was set to 90º. Typical scan rates of 1-2 Hz were used to acquire the data. All imaging was conducted at room temperature in air.

Laser scanning confocal microscopy. Confocal microscopy images of the microcontact printed substrates were taken on a Carl Zeiss LSM 510 microscope with an excitation Ar laser beam of 458 nm wavelength and a 40x objective was used. The emitted fluorescence was collected on a PMT R6357 spectrophotometer. All confocal microscopy images were acquired in air.

XPS. XPS spectra were obtained on a Physical Electronics Quantera Scanning X-ray Multiprobe instrument, equipped with a monochromatic Al Kα X-ray source operated at 1486.7eV and 25 W. Spectra were referenced to the main C 1s peak set at 284.0 eV. XPS data were collected from a surface area of 1000 μm x 300 μm with a pass energy of 224 eV and a step energy of 0.8 eV for survey scans and 0.4 eV for high-resolution scans at a 45˚ take-off angle, whereas the angle between sample surface and the X-ray beam was 90˚. For quantitative analysis, the sensitivity factors used to correct the number of counts under each peak were as follows: C 1s, 1.00; N 1s, 1.59. Charge neutralization was achieved by low-energy electrons and low-energy Ar ions.

Electrochemical measurements. Electrochemical experiments were performed in a conventional electrochemical cell containing a three-electrode system. A Pt plate and a saturated calomel reference electrode (SCE) were used as a counter and reference electrode, respectively. Impedance spectroscopy measurements were performed in 0.1 M K_2SO_4 between –0.4 V_{MSE} and –0.1 V_{MSE}. Cyclic voltammetric capacitance measurements were conducted in 0.1 M K_2SO_4 and 1 mM $Ru(NH_3)_6Cl_2/Ru(NH_3)_6Cl_3$ (1:1) mixture as a redox probe between –0.7 V_{SCE} and 0 V_{SCE} at scan rates ranging from 0.1 V/s to 2 V/s. A gold disk electrode with a diameter of 2.2 mm (geometric surface of 3.8 mm^2) was used for electrochemical measurements.

3.7. References

[1]   A. Ulman, *An Introduction to Ultrathin Organic Films*, Academic Press, Boston, **1991**.

[2]   S. Onclin, B. J. Ravoo, D. N. Reinhoudt, *Angew. Chem. Int. Ed.* **2005**.

[3]   A. Ulman, *Chem. Rev.* **1996**, *96*, 1533-1554.

[4]   T. Pfohl, J. H. Kim, M. Jasa, H. P. Miller, G. C. L. Wong, F. Bringezu, Z. Wen, L. Wilson, M. W. Kim, Y. Li, et al., *Langmuir* **2001**, *17*, 5343-5351.

[5]   P. Ghosh, W. M. Lackowski, R. M. Crooks, *Macromolecules* **2001**, *34*, 1230-1236.

[6]   H. Li, D.-J. Kang, M. G. Blamire, W. T. S. Huck, *Nano Lett.* **2002**, *2*, 347-349.

[7]   U. Schmelmer, R. Jordan, W. Geyer, W. Eck, A. Gölzhäuser, M. Grunze, A. Ulman, *Angew. Chem. Int. Ed.* **2003**, *42*, 559-563.

[8]   S. Pathak, A. K. Singh, J. R. McElhanon, P. M. Dentinger, *Langmuir* **2004**, *20*, 6075-6079.

[9]   D. Qin, Y. Xia, B. Xu, H. Yang, C. Zhu, G. M. Whitesides, *Adv. Mater.* **1999**, *11*, 1433.

[10]   R. Chakrabarti, A. M. Klibanov, *J. Am. Chem. Soc.* **2003**, *125*, 12531-12540.

[11]   M. C. Pirrung, J. D. Davis, A. L. Odenbaugh, *Langmuir* **2000**, *16*, 2185-2191.

[12]   L. A. Kung, L. Kam, J. S. Hovis, S. G. Boxer, *Langmuir* **2000**, *16*, 6773-6776.

[13]   E. A. Smith, M. J. Wanat, Y. Cheng, S. V. P. Barreira, A. Frutos, R. M. Corn, *Langmuir* **2001**, *17*, 2502-2507.

[14]   P. Rigler, W. P. Ulrich, P. Hoffmann, M. Mayer, H. Vogel, *ChemPhysChem* **2003**, *4*, 268-275.

[15]   Y.-Y. Cheng, C. H.-C., G. Hoops, M.-C. Su, *J. Am. Chem. Soc.* **2004**, *126*, 10828-10829.

[16]   D. Stamou, C. Duschl, E. Delamarche, H. Vogel, *Angew. Chem. Int. Ed.* **2003**, *42*, 5580-5583.

[17]   Y. Zhu, C. Gao, X. Liu, J. Shen, *Biomacromolecules* **2002**, *3*, 1312-1319.

[18]   A. K. Vogt, L. Lauer, W. Knoll, A. Offenhäuser, *Biotechnol. Prog.* **2003**, *19*, 1562-1568.

[19]   W.-S. Yeo, M. N. Yousaf, M. Mrksich, *J. Am. Chem. Soc.* **2003**, *125*, 14994-14995.

[20]   Y. N. Xia, G. M. Whitesides, *Angew. Chem. Int. Ed.* **1998**, *37*, 551-575.

[21]   E. Delamarche, H. Schmid, A. Bietsch, N. B. Larsen, H. Rothuizen, B. Michel, H. Biebuyck, *J. Phys. Chem. B* **1998**, *102*, 3324-3334.

[22]   T. P. Sullivan, W. T. S. Huck, *Eur. J. Org. Chem.* **2003**, 17-29.

[23]   M. W. J. Beulen, J. Bugler, M. R. de Jong, B. Lammerink, J. Huskens, H. Schönherr, G. J. Vancso, B. A. Boukamp, H. Wieder, A. Offenhäuser, et al., *Chem. Eur. J.* **2000**, *6*, 1176-1183.

[24]   T. Auletta, B. Dordi, A. Mulder, A. Sartori, S. Onclin, M. C. Bruinink, M. Péter, C. A. Nijhuis, H. Beijleveld, H. Schönherr, et al., *Angew. Chem. Int. Ed.* **2004**, *43*, 369-373.

[25]   A. Mulder, S. Onclin, M. Péter, J. P. Hoogenboom, H. Beijleveld, J. ter Maat, M. F. García-Parajó, B. J. Ravoo, J. Huskens, N. F. van Hulst, et al., *Small* **2005**, *1*, 242-253.

[26]   A. Frutos, J. Brockman, R. M. Corn, *Langmuir* **2000**, *16*, 2192-2197.

[27]   D. Peelen, L. M. Smith, *Langmuir* **2005**, *21*, 266-271.

[28]   N. L. Jeon, K. Finnie, K. Branshaw, R. G. Nuzzo, *Langmuir* **1997**, *13*, 3382-3391.

[29]   X.-M. Li, V. Paraschiv, J. Huskens, D. N. Reinhoudt, *J. Am. Chem. Soc.* **2003**, *125*, 4279-4284.

[30]   B. Michel, A. Bernard, A. Bietsch, E. Delamarche, M. Geissler, D. Juncker, H. Kind, R. J.-P., H. Rothuizen, H. Schmid, et al., *IBM J. Res. & Dev.* **2001**, *45*, 697-719.

[31]   D. Trimbach, K. Feldman, N. D. Spencer, D. J. Broer, C. W. M. Bastiaansen, *Langmuir* **2003**, *19*, 10957-10961.

Chapter 4

Directional movement of dendritic macromolecules on gradient surfaces[*]

A gradient driven methodology has been developed to manipulate the movement of dendritic macromolecules. Poly(propyleneimine) dendrimers, labeled with rhodamine B, are attached to glass substrates via multiple imine bonds. The dendrimers are able to move on the surface by the hydrolysis and reformation of these imine bonds. In the absence of al stimulus, this random movement results in a two-dimensional diffusion on the substrate. However it is possible to bias the movement of the dendrimers by means of an aldehyde gradient on the glass substrate.

4.1. Introduction

Chemotaxis,[1] the response of cells to chemical gradients by directed movement, is a universal phenomenon that is vital to the survival of both microorganisms and multicellular organisms. For example, bacteria are able to sense changes in concentrations of certain chemicals and move toward or away from this chemical by means of altering its tumbling frequency.[2] Likewise, multicellular organisms are able to fight off bacterial infections using white blood cells (neutrophils) that are able to sense chemicals left by bacteria to find and destroy the invading microorganisms. Hence, directional sensing and response play a central role in health and diseases.[3] Fundamentally, the same principles should apply for particles of any size that are able to sense and respond to a gradient, although the mechanism may be completely different.[4,5] In this Chapter, the directed movement of dendritic macromolecules on the glass substrates which contain a density gradient of aldehyde functionality is presented.

Dendrimers have been used in a variety of applications[6-12]; in this case it is the multivalent, globular nature and their ability to deform their shape that is essential for gradient sensing. For our purposes, the dendrimers need to be attached to the substrate, yet have some freedom to move about on the surface, to 'sense' and respond to their environment. This freedom requires that their attachment to the surfaces be reversible to allow the dendrimer to move across the substrate.

Substrates that contain a density gradient[13-19] of self-assembled monolayers, particles or polymers display a gradual change in the chemical and physical properties along their length. Such substrates found an application in directional movement of cells,[20,21] molecules,[22] and immobilization of liquid crystals.[23] Moreover, gradient substrates can serve as an array of surface compositions to be explored within a single experiment.[24]

There are many techniques to prepare the gradient surfaces but the most commonly used are gradual immersion,[4,25,26] contact printing,[27] microfluidic flow,[19,28] microstructuring,[29] thermal[30] and vapor-phase diffusion,[31-35]chemical potential distribution and electrochemical methods,[36-38] photolithographic methods,[39,40] photopolymerization,[41] and corona treatment.[42] In addition, numerous molecules were used to form gradient surfaces, for instance proteins,[19,43-45] thiols,[4,46] alkylsilanes,[34,39] polymer brushes[46] and other.

When the gradient surface is used for the attachment of molecules, one can expect that more molecules will be attached to the part of the substrate that has more reactive groups on the surface. Here, the question would be: what can one expect from a dendrimer, which possesses more than one anchoring group, placed on the surface with the density gradient? An amine terminated dendrimer will attach to a surface containing aldehyde groups by imine

condensation. One or more of these imine bonds can hydrolyze,[47] giving the dendrimer additional freedom to move about and attach itself via imine formation with another aldehyde on the surface. The net result is random motion on the surface, resembling a random walk. In the presence of a gradient, it is more likely for the dendrimer to move in one direction (with the gradient) as it is statistically more likely to form imine bonds where more aldehyde groups are present. The number of imine bonds formed between the two will depend on the availability and proximity of amine and aldehyde groups. On a 5th generation dendrimer there are 64 amine groups, some (approximately 8) of which are used to attach rhodamine labels so it is possible to follow by fluorescence. Although dendrimers do deform on surfaces, flattening to maximize favorable interactions, not all of the amine groups are accessible at the same time for attachment to the surface, hence when the dendrimer moves around, those free amine groups are free to react with aldehyde groups on the substrate.

4.2. Gradient formation and microcontact printing of dendrimers

Reactive aldehyde substrates were prepared by reacting glass slides with trimethoxysilylalkylaldehyde. The aldehyde gradients are achieved by a modified reverse dip-coating procedure, whereas the control substrates were prepared by full immersion of the substrate for a specified amount of time. The dendrimers are labeled with rhodamine B by reacting the 5th generation dendrimer with 8 equiv. rhodamine B isothiocyanate. The resulting labelled dendrimers were applied onto the substrate by microcontact printing. The printed substrates were fully immersed in water overnight then analyzed using confocal microscopy.
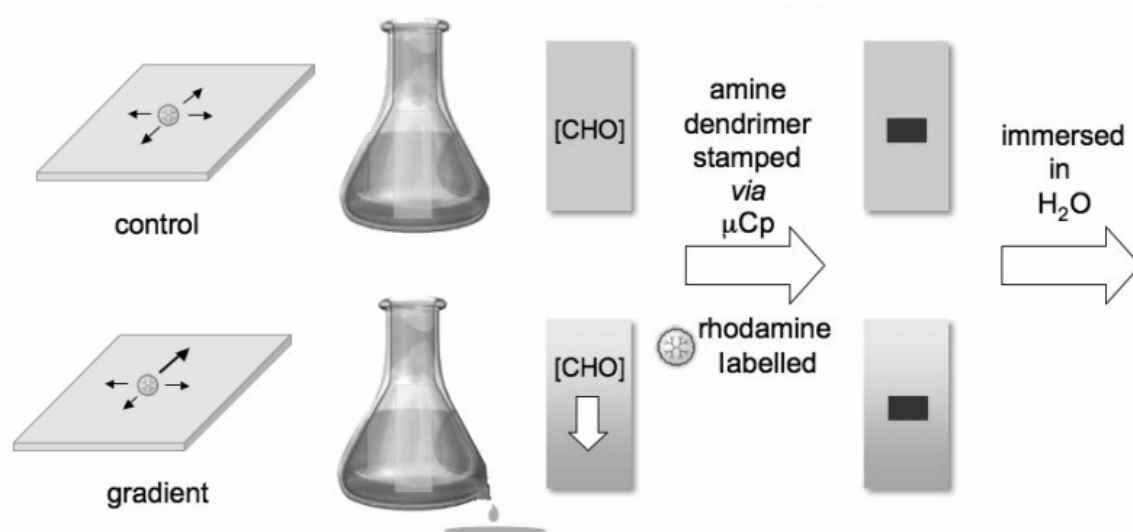

Figure 4-1. Substrate preparation by modified dip coating procedure and microcontact printing of rhodamine-labelled PPI dendrimers.

The fluorescent microscope images of the top and bottom of a rectangular pattern of dendrimers printed on a glass substrate before and after overnight immersion in water are shown in Figure 4-2.
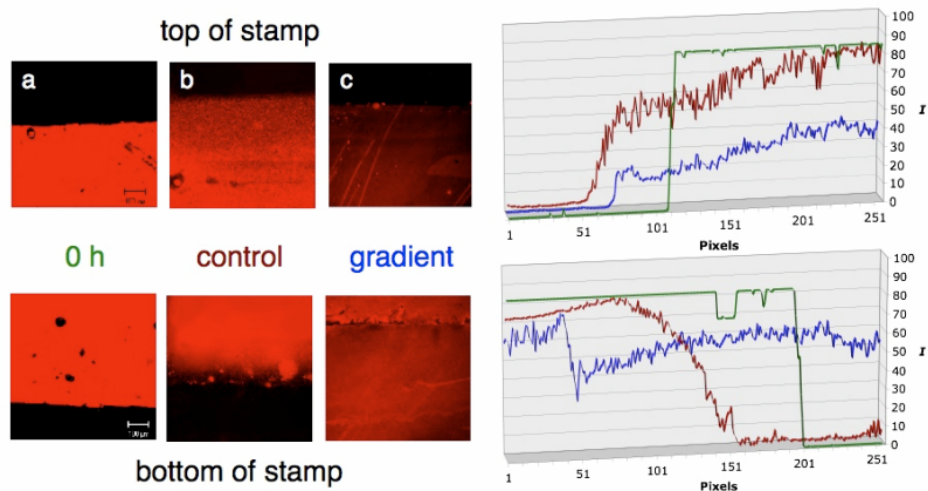

Figure 4-2. Fluorescent confocal microscopy images of the top and bottom edges of stamped dendrimer regions (700 μm x 700 μm), (a) before immersion on a uniform aldehyde substrate, (b) after 16 h of immersion in water and (c) after 16 h immersion on a 15 min gradient substrate. The graphs on the right show the average fluorescence intensity profiles of each picture from top to bottom (left green, middle red, right blue). The graphs were calculated by taking the average fluorescence of six lines in the images from the top to the bottom of the images. The maximum intensity is 255 for white light, since only red light is emitted, the relative maximum is 85. Defects in the stamp and/or the substrate are also taken into account as evidenced by regions of reduced fluorescence.

Before immersion, the image is sharp as can be observed by the edges of the pattern as well as defects in the stamp. This can be seen clearly in the fluorescence intensity graphs, where sharp slopes can be seen at the edges of the stamp. After immersion, the patterns are blurred as a consequence of diffusion of the dendrimers. In the absence of a gradient, we see that the edges are no longer clear, there is migration of dendrimer away from where they were originally stamped and the amount of migration is similar on all edges. The fluorescence intensity is lower after immersion which can be attributed to loss of dendrimers that were either attached to other dendrimers or that were weakly bound. Dendrimers on the gradient substrate, however, appear to move with the gradient. On the top of the stamp, the edge remains sharp whereas at the bottom, large amount of fluorescence past the edge of the stamp.

To observe the behavior of dendrimers on the surfaces of different aldehyde concentrations, smaller patterns were printed using these fluorescent labelled dendrimers. Figure 4-3 shows one such example where circles of approximately 100 μm in diameter are

printed. The pattern is less defined after immersion, the circles are less intense in fluorescence and fluorescence can be detected between the circles. The behavior of the dendrimers is very different and is dependent upon the local aldehyde concentration of the gradient. Towards the top of the stamp with the smallest aldehyde density, depicted in Figure 4-3c, there is minimal diffusion of the dendrimers from their starting positions. Further down the gradient (Figure 4-3d) the movement of dendrimer primarily along the gradient was observed, resulting in an elongation of the pattern. With higher aldehyde concentration, the pattern becomes less defined and diffusion appears to be faster at these concentrations (Figure 4-3e-f).
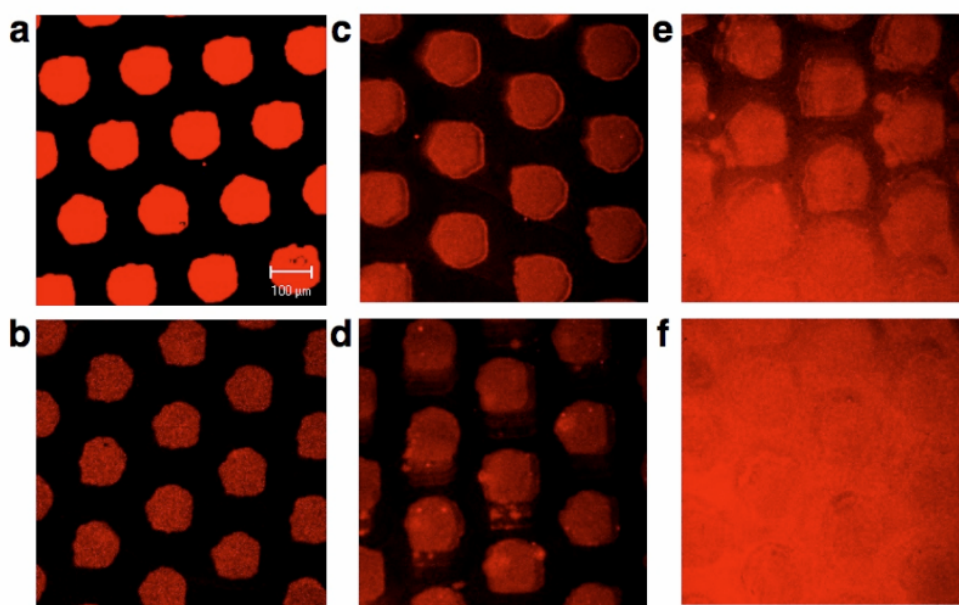
Figure 4-3. Fluorescent confocal microscope images of dendrimers stamped using microcontact printing with circles of ~100 μm in diameter. (a) before immersion, and (b) a uniform aldehyde substrate and (c) – (f) gradient substrates with increasing aldehyde concentrations, after 16 h immersion in water.

It can be seen that dendrimers accumulate at higher aldehyde concentration and it can be observed that dendrimers are almost evenly distributed at regions of higher local aldehyde concentration.

The fluorescence intensity profiles (Figure 4-4) show the preference of dendrimers to migrate toward higher aldehyde concentrations. The edges of the patterns are sharp (Figure 4-4a) before immersion and become less defined after immersion for either the control (Figure 4-4b) or gradient (Figure 4-4c) substrates. In the absence of a gradient (4b) there is some migration in all directions as seen by the slightly shallower slope. With a gradient, the dendrimers exhibit directional preference as indicated by the steep slope on the edges against the gradient and a more gradual change in fluorescence intensity when the dendrimers are moving with the gradient.
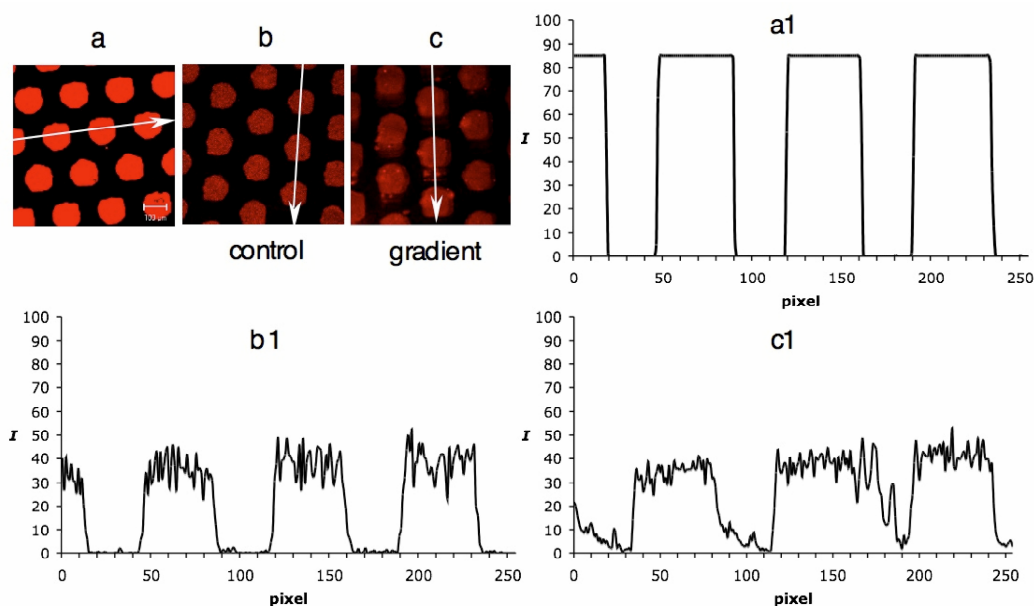
Figure 4-4. Averaged fluorescence profiles and their corresponding fluorescent confocal microscope images of dendrimers (a) before immersion and (b) control and (c) gradient substrates, after 16 h of immersion.

4.3. Conclusions

From these experiments it appears that the diffusion rate increases with increasing aldehyde concentrations. This may initially seem unexpected since a smaller number of attachments to the surface should allow for greater dendrimer mobility. At "low" aldehyde concentration, the dendrimer does have a larger degree of freedom but there are less aldehyde groups available around the dendrimer to allow movement. In addition, once an imine bond is hydrolyzed, there is a relatively high local amine concentration (since few imine bonds are formed, there are many free amine groups) and an imine bond can form between the same aldehyde with another amine on the same dendrimer. The converse should be true for very high aldehyde concentrations. In this case, when an imine bond is hydrolyzed, the free amine can react with another nearby aldehyde group. At this aldehyde concentration, there are probably so many imine bonds between the dendrimer and the surface that there is limited dendrimer movement. There is therefore only a certain aldehyde concentration/gradient range across which biased migration can be observed.

4.4. Experimental section

Materials. The following materials and chemicals were used as received: poly(dimethylsiloxane) (PDMS) (Dow Corning), trimethoxysilylalkylaldehyde (Fluorochem, UK), rhodamine B isothiocyanate (Sigma), dendrimers (PPI, G5) (Aldrich). All solvents were

HPLC grade, and all other reagents were analytical grade. Other solvents or reagents were purchased from either Aldrich or Sigma.

Modification of glass slides. Clean microscope cover glass (Paul Marienfeld Gmbh & Co.KG, Germany) was activated with piranha solution for 45 min (concentrated H_2SO_4 and 33 % aqueous H_2O_2 in a 3:1 ratio) *(Warning! Piranha solution should be handled with caution: it has been reported to detonate unexpectedly.)*, rinsed with water (MilliQ) and immediately immersed in 0.1 vol. % trimethoxysilylalkylaldehyde in toluene for 1 h. Following monolayer formation, the substrates were rinsed with toluene to remove any excess of silanes and subsequently dried in N_2.

Gradient formation. Clean microscope cover glass (size 22 x 40 mm, Paul Marienfeld Gmbh & Co.KG, Germany) was activated with piranha solution for 45 min (concentrated H_2SO_4 and 33 % aqueous H_2O_2 in a 3:1 ratio) *(Warning! Piranha solution should be handled with caution: it has been reported to detonate unexpectedly.)*, rinsed with water (MilliQ) and immediately immersed vertically in an erlenmeyer flask containing a solution of 0.1 vol. % trimethoxysilylalkylaldehyde in toluene. The reagent was removed from the flask via a drip spout; hence the top of the substrate will have the least reaction time and the bottom of the slide the most reaction time to form the gradient. The reaction time was 15 min. The steepness of the gradient will depend on the rate of reactant removal. Hence the slower the solution is drained, the steeper the gradient since the top and bottom of the substrate will have the larger difference in reaction time.

Fabrication of stamps. Silicon wafer-based masters with etched structures were prepared by UV photolithography. The master surface was fluorinated using fluorosilanes. PDMS stamps were fabricated by curing Sylgard 184 on the surface of the master at 60 °C for 12 h.

Microcontact printing of dendrimers. The PDMS stamp was immersed in 1 mM ethanolic solution of dendrimers for 30 s. The stamp was dried with nitrogen and brought into conformal contact with the aldehyde-terminated glass slide for a min. After printing, the stamp was lifted off and the substrate was rinsed with ethanol and subsequently dried with nitrogen.

Immersion of the substrates. The substrates were placed for 16 h in MilliQ water horizontally. The angle the substrate is placed while immersed in water does not appear to make any difference in the direction or amount of diffusion. All the images presented in this letter are immersed horizontally.

4.5. References

[1] M. C. Eisenbach, *Chemotaxis*, Imerial Collage Press, London, UK, **2004**.

[2] R. M. Macnab, D. E. Koshland, *Proc. Nat. Acad. Sci. USA* **1972**, *69*, 2509-2512.

[3] P. Devreotes, C. Janetopoulos, *J. Biol. Chem.* **2003**, *278*, 20445-20448.

[4] T. Kraus, R. Stutz, T. E. Balmer, H. Schmid, L. Malaquin, N. D. Spencer, H. Wolf, *Langmuir* **2005**, *21*, 7796-7804.

[5] H. Liu, Y. Ito, *J. Biomed. Mater. Res.* **2003**, *67*, 1424-1429.

[6] B. Helms, E. W. Meijer, *Science* **2006**, *18*, 929-930.

[7] J. M. Frechet, *Science* **1994**, *25*, 1710-1715.

[8] M. S. Lavine, *Science* **2004**, *30*, 651-653.

[9] S. C. Zimmerman, F. Zeng, D. E. C. Reichert, S. V. Kolotuchin, *Science* **1996** *271*, 1095-1098.

[10] D. Bradley, *Science* **1995**, *22*, 270.

[11] R. F. Service, *Science* **1995**, *27*, 458-459.

[12] J. F. G. A. Jansen, E. M. M. de Brabander-van den Berg, E. W. Meijer, *Science* **1994**, *18*, 1226-1229.

[13] X. Wang, R. T. Haasch, P. W. Bohn, *Langmuir* **2005**, *21*, 8452-8459.

[14] S. Jayaraman, A. C. Hillier, *J. Comb. Chem.* **2004**, *6*, 27-31.

[15] S. Morgenthaler, S. Lee, S. Zürcher, N. D. Spencer, *Langmuir* **2003**, *19*, 10459-10462.

[16] B. Liedberg, P. Tengvall, *Langmuir* **1995**, *11*, 3821-3827.

[17] K. A. Fosser, R. G. Nuzzo, *Anal. Chem.* **2003**, *75*, 5775-5782.

[18] R. H. Terrill, K. M. Balss, P. W. Bohn, *J. Am. Chem. Soc.* **2000**, *122*, 988-989.

[19] N. L. Jeon, S. K. W. Dertinger, D. T. Chiu, I. S. Choi, A. D. Stroock, G. M. Whitesides, *Langmuir* **2000**, *16*, 8311-8316.

[20] B. P. Harris, J. K. Kutty, E. W. Fritz, C. K. Webb, K. J. L. Burg, A. T. Metters, *Langmuir* **2006**, *22*, 4467-4471.

[21] R. C. Gunawan, J. Silvestre, H. R. Gaskins, P. J. A. Kenis, D. E. Leckband, *Langmuir* **2006**, *22*, 4250-4258.

[22] S. Daniel, M. K. Chaudhury, J. C. Chen, *Science* **2001**, *291*, 633-636.

[23] B. H. Clare, K. Efimenko, D. A. Fischer, J. Genzer, N. L. Abbott, *Chem. Mater.* **2006**, *18*, 2357-2363.

[24] N. V. Venkataraman, S. Zurcher, N. D. Spencer, *Langmuir* **2006**, *22*, 4184-4189.

[25] X. Yu, Z. Wang, Y. Jiang, X. Zhang, *Langmuir* **2006**, *22*, 4483-4486.

[26] G. Chen, Y. Ito, *Biomaterials* **2000**, *22*, 24583-24587.

[27] S.-H. Choi, B. Z. Newby, *Langmuir* **2003**, *19*, 7427-7435.

[28] X. Jiang, Q. Xu, S. K. W. Dertinger, A. D. Strook, T. Fu, G. M. Whitesides, *Anal. Chem.* **2005**, *77*, 2338-2347.

[29] A. Shastry, M. J. Case, K. F. Bohringer, *Langmuir* **2006**, *22*, 6161-6167.

[30] A. M. Cazabat, F. Heslot, S. M. Troian, P. Carles, *Nature* **1990**, *346*, 824-826.

[31] M. K. Chaudhury, G. M. Whitesides, *Science* **1992**, *256*, 1539-1541.

[32] S. Daniel, M. J. Chaudhury, *Langmuir* **2002**, *18*, 3404-3407.

[33] R. S. Subramanian, N. Moumen, J. B. McLaughlin, *Langmuir* **2005**, *21*, 11844-11849.

[34] N. Moumen, R. S. Subramanian, J. B. McLaughlin, *Langmuir* **2006**, *22*, 2682-2690.

[35] B. H. Clare, K. Efimenko, D. A. Fischer, J. Genzer, N. L. Abbott, *Chem. Mater.* **2006**, *18*, 2357-2363.

[36]   B. S. Gallardo, V. K. Gupta, F. D. Eagerton, L. I. Jong, V. S. Craig, R. R. Shah, N. L. Abbott, *Science* **1999**, *283*, 57-60.

[37]   R. H. Terrill, K. M. Z. Y. Balss, P. W. Bohn, *J. Am. Chem. Soc.* **2000**, *122*, 988-989.

[38]   T. Sehayek, A. Vaskevich, I. Rubinstein, *J. Am. Chem. Soc.* **2003**, *125*, 4728-4719.

[39]   Y. Ito, M. Heydari, A. Hashimoto, T. Konno, A. Hirasawa, S. Hori, K. Kurita, A. Nakajima, *Langmuir* **2006**.

[40]   K. A. Wier, L. Gao, T. J. McCarthy, *Langmuir* **2006**, *22*, 4914-4916.

[41]   B. P. Harris, A. T. Metters, *Macromolecules* **2006**, *39*, 2764-2772.

[42]   M. S. Kim, K. S. Seo, G. Khang, H. B. Lee, *Bioconjugate Chem.* **2005**, *16*, 245-249.

[43]   C. L. Hypolite, T. L. McLernon, D. N. Adams, K. E. Chapman, C. B. Herbert, C. C. Huang, M. D. Distefano, W.-S. Hu, *Bioconjugate Chem.* **1997**, *8*, 658-663.

[44]   I. Caelen, A. Bernand, D. Juncker, B. Michel, H. Heinzelmann, E. Delamarche, *Langmuir* **2000**, *16*, 9125-9130.

[45]   I. Caelen, H. Gao, H. Sigrist, *Langmuir* **2002**, *18*, 2463-2467.

[46]   C. Xu, T. Wu, C. M. Drain, J. D. Batteas, M. J. Fasolka, K. L. Beers, *Macromolecules* **2006**, *39*, 3359-3364.

[47]   D. I. Rożkiewicz, B. J. Ravoo, D. N. Reinhoudt, *Langmuir* **2005**, *21*, 6337-6343.

Chapter 5

Covalent printing of proteins for cell patterning[*]

Covalent immobilization of cytophilic proteins by microcontact printing (μCP) can be used to pattern cells on substrates. Cytophilic proteins are printed in micropatterns on top of reactive self-assembled monolayers (SAMs) using imine chemistry. In brief, an aldehyde-terminated monolayer on glass or on gold was obtained by the reaction between an amino-terminated monolayer and terephthaldialdehyde. The aldehyde monolayer was used as a substrate for the direct microcontact printing of collagen-derived proteins using an oxidized poly(dimethylsiloxane) (PDMS) stamp. After immobilization of the proteins into adhesive "islands", the remaining areas were blocked with amino-poly(ethylene glycol), which forms a layer that is resistant to cell adhesion. Human malignant (HeLa) cells were seeded and incubated onto the patterned substrate. It was found that the cells adhere and spread selectively on the protein islands, while avoiding the PEG zones. These findings illustrate the importance of microcontact printing as a method for positioning proteins at surfaces. Moreover, they demonstrate the scope of controlled surface chemistry to direct cell adhesion.

5.1. Introduction

Controlling cell positioning and adhesion on surfaces is of interest in fundamental cell biology,[1-3] tissue engineering,[4] cell-based biosensor development,[5, 6] and bioelectronics. Various methods have been used to direct the adhesion of living cells to selected areas of a substrate including micropatterning on polymers,[7] soft lithography,[8-11] patterning through pores in elastomeric membranes,[12] patterning using three dimensional microfluidic systems,[13] laminar flow patterning[14] and local oxidation using microelectrodes.[15,16] One particularly versatile approach to control cell attachment and patterning is the physical or chemical adsorption of extracellular matrix (ECM) proteins to selected areas of a substrate. ECM proteins are cytophilic in the sense that cells preferentially adhere to any surface coated with these proteins. ECM proteins have been locally delivered to a substrate by, for example, ink-jet printing,[17] and electrospray deposition.[18] ECM proteins may also be physisorbed to a substrate patterned with self-assembled monolayers (SAMs) by microcontact printing (μCP).[19-21] Alternatively, proteins may be microcontact printed on a suitable substrate.[22-26] The advantage of microcontact printing is that the size and shape of cell-adhesive patterns can be tailored by designing the required master for poly(dimethylsiloxane) (PDMS) stamp fabrication.

Recently, Huck and co-workers[27] proposed the application of μCP for the *in situ* synthesis of oligopeptides exclusively in the contact areas between substrate and PDMS stamp. The advantage of covalent μCP of peptides is that there is a chemical bond between the protein and the substrate SAM. Hence, there is no diffusion of the pattern on the surface. On the other hand, it is unlikely that elaborate protein patterns can be efficiently prepared by multistep synthesis in the confinement between substrate and stamp.

In this work, aldehyde-terminated SAM on gold and silicon oxide substrates was used as a reactive layer for *covalent* microcontact printing of a cytophilic, collagen-like protein. Specific regions of the SAM were patterned with the cytophilic protein while others were made non-adhesive by immobilization of poly(ethylene glycol) (PEG) molecules. The protein, which was used for the cell attachment was a gelatin-like, hydrophilic protein Col3a1 that is a recombinant of non-hydroxylated gelatin based on the mouse type I and rat type III collagen sequences.[28] Col3a1 was secreted from the methylotrophic yeast *Pichia pastoris*, using the *Saccharomyces cerevisiae* α-mating factor prepro signal.[28] This protein contains the tripeptide RGD (Arg-Gly-Asp) characteristic for cell adhesion. The RGD sequence is present in many ECM proteins such as fibronectin, laminin and collagen. This tripeptide is the minimal structure required for recognition by cell-surface receptors. Studying cell–ECM component interactions can help in understanding cell adhesion phenomena. The Col3a1 protein is a random coil without any

secondary structure, which might favor the exposure of the RGD sequence on the surface and make RGD more readily available for interactions with cell membrane receptors than in conventional ECM proteins.
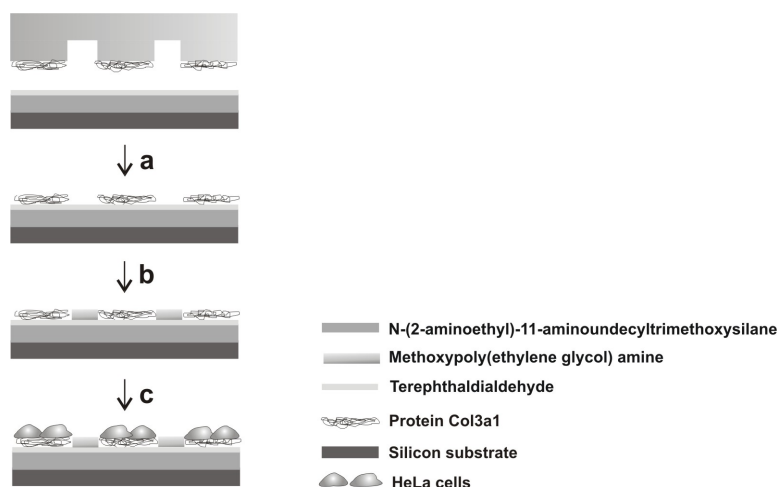

Figure 5-1. Schematic representation of cell patterning via direct microcontact printing of protein Col3a1. a) microcontact printing of Col3a1 onto aldehyde-terminated SAM, b) reaction between remaining aldehyde groups and amino-PEG, c) incubation of HeLa cells.

The methodology is outlined in Figure 5-1. In brief, the gold and silicon oxide substrates were modified with amino-terminated SAMs and then the amino groups were converted into aldehyde groups by the reaction with terephthaldialdehyde (see Chapter 3). Substrates modified in this manner can be directly patterned with collagen-like proteins by microcontact printing using a PDMS stamp. Amino residues in the protein form imine bonds with the aldehyde SAM. The remaining areas of the aldehyde SAM can subsequently be blocked with amino-PEG forming areas resistant to cell adhesion. Human malignant (HeLa) cells were seeded and incubated on the patterned substrates. The cells adhere and spread selectively on the protein islands.

5.2. Surface modification for protein and cell attachment

The protein monolayers presented in Figure 5-2 can be prepared on gold and silicon oxide (or glass) surfaces. The aldehyde-terminated substrates were prepared according to a previously shown procedure (see Chapter 3).
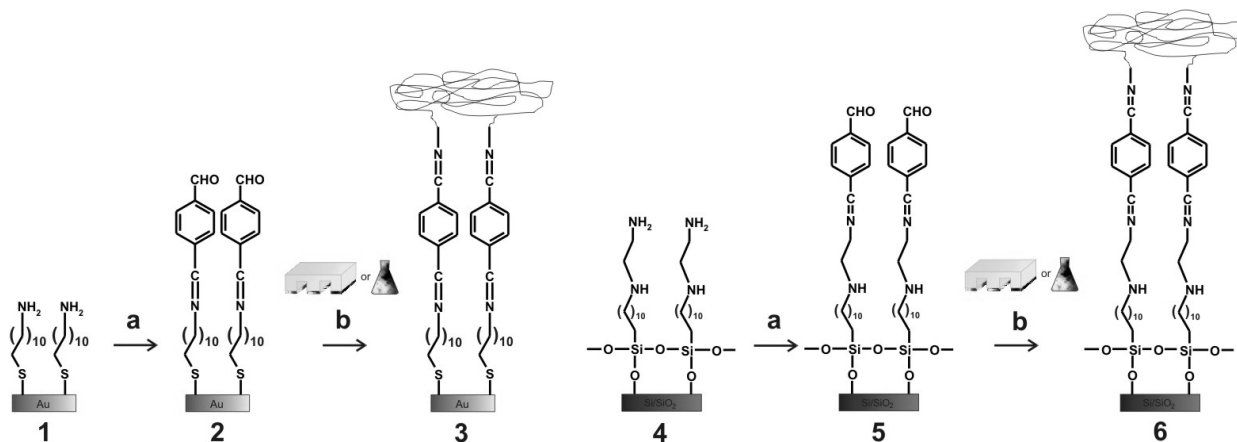
Figure 5-2. Synthetic route to covalent immobilization of protein Col3a1 on the gold and silicon oxide surface. **1**, **4** – amino-terminated substrates, **2**, **5** - aldehyde-terminated substrates, **3**, **6**- substrates with immobilized Col3a1 protein, **a** – terephthaldialdehyde, **b** – proteins Col3a1.

Col3a1 proteins were covalently attached to aldehyde-terminated surfaces by reaction from a 1 mM solution in buffer solution (PBS) at room temperature (**3**, **6**). Also, they were immobilized by direct μCP (using 1 mM solution of Col3a1 in PBS buffer) with a flat, hydrophilic PDMS stamp that was treated with UV/ozone plasma for 30 minutes (**6***). All monolayers were extensively rinsed with PBS, water, and ethanol after each reaction step in order to remove all physisorbed material. The monolayers were characterized by water contact angle goniometry, X-ray photoelectron spectroscopy (XPS), infrared spectroscopy (FT-IRRAS) and ellipsometry measurements.

Table 5-1. Water contact angle (advancing and receding), atomic ratios of elements C, N from XPS, and the ellipsometric thickness of monolayers **1** - **6***.

SAM	θ_{adv} [deg]	θ_{rec} [deg]	C/N (XPS)	C/N (calcd)	Ell. thickness [nm]
1	62±2	50±2	10.6±0.7	11	n. a.
2	77±2	62±2	13.9±0.4	14	n. a.
3	< 10	< 10	9±1.8	10	n. a.
4	57±2	45±2	8±0.6	6.5	2.4±0.2
5	65±2	54±2	12±0.4	10.5	3.14±0.2
6	< 10	< 10	7.2±1.5	10	4.62±0.3
6*	< 10	< 10	8.9±1.2	10	5.3±0.3

θ_{adv} – advancing water contact angle
θ_{rec} – receding water contact angle
n. a. – not available
6*-proteins immobilized on the substrate **6** by direct μCP with flat PDMS stamp.

Values for the water contact angle of monolayers **1-6** are shown in Table 5-1. It is seen that after attachment of hydrophilic protein Col3a1, the water contact angle decreases dramatically (SAMs **3**, **6**, **6***) and the values approach a range beyond the limit of measurement (<10 °). The thickness of the monolayers on the silicon substrates **4-6*** was investigated by ellipsometry (Tale 5-1). It was observed that the thickness of the monolayers increases after each synthesis step and is consistent with the anticipated values. Furthermore, the C/N ratios from XPS measurements for amine and aldehyde SAMs are in agreement with the molecular composition and C/N ratio of the protein monolayers **3, 6, 6*** is in accordance with the molecular composition of protein Col3a1. The protein is exposed on the surface and at the same time is shielding the underlying monolayer. The variation of the XPS signal intensity as a function of take-off angle may give information about the vertical position of the corresponding element within the depth sampled by XPS. The intensity was translated into an atomic concentration and the dependence of the take-off angle was plotted in Figure 5-3. Angle dependent XPS measurements of **3** show that the atomic concentration of Au (4f) increases as a function of electron take-off angle, while the atomic concentration of C (1s) and N (1s) decrease. (The variation of concentration of O (1s) is smaller than the experimental error.). These findings confirm that the protein is absorbed on top of the SAM on gold.
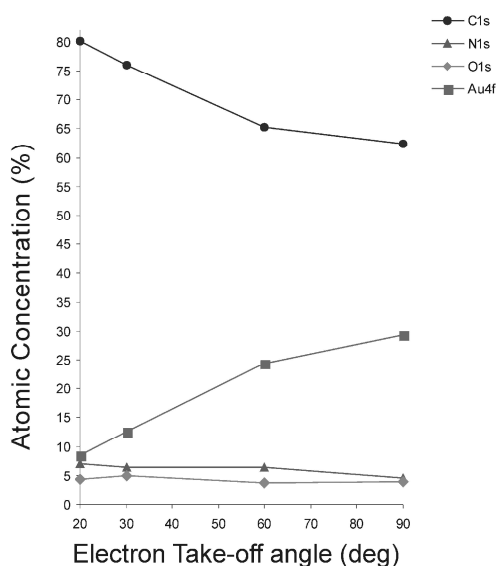

Figure 5-3. XPS atomic concentrations of C (1s), N (1s), O (1s) and Au (4f) after immobilization of protein Col3a1 onto aldehyde-terminated monolayer 3 measured at different electron take-off angles.

After each synthetic step, the surface was thoroughly rinsed with the proper solvent and dried under a nitrogen stream before Fourier transform infrared reflection-adsorption spectroscopy (FT-IRRAS) spectra were collected (Figure 5-4). After exposure of the 11-aminoundecanethiol (11-AUT) SAM **1** (with its characteristic bands for amino and CH_2 vibrations) to

terephthaldialdehyde (SAM **2**), several changes were observed in the spectra. The broad peak of the amino group disappeared, indicating complete reaction on the surface. Furthermore, several new bands appeared: imine C=N stretching vibration at 1645 cm^{-1} and a band at 1705 cm^{-1} assigned to the C=O stretching vibration of the second aldehyde group attached to the aromatic ring. The presence of these characteristic imine and aldehyde bands and the absence of the bands assigned to the amine group provide strong evidence that terephthaldialdehyde was attached covalently via an imine bond, leaving reactive aldehyde groups on the surface, consistent with our earlier reports (see Chapter 3).
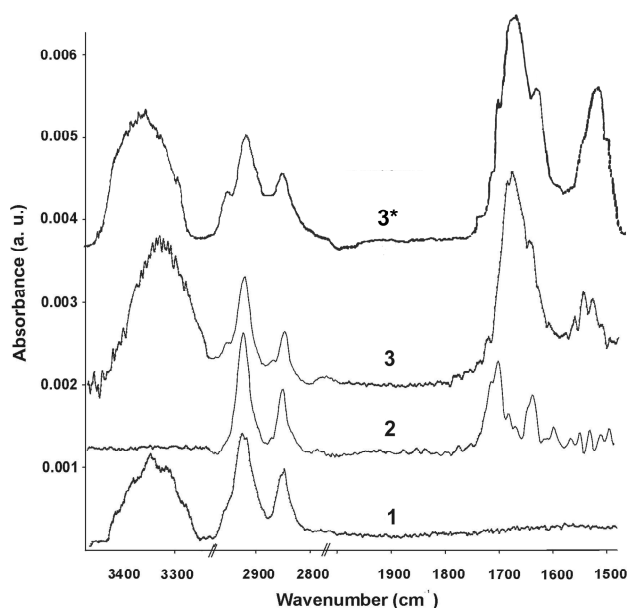
Figure 5-4. FT-IRRAS spectra of functionalized monolayers obtained by sequential exposure of Au surface to 11-AUT (**1**), terephthaldialdehyde (**2**), and protein Col3a1 (**3, 3*** - directly printed via oxPDMS).

After protein immobilization to the monolayer **2** several new peaks in the spectra appeared. The broad band at approximately 3350 cm^{-1} can be assigned to the N-H stretching vibration of the amino groups and amides in the protein (Figure 4, spectrum **3**). Bands at 2926 and 2854 cm^{-1} indicate CH$_2$ asymmetrical and symmetrical stretching vibrations of the substrate SAM. Furthermore, a shoulder at 1645 cm^{-1} overlapping with the 1678 cm^{-1} amide I band can be assigned to the C=N stretching vibration of the imine group, resulting from the reaction between the protein amine groups and the aldehyde groups from the SAM. Finally the band at 1546 cm^{-1} was assigned to the amide II stretching vibration. Spectra of microcontact printed protein were also taken (Figure 5-4, spectrum 3*). Col3a1 was printed onto aldehyde-terminated SAM **2** with a flat, oxidized PDMS stamp. The FT-IRRAS spectra of SAM **3** (obtained by 1 hour chemisorption of Col3a1 from solution) and SAM **3*** (obtained by 15 min μCP) are virtually

identical, once more confirming the remarkable efficiency of the immobilization reaction in the confinement between stamp and substrate.[27,29]

To investigate the structure and distribution of the protein onto the aldehyde-terminated SAM **2**, tapping mode AFM images were taken directly after immobilization of protein Col3a1 (Figure 5-5)**.** The molecules that were not attached covalently to the surface were removed by sonication and vigorous rinsing of the surface. Col3a1 forms a homogenous but relatively low-coverage adlayer. The average height of the Col3a1 molecules ranges from 1 to 4 nm, consistent with the data from ellipsometry (Table 5-1). Each molecule (or small aggregate) of protein is attached to the surface while avoiding the neighboring protein molecules as a consequence of electrostatic and steric repulsion.
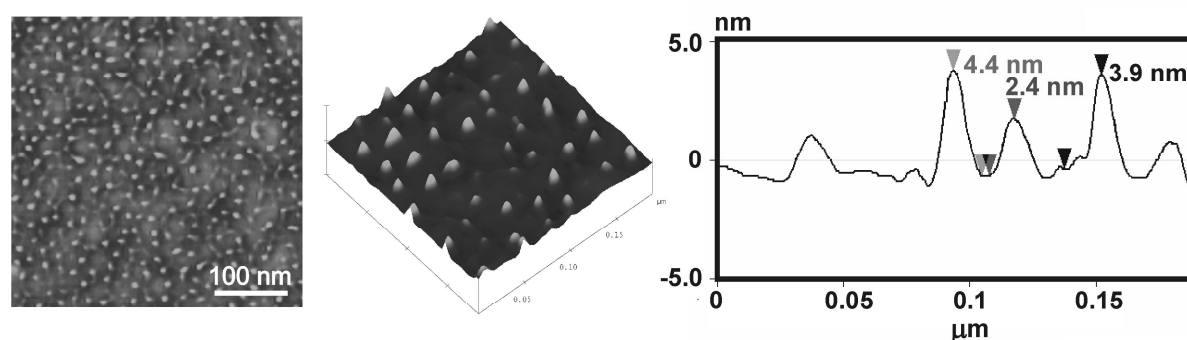
Figure 5-5. Tapping mode AFM height images of immobilized protein Col3a1 on aldehyde-terminated gold substrate (SAM **3**).

The adhesion of cells was investigated onto the substrates with different proteins. Cells were incubated on modified substrates for 24 h, at 37 ˚C (in the incubator), 5 % CO_2, 95 % air, in the concentration of 3 x 10^4 cells/cm^2, in Iscove's modified Dulbecco's medium. The comparison of HeLa cells attachment onto glass slides modified with Col3a1 and proteins/peptides similar in sequence or structure such as gelatin type B, P4, and Col1a1-1* (Figure 5-6) was conducted.[28] P4 is a very hydrophilic protein with a sequence similar to Col3a1. Gelatin is a denatured and partially degraded form of collagen. Col1a1-1* has a similar sequence to Col3a1, where the alpha 1 chain has a part of type I collagen but lacks the RGD tripeptide. The highest number of attached cells was found on Col3a1-modified substrate (980 cells/mm^2). A significant number of cells was also found on the P4 modified substrate (790 cells/mm^2), which is surprising since this protein does not present a binding motif RGD in its structure. Gelatin gives the lowest adhesion of HeLa cells from all compared substrates. Col1a1-1* is about half as efficient in terms of cell adhesion as Col3a1.
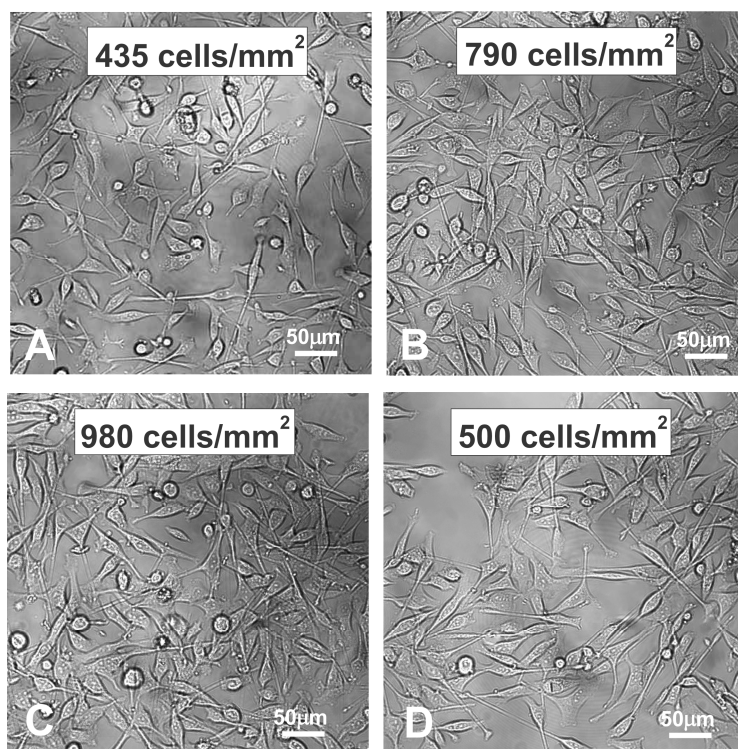
Figure 5-6. HeLa cells on the glass slides modified with A) gelatin, B) P4 protein, C) Col3a1, D) Col1a1-1* protein.

5.3. Protein and cell patterning

Col3a1 was microcontact printed in 3 µm lines using a hydrophilic, oxidized PDMS stamp (treated with an UV/ozone plasma for 30 min and stored in water) onto aldehyde-terminated SAM **2**. Unmodified PDMS provides a hydrophobic surface that is not suitable for aqueous inks. The ink concentration was 1 mM (in PBS) and the contact time was 15 min. After this contact time the surface was sonicated in PBS for 5 min, vigorously rinsed with PBS and water and dried with nitrogen. The surface was imaged with tapping mode AFM after printing (Figure 5-7A). The contrast in height images (average height of the pattern is about 1.3 nm) confirms the formation of a protein pattern on the surface. The height of the printed protein layer is consistent with ellipsometry and also with the observed height from of chemisorbed Col3a1 (see above). Furthermore, to confirm immobilization of proteins via covalent imine bonds (and not physisorption), the proteins were removed through acid-catalyzed hydrolysis. Indeed, after hydrolysis no pattern was observed on the SAM (Figure 5-7B).
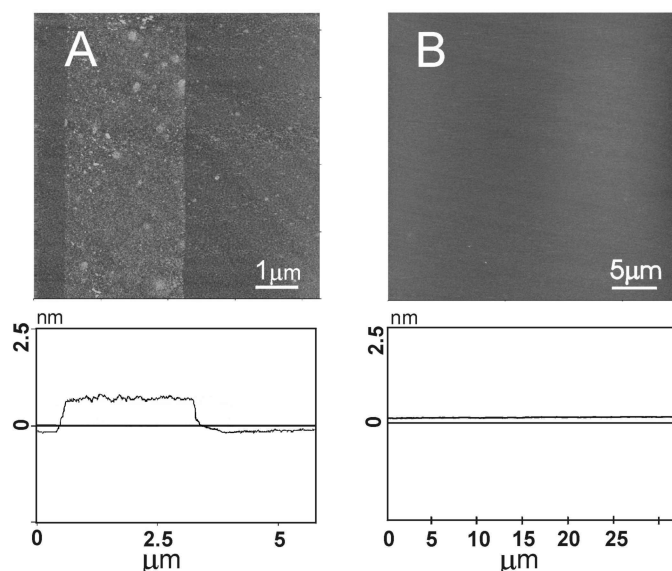
Figure 5-7. Tapping mode AFM images of microcontact printed Col3a1 proteins onto aldehyde-terminated substrates using A) hydrophilic, oxidized PDMS, B) after acid catalyzed hydrolysis of microcontact printed proteins.

The covalent microcontact printing of proteins was additionally investigated by fluorescence microscopy. Firstly, Col3a1 was directly printed in 100 µm dots onto an aldehyde-terminated glass slide, sonicated the substrate in PBS and vigorously rinsed with PBS and water (Milli-Q). Secondly, the remaining aldehyde gaps were reacted with methoxypoly(ethylene glycol) amine. Immobilized protein Col3a1 was then labeled with a fluorescent dye, Lissamine rhodamine B, from ethanolic solution for 1 h at room temperature (Figure 5-8). It is evident from the fluorescence image that lissamine labeled Col3a1 is present exclusively in the contact regions (100 µm dots) and not in the poly(ethylene glycol) coated areas in between.
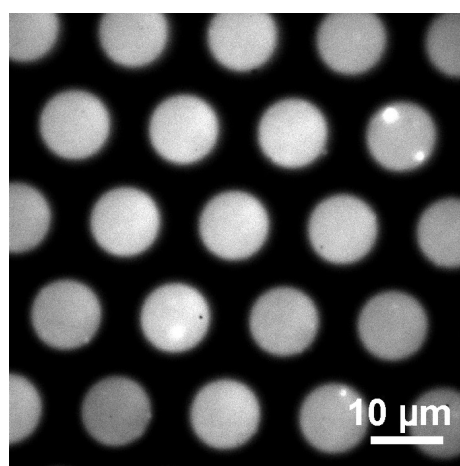
Figure 5-8. Fluorescent confocal microscopy image of directly printed Col3a1 proteins patterns (10 µm dots) labeled with fluorescent dye - lissamine rhodamine B.

To explore patterns of HeLa cells on the surface, the substrates that were pre-patterned with covalently attached Col3a1 proteins were used. These substrates were obtained by direct µCP of proteins onto aldehyde-terminated SAM and subsequent blocking of the remaining aldehyde groups with amino-PEG (Figure 5-1). It is important to choose the right dimension of the pattern on the surface. Cells are constrained and inhibited if they are confined in areas similar to or smaller than their natural dimensions. If the separation between the patterned cells is not enough, cells communicate with each other and readily occupy the space between the patterns. The pattern that was chosen for this experiment had 100 µm dots with 100 µm spacing between dots. HeLa cells were seeded onto the substrate (6*) patterned with adhesive "islands" and incubated for 24 h, at 37 ˚C (in the incubator), 5 % CO_2, 95 % air, at a concentration of 3 x 10^4 cells/cm^2, in Iscove's modified Dulbecco's modified medium. The HeLa cells attach onto each island, spread to the limits of the printed pattern and stay on the pattern even after vigorous rinsing of the substrate with PBS (Figure 5-9). On average, there were more than 9 out of 10 cells adhering to the islands and less than 1 out of 10 outside the islands.
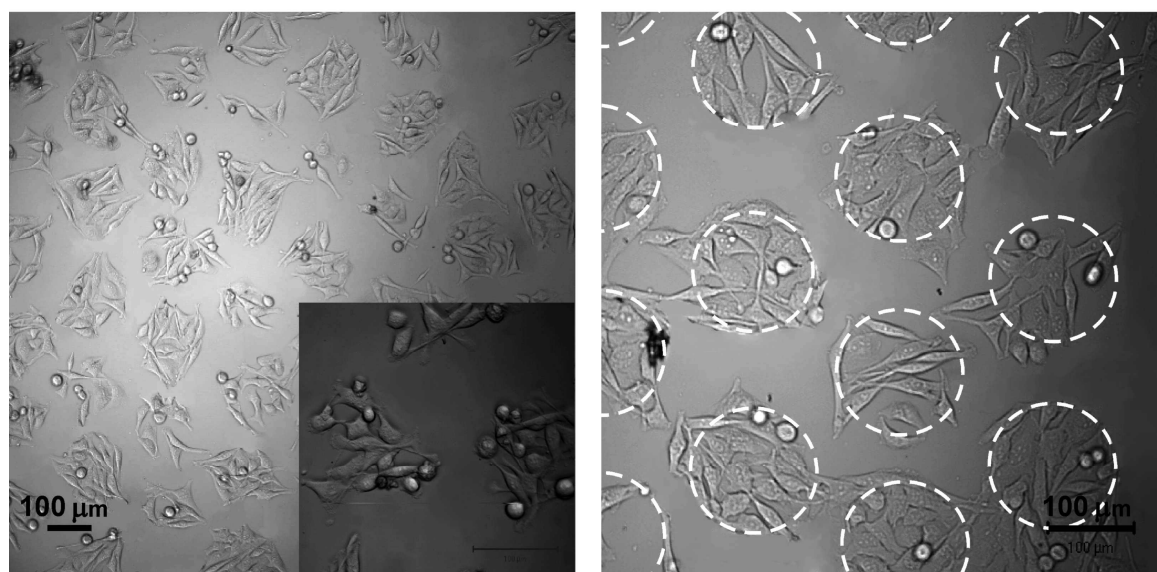

Figure 5-9. Patterns of HeLa cells obtained by microcontact printing 100 µm dots of protein Col3a1.

As a control experiment, a glass substrate that was homogenously covered with Col3a1 proteins (without pattern) was used. Cells were seeded at a concentration of 3 x 10^4 cells/cm^2 and after incubation (24 h, at 37 ˚C in the incubator, 5 % CO_2, 95 % air, in Iscove's medium) cells attached to the substrate without forming any pattern (Figure 5-6).
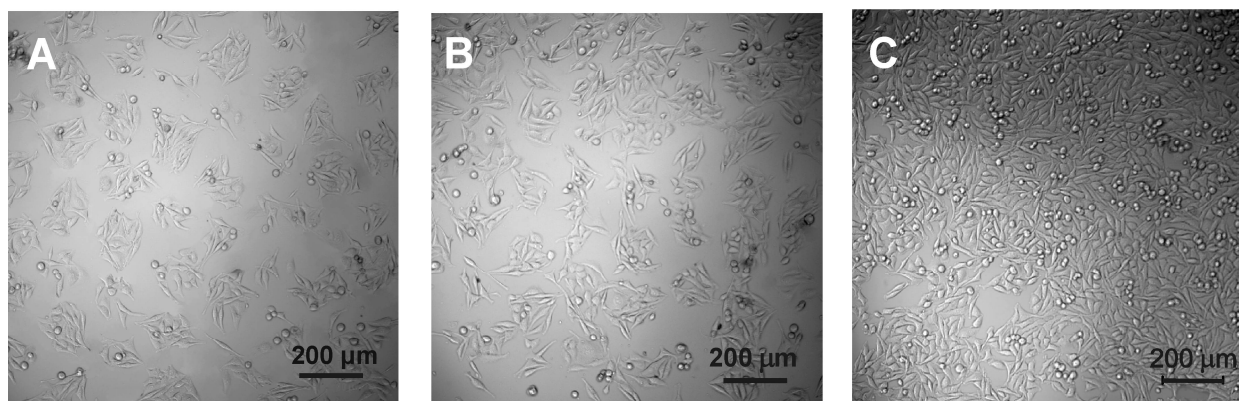
Figure 5-10. Images of HeLa cells on the substrate with printed protein Col3a1 A) after 24 h of incubation, B) after 48 h incubation, C) after 72 h incubation.

The stability of the cell pattern after 24 h, 48 h and 72 h was also investigated (Figure 5-10). After 24 h of incubation the pattern was visible and well separated and cells adhered mostly only to the part of the substrate where Col3a1 was immobilized. After 48 h of incubation cells started occupying the space between the pattern and after 72 h of incubation the pattern was not visible. Cells crawled onto the non-adhesive regions, and overgrew areas that were resistant to cell adhesion.

After 48 h of incubation, the cells started to change their shape. The elongated membrane protrusions from the leading edge (more than 50 μm in length) could be observed. In addition, cells began to crawl and migrate onto cell-resistant areas (Figure 5-11). This might confirm cell-to-cell communication between cells on the pattern and possible also secretion of ECM proteins by the HeLa cells that similarly to Col3a1 enhance adhesion of the cells to the substrate. Alternatively, the cells may secrete degradative enzymes that can affect the patterned substrate. It was previously reported that cells can also indirectly degrade non-adhesive surfaces by exerting local physical stresses such as mechanical strain or pH change.[30]
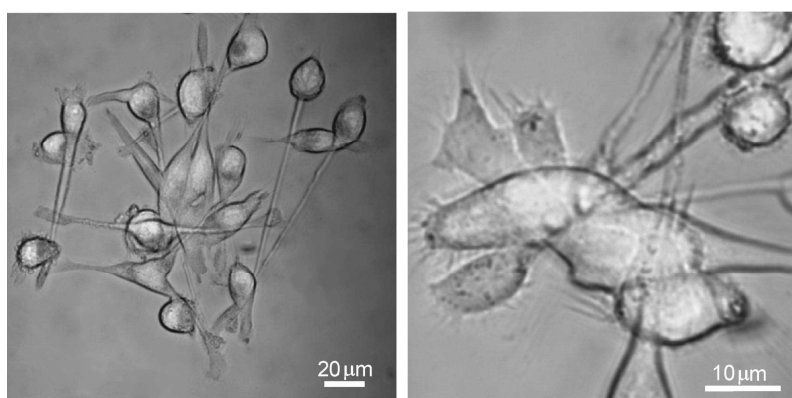

Figure 5-11. Patterned substrates with HeLa cells after 48 h of incubation. Cells show long (more than 50 μm in length) actin tubes and migrate towards cell-resistant areas.

5.4. Conclusions

Covalent microcontact printing of protein Col3a1 onto aldehyde-terminated substrates can be used to obtain stable protein patterns that can be applied for cell patterning. Col3a1 shows the highest adhesion in comparison to other, similar proteins like Col1a1-1*, P4, or gelatin. Direct covalent immobilization of proteins by microcontact printing is fast, simple, and delivers protein in well-defined, spatially and geometrically-controlled areas to the substrate. By blocking not printed areas on the substrate cells can be positioned and separated in confined domains. Cells spread and flatten on the Col3a1 pattern. After longer incubation (72 h) cells proliferate, migrate and grow on the pattern and fill in the cell-resistant spaces. There are several advantages of this technique; it is easy, inexpensive, fast and straightforward. The pattern can be tailored according to the desired application by designing the geometry of the master for PDMS stamp fabrication. It can be useful in generating large areas of addressable arrays of cells in a variety of shapes dependent on the shape of the stamp. This method for patterning the cells can be useful in understanding how spatial or geometric modification of active surfaces can influence cellular behavior such as cell-cell interaction, signaling between cells, and cell motility.

5.5. Experimental section

Materials. The following materials and chemicals were used as received: 11-aminoundecanethiol (Dojindo Laboratories), terephthaldialdehyde 99% (Aldrich), poly(dimethylsiloxane) (PDMS) (Dow Corning), N-(2-aminoethyl)-11-aminoundecyltrimethoxysilane (Gelest, Inc.), Lissamine rhodamine B (Molecular Probes), methoxypoly(ethylene glycol) amine (Fluka). Proteins Col3a1, Col1a1-1*, P4 were biosynthesized at Wageningen UR, Agrotechnology and Food Innovations.[28] Collagen from rat tail (type I) and gelatin type B from bovine skin were purchased form Sigma-Aldrich. Serum and materials for cell culture were purchased from Gibco or Invitrogen. All solvents were HPLC grade, and all other reagents were analytical grade. Other solvents or reagents were purchased from either Aldrich or Sigma.

Monolayer formation. Monolayers on gold and silicon substrates were prepared according to previously published procedures.[29] The procedure for immobilization of Col3a1 protein is the same for gold and silicon surfaces. The substrates were immersed for 1 hour in protein solution (1 mM Col3a1 PBS solution). Subsequently the substrates were copiously rinsed with MilliQ water and dried under a stream of nitrogen. In the direct µCP method

(substrates with full-coverage of proteins), a flat, oxidized PDMS stamp (treated for 30 min with an UV/ozone plasma and stored under Milli-Q water) was inked with 1 mM solution of Col3a1 proteins in buffer (PBS), dried under a stream of nitrogen, and placed on aldehyde-terminated substrate for 15 min at 35 °C. After reaction time the stamp was lifted off and the substrate sonicated in PBS for 5 min, copiously rinsed with Milli-Q water (to remove all physisorbed material) and dried under a stream of nitrogen.

Preparation of protein-modified substrates for cell attachment. Aldehyde-terminated glass slides were prepared as described.[29] The substrates were immersed for 1 hour in protein solution (1 mM Col3a1 PBS solution, 1 mM Co1a1-1* PBS solution, 1mM P4 PBS solution, 0.1 mM aq. gelatin solution). Subsequently the substrates were copiously rinsed with MilliQ water and dried under stream of nitrogen.

Direct printing of proteins on aldehyde-terminated gold and glass/silicon oxide substrates. Aldehyde-terminated glass slides (or silicon oxide) and gold substrates were prepared according to procedures mentioned above. PDMS stamps were oxidized in UV/ozone reactor for 30 min and then placed in Milli-Q water for 20 min to maintain its hydrophilic properties. Subsequently the stamp was inked with 1 mM solution of Col3a1 in PBS, dried with N_2 and brought into conformal contact with the substrate for 15 min at 35 °C. After that time the stamp was removed and the substrate was sonicated in buffer for 5 min and thoroughly rinsed with PBS and Milli-Q water. The remaining gaps on the substrate (containing aldehyde groups) were reacted with 1 mM methoxy-PEG amine aqueous solution with triethylamine residues for 30 min at room temperature. After reaction time the substrate was rinsed with water and dried with nitrogen.

Control experiment for protein attachment. The imine monolayer that was formed by the reaction between amino-terminated SAM and terephthaldialdehyde and Col3a1 was hydrolyzed by immersing the substrate in aqueous acetic acid solution (pH 3) for 1 h at room temperature.[29]

Fluorescent labeling of protein Col3a1. The reaction of protein Col3a1 with Lissamine rhodamine B was performed by soaking the substrate with immobilized proteins into 1 mM ethanolic solution of the dye for 1 h. Subsequently the surface was thoroughly rinsed with ethanol and water and dried under nitrogen.

Cell culture and seeding onto the substrates. HeLa cells (human cervix epithelial cell line) were cultured with Iscove's modified Dulbecco's medium supplemented with 10 % fetal calfs serum (Gibco 16000), 2 mM L-glutamine, 1% antibiotics/antimycotic-solution. The cells were trypsinized in a 0.05 % trypsin-EDTA solution and seeded onto the patterned glass slides in the concentration of 3 x 10^4 cells/cm^2, in Iscove's modified Dulbecco's medium. Substrates with cells were incubated for 24 h, at 37 °C, 5 % CO_2. Following the incubation substrates were rinsed with PBS to wash away cells that did not attach to the pattern and imaged with an optical microscope. Using the same protocol, HeLa cells were seeded onto substrates with homogeneously immobilized proteins (Col3a1, P4, gelatin, and Co1a1-1*). Cells were incubated in Iscove's modified Dulbecco's medium, for 24 h, at 37 °C, 5 % CO_2, 95 % air.

Instrumentation. *Contact angle measurements.* Contact angles were measured on a Krüss G10 goniometer, equipped with a CCD camera. Advancing and receding contact angles (θ_a and θ_r) were determined automatically during growth and shrinkage of the droplet by a drop shape analysis. Milli-Q water (18.4 MΩ·cm) as a probe liquid. Both angles (advancing and receding) were measured on at least three different locations on each sample.

Ellipsometry. Ellipsometric layer thickness measurements were performed on a Plasmos Ellipsometer ($\lambda = 632.8$ nm) assuming a refractive index of 1.5 for the monolayers and 1.465 for the underlying native oxide. The thickness of the SiO_2 layer was measured separately on an unmodified part of the same wafer and subtracted from the total layer thickness determined for the monolayer covered silicon substrate.

FT-IRRA spectroscopy. FT-IRRA spectra in the mid-IR region of 1024 scans at 4 cm^{-1} resolution, 20 kHz speed, were recorded on a BIO-RAD FTS-60A spectrometer with a liquid nitrogen-cooled cryogenic, external mercury cadmium telluride (MCT) detector, with its sample area modified to accommodate an external reflection sampling geometry. The sample area was purged by dry nitrogen. Background spectra consisting of 1024 averaged scans were taken before collecting each sample spectra.

Atomic force microscopy (AFM) imaging. AFM measurements were carried out with a digital multimode Nanoscope III (Digital Instruments, Santa Barbara, CA, USA) scanning force microscope in tapping mode, with 512 x 512 data acquisitions, using n(+)-silicon AFM pointprobes tips, type NCH-W with nominal spring constant 37-56 N/m (Nanoprobes, Digital Instruments) and E-scanner. Typical scan rates of 0.8-1 Hz were used to acquire the data. All imaging was conducted at room temperature in air.

Laser scanning confocal microscopy/optical microscopy. Microcontact printed substrates with and without cells were imaged with a Carl Zeiss LSM 510 scanning confocal microscope with an excitation HeNe laser beam of 543 nm wavelength and a 10, 40 and 60 x objective was used. The emitted fluorescence was collected on a R6357 spectrophotometer. All confocal microscopy images were acquired in liquid.

XPS analysis. XPS spectra were obtained on a Physical Electronics Quantera Scanning X-ray Multiprobe instrument, equipped with a monochromatic Al Kα X-ray source operated at 1486.7eV and 25 W. Spectra were referenced to the main C 1s peak set at 284.0 eV. XPS data were collected from a surface area of 700 μm x 300 μm with a pass energy of 224 eV and a step energy of 0.8 eV for survey scans and 0.4 eV for high-resolution scans at a 45˚ takeoff angle, whereas the angle between sample surface and the X-ray beam was 90˚. For quantitative analysis, the sensitivity factors used to correct the number of counts under each peak were as follows: C 1s, 1.00; N 1s, 1.59. Charge neutralization was achieved by low-energy electrons and low-energy argons ions.

5.6. References

[1]   C. S. Chen, M. Mrksich, S. Huang, G. M. Whitesides, D. E. Ingberg, *Science* **1997**, *276*, 1425-1429.

[2]   A. Folch, H. Jo, O. Hurtado, D. J. Beebe, M. Toner, *J. Biomed. Mater. Res.* **2000**, *52*, 346-353.

[3]   S. Raghavan, C. S. Chen, *Adv. Mater.* **2004**, *16*, 1303-1313.

[4]   R. Langer, J. P. Vacanti, *Science* **1993**, *260*, 920-926.

[5]   J. J. Pancrazio, J. P. Whelan, D. A. Borkholder, D. A. Stenger, *Ann. Biomed. Eng.* **1999**, *27*, 697-711.

[6]   T. H. Park, M. L. Shuler, *Biotechnol. Prog.* **2003**, *19*, 243-253.

[7]   R. S. Kane, S. Takayama, E. Ostuni, D. E. Ingber, G. M. Whitesides, *Biomaterials* **1999**, *20*, 2363-2376.

[8]   P. Ghosh, A. M. L., W. M. Lackowski, M. V. Pishko, R. M. Crooks, *Angew. Chem. Int. Ed.* **1999**, *38*, 1592-1595.

[9]   J. Lahann, M. Balcells, T. Rodon, J. Lee, J. S. Choi, K. F. Jensen, R. Langer, *Langmuir* **2002**, *18*, 3632-3638.

[10] D. R. Reyes, E. M. Perruccio, S. P. Becerra, L. E. Locascio, M. Gaitan, *Langmuir* **2004**, *20*, 8805-8811.

[11] H. Ma, J. Hyun, Z. Zhang, T. P. Beebe, A. Chilkoti, *Adv. Funct. Mater.* **2005**, *15*, 529-540.

[12] E. Ostuni, R. Kane, C. S. Chen, D. E. Ingber, G. M. Whitesides, *Langmuir* **2000**, *16*, 7811-7819.

[13] D. T. Chiu, N. L. Jeon, S. Huang, R. S. Kane, C. J. Wargo, I. S. Choi, D. E. Ingberg, G. M. Whitesides, *Proc. Natl. Acad. Sci. USA* **2000**, *97*, 2408-2413.

[14] S. Takayama, J. C. McDonald, E. Ostuni, M. N. Liang, P. J. Kenis, R. F. Ismagilov, G. M. Whitesides, *Proc. Natl. Acad. Sci. USA* **1999**, *96*, 5545-5548.

[15] M. Nishizawa, K. Takoh, T. Matsue, *Langmuir* **2001**, *18*, 3645-3649.

[16] H. Kaji, K. Tsukidate, T. Matsue, M. Nishizawa, *J. Am. Chem. Soc.* **2004**, *126*, 15026-15027.

[17]   L. Pardo, W. C. Wilson, T. Boland, *Langmuir* **2003**, *19*, 1462-1466.

[18]   N. V. Avseenko, T. Y. Morozova, F. I. Ataullakhanov, V. N. Morozov, *Anal. Chem.* **2001**, *73*, 6047-6052.

[19]   M. Mrksich, C. S. Chen, Y. N. Xia, D. E. Ingberg, G. M. Whitesides, *Proc. Natl. Acad. Sci. USA* **1996**, *93*, 10775-10778.

[20]   M. Mrksich, L. E. Dike, J. Tien, D. E. Ingberg, G. M. Whitesides, *Exp. Cell Res.* **1997**, *235*, 305-313.

[21]   A. A. Oliva, C. D. James, C. E. Kingman, H. G. Craighead, G. A. Banker, *Neurochem. Res.* **2003**, *28*, 1639-1648.

[22]   A. Bernard, E. Delamarche, H. Schmid, B. Michel, H. R. Bosshard, H. Biebuyck, *Langmuir* **1998**, *14*, 2225-2229.

[23]   A. Bernard, J. P. Renault, B. Michel, H. R. Bosshard, E. Delamarche, *Adv. Mater.* **2000**, *12*, 1067-1070.

[24]   L. Kam, S. G. Boxer, *J. Biomed. Mater. Res.* **2001**, *55*, 487-495.

[25]   L. Kam, W. Shain, J. N. Turner, R. Bizios, *Biomaterials* **2001**, *22*, 1049-1054.

[26]   N. Sgarbi, D. Pisignano, F. Di Benedetto, G. Gigli, R. Cingolani, R. Rinaldi, *Biomaterials* **2004**, *25*, 1349-1353.

[27]   T. P. Sullivan, M. L. van Poll, P. Y. W. Dankers, W. T. S. Huck, *Angew. Chem. Int. Ed.* **2004**, *43*, 4190-4193.

[28]   M. W. T. Werten, T. J. Van den Bosch, R. D. Wind, H. Mooibroek, F. A. De Wolf, *Yeast* **1999**, *15*, 1087-1096.

[29]   D. I. Rożkiewicz, B. J. Ravoo, D. N. Reinhoudt, *Langmuir* **2005**, *21*, 6337-6343.

[30]   C. M. Nelson, S. Raghavan, J. L. Tan, C. S. Chen, *Langmuir* **2003**, *19*, 1493-1499.

[31]   P. Kohe, R. M. Kannan, *Biomacromolec.* **2003**, *4*, 173-180.

[32]   A. Papra, A. Bernard, D. Juncker, N. B. Larsen, B. Michel, E. Delamarche, *Langmuir* **2001**, *17*, 4090-4095.

Chapter 6

Dendrimer-mediated transfer printing of DNA and RNA microarrays[*][§]

A new method for the transfer printing of DNA and RNA is presented in this Chapter. The method, which facilitates positioning of nucleic acids with high lateral resolution by microcontact printing (μCP) is based on the modification of PDMS stamps with dendrimers ("dendri-stamps"). The modification of PDMS stamps with poly(propyleneimine) (PPI) dendrimers gives a high density of positive charge on the stamp surface that can attract negatively charged DNA and RNA molecules in a "layer-by-layer" arrangement. The electrostatic interactions between dendrimers and oligonucleotides ensure successful transfer of DNA or RNA to the target surface. Here, imine chemistry is applied to bind covalently amino-modified DNA/RNA molecules to an aldehyde-terminated substrate. The labile imine bond is reduced to a stable secondary amine bond forming a robust connection between the nucleic acid strand and the solid support. Microcontact printed oligonucleotides are distributed homogeneously within the patterned area and they are available for hybridization. In combination with a robotic spotting system, an array of multiple oligonucleotides can be introduced to the surface of a flat, dendrimer-modified stamp and subsequently used for repeated replication of the entire microarray by microcontact printing. The printed microarrays are characterized by a homogeneous probe density and regular spot morphology. In addition, a similar method for the modification of atomic force microscopy (AFM) tips to transfer and deliver DNA molecules to a target surface was developed. The procedure relies on the immobilization of PPI or PAMAM dendrimers on the oxidized surface of silicon nitride tips. Dip-pen nanolithography (DPN) was utilized to create nanometer size patterns of DNA on the surface.

6.1. Introduction

DNA microarrays have rapidly developed into a fundamental tool for high-throughput genetic analysis. DNA chips were applied among others as tools for large-scale parallel analyses of genome sequence and gene expression,[1] for the evaluation of the clinical course of tumors,[2] for detection of viruses and other pathogens,[3] for monitoring mRNA expression[4] and classification of human tumors.[5] Immobilization of oligonucleotides on solid surfaces is central to the design, fabrication and operation of DNA-based microarrays. In general, there are two methods for DNA microarray fabrication: immobilization of synthetic oligonucleotides or DNA onto solid supports or direct synthesis of DNA on a chip (mostly up to 25 nucleotides).[6-11] The immobilization of DNA can be carried out by automated spotting conducted by contact printing or non-contact printing. Contact printing employs robotic systems equipped with a set of pins for dispensing pico- or nanoliters of DNA solution, where the surface is contacted for probe deposition. Non-contact printing ("ink-jetting") relies on depositing the spotting solution from an array of e.g. piezo-electrically driven pipettes onto the solid support without direct contact with the surface. DNA can be immobilized covalently by reaction between DNA modified with reactive group (e.g. an amine) and a reactive solid support (exposing e.g. aldehyde or epoxide groups). Alternatively, DNA can be immobilized non-covalently by the adsorption on positively charged surfaces, or using Van der Waals, or hydrophobic interaction, or other. [6-14] Surfaces modified with self-assembled monolayers (SAMs),[3,13,14] polyacrylamide gel,[15] polyamidoamine (PAMAM) dendrimers[16] or agarose films[17] were used as substrates for DNA microarrays. Typically, probes are modified at the 5'-terminus with a reactive group that can bind covalently with the support.

The synthesis of DNA on a chip can be conducted by either piezoelectric printing (ink-jetting), photolithographic synthesis[6-8] or physical confinement of nucleotide precursors using microfluidic devices.[6-11] Methods such as chemical nanoprinting,[18] dip-pen nanolithography,[19] and nanografting[20] were also applied for the fabrication of DNA microarrays.

Ideally, a DNA chip would have the following properties: (1) high and homogeneous probe density for optimal signal read-out, (2) submicron spot size and nanoscale spot resolution for high data density, (3) many thousands of different probes spotted identically and rapidly for large probe arrays; (4) simple, parallel manufacturing and analysis. It is evident that state-of-the-art DNA microarray technology falls short of this ideal.[6,9,10,12] Inhomogeneous spots result from printing from pins or pipettes due to the evaporation of solvent. Higher DNA concentrations remain at the edges ("doughnut effect") or DNA aggregates at a few points

within a spot. Spot sizes are typically in the 50 micron range, spots are separated by at least 50 micron, and smaller spots can only be produced accurately by time-consuming serial processes. Soft lithography methods such as microcontact printing are not useful to pattern multiple probes simultaneously.[26-28]

In this Chapter a simple but efficient method to transfer DNA as well as RNA to a glass substrate and facilitate positioning of oligonucleotides in molecular monolayers with submicron edge resolution by microcontact printing (µCP) is described. An essential novelty of this method is the modification of PDMS stamps with fifth generation poly(propylene imine) (G5-PPI) dendrimers ("dendri-stamps"). In addition the combination of microcontact printing with contact printing robotic systems to deposit hundreds of oligonucleotide spots and print them repeatedly from one stamp with good spot uniformity is here presented.

The key to this work is the electrostatic interaction between a negatively charged, oxidized PDMS stamp and positively charged G5-PPI. Dendrimers such as PPI and poly(amidoamine) (PAMAM) have become an interesting alternative for surface modifications and immobilization of biomolecules. Dendrimer-modified substrates were previously used for the attachment of DNA.[13,16,21,22] Dendron-modified glass slides were used to obtain controlled spacing between immobilized DNA molecules.[3,23] "Dendri-slides" (dendrimers covalently attached to a glass substrate) generate a high surface coverage of oligonucleotides that can be further hybridized with high yield.[21] Grafting of DNA on such substrates resulted in uniform and high density layers. Moreover, dendrimers were used as DNA transport agents in gene therapy to deliver genetic material to diseased sites.[4,24,25] G5-PPI possesses 64 amino groups at the periphery, providing a high density of terminal amino groups at the outer sphere.[30] At neutral pH, a significant fraction of the peripheral and internal amines are protonated, and the dendrimers can bind electrostatically to the negatively charged phosphate backbone of DNA.[4,25,30-32] All types of nucleic acids, including plasmid DNA, single-stranded and double-stranded oligonucleotides, and RNA, can form complexes via electrostatic interactions with PPI or PAMAM dendrimers.[4] The modification of PDMS stamps with G5-PPI ensures a high density of positive charge on the stamp surface that can attract negatively charged DNA and RNA molecules in a "layer-by-layer" arrangement.[33] PDMS stamps modified in this manner are able to transfer DNA to suitable solid supports creating patterns characterized by homogeneous distribution, high coverage and efficient hybridization. Here, the imine chemistry was applied to bind covalently amino-modified DNA and RNA molecules to an aldehyde-terminated substrate. The labile imine bond was reduced to a stable secondary amine bond forming a robust connection between the oligonucleotide strand and the solid support.

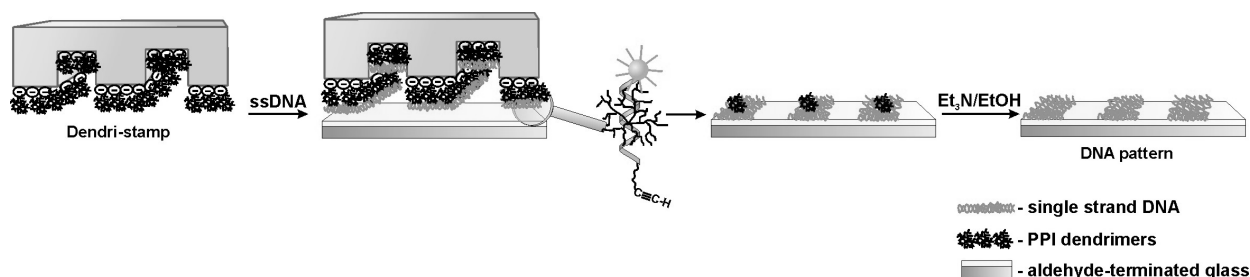## 6.2.   Microcontact printing of oligonucleotides

Figure 6-1. Schematic representation of microcontact printing of oligonucleotides with dendri-stamps. An oxidized PDMS stamp is first inked with dendrimers and subsequently incubated with fluorescein-labeled DNA. After transfer printing DNA onto the solid support, the substrate is rinsed with EtOH/Et$_3$N to wash residual dendrimers from the DNA substrate.

Figure 6-1 briefly outlines the protocol of printing DNA or RNA using dendrimer-modified PDMS stamps ("dendri-stamps"). An oxidized PDMS stamp was modified with dendrimers by immersion in 1 μM ethanolic solution of G5 PPI dendrimers for 30 s and dried with N$_2$. 3'-fluorescein-labeled 5'-amino-functionalized single-stranded DNA was incubated on the modified PDMS stamp for 20 min at RT. The stamp was dried with N$_2$ and brought into conformal contact with the aldehyde-modified glass slide for a contact time of 15 s. The substrate was rinsed with ethanol containing a drop of Et$_3$N (to remove residual PPI dendrimer) and subsequently with water. To ensure that the imine linkage between the DNA strand and the substrate will not be susceptible to hydrolysis, the imine bond was reduced to the corresponding amine by reaction with sodium borohydride. There was no loss of signal intensity of printed DNA due to the imine reduction reaction. To study the influence of the dendrimer concentration on the quality of microcontact printing different concentrations of that solution were prepared: 5 mM, 1 mM, and 1 μM. Fluorescent images taken after transfer printing of DNA with the dendri-stamp and after imine reduction are shown in Figure 6-2.
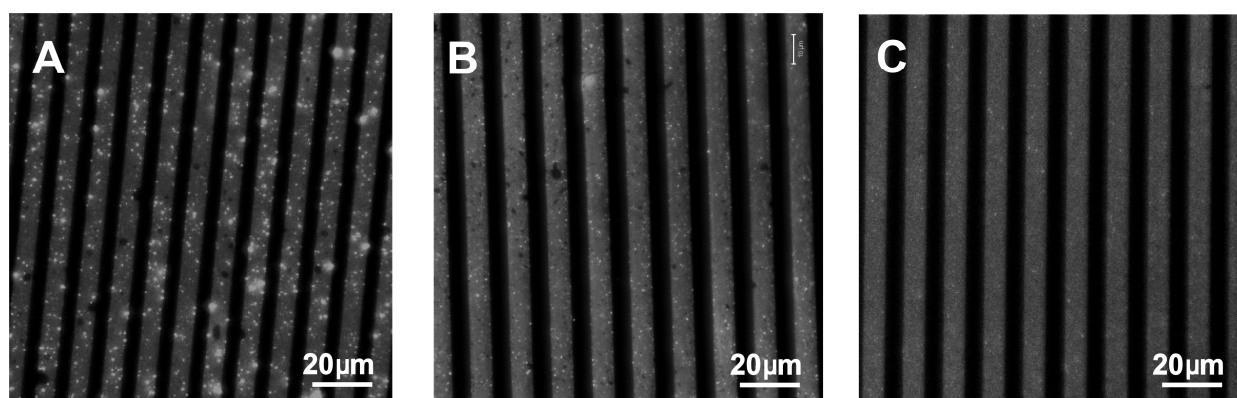
Figure 6-2. DNA patterns obtained by printing with dendri-stamps. An oxidized PDMS stamp was modified with A) 5 mM, B) 1 mM, C) 1 µM solution of G5-PPI dendrimers.

Using the same settings and parameters for signal detection, stamps modified with the 1 µM solution of dendrimers showed the best results of the microcontact printed pattern. The pattern of printed oligonucleotides was homogeneous while the patterns obtained by printing with the stamps modified by the solutions with higher concentration of dendrimers show a heterogeneous density of oligonucleotides in the patterned area. This phenomenon could be related to the formation of aggregates between dendrimers and oligonucleotides. If there is an excess (i.e. more than a monolayer) of dendrimers on the stamp, they could possibly mix with deposited oligonucleotides and form aggregates ("polyplexes"[24,25]) that are later difficult to remove just by rinsing.

DNA was also incubated on an oxidized PDMS stamp *without* modification with dendrimers. After printing *no* pattern was observed. Even though the oxidized stamp is hydrophilic it is also slightly negatively charged which might act repulsive for DNA. In addition, the transfer of DNA molecules with a dendri-stamp with a PDMS stamp that was modified with 3-aminopropyltriethoxysilane (APTES) was compared.[26] A solution of fluorescein-labeled oligonucleotides (1 µM in Tris-EDTA buffer) was incubated on top of the amino-modified PDMS stamps for 20 min at RT. Subsequently, the stamps were dried with nitrogen and brought into conformal contact with aldehyde-modified glass slides for 15 s. The substrates were washed with ethanol containing a drop of triethylamine, dried with nitrogen and imaged with laser scanning confocal microscope. Both substrates were imaged using the same microscope settings (Figure 6-3). The intensity of the pattern made by printing oligonucleotides via the dendri-stamp is 10 times higher than measured on the substrate printed via APTES-modified PDMS stamp. This phenomenon is probably related to the lower surface concentration of positively charged amino groups that attract negatively charged oligonucleotides.
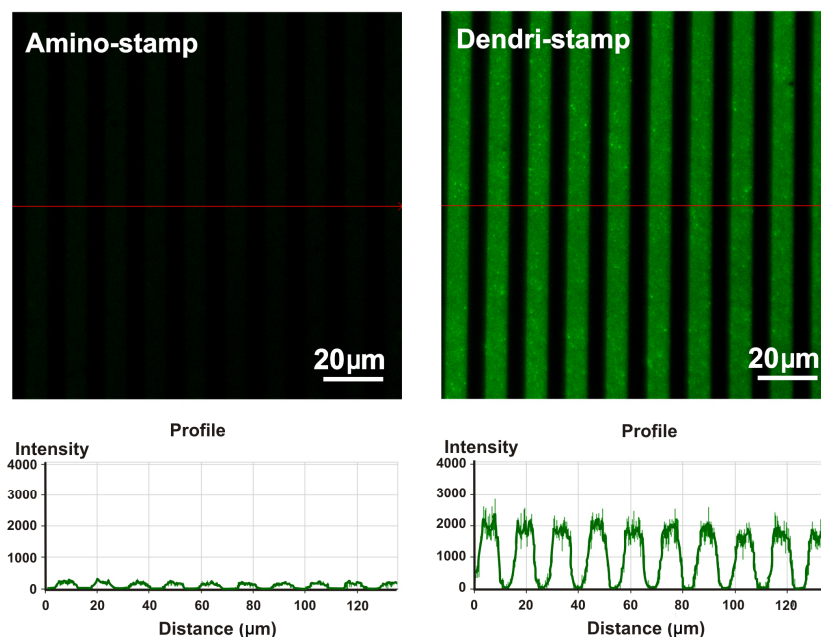
Figure 6-3. DNA patterns obtained by microcontact printing using APTES-modified PDMS stamp (left image) and transfer printing with a dendri-stamp (right image).

AFM was used to investigate the topography and distribution of DNA on the substrate after transfer printing with the dendri-stamp and after DNA immobilization from solution (i.e. the substrate was immersed in the solution of oligonucleotide for overnight, rinsed and dried with nitrogen). The packing of DNA strands was almost identical (Figure 6-4) but the time necessary for the proper immobilization was drastically different - 15 s for µCP and 16 h for immobilization from solution.
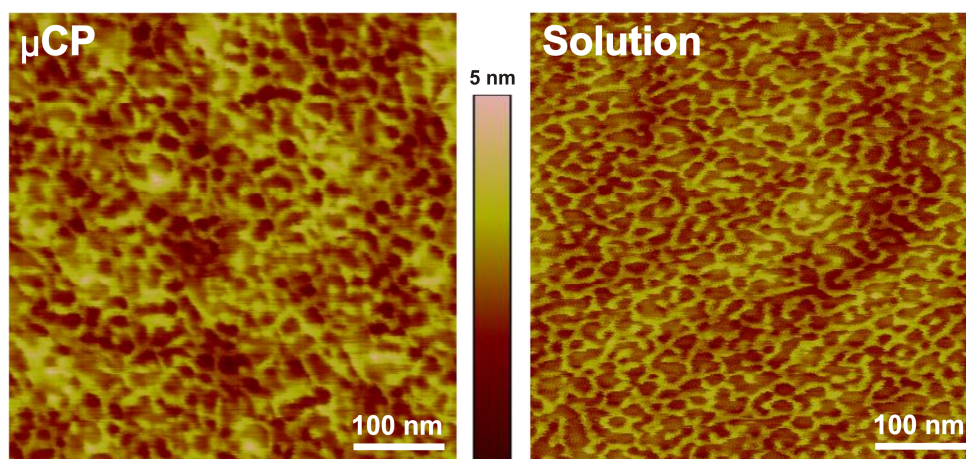
Figure 6-4. AFM tapping mode images of immobilized DNA using transfer printing with a dendri-stamp (left image) and from solution (right image).

From AFM measurements it appears that during printing DNA strands are transferred and immobilized into a meshwork. These features are approximately 2 nm in height and 7 nm in width (Figure 6-5).
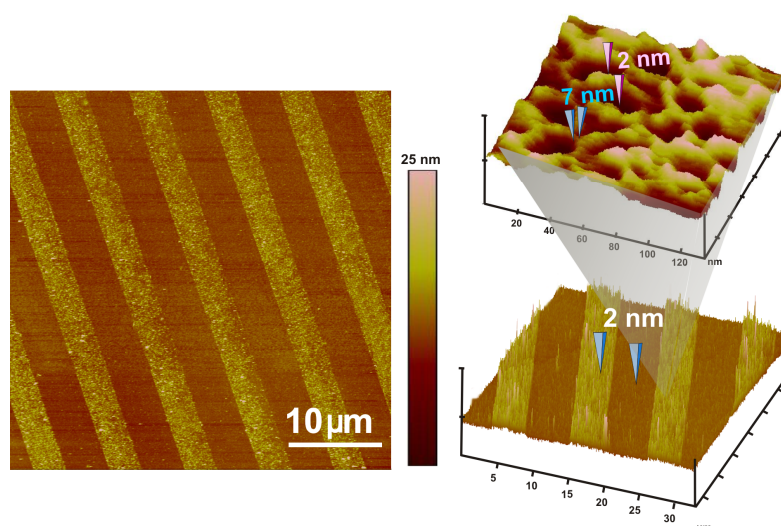
Figure 6-5. DNA pattern made by microcontact printing onto aldehyde-terminated glass support using dendri-stamps. The size of the DNA meshwork is 2 nm in height and 7 nm in width and the height of the strand corresponds to the height of the pattern.

6.3. Hybridization of printed oligonucleotides

To investigate whether the printed DNA is available for hybridization, the pattern was reacted with complementary, Cy5-labeled oligonucleotides. It was also important to examine if dendrimers can affect the conformation of DNA on the surface which subsequently might have an influence on hybridization. Hybridization with complementary strand was carried out overnight in 1 μM (4 x SSC, 0.2 % SDS) solution. Both strands – the probe (green fluorescein dye) and target (red Cy5 dye) - are clearly visible in the fluorescence microscope (Figure 6-6).
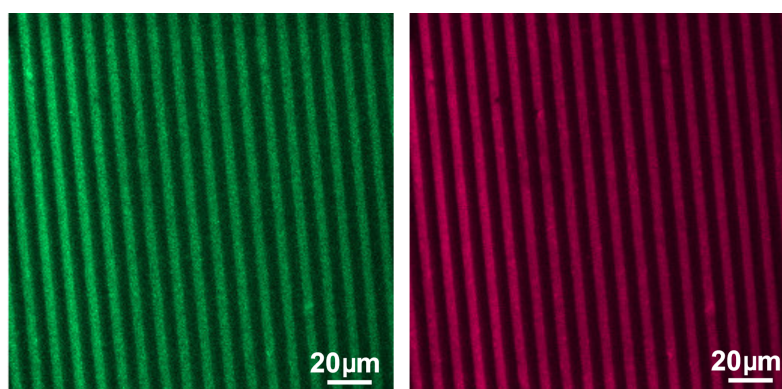
Figure 6-6. Simultaneous imaging of DNA patterns after hybridization between fluorescein-labeled probe (left image) and Cy5-labeled target (right image) by fluorescent confocal microscope.

To examine the specificity of the hybridization the extent of mismatch was essayed by the reaction with a strand that differs just in one nucleotide in the middle of the sequence and with a strand that has a completely non-complementary sequence. Printed oligonucleotides were subsequently reacted with Cy5-labeled oligonucleotides. The fluorescence signals acquired after

hybridization show marginal signal with the mismatch oligonucleotide and no signal with the oligonucleotide probe of unrelated sequence (Figure 6-7). These experiments also confirm that no significant amount of dendrimer is left on the substrate since residual dendrimers would likely bind any nucleotide sequence in an unspecific (electrostatic) manner.
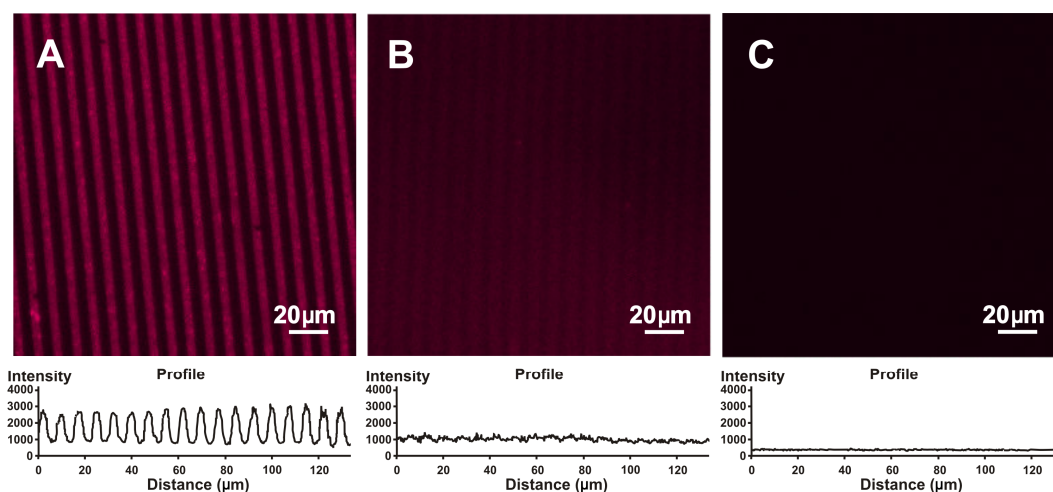

Figure 6-7. DNA patterns after hybridization of the transfer printed oligonucleotide with Cy5-labeled oligonucleotide having A) complementary sequence, B) sequence with one mismatch, C) non-complementary sequence.

6.4. DNA and RNA spotting by contact printing system

To expand this method to multiple-probes printing, spotting (contact printing) was combined with microcontact printing technique. By using robotic system (MicroGrid, Apogent Discoveries) an array of amino-modified, fluorescein labeled oligonucleotide spots was fabricated onto a flat dendri-stamp.
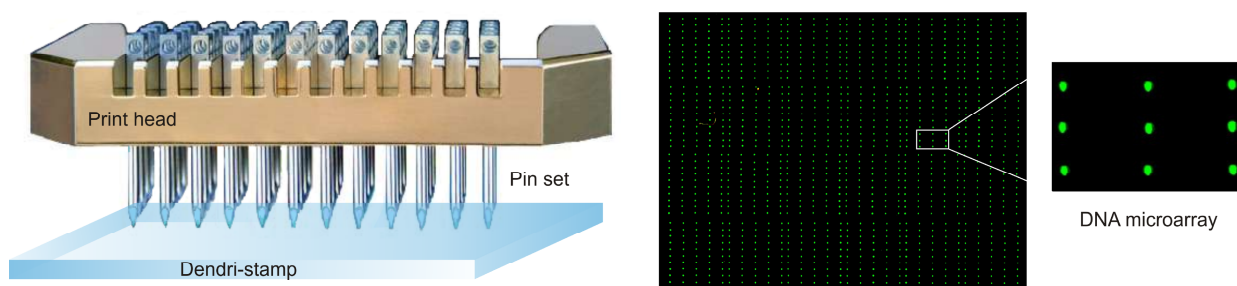
Figure 6-8. Contact printing of DNA onto a flat dendri-stamp (left illustration). Fragment of fluorescence image of an aldehyde-terminated glass slide with an array of 400 spots of fluorescein labeled oligonucleotide using a dendri-stamp (right images).

The average spot size in this array was ca. 100 micron. The DNA-spotted dendri-stamp was brought into conformal contact with an aldehyde-terminated glass slide for 15 s contact time. The microarray on the stamp was replicated faithfully as a microarray on the aldehyde substrate. The spot size was regular and probe density was homogeneous (Figure 6-8).

In a second experiment, an array of an amino-modified oligonucleotide labeled with fluorescein, and two mixtures of polyadenylated RNA labeled with Cy3 and Cy5, respectively, was fabricated onto a flat dendri-stamp. The spotted dendri-stamp was brought into conformal contact with an aldehyde-terminated glass slide for 15 s contact time and subsequently used for 3 additional prints without supplementary reloading with oligonucleotides. After each microcontact print, the substrates were rinsed thoroughly with ethanol containing a drop of triethylamine, ethanol and water. The first three prints exhibit almost equal intensities and densities of oligonucleotides and RNA mixtures on the aldehyde substrate. A significant decrease of intensity is noticed during the fourth print (Figure 6-9). Microcontact printed spots of oligonucleotides and RNA mixtures on the aldehyde-terminated glass slides have a good spot uniformity. This experiment demonstrates that a microarray of hundreds of probes can be replicated faithfully several times by microcontact printing using the dendri-stamps and that DNA and RNA are both printed equally well.
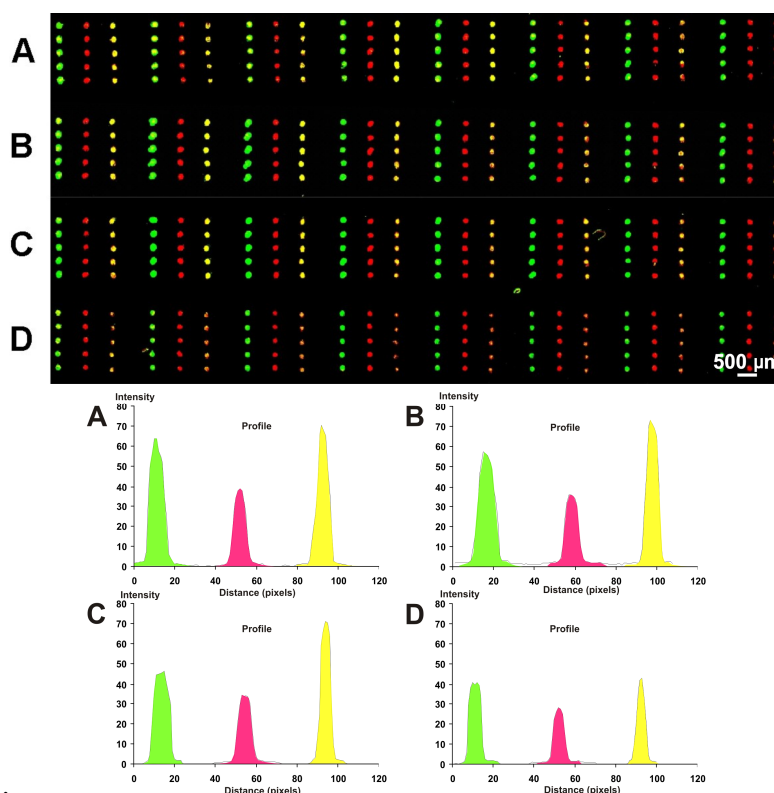

Figure 6-9. Fluorescence microscopy image of an array of four microcontact printed patterns (from A to B) that were fabricated using one dendri-stamp with spotted different oligonucleotides. Total number of spots: 120. A)-First print, B)-Second print, C)-Third print, D)-Fourth print. Bottom: Average intensity

profiles of three different dyes: fluorescein (green), Cy5 (red), Cy3 (yellow) attached to DNA (green) or RNA (red and yellow).

6.5. Modification of AFM tips for DNA delivery

One of the promising methods that could minimize the spot size of biomolecules and create ultra-high density arrays is dip-pen nanolithography (DPN) which is capable to fabricate sub-100 nm patterns with high precision and registry (see Chapter 2). In a typical DPN experiment, alkanethiols are used to coat the AFM tip and these are deposited from the tip through a water meniscus on the gold substrate as a self-assembled monolayer. [34,35] The diffusion-based process is using the dependence between dwell time and feature size; the longer tip is contacting the substrate the larger features are produced. This technique is compatible with a wide variety of substrates and (bio)molecules such as DNA,[36,37] proteins[38,39] or peptides[40,41] as an ink. Due to its direct deposition nature, this technique seems to be a universal method for the fabrication of sub-micrometer size patterns. The main requirement for successful pattern fabrication is the specific interaction (covalent, electrostatic, or physical) between the ink and the surface of the substrate. For the patterning of biomolecules by DPN several approaches have been proposed (see Chapter 2). DNA possessing a thiol linker at one terminus was used as an ink and deposited on gold substrates.[36] A similar strategy has been proposed for the patterning of proteins containing cysteine residues.[42] Often an indirect method of DPN is used to immobilize biomolecules (such as DNA), cells or viruses.[43] This method relies on "writing" with mercaptohexadecanoic acid (MHA) on gold and subsequent immobilization of linkers and biomolecules.[35,44]

The DPN process can be facilitated by several factors including careful functionalization of the AFM tip, precise control of humidity and ink-substrate combination. Ginger *et al.* have shown that by activation of the AFM tips with aminosilanes ((aminopropyl)triethoxysilane) and humidity up to 95 %, it is possible to pattern directly DNA onto diverse substrates. On the other hand, in previous sections it was shown that a PDMS stamp modified with amino-functionalized dendrimers, characterized by a high density of positive charge on the surface of that stamp, is able to attract large quantity of natively charged DNA molecules. This idea was here utilized to functionalize AFM tips with PPI or PAMAM dendrimers and immobilize DNA molecules for the transfer and delivery to the activated glass slide. DNA molecules that were used in this experiment were modified with a C6-NH_2 linker to introduce specific binding between "ink" and aldehyde-terminated glass substrate. The probe sequence was: 5'-NH_2-C6-GTG CAC CTG ACT CCT GTG-3'-fluorescein. To facilitate the attachment of DNA to the AFM tip surface in a

simple manner and "load" the tip with high yield, silicon nitride tips were oxidized to expose silanol groups on the surface and bind dendrimers via electrostatic interactions. Once dendrimers are bound to the tip they introduce a high density of positive charge to the surface of the tip and at the same time they are able to attract negatively charged DNA molecules in a "layer-by-layer" fashion (Figure 6-10).
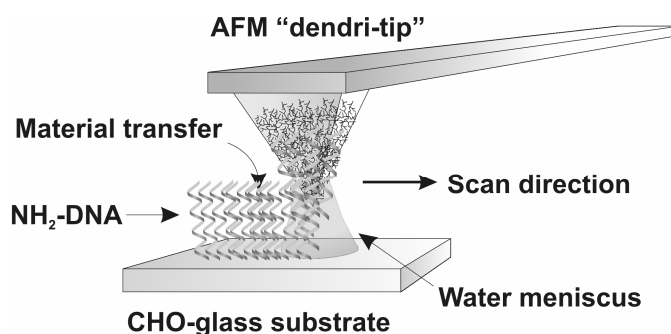

Figure 6-10. An AFM "dendri-tip" which is used to generate DNA patterns on an aldehyde functionalized glass substrate. The silicon nitride tip is first oxidized and coated with PPI or PAMAM dendrimers. The modified tip ("dendri-tip") is then incubated with the solution of DNA and used directly for writing DNA structure on the substrate.

By contacting the inked tip with the functionalized surface, DNA molecules were deposited through the water meniscus and immobilized in a specific pattern. The dwell time needed for the sufficient DNA attachment was in the range between 10-30 s, (humidity ca. 30 % and a temperature 25 ℃). Several patterns of DNA which were fabricated using the "dendri-tip" are shown in Figure 6-11. The average width of DNA lines (Figure 6-11) was 200 nm and similarly, the diameter of the fabricated DNA spots was also 200 nm.
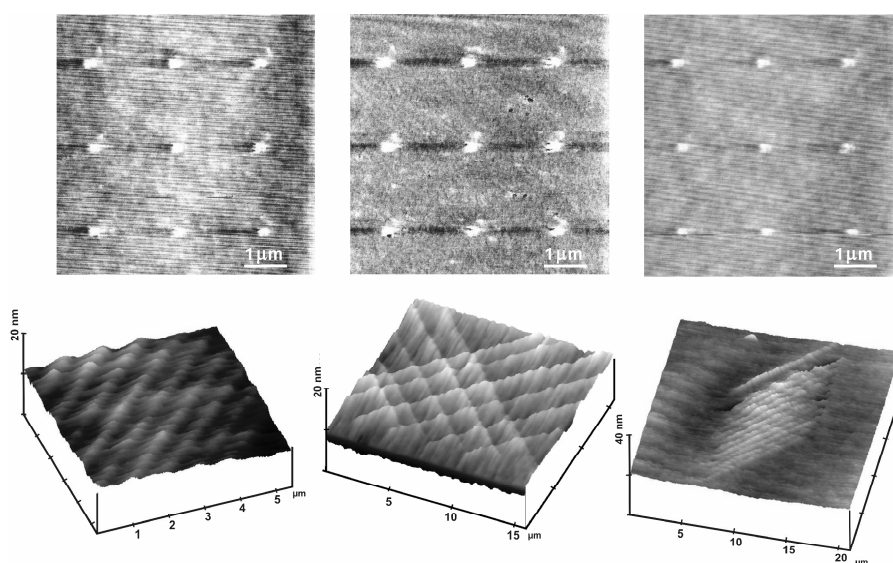

Figure 6-11. AFM height images of DNA patterns on an aldehyde-functionalized glass substrate created using the AFM tips modified with PPI or PAMAM dendrimers which were incubated with DNA solution.

After pattern formation by DPN the substrates were rinsed thoroughly with Et$_3$N/EtOH and MilliQ water in order to remove possible dendrimer residues adsorbed onto the DNA pattern. To confirm that transferred molecules were in fact DNA molecules, squares of 80 µm were drawn and the substrate was investigated by using a fluorescent microscope. The results are illustrated in Figure 6-12.
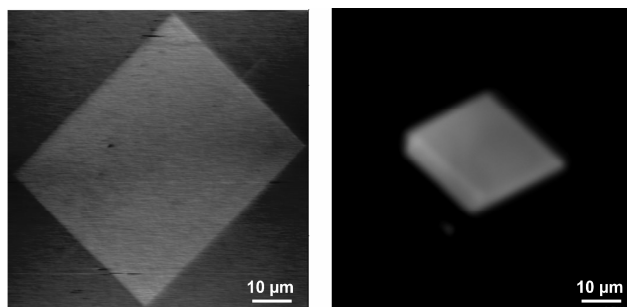

Figure 6-12. Left image: AFM height image of DNA on an aldehyde-functionalized glass substrate fabricated using a "dendri-tip". Right image: fluorescence microscopy image of a fluorescein-labeled-DNA pattern fabricated using an AFM "dendri-tip".

Analysis of the cross section shows that the written patterns were approximately 2 nm in height which corresponds to the size of the immobilized DNA strands (Figure 6-13). This result is also consistent with the height of DNA features printed using dendri-stamp (Figure 6-5). The important feature of fabricated patterns is that lines are continuous without any failure which is essential when considering further applications towards, for example nanowires.
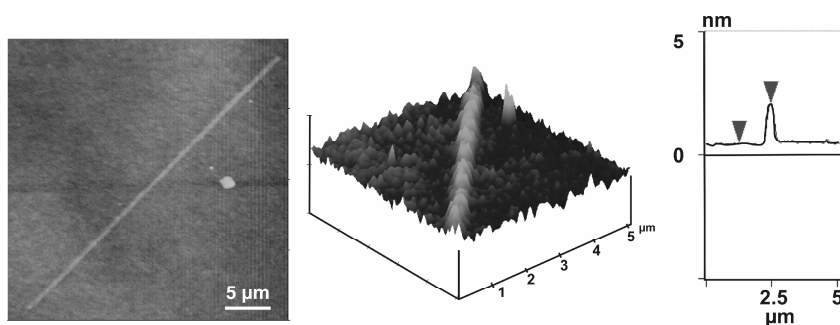

Figure 6-13. Cross section analysis of DNA line fabricated using dendrimer-functionalized silicon nitride tip (AFM height image). The average height of the line is 2 nm.

6.6. Conclusions

In conclusion, a new method to transfer DNA and RNA to a target surface and to replicate an array has been developed. By printing oligonucleotides using PDMS stamps modified with amino-dendrimers very homogeneous patterns of the probe with a high intensity signal can be obtained. There is no difference between the edge and the middle of the pattern, the so called "doughnut effect".[11] Oligonucleotides printed in 15 s are of the same density as a

probe that was immobilized from the solution during at least 16 h. In addition, patterns of oligonucleotides printed with dendri-stamp show 10 times higher intensity than patterns obtained by printing DNA with an APTES-modified PDMS stamp. This suggests that also the probe surface concentration is much higher. DNA that is printed in this manner is available for hybridization. The fabrication of uniform patterns does not require specialized equipment, cleanroom facilities, complex technology or time consuming modifications of PDMS. This fabrication method of uniform oligonucleotide patterns can subsequently be combined with spotting systems which enable introduction of thousands of different oligonucleotides on the same dendri-stamp. This array can be microcontact printed multiple times with good spot uniformity. From one "master" DNA/RNA array on the dendri-stamp it is possible to obtain 3-4 copies of that array possessing good DNA/RNA density and good spot homogeneity. Moreover, RNA molecules appear to be transferred equally well compared to DNA oligonucleotides. This method can be readily extended to arrays of many thousands of probes and should facilitate and improve microarray-fabricated substrates.

Modification of an AFM tip with PPI or PAMAM dendrimers introduces a high density of positive charge to the surface of the tip. Such a tip is able to attract negatively charged molecules like oligonucleotides through electrostatic interactions. To immobilize DNA on the surface specific interactions between ink and the substrate must be involved. Here, it has been shown that amino-modified oligonucleotides are able to react with aldehyde-functionalized glass surfaces simply by applying a contact between dendri-tip and the surface. The advantage of this method is that the writing process can be conducted in ambient laboratory condition without the need of enhancing humidity since 30 % relative humidity (i.e. standard air humidity) is already sufficient to induce the transfer of DNA from the tip. The tip modification is simple, fast and does not require additional process steps such as silanization or gold evaporation which is commonly used in tip functionalization.

6.7.   Experimental section

Materials. All oligonucleotides were purchased from Sigma. The probe sequence employed in surface studies had sequence 5'-GTG CAC CTG ACT CCT GTG GAG-3' (single strand of mutant β-globin gene) and was modified at the 5' terminus with a six-carbon linker and amino group (NH_2-$(CH_2)_6$-) and at the 3' with fluorescein. The target sequence was 5'- CTC CAC AGG AGT CAG GTG CAC-3', 5'-CTC <u>CTC</u> AGG AGT CAG GTG CAC-3' (single mismatch) , 5'- CAC GTG GAC TGA GGA ACA CCT-3' (total mismatch, reverse sequence) all with the Cy5 modification at the 5' terminus. All the nucleotides had were HPLC purified

and modified by the manufacturer. The probe concentration was 1 μM in Tris-EDTA buffer pH 8 and the target concentration was 1 μM in 4 x SSC, 0.2 % SDS solution. Before use, oligonucleotides were denatured at 95 °C for 5 min. All buffers and immobilization solutions were prepared with 18 MΩ·cm distilled water (MilliQ). The following materials and chemicals were used as received: poly(dimethylsiloxane) (PDMS) (Dow Corning), $NaBH_4$ (Aldrich), trimethoxysilylalkylaldehyde (Fluorochem), polypropyleneimine tetrahexacontaamine dendrimers, generation 5 (Aldrich), 3-aminopropyltriethoxysilanes (APTES) (Aldrich). All solvents were HPLC grade, and all other reagents were analytical grade. Other solvents or reagents were purchased from either Aldrich or Sigma.

Modification of glass slides. Clean microscope cover glass (Paul Marienfeld Gmbh & Co.KG, Germany) was activated with piranha solution for 45 min (concentrated H_2SO_4 and 33 % aqueous H_2O_2 in a 3:1 ratio) *(Warning! Piranha solution should be handled with caution: it has been reported to detonate unexpectedly.)*, rinsed with water (MilliQ) and immediately immersed in 0.1 vol. % trimethoxysilylalkylaldehyde in toluene for 1 h. Following monolayer formation, the substrates were rinsed with toluene to remove any excess of silanes and subsequently dried in N_2.

Modification of gold substrates. Aldehyde-terminated monolayers on annealed gold substrates were prepared according to previously published procedures (see Chapter 3).

Fabrication of stamps. Silicon wafer-based masters with etched structures were prepared by UV photolithography. The master surface was fluorinated using fluorosilanes. PDMS stamps were fabricated by curing Sylgard 184 on the surface of the master at 60 °C for 12 h.

Microcontact printing of DNA with dendrimers. PDMS stamps were first oxidized in UV/ozone plasma reactor (Ultra-Violet Products, model PR-100) for 30 min at a distance of about 2 cm from the plasma source. [This reactor contains a low-pressure mercury UV light operating with UV emissions at 185 nm (1.5 mW cm^{-2}) and 254 nm (15 mW cm^{-2}) to generate molecular oxygen]. Subsequently the hydrophilic stamps were immersed in 1 μM ethanolic solution of dendrimers for 30 s and blow dried with nitrogen. A drop of oligonucleotide solution was incubated on the stamp for 20 min at room temperature. The probe concentration was 1 μM in Tris-EDTA buffer pH 8 solution. The stamp was dried with nitrogen and brought into conformal contact with the aldehyde-terminated glass slide for 15 s. After printing, the stamp

was lifted off and the substrate was rinsed with 30 mL of ethanol containing a drop of triethylamine in order to remove the dendrimer layer and subsequently dried with nitrogen.

Reduction of imines on the surface. After printing amino-modified oligonucleotides onto the aldehyde-terminated substrate, the glass slide was immersed in solution containing 50 mg $NaBH_4$ in 30 mL PBS with 10 mL EtOH for 5 min as described in Ref. [17]. After reaction time the substrate was washed in 0.2 % SDS solution for 2 min under agitation, in water for 1 min and subsequently dried with nitrogen.

Hybridization on the substrate surface. For hybridization, a 5'-Cy5-labeled oligonucleotide was diluted to 1 µM in 4 x SSC containing 0.2 % SDS and applied to the surface of the modified glass slide as described by Afanassiev et al.[17] A coverslip was mounted gently on the top of the solution and the substrates where transferred to the hybridization oven at 42.3-47.3 °C for overnight. The unhybridized probes were removed by washing with vigorous agitation in the 1 x SSC with 0.1 % SDS solution for 5 min at hybridization temperature, 0.1 x SSC with 0.1 % SDS for 5 min at RT, and subsequent washing in water for 5 min. After washing, the glass slides were dried with nitrogen and scanned on a confocal fluorescent microscope (Zeiss 510) to visualize hybridization signals.

Tip modification. The silicon nitride contact mode tip was oxidized in an oxygen plasma reactor for 10 min and immediately immersed in 1 µM solution of PPI dendrimers for 10 s. Subsequently the tip was immersed in an oligonucleotide solution 1 µM in TE for 20 min and directly used for DPN.

Dip-pen nanolithography. DPN was carried out on a NScriptor (NanoInk, Chicago, IL, USA) and on Dimension 3100/Nanoscope IVa (Digital Instruments, Santa Barbara, CA, USA) in contact mode, with 512 x 512 data acquisitions, using single and multipen arrays type E, F, M NScriptor (NanoInk, Chicago, IL, USA). DPN was conducted at room temperature in air, at 30 % relative humidity. The contact time between the tip and aldehyde-functionalized substrate was 10-30 s. After nanolithography the substrates were rinsed thoroughly with Et_3N/EtOH, water and dried with nitrogen.

Instrumentation. *Atomic force microscopy (AFM) imaging.* AFM measurements were carried out on a Dimension 3100/Nanoscope IVa (Digital Instruments, Santa Barbara, CA, USA) in tapping mode, with 512 x 512 data acquisitions, using ultrasharp tips (MikroMash,

Spain). All imaging was conducted at room temperature in air. Annealed gold substrates with aldehyde-terminated thiol monolayers[45] were used as substrates for AFM imaging.

Fluorescence microscopy. Fluorescence images were acquired with a Carl Zeiss LSM 510 scanning confocal microscope. Red- and green-labeled DNA were visualize at $\lambda_{ex} = 650$ nm ($\lambda_{em} = 670\text{-}700$ nm) and $\lambda_{ex} = 495$ nm ($\lambda_{ex} = 517$ nm) respectively. The emitted fluorescence was collected on a R6357 spectrophotometer.

Contact printing by robotic systems. The spots of oligonucleotides were fabricated using MicroGrid, Apogent Discoveries. Flat, 2-3 mm thin dendri-stamps were used as substrates for contact printing. Following probes were used for spotting experiment: 5'-NH$_2$-C$_6$-GTG CAC CTG ACT CCT GTG GAG-fluorescein-3', and mixtures polyA-RNA of *Bacillus subtilus* genes (ycxA, yceG, ybdO, ybbR, ybaS, ybAF) labeled with Cy-5 and (ybaC, yacK, yabQ, Trp, Thr, Dap, Phe, Lys) labeled with Cy-3 using the ULS labeling system (Kreatech BV, Amsterdam). The spotting solution of probe was 1 μM in Tris-EDTA buffer pH 8 solution. After printing the substrates were left to dry under ambient conditions and used for microcontact printing.

6.8. References

[1] M. O. Noordewier, P. V. Warren, *Trends Biotechnol.* **2001**, *19*, 412.

[2] T. R. Golub, D. K. Slonim, P. Tamayo, C. Huard, M. Gaasenbeek, J. P. Mesirov, H. Coller, M. L. Loh, J. R. Downing, M. A. Caligiuri, C. D. Bloomfield, E. S. Lander, *Science* **1999**, *286*, 531.

[3] B. J. Hong, S. J. Oh, T. O. Youn, S. H. Kwon, J. W. Park, *Langmuir* **2005**, *21*, 4257.

[4] W. Heiser, *Methods in molecular biology. Gene delivery to mammalian cells. Vol. 1. Nonviral gene transfer technique*, Human Press, **2004**.

[5] C. M. Perou, *Nature* **2000**, *406*, 747.

[6] C. Heise, F. F. Bier, *Top Curr. Chem.* **2006**, *261*, 1.

[7] S. P. Fodor, J. L. Read, M. C. Pirrung, L. Stryer, A. Y. Lu, D. Solas, *Science* **1991**, *251*, 767.

[8] G. H. McGall, A. D. Barone, M. Diggelmann, S. P. A. Fodor, E. Gentalen, N. Ngo, *J. Am. Chem. Soc.* **1997**, *119*, 5081.

[9] A. del Campo, I. J. Bruce, *Top Curr. Chem.* **2005**, *260*, 77.

[10] M. C. Pirrung, *Angew. Chem. Int. Ed.* **2002**, *41*, 1276.

[11] F. Diehl, S. Grahlmann, M. Beier, J. D. Hoheisel, *Nucleic Acids Res.* **2001**, *29*, e38.

[12] V. G. Cheung, M. Morley, F. Auilar, R. Kucherlapati, G. Childs, *Nature Genet.* **1999**, *21*, 15.

[13] M. Beier, J. D. Hoheisel, *Nucleic Acids Res.* **1999**, *27*, 1970.

[14] N. Zammatteo, L. Jeanmart, S. Hamels, S. Courtois, P. Louette, L. Hevesi, J. Remacle, *Anal. Biochem.* **2000**, *280*, 143.

[15] E. Fahy, G. R. Davis, L. J. DiMichele, S. S. Ghosh, *Nucleic Acids Res.* **1993**, *21*, 1819.

[16] R. Benters, C. M. Niemeyer, D. Drutschmann, D. Blohm, D. Wöhrle, *Nucleic Acids Res.* **2002**, *30*, e10.

[17] V. Afanassiev, V. Hanemann, S. Wölfl, *Nucleic Acids Res.* **2000**, *28*, e66.

[18]   A. Kumar, Z. Liang, *Nucleic Acids Res.* **2001**, *29*, e2.

[19]   L. M. Demers, D. S. Ginger, S. J. Park, Z. Li, S. W. Chung, C. A. Mirkin, *Science* **2002**, *296*, 1836.

[20]   S. Xu, G. Y. Liu, *Langmuir* **1997**, *13*, 127.

[21]   V. Le Berre, E. Trévisiol, A. Dagkessamanskaia, S. Sokol, A.-M. Caminade, J.-P. Majoral, B. Meunier, J. François, *Nucleic Acids Res.* **2003**, *31*, e88.

[22]   R. Benters, C. M. Niemeyer, D. Wöhrle, *ChemBioChem* **2001**, *2*, 686.

[23]   B. J. Hong, V. Sunkara, J. W. Park, *Nucleic Acids Res.* **2005**, *33*, e106.

[24]   B. H. Zinselmeyer, S. P. Mackay, A. G. Schatzlein, I. F. Uchegbu, *Pharmaceutical Research* **2002**, *19*, 960.

[25]   C. S. Braun, J. A. Vetro, D. A. Tomalia, G. S. Koe, C. R. Middaugh, *J. Pharm. Sci.* **2005**, *94*, 423.

[26]   S. A. Lange, V. Benes, D. P. Kern, J. K. H. Hober, A. Bernard, *Anal. Chem.* **2004**, *76*, 1641.

[27]   C. Xu, P. Taylor, M. Ersoz, P. D. J. Fletcher, V. Paunov, *J. Mater. Chem.* **2003**, *13*, 3044.

[28]   P. Björk, S. Holmström, O. Inganäs, *Small* **2006**, *2*, 1068.

[29]   F. Zeng, S. C. Zimmerman, *Chem. Rev.* **1997**, *97*, 1681.

[30]   A. W. Bosman, H. M. Janssen, E. W. Meijer, *Chem. Rev.* **1999**, *99*, 1995.

[31]   V. A. Kabanov, A. B. Zezin, V. B. Rogacheva, Z. G. Gulyaeva, M. F. Zansochova, J. G. H. Joosten, J. Brackman, *Macromolecules* **1999**, *32*, 1904.

[32]   R. C. van Duijvenbode, M. Borkovec, G. J. M. Koper, *Polymer* **1998**, *39*, 2657.

[33]   G. Decher, *Science* **1997**, *277*, 1232.

[34]   R. D. Piner, J. Zhu, F. Xu, S. H. Hong, C. A. Mirkin, *Science* **1999**, *283*, 661.

[35]   D. S. Ginger, H. Zhang, C. A. Mirkin, *Angew. Chem. Int. Ed.* **2004**, *43*, 30.

[36]   L. M. Demers, D. S. Ginger, S.-J. Park, Z. Li, S.-W. Chung, C. A. Mirkin, *Science* **2002**, *7*, 1836.

[37]   S.-W. Chung, D. S. Ginger, M. W. Morales, Z. Zhang, V. Chandrasekhar, M. A. Ratner, C. A. Mirkin, *Small* **2005**, *1*, 64.

[38]   K. Y. Lee, L. J. H., C. A. Mirkin, *J. Am. Chem. Soc.* **2003**, *125*, 5588.

[39]   J.-H. Lim, D. S. Ginger, K.-B. Lee, J. Heo, J.-M. Nam, C. A. Mirkin, *Angew. Chem. Int. Ed.* **2003**, *42*, 2309.

[40]   Y. Cho, A. Ivanisevic, *J. Phys. Chem. B* **2004**, *108*, 15223.

[41]   Y. Cho, A. Ivanisevic, *J. Phys. Chem. B* **2005**, *109*, 6225.

[42]   J. C. Smith, K.-B. Lee, Q. Wang, M. G. Finn, J. E. Johnson, M. Mrksich, C. A. Mirkin, *Nano Lett.* **2003**, *3*, 883.

[43]   R. A. Vega, D. Maspoch, K. Salaita, C. A. Mirkin, *Angew. Chem. Int. Ed.* **2005**, *44*, 6013.

[44]   K. Salaita, Y. Wang, C. A. Mirkin, *Nature Nanotechnology* **2007**, *2*, 145.

[45]   D. I. Rożkiewicz, B. J. Ravoo, D. N. Reinhoudt, *Langmuir* **2005**, *21*, 6337.

Chapter 7

"Click" chemistry by microcontact printing[*][§]

"Click" chemistry can be efficiently combined with microcontact printing. 1,3-dipolar cycloaddition where alkynes and azides react to give triazoles can serve as a good example for the reaction conducted under stamp confinement. Usually this reaction needs Cu(I) catalyst to accelerate the rate of reaction. In this Chapter it will be shown that synthesis in the nanoscale confinement between an elastomeric stamp and a reactive substrate leads to the desired product within a short period of time, without a catalyst, and under mild conditions.

7.1. Introduction

Microcontact printing (μCP) is commonly used to pattern self-assembled monolayers (SAMs) as etch resists or chemical templates on gold and silicon oxide substrates.[1-4] However, μCP can also be used for chemical synthesis on gold and silicon oxide in the nano-scale confinement between stamp and substrate. Amines can be printed onto reactive anhydride SAMs.[5-7] Peptides can be synthesized by printing *N*-protected amino acids onto an amine SAM.[3] It has been proposed that the confinement of the ink at the interface between the elastomeric stamp and the self-assembled monolayer, in combination with the pre-organization of the reactants in the monolayer, facilitates the formation of covalent peptide bonds.[8] Recently, imine formation via μCP of amines on aldehyde SAMs was demonstrated [9] and applied this chemistry to direct the immobilization of cytophilic proteins.[10] In this chapter a Huisgen *1,3*-dipolar cycloaddition will be presented, as a representative example of the Sharpless "click" chemistry, induced *without any catalyst* by μCP of acetylenes onto azide-terminated SAMs on silicon oxide substrates.

"Click" chemistry includes a range of reactions that proceed in high yield under simple conditions, preferably in water, with regioselectivity and broad tolerance of functional groups.[11] The Cu catalyzed 1,3-dipolar cycloaddition reaction of azides and acetylenes is known as the "cream of the crop" of all "click" reactions.[12, 13] This cycloaddition is irreversible and proceeds in quantitative yield without any side products in many solvents, including water. Acetylenes and azides are stable educts that do not react between themselves. Azides are known for their ease of introduction, and both azides and acetylenes show great tolerance of other functionalities. The triazole group is a thermally and hydrolytically stable, conjugated linkage. Increasingly, "click" chemistry is used for the preparation of biological conjugates and the immobilization of biomacromolecules.[14-18] Triazole formation on surfaces was applied for the modification of SAMs on gold substrates,[19-22] SAMs on silicon oxide,[23] carbon nanotubes,[24] and polymer adhesives.[25] Azide-terminated monolayers were utilized for the immobilization of substituted acetylenes (including ferrocene and oligonucleotides)[19-23,26] via triazole linkage. The majority of Huisgen reactions - in particular those which involve electron-rich acetylenes – need a Cu catalyst, which may accelerate the reaction by a factor of 10^7. This catalyst is usually Cu(I), generated from Cu(II) by an excess of reducing agent such as for instance sodium ascorbate.[12,13] In this Chapter it will be shown that the high local concentration of reagents in the contact area of the elastomeric stamp and the monolayer surface is sufficient to obtain full conversion reaction within *minutes* of contact time, even *without* a Cu catalyst. In particular for the immobilization of biomolecules it is advantageous to exclude the toxic Cu catalysts.

7.2.   Synthesis under elastomeric stamp confinement

Azide-terminated SAM on silicon oxide was prepared by the substitution of a bromide-terminated monolayer with NaN$_3$.[27] The bromide-terminated SAM was obtained by the immersion of a 1 x 1 cm piece of silicon wafer (cleaned and activated with piranha) in 0.1 % (v/v) *11*-bromoundecyltrichlorosilane in toluene for 20 min at 20 °C. To substitute the bromide for the azide group we used a saturated solution of NaN$_3$ in DMF for 48 h at 70 °C.[27] The substrate was rinsed with MilliQ water and ethanol and dried with nitrogen. The preparation of the azide-terminated SAMs and the subsequent "click" chemistry by µCP of acetylenes are outlined in Figure 7-1.
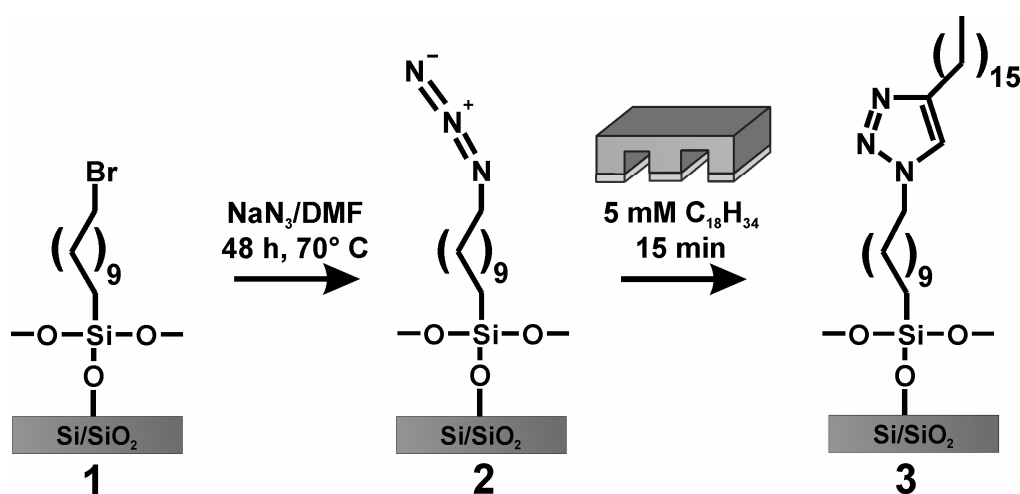
Figure 7-1. Schematic representation of "click" chemistry by microcontact printing (µCP). **1** Bromide-terminated SAM on a Si/SiO$_2$ substrate. **2** Azide-terminated SAM. **3** Triazole SAM after µCP of 1-octadecyne onto azide-terminated SAM.

As a first illustration of the potential of µCP of acetylenes onto azide-terminated SAMs on silicon substrate *1*-octadecyne was printed with a poly(dimethylsiloxane) (PDMS) stamp with features of 3 x 5 µm. The stamp was inked in 5 mM ethanolic solution of *1*-octadecyne for 1 min, dried with nitrogen and brought into contact with the substrate SAM for 15 min and with a load of 35 g. After rinsing with ethanol the substrate was imaged with AFM. Figure 7-2 depicts the pattern made by printing *1*-octadecyne on substrate **2**. Evidently, the 3 x 5 µm features of the stamp are reproduced faithfully on the substrate. The average height of the 3 µm wide lines in the pattern is approximately 1 nm.
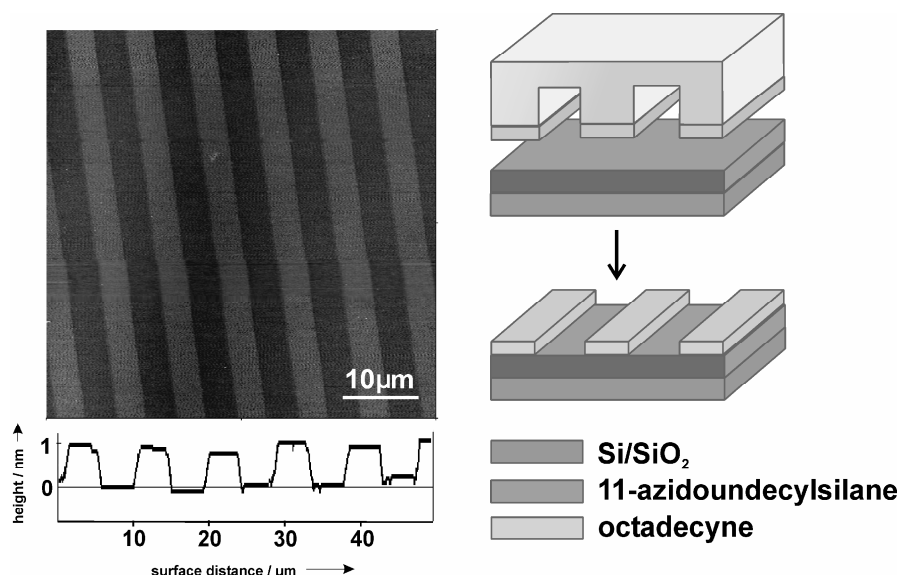
Figure 7-2. Tapping mode AFM image (50 μm x 50 μm) and line section of a 3 x 5 μm line pattern obtained by printing 1-octadecyne onto azide-terminated SAM **2** on a silicon oxide substrate.

To verify triazole formation on the azide SAM, the reaction between the azide SAM and *1*-octadecyne induced μCP and from solution was compared. To demonstrate triazole formation via μCP first a flat, featureless PDMS stamp was used. The stamp was inked with 5 mM ethanolic solution of *1*-octadecyne and brought into conformal contact with the azide-terminated SAM for 15 min with a load of 35 g (to ensure conformal contact with the substrate for the reaction time). After printing, the substrate was rinsed with ethanol and dried with nitrogen. To investigate the reaction with acetylene from solution, the azide substrate was exposed to a 5 mM solution of *1*-octadecyne in ethanol for 48 h at room temperature. After reaction, the substrate was rinsed with ethanol and dried with nitrogen. The [2+3] cycloaddition of azides and electron-rich acetylenes like *1*-octadecyne is normally very slow in the absence of Cu catalyst. Indeed Collman *et al.*[19] and Lummerstorfer and Hoffman[23] report that no reaction occurs between azide SAMs and electron-rich acetylenes in the absence of Cu catalyst.[28, 29] To scavenge any adventitious metal contamination in solvents, reactants, PDMS stamps or substrates, the cycloaddition reaction was also performed in the presence of 0.05 % EDTA. There was no change in the reaction of the azide SAM either by μCP or from solution.

The X-ray photo-electron spectroscopy (XPS) spectrum of bromide-terminated SAM **1** shows a pronounced Br (3d) peak at 70.5 eV (Figure 7-3). After substitution with NaN$_3$, the Br (3d) peak disappeared and a N (1s) peak appeared at 400 eV, confirming complete reaction. When *1*-octadecyne was introduced in 15 min by μCP using a flat PDMS stamp (**3**) or in 48 h by reaction from solution (**3***), the intensity of C1s peak increased while the intensity of N1s

peak decreased. The C/N ratio calculated from the elemental composition revealed that when the triazole monolayer was formed from solution the ratio of C/N was 9.7 while after printing the ratio was C/N=10.8. The theoretical ratio C/N = 10. Hence, XPS indicates that the triazole is formed by reaction from solution and by reaction using μCP, but the cycloaddition occurs much faster by μCP than by reaction from solution.
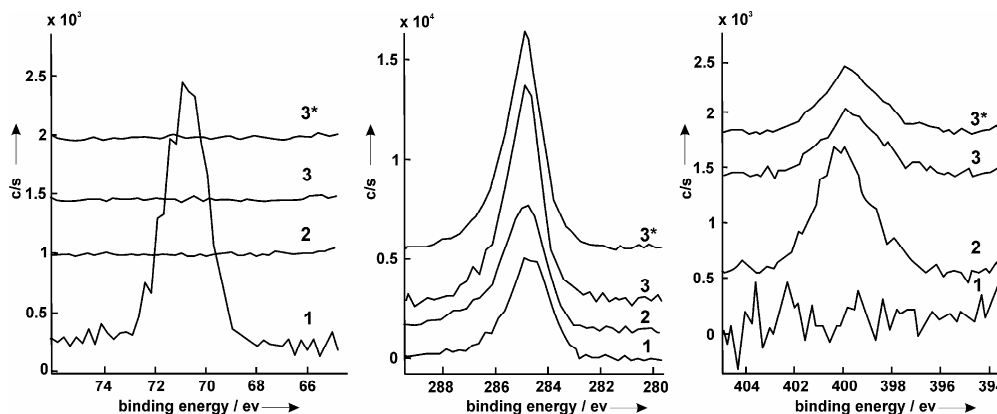

Figure 7-3. Element XPS scans for a) bromine, b) carbon, c) nitrogen in: **1** Bromide-terminated SAM. **2** Azide-terminated SAM. **3** Triazole SAM prepared by μCP of 1-octadecyne on SAM 2 for 15 min. 3* Triazole SAM prepared by reaction from solution of 1-octadecyne with SAM 2 for 48 h.
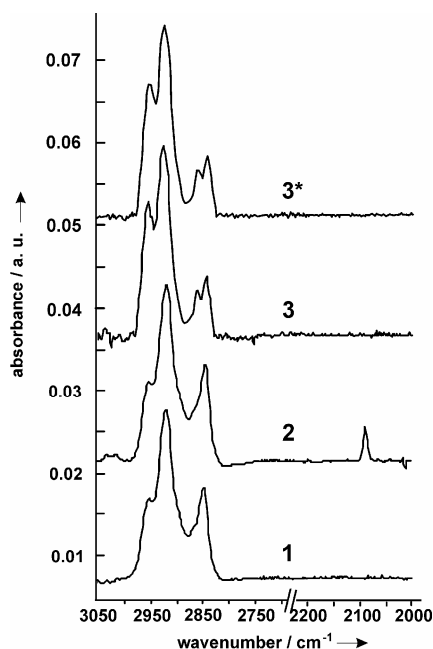
Figure 7-4. GA-IS spectra of functionalized monolayers on a silicon oxide substrate. **1** Bromide-terminated SAM. **2** Azide-terminated SAM. **3** Triazole SAM prepared by μCP of 1-octadecyne on SAM 2 for 15 min. **3*** Triazole SAM prepared by reaction from solution of 1-octadecyne with SAM **2** for 48 hours.

Grazing-angle infrared spectroscopy (GA-IS) of bromide-terminated SAM **1** revealed the typical methylene bands at 2924 cm^{-1} and 2852 cm^{-1} (Figure 7-4, **1**). After exposure of the bromide-terminated SAM **1** to NaN$_3$, the azide-terminated monolayer showed absorption at 2089 cm^{-1} (v_{as} (N$_3$)) in addition to the methylene absorption bands (Figure 7-3A, **2**). When SAM **2** was reacted for 48 h with *1*-octadecyne from solution (Figure 7-4, **3***) the azide peak disappeared and in addition two bands responsible for methyl stretching were visible at 2960 cm^{-1} (v_{as} (CH$_3$)) and at 2871 cm^{-1} (v_s (CH$_3$)). The bands at 2935 cm^{-1} and 2855 cm^{-1} are the methylene stretching modes. After µCP of *1*-octadecyne via a flat PDMS stamp for 15 min (Figure 7-4, **3**) the IR spectrum was identical for the reaction conducted from solution. In summary, the cycloaddition reaction is confirmed by the disappearance of the v_{as} (N$_3$) and the appearance of v (CH$_3$) peaks.[19]

In addition, the cycloaddition reaction of azide substrate **2** with *1*-octadecyne was monitored with ellipsometry. It was found that bromide SAM **1** has a thickness $d = 1.34 \pm 0.08$ nm and azide SAM **2** has $d = 1.48 \pm 0.10$ nm, while for triazole SAM **3** $d = 2.10 \pm 0.14$ nm and for triazole SAM **3*** $d = 1.88 \pm 0.17$ nm. Hence, the cycloaddition leads to a significant increase of the thickness of the SAM, consistent with the AFM height scan (Figure 7-2). The increase in d (0.5-1.0 nm) indicates that the triazole alkyl chain is substantially tilted relative to the surface.

7.3. Printing with fluorescent ink

Furthermore, to illustrate the power and scope of the triazole click reaction by µCP a fluorescent alkyne **4** on azide SAM **2** was printed (Figure 7-5). In this case, the PDMS stamp was oxidized with UV/ozone plasma for 30 min in order to increase the wettability and improve the spreading of the polar ink on the stamp. Directly after oxidation the stamp was inked with 1 mM solution of alkyne **4** in ethanol, dried with nitrogen for 1 min and brought into conformal contact with azide-terminated SAM **2** on a glass slide for 1 min. The substrate was vigorously rinsed with MilliQ water, sonicated in ethanol for 5 min and dried with nitrogen. It is evident from the confocal microscopy image in Figure 7-5 that the 20 µm dot features of the stamp are reproduced faithfully on the substrate and that the ink is distributed homogeneously over the contact area. Since the alkyne **4** is still present on the surface in spite of extensive rinsing and sonication, any type of absorption other than covalent immobilization through triazole formation should be confidently excluded. To scavenge any adventitious metal contamination, µCP of alkyne **4** on SAM **2** in the presence of 0.05 % EDTA was performed. No change was observed. However, when the microcontact printing of alkyne **4** on an "inert" SAM of *n*-dodecyltriethoxysilane was performed, no evidence of immobilization of **4** was observed. This

could explain the remarkable efficiency of the click reaction of alkyne **4** printed on SAM **2** from the high local concentration of the polar ink at the surface of the oxidized PDMS stamp.
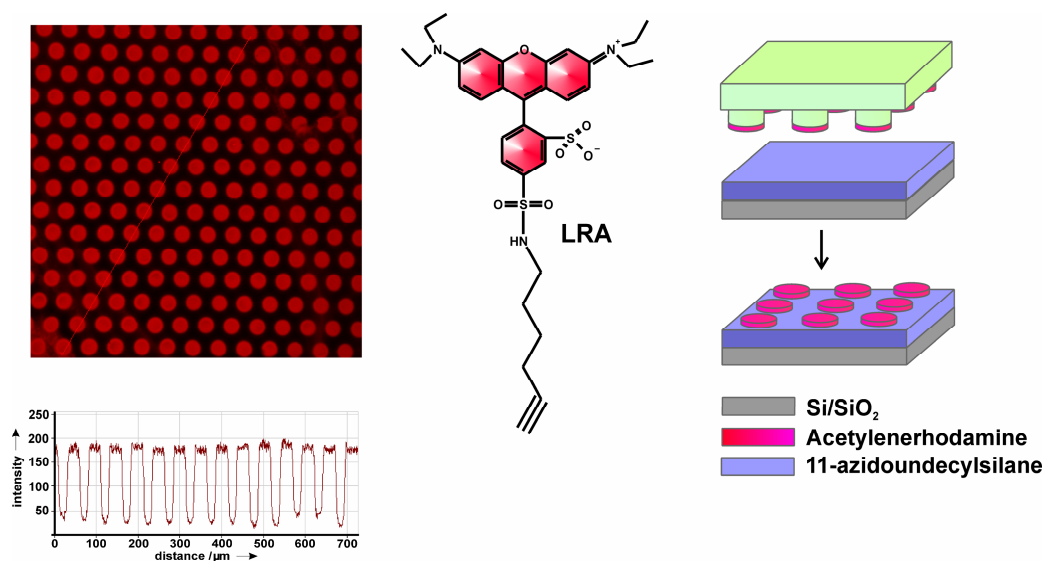

Figure 7-5. Fluorescent microscopy image (700 x 700 μm) of lissamine rhodamine with a terminal acetylene unit printed onto azide-terminated SAM 2. Schematic representation of the μCP induced "click" reaction between the fluorescent alkyne and the azide-terminated glass slide.

7.4. Conclusions

The above presented experiments show that "click" chemistry can be applied for the microcontact printing of acetylenes onto azide-terminated SAMs. Synthesis in the nanoscale confinement between a PDMS stamp and a reactive substrate leads to the desired product within a short period of time, without a catalyst, and under mild conditions. These experiments suggest that "click" chemistry by μCP can be applied using a wide variety of acetylenes and immobilized azides, as well as azides and immobilized acetylenes. In particular, this methodology will be useful for the directed immobilization of (bio)molecules that are modified with either acetylene or azide units. "Click" chemistry by μCP should serve the development of biological arrays that can be obtained within short reaction time, under mild reaction conditions, with no toxic catalyst required, with high selectivity and quantitative yields, and tolerance for a wide range of functionally complex substances.

7.5.   Experimental section

Materials. The following materials and chemicals were used as received: poly(dimethylsiloxane) (PDMS) (Dow Corning), NaN_3, rhodamine lissamine (Sigma), octadecyne (Aldrich), *11*-bromoundecyltrichlorosilane (Sigma), *n*-dodecyltriethoxysilane (Sigma). All solvents were HPLC grade, and all other reagents were analytical grade. Other solvents or reagents were purchased from either Aldrich or Sigma.

Modification of glass slides. Clean microscope cover glass (Paul Marienfeld Gmbh & Co.KG, Germany) was activated with piranha solution for 45 min (concentrated H_2SO_4 and 33 % aqueous H_2O_2 in a 3:1 ratio) *(Warning! Piranha solution should be handled with caution: it has been reported to detonate unexpectedly.)*, rinsed with water (MilliQ) and immediately immersed in 0.1 vol. % *11*-bromoundecyltrichlorosilane in toluene for 20 min at 20 °C. Following monolayer formation, the substrates were rinsed with toluene to remove any excess of silanes and subsequently dried in N_2. The bromide substitution for the azide group was conducted by the reaction with a saturated solution of NaN_3 in DMF for 48 h at 70 °C.[22] The substrate was rinsed with MilliQ water and ethanol and dried with nitrogen.

Fabrication of stamps. Silicon wafer-based masters with etched structures were prepared by UV photolithography. The master surface was fluorinated using fluorosilanes. PDMS stamps were fabricated by curing Sylgard 184 on the surface of the master at 60 °C for 12 h.

Microcontact printing with octadecyne. The PDMS stamp was inked in 5 mM ethanolic solution of *1*-octadecyne for 1 min, dried with nitrogen and brought into contact with the substrate SAM for 15 min and with a load of 35 g. The substrate was vigorously rinsed with ethanol, sonicated in ethanol fro 5 min and dried with stream of nitrogen.

Microcontact printing with fluorescent ink. The PDMS stamp was oxidized with UV/ozone plasma for 30 min in order to increase the wettability and improve the spreading of the polar ink on the stamp. Directly after oxidation the stamp was inked with 1 mM solution of alkyne **4** in ethanol, dried with nitrogen for 1 min and brought into conformal contact with azide-terminated glass slide for 1 min. The substrate was vigorously rinsed with MilliQ water, sonicated in ethanol for 5 min and dried with nitrogen.

Synthesis of lissamine rhodamine modified with acetylene unit. The synthesis of LRA was conducted according to the Scheme 7-1.
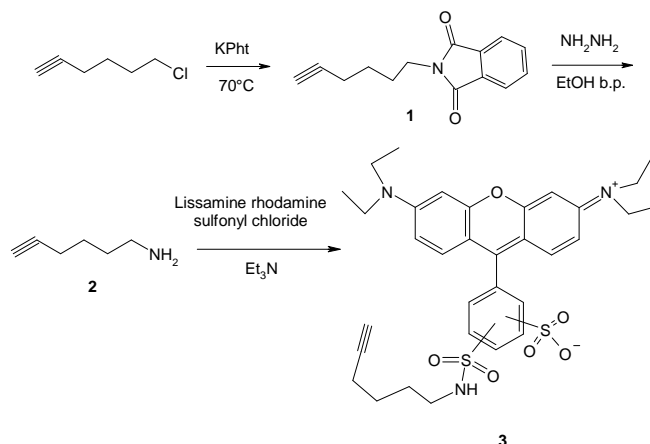
Scheme 7-1. Synthetic route to the acetylene-modified lissamine rhodamine (LRA).

6-Phtalimido-1-hexyne (1). Potassium phtalimide (12.428 g, 67 mmol) was added to the solution of 6-chloro-1-hexyn (5 mL, 41 mmol) in 100 ml of DMF. After stirring for 16 h at 70 °C the solvent was evaporated and the solid residue was suspended in CH_2Cl_2 and filtered through a layer of silica gel 60. Evaporation of the solvent resulted in title product (7.90 g, 35 mmol, 85 %). ^{1}H NMR (300 MHz, $CDCl_3$): δ = 7.85 – 7.83, 7.72 – 7.69 (m, 4 H, Ph), 3.72 (t, 2 H, J = 6.9 Hz, C*H*$_2$N), 2.57 (m, 2 H, CH$_2$C*H*$_2$CCH), 1.93 (t, 1 H, J = 2.7 Hz, CH$_2$CH$_2$CC*H*), 1.85 – 1.78, 1.61 – 1.50 (m, 4 H, CH$_2$). ^{13}C NMR ($CDCl_3$, 75MHz): δ = 168.6 (CO), 131.1, 132.3, 123.4 (Ph), 83.9, 69.0 (CH$_2$*CC*H), 37.6, 27.9, 25.8, 18.2 (CH$_2$); FAB MS measured 228.1, calculated for $[C_{14}H_{13}N + H]^+$ 228.1.

6-Amino-1-hexyne (2). Hydrazine hydrate (2 mL, 42 mmol) was added to a solution of 6-phtalimido-1-hexyn (**1**) (2.79 g, 12 mmol) in ethanol. The mixture was stirred under reflux for 1h, then cooled to room temperature and filtered, after solvent evaporation resulting with product (0.53 g, 5.4 mmol, 45 %). ^{1}H NMR ($CDCl_3$, 300MHz) 2.78 (t, 2 H, J = 6 Hz, C*H*$_2$NH$_2$), 2.62 (br, 2 H, NH$_2$), 2.57 (m, 2 H, CH$_2$C*H*$_2$CCH), 1.95 (t, 1 H, J = 2.4 Hz, CH$_2$CH$_2$CC*H*), 1.64 – 1.55 (m, 4 H, CH$_2$); ^{13}C NMR ($CDCl_3$, 75MHz) δ = 84.5, 68.6 (CH$_2$*CC*H), 41.8, 32.7, 26.0, 18.5 (CH$_2$); FAB MS measured 98.1, calculated for $[C_6H_{11}N + H]^+$ 98.1.

Lissamine rhodamine B sulfonyl acetylene amide (LRA), (3). 6-amino-1-hexyne (**2**) (0.198 g, 2.67 mmol) was added to a solution of lissamine rhodamine B sulfonyl chloride (mixture of isomers), (0.295 g, 0.34 mmol) in 40 mL of dry THF. Subsequently 0.1 mL of triethyl amine was added and the mixture was stirred at the room temperature for 3 h and then

left at -20 °C for 16 h. After addition of 3 mL of 1 M NaOH and 20 ml of EtOH the mixture was filtrated and the solvent was evaporated resulting in a product (0.161 g, 0.252 mmol, 74 %). The product (a mixture of isomers) was used later without further purification. FAB HRMS measured 660.21416, calculated for $[C_{33}H_{39}N_3O_6S_2 + Na]^+$ 660.21780.

Instrumentation. *Contact angle measurements.* Contact angles were measured on a Krüss G10 goniometer, equipped with a CCD camera. Advancing and receding contact angles (θ_a and θ_r) were determined automatically during growth and shrinkage of the droplet by a drop shape analysis. MilliQ water (18.4 MΩ cm) as a probe liquid. Both angles (advancing and receding) were measured on at least three different locations on each sample.

Grazing-angle infrared spectroscopy (GA-IS). Ga-IS spectra in the mid-IR region of 1024 scans at 4 cm^{-1} resolution, 20 kHz speed, were recorded on a BIO-RAD FTS-60A spectrometer with a liquid nitrogen-cooled cryogenic, external mercury cadmium telluride (MCT) detector, with its sample area modified to accommodate an external reflection sampling geometry. The sample area was purged by dry nitrogen. Background spectra consisting of 1024 averaged scans were taken before collecting each sample spectra.

Atomic force microscopy (AFM) imaging. AFM measurements were carried out with a digital multimode Nanoscope III (Digital Instruments, Santa Barbara, CA, USA) scanning force microscope in contact mode, with 512 x 512 data acquisitions, using V-shaped Si_3N_4 AFM tips (Nanoprobes, Digital Instruments) with a nominal spring constant of 0.32 N/m. The scan angle was set to 90°. Typical scan rates of 1-2 Hz were used to acquire the data. All imaging was conducted at room temperature in air.

Ellipsometry. Ellipsometric layer thickness measurements were performed on a Plasmos Ellipsometer (λ = 632.8 nm) assuming a refractive index of 1.5 for the monolayers and 1.465 for the underlying native oxide. The thickness of the SiO_2 layer was measured separately on an unmodified part of the same wafer and subtracted from the total layer thickness determined for the monolayer covered silicon substrate.

Laser scanning confocal microscopy/optical microscopy. Microcontact printed substrates with and without cells were imaged with a Carl Zeiss LSM 510 scanning confocal microscope with an excitation Ar-Kr laser beam of 568 nm wavelength and a 40 x objective was used. The emitted fluorescence was collected on a R6357 spectrophotometer.

XPS analysis. XPS spectra were obtained on a Physical Electronics Quantera Scanning X-ray Multiprobe instrument, equipped with a monochromatic Al Kα X-ray source operated at 1486.7eV and 25 W. Spectra were referenced to the main C 1s peak set at 284.0 eV. XPS data were collected from a surface area of 700 μm x 300 μm with a pass energy of 224 eV and a step energy of 0.8 eV for survey scans and 0.4 eV for high-resolution scans at a 45˚ takeoff angle, whereas the angle between sample surface and the X-ray beam was 90˚. For quantitative analysis, the sensitivity factors used to correct the number of counts under each peak were as follows: C 1s, 1.00; N 1s, 1.59. Charge neutralization was achieved by low-energy electrons and low-energy argons ions.

7.6. References

[1]   A. Kumar, G. M. Whitesides, *Appl. Phys. Lett.* **1993**, *63*, 2002-2004.

[2]   N. L. Jeon, K. Finnie, K. Branshaw, R. G. Nuzzo, *Langmuir* **1997**, *13*, 3382-3391.

[3]   Y. N. Xia, G. M. Whitesides, *Angew. Chem. Int. Ed.* **1998**, *37*, 551-575.

[4]   B. Michel, A. Bernard, A. Bietsch, E. Delamarche, M. Geissler, D. Juncker, H. Kind, J.-P. Renault, H. Rothuizen, H. Schmid, et al., *IBM J. Res. & Dev.* **2001**, *45*, 697-719.

[5]   L. Yan, X.-M. Zhao, G. M. Whitesides, *J. Am. Chem. Soc.* **1998**, *120*, 6179-6180.

[6]   L. Yan, W. T. S. Huck, X.-M. Zhao, G. M. Whitesides, *Langmuir* **1999**, *15*, 1208-1214.

[7]   J. Lahiri, E. Ostuni, G. M. Whitesides, *Langmuir* **1999**, *15*, 2055-2060.

[8]   T. P. Sullivan, M. L. van Poll, P. Y. W. Dankers, W. T. S. Huck, *Angew. Chem. Int. Ed.* **2004**, *43*, 4190-4193.

[9]   D. I. Rożkiewicz, B. J. Ravoo, D. N. Reinhoudt, *Langmuir* **2005**, *21*, 6337-6343.

[10]   D. I. Rożkiewicz, Y. Kraan, M. W. T. Werten, F. A. de Wolf, V. Subramaniam, B. J. Ravoo, D. N. Reinhoudt, *Chem. Eur. J.* **2006**, *12*, 6290-6297.

[11]   H. C. Kolb, M. G. Finn, K. B. Sharpless, *Angew. Chem. Int. Ed.* **2001**, *40*, 2004-2021.

[12]   V. V. Rostovtsev, L. G. Green, V. V. Fokin, K. B. Sharpless, *Angew. Chem. Int. Ed.* **2002**, *42*, 2596-2599.

[13]   C. W. Tornøe, C. Christensen, M. Meldal, *J. Org. Chem.* **2002**, *67*, 3057-3064.

[14]   T. S. Seo, Z. M. Li, H. Ruparel, J. Y. Ju, *J. Org. Chem.* **2003**, *68*, 609-612.

[15]   A. J. Link, D. A. Tirrell, *J. Am. Chem. Soc.* **2003**, *125*, 11164-11165.

[16]   A. T. Poulin-Kerstien, P. B. Dervan, *J. Am. Chem. Soc.* **2003**, *125*, 15811-15821.

[17]   B. Parrish, R. B. Breitenkamp, T. Emrick, *J. Am. Chem. Soc.* **2005**, *127*, 7404-7410.

[18]   V. P. Mocharla, B. Colasson, L. V. Lee, S. Roper, K. B. Sharpless, C. H. Wong, H. C. Kolb, *Angew. Chem. Int. Ed.* **2005**, *44*, 116-120.

[19]   J. P. Collman, N. K. Devaraj, C. E. D. Chidsey, *Langmuir* **2004**, *20*, 1051-1053.

[20]   J. K. Lee, Y. S. Chi, I. S. Choi, *Langmuir* **2004**, *20*, 3844-3847.

[21]   R. Zirbs, F. Kienberger, P. Hinterdorfer, W. H. Binder, *Langmuir* **2006**, *21*, 8414-8421.

[22]   N. K. Devaraj, P. H. Dinolfo, C. E. D. Chidsey, J. P. Collman, *J. Am. Chem. Soc.* **2006**, *128*, 1794-1795.

[23]   T. Lummerstorfer, H. Hoffmann, *J. Phys. Chem. B* **2004**, *108*, 3963-3966.

[24]   H. Li, F. Cheng, A. M. Duft, A. Adronov, *J. Am. Chem. Soc.* **2005**, *127*, 14518-14524.

[25]   D. D. Diaz, S. Punna, P. Holzer, A. K. McPherson, K. B. Sharpless, V. V. Fokin, M. G. Finn, *J. Polym. Sci. Part A: Polym. Chem.* **2004**, *42*, 4392-4403.

[26]   N. K. Devaraj, G. P. Miller, W. Ebina, B. Kakaradov, J. P. Collman, E. T. Kool, C. E. D. Chidsey, *J. Am. Chem. Soc.* **2005**, *127*, 8600-8601.

[27]   N. Balachander, C. Sukenik, *Langmuir* **1990**, *6*, 1621-1627.

[28]   D. G. Kurth, T. Bein, *Langmuir* **1993**, *9*, 2965-2973.

[29]   T. P. Sullivan, W. T. S. Huck, *Eur. J. Org. Chem.* **2003**, 17-29.

Chapter 8

Transfer printing of DNA by "click" chemistry[*]

This Chapter demonstrates the use of dendri-stamps to transfer and deliver acetylene-modified oligonucleotides to the azide-functionalized surface by microcontact printing. The oligonucleotides are immobilized via 1,3-dipolar cycloaddition reaction without the use of a Cu(I) catalyst. When the acetylene unit is located at the termini of the DNA strand, it shows the highest efficiency of the hybridization when reacted with complementary strand.

8.1. Introduction

Microcontact printing (μCP) is a successful tool for patterning and functionalization of surfaces by direct synthesis under elastomeric stamp confinement.[1-3] Huck and coworkers reported the synthesis of a RGD peptide and a 20-mer peptide nucleic acid (PNA) by microcontact printing.[4] Another example where the PDMS stamp was used as a tool to locally transfer and covalently bind enzymes was presented by Wilhelm and Wittstock.[5] In that case, enzyme glucose oxidase (GOx) was mixed together with coupling agent (EDAC, *N*-(3-dimethylaminopropyl)-*N*-ethylcarbodiimide hydrochloride) and printed directly onto amino-terminated glass substrate. Recently, imine formation via μCP of amines on aldehyde SAMs have been demonstrated and this chemistry has been applied to direct the immobilization of cytophilic proteins.[6,7] Moreover, "click" chemistry was applied in microcontact printing to couple molecules bearing acetylene moieties to the azide-terminated surface, without the need of the catalyst.[8]

"Click" chemistry was developed by Sharpless *et al.* as a modular approach which uses reliable chemical transformations that couple two molecules irreversibly under mild conditions.[9,10] The Huisgen 1,3-dipolar cycloaddition of alkynes and azides yielding triazoles is a typical example of a "click" reaction.[11-16] Azides and alkynes are easy to introduce, they are inert towards biological molecules and stable under physiological cell conditions.[17-22] In addition, the obtained triazoles are also very stable, and almost impossible to oxidize or reduce.[13] This cycloaddition reaction is accelerated by Cu(I) catalysis. [11,12]

Due to its perfect biocompatibility, the Huisgen 1,3-dipolar cycloaddition was widely used in DNA immobilization and DNA modification strategies. Sharpless "click" chemistry was successfully applied by Chidsey and coworkers in surface immobilization of acetylene-bearing oligodeoxynucleotides onto azide-terminated surface with the presence of copper(I) tris (benzyltriazolylmethyl)amine (TBTA) catalyst.[23-25] Seo *et al.* have constructed DNA microarray by using triazole formation to attach azido-modified DNA onto alkyne-functionalized glass chip at room temperature under aqueous conditions in the presence of CuI catalyst.[26] The biocompatibility between the 1,3-dipolar cycloaddition and oligonucleotides was demonstrated in postsynthethic labeling of alkyne-modified DNA.[27,28] Triazole formation was applied to construct fluorescent oligonucleotides for DNA sequencing,[17] for oligonucleotide conjugation,[29] and lately for the synthesis of multiple-labeled carbohydrate oligonucleotide on solid supports.[30]

In Chapter 7, it was demonstrated that "click" chemistry can be applied in direct microcontact printing of acetylene-bearing molecules onto azide-terminated substrates without the need of the

catalyst.[8] In this Chapter, the focus will be on expanding these findings to the microcontact printing of oligonucleotides possessing acetylene units in its sequence on azide-terminated glass slides.

8.2.   Immobilization of DNA by "click" chemistry

An azide-terminated monolayer was prepared according to a previously published procedure[31] by formation of *11*-bromoundecyltrichlorosilane monolayer on the activated glass slide and substitution of bromide for azide by the reaction with saturated solution of NaN_3. Modified oligodeoxynucleotides (ODN) were synthesized with the acetylene unit in different positions of each strand (Table 8-1 and Figure 8-1). In ODN-1 a single alkyne unit is positioned in the middle of the strand, in ODN-2 two acetylene units are in two locations in the middle of the strand, and in ODN-3 a single unit is located at the 5'-terminus. ODN-1 is complementary to ODN-a (fragment) and ODN-b (full length). ODN-2 is complementary to ODN-c (fragment) and ODN-d (full length). ODN-3 is complementary to ODN-e (full length).

Table 8-1. Sequences of oligonucleotides containing acetylene-modified monomers **1** (X) and **2** (Y). Melting (T_m) and hybridization (T_H) temperatures of complementary strands.

Symbol	Sequence	T_m (˚C)	T_H (˚C)
ODN-1	5'-GCG CTG T**X**C ATT CGC G-3'		
ODN-2	5'-TTA ATT GAA TTC GAT T**X**G GGC CGG A**X**T TGT TTC-3'		
ODN-3	5'-**Y**GC GCT GTT CAT TCG CG-3'*-fluorescein*		
ODN-a	*Cy5*-5'-CGC GAA T-3'	15	2.0
ODN-b	*Cy5*-5'-CGC GAA TGA ACA CGC-3'	65.7	45.7
ODN-c	*Cy5*-5'-GAA TTC AAT TAA-3'	26.2	6.2
ODN-d	*Cy5*-5'-GAA ACA ATC CGG CCC AAT CGA ATT CAA TTA A-3'	75.3	56.3
ODN-e	*Cy5*-5'-CGC GAA TGA ACA GCG C-3'	65.7	45.7
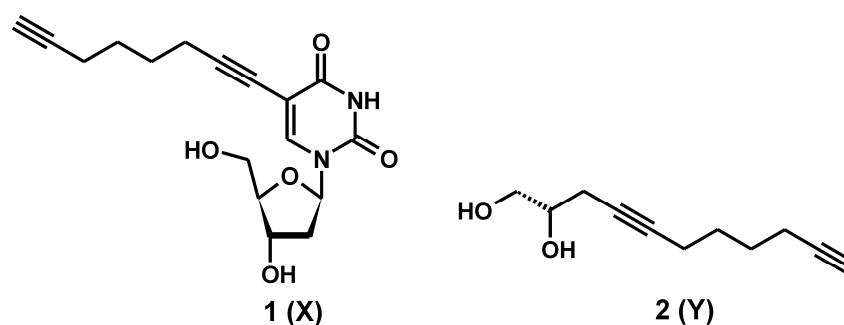
Figure 8-1. Monomers used in solid phase synthesis of acetylene-modified oligonucleotides.

Dendri-stamps[32] were described in details in Chapter 6 (Figure 6-1) as a successful tool to transfer and deliver oligodeoxynucleotides to the activated surface. DNA is attracted to the dendri-stamp by electrostatic interactions between negatively charged phosphate backbone of DNA strand and positively charged dendrimers attached to the oxidized PDMS stamp. After incubation of acetylene-modified oligonucleotides (15-mer, 31-mer and 16-mer) to the dendri-stamp, drying with nitrogen, the inked stamp (*without the copper(I) catalyst*) was brought into conformal contact with azide-terminated substrate for 1 h at room temperature with the weight of 120 g to ensure the contact between the stamp and the substrate (Figure 6-1). After contact time, the stamp was removed and the substrate rinsed thoroughly with ethanol containing triethylamine to remove any residues of dendrimers.

8.3. Analysis of the DNA pattern

In order to visualize the printed pattern of oligonucleotides, strands that did not possess fluorescent dyes in their structure (ODN-1 and ODN-2) were subjected, after printing, to labeling by fluorescent molecules (TOTO-1). This dye is known to bind to single stranded DNA. After binding, the substrates were imaged by using a laser-scanning fluorescent confocal microscope. The topological pattern of the stamp was faithfully replicated as a line or dot pattern of immobilized, fluorescent oligonucleotide (Figure 8-2). The signal-to-noise ratio as measured by a line scan was invariably higher than 100, and often higher than 1000.
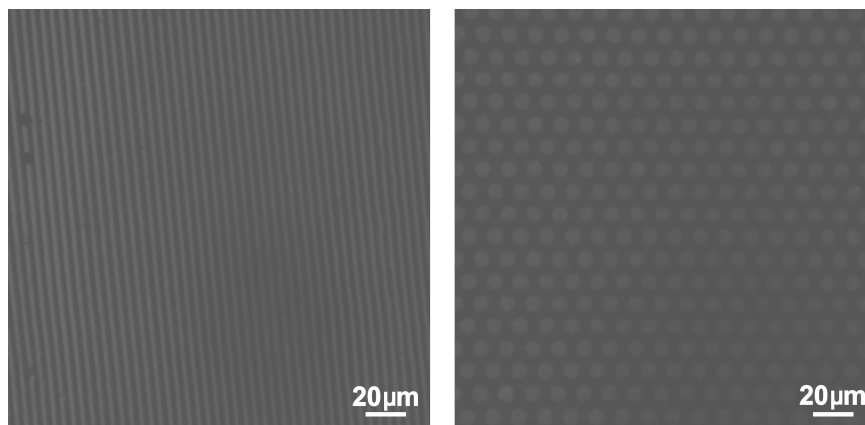
Figure 8-2. Fluorescence microscopy images of ODN 1 (left) and ODN 2 (right) printed via dendri-stamp, after intercalation of TOTO-1 dye.

These patterns were also investigated with an atomic force microscope. The pattern comprised of homogeneously distributed oligonucleotides forming a uniform coating with an average height of printed patterns of 3 nm (Figure 8-3). The height of the pattern is consistent with a monolayer of oligonucleotides.
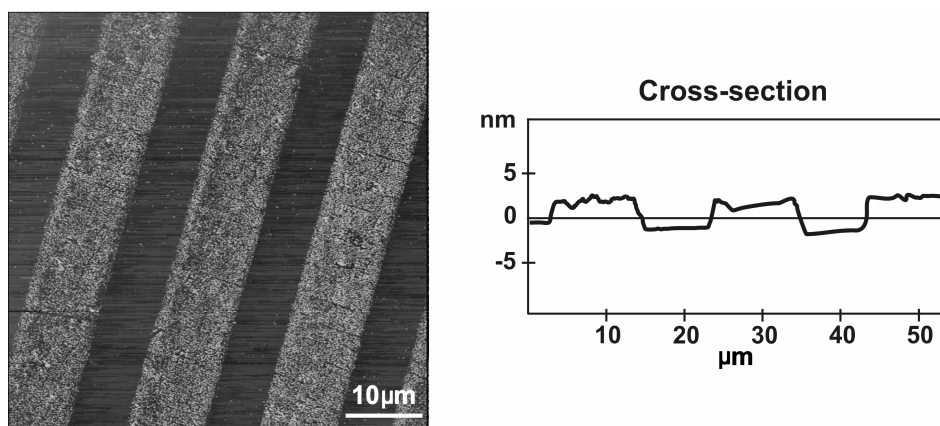
Figure 8-3. AFM height image of microcontact printed ODN-3 pattern on azide-terminated glass surface.

8.4. Hybridization

In the next step, immobilized oligonucleotides were hybridized with complementary strands. To investigate whether the immobilization via triazol linkage in the middle of the strand can affect the subsequent hybridization we investigated this re-association with complementary strands of different-length (Figure 8-4). In case of ODN-1 and ODN-2 the hybridization was examined with two different strands: with fragment strands (ODN-a, ODN-c) and with full-length strands which have the same number of oligonucleotides as the probes (ODN-b, ODN-d), respectively.
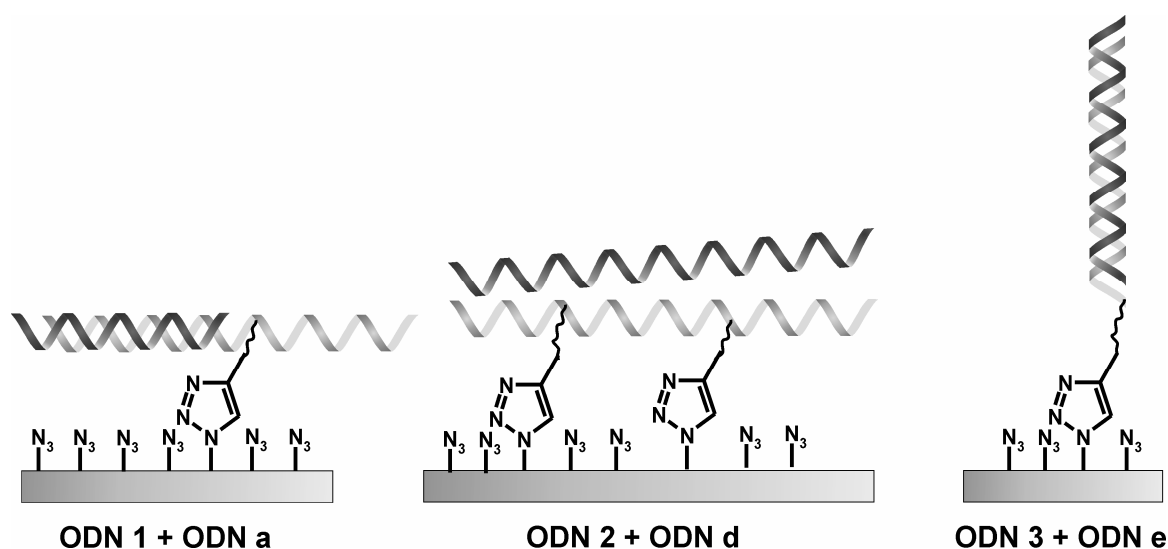
Figure 8-4. Immobilization of oligonucleotides ODN-1, ODN-2, ODN-3 possessing acetylene units in different positions and hybridization with complementary strands ODN-a, ODN-d, ODN-e.

ODN-1 and ODN-2 did not hybridize with full-length, complementary strands (ODN-b, ODN-d). However, ODN-1 hybridized with the short fragment of complementary, Cy5-labeled strand

ODN-a. The strands that hybridized successfully showed a visible, fluorescent pattern (Figure 8-5).
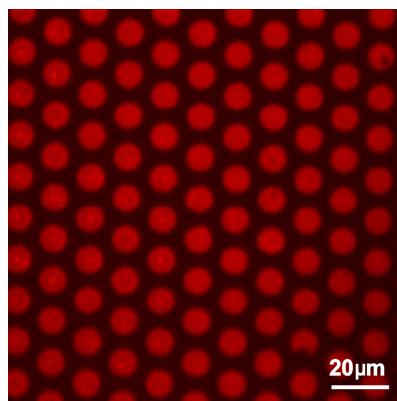
Figure 8-5. Fluorescence microscopy image of Cy5-labeled ODN-a strand hybridized to the ODN-1.

The hybridization with short, complementary strand ODN-c and ODN-2 was not successful. The short fragment of complementary strand probably had too low GC content to be hybridized. Attempts to hybridize the full-length complementary strand resulted in incomplete and variable level of intensity patterns which could be due to the double point of immobilization of the probe strand or due to the highly unfavorable formation of the double strand complex parallel to the surface. Finally, immobilized probe ODN-3 hybridizes readily with full-length, complementary, Cy5-labeled ODN-e strand (Figure 8-6) which could be expected since the immobilization point of ODN-3 is located at the terminus of the strand. The signal-to-noise ratio of the hybridized oligonucleotide pattern as measured by a line scan was invariably higher than 100, and often higher than 1000.
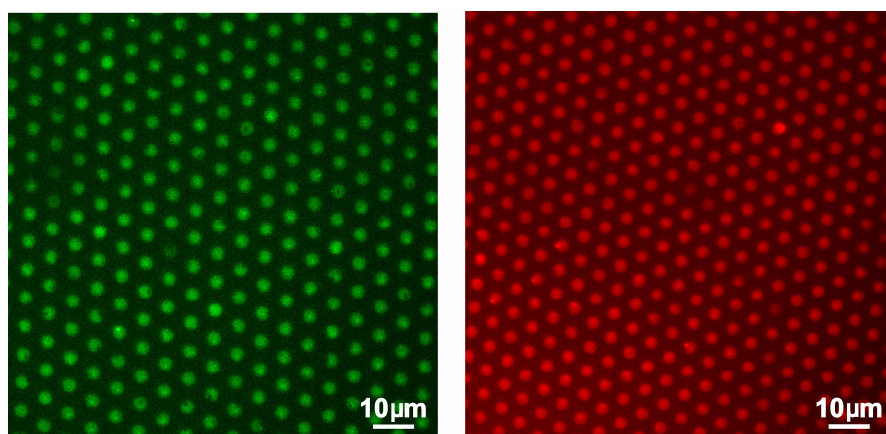
Figure 8-6. Fluorescence microscopy images of ODN-3 patterns made by microcontact printing using dendri-stamp. Before hybridization, fluorescein-labeled probe (left image) and after hybridization with the complementary Cy5-labeled probe, ODN-e (right image).

8.5.   Conclusions

In summary, the simple and straightforward procedure to immobilize oligodeoxynucleotides was presented in this Chapter. The method relies on the attachment of DNA to the surface in well-defined patterns by microcontact printing using a "dendri-stamp" via "click" chemistry reaction without the use of copper catalyst. Acetylene-modified oligonucleotides were reacted with azide-terminated glass slide under the dendri-stamp confinement. The immobilization is irreversible, covalent and one-step reaction resulting in a stable attachment of ODN. The ODN strand with the acetylene-modification at the 5'-termini brought the best result in hybridization with full-length, complementary targets. Strands with more than one acetylene linkers showed lack of hybridization. This method can be extended to other (bio)molecules that are modified with acetylene unit and can be attached to azide-terminated monolayer. Moreover, this strategy can be utilized in microarray fabrication in combination with microfluidic devices, in new immobilization approaches, in DNA studies on the surface such as influence of the linker and its position on probe immobilization and hybridization.

8.6.   Experimental Section

Materials. The probes employed in surface studies ODN-1, ODN-2, ODN-3 were synthesized according to the procedures listed below. The complementary strands were purchased from Sigma. The target sequence was Cy5-5'-ACA GCG C-3', Cy5-5'-CGC GAA TGA CAG CGC-3', Cy5-5'-GAA ACA ATC CGG CCC AAT CGA ATT CAA TTA A-3', Cy5-5'-AAT CGA ATT CAA TTA A-3', Cy5-5'-CGC GAA TGA ACA GCG C-3'. All the nucleotides were HPLC purified and modified by the manufacturer. The probe concentration was 1 μM in Tris-EDTA buffer pH 8 and the target concentration was 1 μM in 4 x SSC, 0.2 % SDS solution. Before use, oligonucleotides were denatured at 95 °C for 5 min. All buffers and immobilization solutions were prepared with 18 MΩ·cm distilled water (MilliQ). The following materials and chemicals were used as received: poly(dimethylsiloxane) (PDMS) (Dow Corning), polypropyleneimine tetrahexacontaamine dendrimers, generation 5 (Aldrich), NaN_3, *11*-bromoundecyltrichlorosilane (Sigma). All solvents were HPLC grade, and all other reagents were analytical grade. Other solvents or reagents were purchased from either Aldrich or Sigma.

Synthesis of monomers and oligonucleotides. The solid phase building block for monomer **1** was synthesized according to literature procedures.[27] The monomer **2** was synthesised according to Scheme 1.
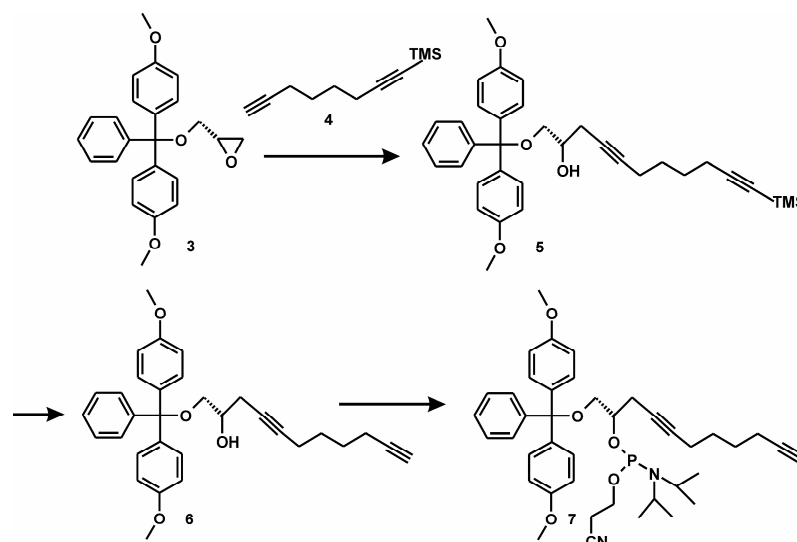
Scheme 1. Synthesis of the solid phase building block for monomer **2**.

Compound 5:[33] To a cooled solution (-78°C) of 1-trimethylsilyl-1,7-octadiyne **4**[34] (159 mg, 0.9 mmol, 1.2 eq.) in diethylether was added *n*-butyl lithium (360 µL, 0.9 mmol, 1.2 eq.) within 5 minutes. The reaction was stirred for an additional 20 minutes. Then BF$_3$·Et$_2$O (90 µL, 0.9 mmol, 1.2 eq.) was added within 2 minutes and the reaction again stirred for an additional 20 minutes. Then a solution of R-1-(dimethoxytritylmethoxymethyl)-oxirane **3**[35] (281 mg, 0.75 mmol, 1.0 eq.) in diethylether was added and the reaction stirred for 2 hours at -78 °C. The reaction was quenched with saturated NaHCO$_3$ solution and the solution was allowed to warm to room temperature. The product was extracted with diethylether (3x) and the organic phases were washed with water (3x) and brine (3x). The solvents were removed *in vacuo* and the raw product purified by column chromatography (hexane with 10 % à 15 % ethyl acetate). The product **5** was obtained as colourless oil (414 mg, 99 %) and used directly in the next step.

R$_f$ 0.22 (hexane/20 % EtOAc);

Compound 6: **5** (414 mg, 0.75 mmol) was dissolved in THF:MeOH (1:1; 20 mL), dry K$_2$CO$_3$ (515 mg, 3.74 mmol, 5.0 eq.) was added and the reaction stirred overnight. The reaction mixture was diluted with MeOH (200 mL) and filtered through celite and concentrated. Column chromatography (hexane with 20% ethyl acetate + 1 % pyridine) afforded product **6** (110 mg, 29 %)

R$_f$ 0.2 (hexane with 20% ethyl acetate); ^{1}H NMR (600 MHz, CDCl$_3$) δ= 1.57-1.50 (m, 4H, CH$_2$-CH$_2$), 1.94 (t, *J* = 2.63, 2.63 Hz, 1H, C≡CH), 2.14 (td, *J* = 8.50, 3.25 Hz, 2H, CH$_2$), 2.17 (dt, *J* = 6.56, 2.57 Hz, 2H, CH$_2$), 2.34 (d, *J* = 4.96 Hz, 1H, OH), 2.41-2.45 (m, 2H, CH$_2$), 3.21 (ddd, *J* = 15.37, 9.32, 5.31 Hz, 2H, CH$_2$), 3.79 (s, 6H, CH$_3$), 3.84-3.90 (m, 1H, CH), 6.85-6.80 (m, 4H), 7.21 (t, *J* = 7.32 Hz, 1H), 7.27-7.33 (m, 6H), 7.45-7.41 (m, 2H); ^{13}C-NMR (151 MHz, CDCl$_3$) δ= 17.9 (CH$_2$), 18.2 (CH$_2$), 24.2 (CH$_2$), 27.5 (CH$_2$), 27.8 (CH$_2$), 55.2 (CH$_3$), 66.0 (CH$_2$), 68.4, 69.6 (CH), 76.0, 82.2, 84.2, 86.1, 113.1 (CH), 126.8 (CH), 127.8 (CH), 128.1, (CH), 130.0 (CH), 136.0, 144.8, 158.5; HR-MS (ESI-FT-ICR$^+$): calc. for [M+Na$^+$]$^+$: [C$_{32}$H$_{34}$O$_4$Na]$^+$: 505.2349 found 505.2329.

Compound 7: To a solution of **6** (100 mg, 0.21 mmol, 1.0 eq.) in dichloromethane (3 mL) was added *N,N′* -diisopropylethylamine (72 µL, 0.42 mmol, 2.0 eq.) and the reaction was stirred for 10 minutes at room temperature. Then 2-cyanoethoxy-*N,N′* -diisopropylchlorophosphoramidite (70 µL, 0.31 mmol, 1.5 eq.) was added and the reaction stirred for 1.5 hours. The solvent was removed under vacuum and the raw product by column chromatography (deactivated silica; hexane with 10 % ethyl acetate + 1 % pyridine). The product **7** was obtained as a mixture of diastereomers (123 mg, 86 %).

^{31}P-NMR (81 MHz, CD$_2$Cl$_2$) δ= 149.59, 149.67.

Modification of glass slides. Clean microscope cover glass (Paul Marienfeld Gmbh & Co.KG, Germany) was activated with piranha solution for 45 min (concentrated H$_2$SO$_4$ and 33 % aqueous H$_2$O$_2$ in a 3:1 ratio) *(Warning! Piranha solution should be handled with caution: it has been reported to detonate unexpectedly.)*, rinsed with water (MilliQ) and immediately immersed in 0.1 vol. % *11*-bromoundecyltrichlorosilane in toluene for 20 min at 20 °C. Following monolayer formation, the substrates were rinsed with toluene to remove any excess of silanes and subsequently dried in N$_2$. To substitute the bromide for the azide group we used a saturated solution of NaN$_3$ in DMF for 48 h at 70 °C.[31] The substrate was rinsed with MilliQ water and ethanol and dried with nitrogen.

Fabrication of stamps. Silicon wafer-based masters with etched structures were prepared by UV photolithography. The master surface was fluorinated using fluorosilanes. PDMS stamps were fabricated by curing Sylgard 184 on the surface of the master at 60 °C for 12 h.

Microcontact printing of DNA with dendrimers. PDMS stamps were first oxidized in UV/ozone plasma reactor (Ultra-Violet Products, model PR-100) for 30 min at a distance of about 2 cm from the plasma source. [This reactor contains a low-pressure mercury UV light operating with UV emissions at 185 nm (1.5 mW cm^{-2}) and 254 nm (15 mW cm^{-2}) to generate molecular oxygen]. Subsequently the hydrophilic stamps where immersed in 1 µM ethanolic solution of dendrimers for 30 s and blow dried with nitrogen. A drop of oligonucleotide solution was incubated on the stamp for 20 min at room temperature. The probe concentration was 1 µM in Tris-EDTA buffer pH 8 solution. The stamp was dried with nitrogen and brought into conformal contact with the aldehyde-terminated glass slide for 15 s. After printing, the stamp was lifted off and the substrate was rinsed with 30 mL of ethanol containing a drop of triethylamine in order to remove the dendrimer layer and subsequently dried with nitrogen.

Intercalation of TOTO-1 to the patterned ODN. 1μM TOTO-1 solution in DMSO was dropped onto the patterned with ODN glass slide for 5 min, rinsed with DMSO, ethanol and water. The substrate was dried with nitrogen.

Hybridization on substrate surface. For hybridization, a 5'-Cy5-labeled oligonucleotide was diluted to 1 μM in 4 x SSC containing 0.2 % SDS and applied to the surface of the modified glass slide as described by Afanassiev *et al.*[36] A coverslip was mounted gently on the top of the solution and the substrates where transferred to the hybridization oven at the hybridization temperature (T_h) for overnight. The unhybridized probes were removed by washing with vigorous agitation in the 1 x SSC with 0.1 % SDS solution for 5 min at hybridization temperature, 0.1 x SSC with 0.1 % SDS for 5 min at RT, and subsequent washing in water for 5 min. After washing, the glass slides were dried with nitrogen and scanned on a confocal fluorescent microscope (Zeiss 510) to visualize hybridization signals.

Instrumentations. *Atomic force microscopy imaging (AFM).* AFM measurements were carried out on a Dimension 3100/Nanoscope IVa (Digital Instruments, Santa Barbara, CA, USA) in tapping mode, with 512 x 512 data acquisitions, using ultrasharp tips (MikroMash, Spain). All imaging was conducted at room temperature in air.

Fluorescence microscopy: Fluorescent images were acquired with a Carl Zeiss LSM 510 scanning confocal microscope. Red- and green-labeled DNA were visualize at $\lambda_{ex} = 650$ nm (λ_{em} =670-700 nm) and λ_{ex}= 495 nm (λ_{em} =517 nm) respectively. The emitted fluorescence was collected on a R6357 spectrophotometer.

8.7. References

[1]   J. Lahiri, E. Ostuni, G. M. Whitesides, *Langmuir* **1999**, *15*, 2055.

[2]   K. B. Lee, D. J. Kim, Z. W. Lee, S. I. Woo, I. S. Choi, *Langmuir* **2004**, *20*, 2531.

[3]   J. H. Hyun, H. W. Ma, P. Banerjee, J. Cole, K. Gonsalves, A. Chilkoti, *Langmuir* **2002**, *18*, 2975.

[4]   T. P. Sullivan, M. L. van Poll, P. Y. W. Dankers, W. T. S. Huck, *Angew. Chem. Int. Ed.* **2004**, *43*, 4190-4193.

[5]   T. Wilhelm, G. Wittstock, *Langmuir* **2002**, *18*, 9485-9493.

[6]   D. I. Rożkiewicz, B. J. Ravoo, D. N. Reinhoudt, *Langmuir* **2005**, *21*, 6337-6343.

[7]   D. I. Rożkiewicz, Y. Kraan, M. W. T. Werten, F. A. de Wolf, V. Subramaniam, B. J. Ravoo, D. N. Reinhoudt, *Chem.Eur. J.* **2006**, *12*, 6290-6297.

[8]   D. I. Rożkiewicz, D. Jańczewski, W. Verboom, B. J. Ravoo, D. N. Reinhoudt, *Angew. Chem. Int. Ed.* **2006**, *45*, 5292-5296.

[9]   H. C. Kolb, M. G. Finn, K. B. Sharpless, *Angew. Chem. Int. Ed.* **2001**, *40*, 2004-2021.

[10]   W. D. Sharpless, P. Wu, T. V. Hansen, J. G. Lindberg, *J. Chem. Educ.* **2005**, *82*, 1833-1836.

[11]   V. V. Rostovtsev, L. G. Green, V. V. Fokin, K. B. Sharpless, *Angew. Chem. Int. Ed.* **2002**, *42*, 2596-2599.

[12]   C. W. Tornøe, C. Christensen, M. Meldal, *J. Org. Chem.* **2002**, *67*, 3057-3064.

[13]   H. C. Kolb, K. B. Sharpless, *Drug Discovery Today* **2003**, *8*, 1128-1137.

[14]   S. Narayan, J. Muldoon, M. G. Finn, V. V. Fokin, H. C. Kolb, K. B. Sharpless, *Angew. Chem. Int. Ed.* **2005**, *44*, 3275-3279.

[15]   D. D. Diaz, S. Punna, P. Holzer, A. K. McPherson, K. B. Sharpless, V. V. Fokin, M. G. Finn, *J. Polym. Sci., Part A: Polym. Chem.* **2004**, *42*, 4392-4403.

[16]   J.-F. Lutz, *Angew. Chem. Int. Ed.* **2007**, *46*, 2-10.

[17]   T. S. Seo, Z. Li, H. Ruparel, J. Ju, *J. Org. Chem.* **2003**, *68*, 609-612.

[18]   A. J. Link, D. A. Tirrell, *J. Am. Chem. Soc.* **2003**, *125*, 11164-11165.

[19]   A. T. Poulin-Kerstien, P. B. Dervan, *J. Am. Chem. Soc.* **2003**, *125*, 15811-15821.

[20]   B. Parrish, R. B. Breitenkamp, T. Emrick, *J. Am. Chem. Soc.* **2005**, *127*, 7404-7410.

[21]   V. P. Mocharla, B. Colasson, L. V. Lee, S. Roper, K. B. Sharpless, C. H. Wong, H. C. Kolb, *Angew. Chem. Int. Ed.* **2005**, *44*, 116-120.

[22]   Q. Wang, T. R. Chan, R. Hilgraf, V. V. Fokin, K. B. Sharpless, M. G. Finn, *J. Am. Chem. Soc.* **2003**, *125*, 3192-3193.

[23]   N. K. Devaraj, G. P. Miller, W. Ebina, B. Kakaradov, J. P. Collman, E. T. Kool, C. E. D. Chidsey, *J. Am. Chem. Soc.* **2005**, *127*, 8600-8601.

[24]   J. P. Collman, N. K. Devaraj, C. E. D. Chidsey, *Langmuir* **2004**, *20*, 1051-1053.

[25]   J. P. Collman, N. K. Devaraj, T. P. A. Eberspacher, C. E. D. Chidsey, *Langmuir* **2006**, *22*, 2457-2464.

[26]   T. S. Seo, X. Bai, H. Ruparel, Z. Li, N. J. Turro, J. Ju, *PNAS* **2004**, *101*, 5488-5493.

[27]   J. Gierlich, G. A. Burley, P. M. E. Gramlich, D. M. Hammond, T. Carell, *Org. Lett.* **2006**, *8*, 3639-3642.

[28]   G. A. Burley, J. Gierlich, M. R. Mofid, H. Nir, S. Tal, Y. Eichen, T. Carell, *J. Am. Chem. Soc.* **2006**, *128*, 1398-1399.

[29]   D. Graham, A. Enright, *Curr. Org. Synth.* **2006**, *3*, 9-17.

[30]   C. Bouillon, A. Meyer, S. Vidal, A. Jochum, Y. Chevolot, J.-P. Cloarec, J.-P. Praly, J.-J. Vasseur, F. Morvan, *J. Org. Chem.* **2006**, *71*, 4700-4702.

[31]   N. Balachander, C. Sukenik, *Langmuir* **1990**, *6*, 1621-1627.

[32]   D. I. Rożkiewicz, B. J. Ravoo, D. N. Reinhoudt, **2007**.

[33]   M. Yamaguchi, I. Hirao, *Tetrahedron Lett.* **1983**, *24*, 391-394.

[34]   J. Gierlich, G. A. Burley, P. M. E. Gramlich, D. M. Hammond, T. Carell, *Org. Lett.* **2006**, *8*, 3639-3642.

[35]   L. Zhang, A. E. Peritz, P. J. Carroll, E. Meggers, *Synthesis* **2006**, *4*, 645-653.

[36]   V. Afanassiev, V. Hanemann, S. Wölfl, *Nucleic Acids Res.* **2000**, *28*, e66.

Chapter 9

Matrix-assisted dip-pen nanolithography of biomolecules[*]

This Chapter describes a method for the direct transfer of (bio)molecules encapsulated within a fluid viscous matrix by dip-pen nanolithography (DPN). The method relies on the preparation of an ink that is used as a" universal" carrier of biomolecules such as DNA or proteins for the fabrication of nanoarrays on activated glass substrates. This carrier offers unique and biocompatible properties and can be easily mixed with almost any type of biomolecules and transferred to the target support.

9.1. Introduction

The encapsulation of biomolecules within a matrix plays an important role in many areas such as stabilization of biomolecules, tissue engineering, bioprocess applications, drug delivery, preservation of biomolecule activity and unfolding, or stabilization of electrostatic interactions.[1-4] Moreover many biologically active compounds such as enzymes, antibodies, oligonucleotides, hormones, but also cells can be encapsulated while retaining their bioactivity. There are numerous techniques like covalent attachment, physical adsorption or entrapment to encapsulate biomolecules in polymer and inorganic matrices. These techniques have been explored as robust immobilization methods which preserve the activity of biologically active molecules. There are many host matrix materials which are biocompatible and commonly used for the encapsulation of biomolecules such as alginate,[5] chitosan,[6] collagen,[7] gelatin,[8] cross-linked poly(2-hydroxyethylmethacrylate),[9] poly(N-isopropylacrylamide),[10] poly(ethylene oxide) copolymers[11] and others. Hydrogels such as agarose or dextrans are often used as vehicles for delivery of drugs, cells, DNA, and enzymes since they can integrate biological molecules in their matrix and preserve their reactivity.[12,13]

Agarose is a linear polysaccharide extracted from marine red algae, consisting of alternating copolymers of (1-3)-linked β-D-galactose and (1-4)-linked (3-6)-anhydro-α-L-galactose.[14,15] This polysaccharide can form thermoreversible gels in aqueous solutions. When agarose is in the gel form it forms bundles of associated helices where the junction zones consists of multiple chain aggregation while water stabilizes the gel network.[16,17,19] Agarose exhibits a temperature-sensitive water solubility that can be utilized to entrap other molecules or cells.[3] In addition, agarose is biocompatible even when implanted *in vivo*.[18] It has a gelation temperature in the range of 15-30 °C depending on the concentration. The gelation mechanism of agarose is governed mainly by the hydrogen bonding and the physical structure of the gel, and is mainly controlled by the agarose concentration, which determines the pore size. In biosensing applications, agarose matrices offer many advantages such as optical transparency which makes them ideal for fluorescence or light transmission microscopy. The advantages of agarose as a patterning medium was noted by Whitesides and coworkers who prepared agarose stamps to pattern proteins (see Chapter 2).[20]

In this Chapter agarose was employed as a carrier of biomolecules for the fabrication of nanometer-scale patterns on a surface. Agarose was used as a polymeric framework that surrounds biomolecules, separating them from each other, stabilizing and protecting them from aggregation and unfolding. This matrix is chemically inert, hydrophilic, and inexpensive. The

agarose matrix can act as a reservoir of water thereby enhancing its ability to maintain the biological activity of entrapped enzymes, antibodies, and cells.

In various types of arrays (DNA, proteins or carbohydrates) there is a great demand to decrease spot size below the micrometer regime thereby increasing the density of spots per substrate. Currently in microarray fabrication the average spot size that is manufactured is in the range of 70-150 µm (see Chapter 2). Dip-pen nanolithography (DPN) offers the potential for the fabrication and development of highly dense nanoarrays of (bio)molecules with spot sizes as small as 100 nm.[21-23] In combination with the multi-pen array, DPN can offer high throughput multi-component parallel arrays fabrication.[21,24] DPN, with its flexibility in design and large choice of inks is a very attractive method for nanofabrication. Although possessing many advantages as a technique for patterning nanometer scale features, DPN is very often rejected as a method to position biomolecules due to the lack of enhancing the adhesion and transport of bio-ink to the tip. Most AFM tips are made of silicon nitride, which is chemically inert, resistant to oxidation, hydrophilic and almost "anti-sticky". Biomolecules such as DNA or proteins which are usually re-suspended in buffer solution hardly attach spontaneously to Si_3N_4. Many modifications of these tips were done (see Chapter 2 and Chapter 6) to improve the adhesion of biomolecules. One commonly used technique for Si_3N_4 tips modification is silanization with poly(ethylene glycol) (PEG)-containing silanes or amino-functionalized silanes.[25,26] Besides modification of the tip there must also be a certain specificity/chemistry involved to attract or bind biomolecules to the tip and release them to the surface. This chemistry or specificity between the biomolecule and the surface plays a very important role. However, the biomolecule should be first temporarily immobilized on the tip forming a coating on the tip before it can be delivered. An ideal carrier-ink would provide a 3D structure with high loading capacity, would be biologically inert, would facilitate homogeneous mixing of the ink components, would be non-diffusive and would be able to create nm-size features without spreading. This Chapter describes a simple method for the transfer of the biomolecule-containing inks from the tip to the surface without the need of the modification of the tip surface. The idea is based on the preparation of a gel matrix that is "mixable" with a solution of biomolecules. This medium can be easily used for effective tip coating and can be delivered to the surface.

9.2.   The AFM "gel-pen"

Agarose gels can be prepared very quickly and can be immediately used for coating AFM tips. The hydrophilic nature of the agarose gel should allow for the easy transport of water and other hydrophilic molecules such as substrates and products of enzymatic reactions.

Because agarose is highly porous it is an excellent material for encapsulation and transportation of biological entities within a 3D gel matrix. Once the ink is deposited on the surface, the encapsulated biomolecules can react with reactive groups on the substrate. The matrix can be removed by rinsing with water. This matrix behaves as liquid-swelled polymers with mechanical characteristics resembling those of extracellular matrix. In addition agarose gel is permeable to oxygen, and water-soluble metabolites which is important when enzymes have to be transferred.
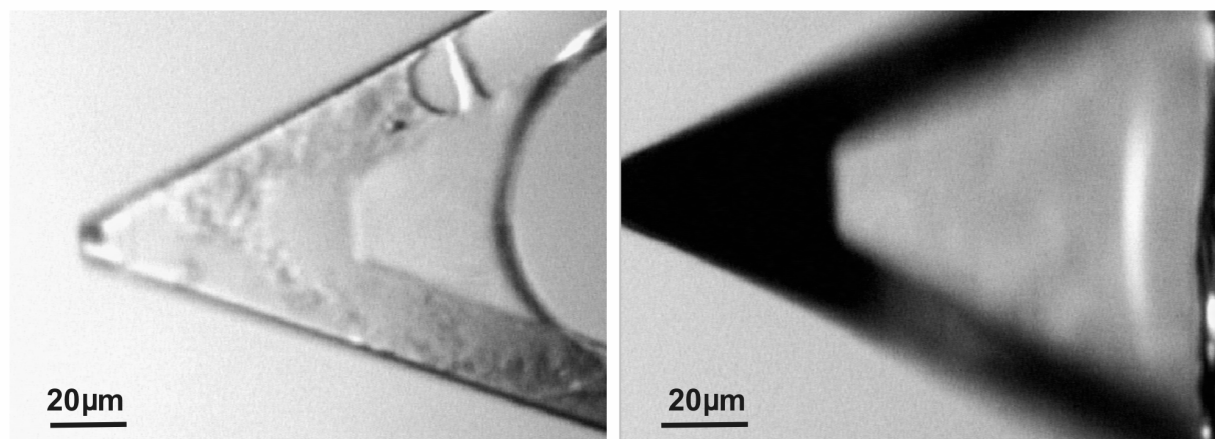
Figure 9-1. Images of AFM contact mode, Si_3N_4 tips coated with agarose matrix mixed with biomolecules.

The agarose matrix was prepared by mixing of 0.3 % agarose with water and diluting it in a 1:1 ratio with a solution of biomolecules to a final concentration of 0.15 %. In the first experiment, a solution of Cy3-labeled DNA possessing a C6-NH$_2$ linker at the 5'-end and a solution of a protein (cholera toxin labeled with Alexa 594) were used as model compounds for the patterning of biomolecules via this matrix-delivery system on an aldehyde-functionalized glass surface. The mixture was used to coat the AFM tip by dipping the tip for 5 s (Figure 9-1). This coating can serve as a reservoir of ink that by adjusting humidity can flow continuously from the tip to the surface.

9.3. Ink transport – DNA and protein nanoarrays

Single stranded, amino-functionalized and fluorescently labeled DNA was used as a model biomolecule in the agarose-gel matrix. To investigate the relation between the spot size and the dwell time, four nanoarrays were fabricated using an 18-pen probe (Figure 9-2). Each nanoarray contains 49 DNA spots and was fabricated using different dwell time (20 s, 10 s, 7 s and 5 s) onto an aldehyde-functionalized glass substrate. After DPN the substrate was washed vigorously with water.
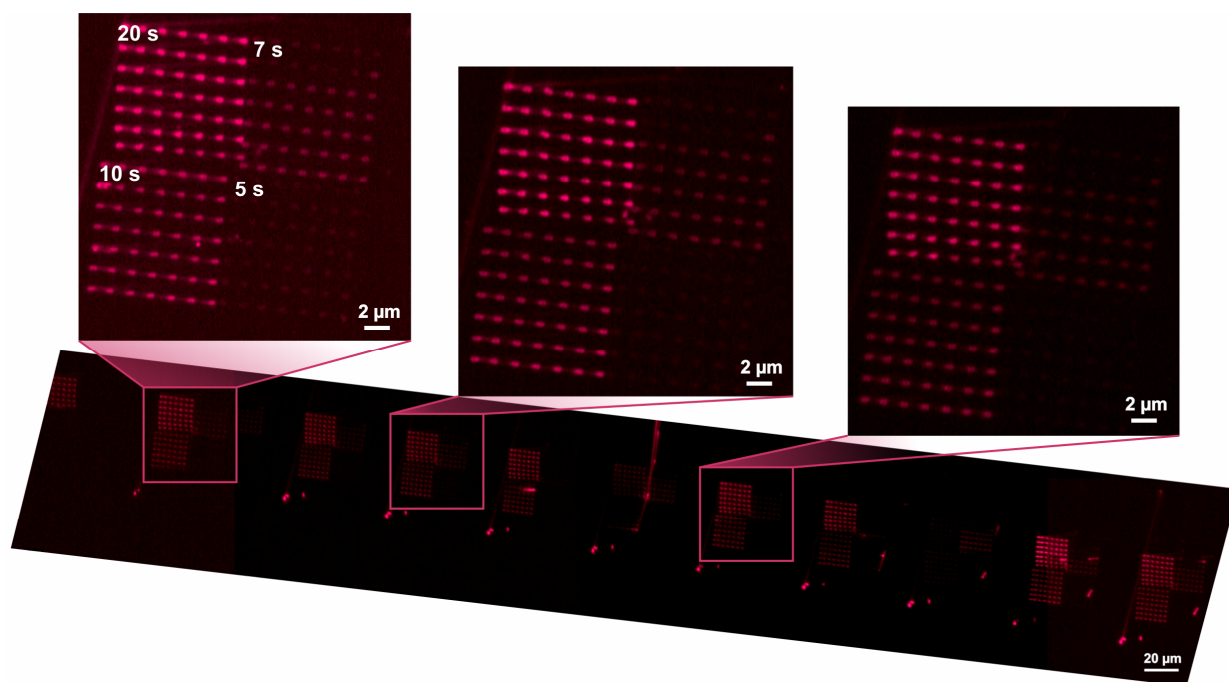
Figure 9-2. Fluorescence microscopy image of DNA nanoarrays fabricated by agarose matrix assisted DPN using an 18-pen probe (fragment of the slide). Each pen has produced 4 arrays of 49 DNA spots (which differ in dwell time: 20 s, 10 s, 7 s, and 5 s) on the aldehyde-terminated glass substrate.

The fluorescence intensity within the spot is very homogeneous which is important when the array is used for the analytical purposes. The size and intensity of the spots differ depending on the dwell time. The average size of spots fabricated with a 20 s dwell time was 700 nm, while 10 s yielded 500 nm sized features. Spots with a contact time of 7 and 5 s had sizes of 350 and 200 nm, respectively. The intensity and the size of spots decreases with the decrease of dwell time. For the fluorescence microscopy analysis spots should be ideally as small as possible (to obtain high density arrays) but at the same time they should have a high fluorescence intensity to be easily analyzed. These requirements are most adequately balanced by employing a 10 s dwell time for the generation of 500 nm sized spots. The spacing between the spots was 2 µm ensuring clear contrast and space resolution between fluorescent features and the background.

To extend matrix assisted DPN to a different kind of biomolecules, cholera toxin protein labeled with Alexa 594 was mixed with agarose gel and used as an ink (Figure 9-3). This toxin is an AB_5 hexameric assembly secreted by *Vibrio cholerae*.[27] Cholera toxin is widely used in research in development of anti-secretory agents. A solution of protein was mixed with the agarose matrix (1:1 v/v) and applied to the AFM tip array. The contact time between the tip (18-pen AFM probe) and the aldehyde-terminated glass surface was 10 s. The spot size was 500 nm and the spots were separated by 2 µm spacing. After DPN the substrate was rinsed with water.
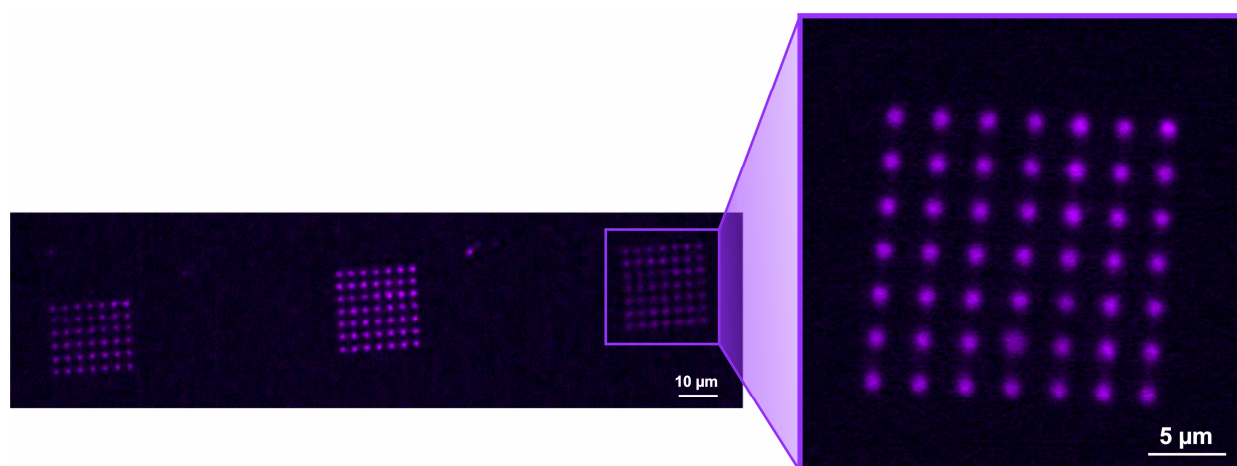
Figure 9-3. Fluorescence microscopy image of cholera toxin protein nanoarray fabricated by matrix-assisted DPN method onto aldehyde-terminated glass slide (fragment of the slide).

An array of 202 DNA spots was fabricated on the aldehyde-functionalized glass substrate without the need of re-inking the 18-pen AFM probe (Figure 9-4). Spots were characterized by uniform fluorescence intensity and size within each array. The contact time between each tip and the surface was 10 s. This indicates the gel matrix is the most important factor influencing the rate of transfer between the tip and substrate. The diffusion constant is thus independent of the type of biomolecule encapsulated within the gel.
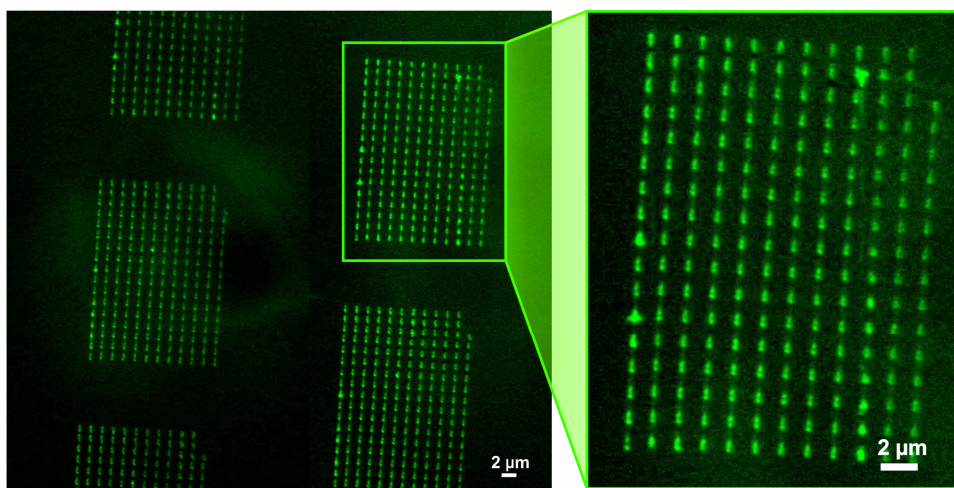
Figure 9-4. Fluorescence microscopy image of DNA nanoarray fabricated by AFM 18-pen probe inked with matrix/DNA (fragment of the slide). The array of 202 DNA spots per pen was fabricated without additional re-inking on an aldehyde-functionalized glass substrate.

9.4. Gradient patterning

Surfaces containing concentration or size gradients of chemical components are central to the investigation of combinatorial screening for macromolecules, droplets and wettability or cells (see Chapter 4). The advantage of such systems is that range of experiments related to, for

example, different surface concentration can be conducted using a single sample. There are many approaches to make a chemical gradient surface such as diffusion of thiol solutions through a polysaccharide matrix,[28,29] gradual immersion of a gold-coated substrate in a dilute thiol solution,[30] microcontact printing with the stamp having a thickness gradient,[31] selective desorption of thiols using electrochemistry[32] or by using titanium dioxide remote photocatalytic lithography.[33]

Alternatively, utilizing the transfer dependency between a force applied to the tip (setpoint) or the dwell time and the size and intensity of spots, gradient patterns can also be fabricated by DPN. As a model biomolecule, DNA encapsulated within agarose matrix was used to create spots on an aldehyde-terminated glass slide. The setpoint was gradually varied between 1 N/m^2 and 0 N/m^2 during nanolithography. The fabricated DNA spots had different local concentration, intensity and size (Figure 9-5).
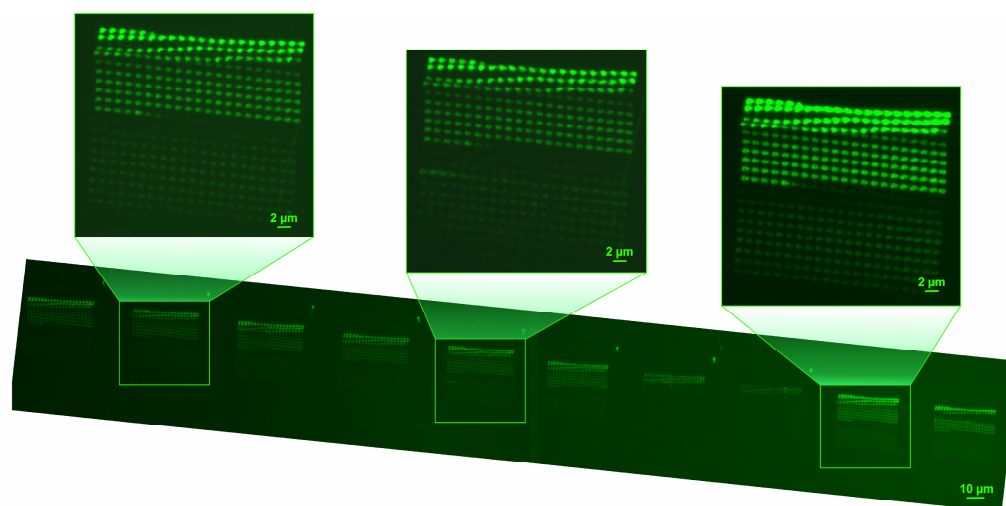
Figure 9-5. Fluorescence microscopy image of gradient of 420 DNA spots obtained by DPN using 18-pen array (fragment of the slide). The drifts in the pattern are related to the scanner movements.

The spot size varies between 400 and 700 nm depending on the applied setpoint. Drifts related to tip positioning or piezo-element movements can cause small defects in patterning such as different distance between the dots. Similar arrays could be fabricated by varying the dwell time while keeping the setpoint constant to obtain different size or intensity spots. In this experiment 420 spots were fabricated without the need for secondary inking.

9.5. Conclusions

In summary, a new approach for the nanopatterning of biomolecules by DPN has been developed via a biocompatible matrix. This agarose matrix shows a similar rate of transfer

regardless of the type of encapsulated biomolecule, which suggest that this universal carrier alone influences the diffusion characteristics of the ink. Moreover, matrix inks can form a dense layer around the tip and the cantilever serves as a large reservoir for the process of writing. More than 200 spots possessing almost equal size and intensity can be fabricated without re-inking. By applying different setpoints to the tip or different dwell times, patterns with different spot sizes and intensity as well as gradient patterning can be achieved. This method has the potential to be a universal technique with high loading capacity of ink for the patterning of biomolecules in the nanometer regime.

9.6. Experimental section

Materials. Oligonucleotides were purchased from Integrated DNA Technologies, Inc. San Diego, USA. The probe sequence employed in surface studies was 5'-GTG CAC CTG ACT CCT GTG GAG-3' (single strand of mutant β-globin gene) and was modified at the 5' terminus with a six-carbon linker and amino group (NH_2-$(CH_2)_6$-) and at the 3' with Cy3. The probe concentration was 30 μM in Tris-EDTA buffer pH 8. All buffers and immobilization solutions were prepared with 18 MΩ·cm distilled water (MilliQ). The following materials and chemicals were used as received: trimethoxysilylalkylaldehyde (United Chemical Technologies, Inc.), agarose low melting (FisherBiotech, BP165-25), cholera toxin protein (1 mg/ml) Alexa 594.

Modification of glass slides. Clean microscope cover glass (Fisher Scientific) was activated in an oxygen plasma reactor for 15 min and immediately submitted to vapor deposition of trimethoxysilylalkylaldehyde for 20 min. Following monolayer formation, the substrates were rinsed with ethanol to remove any excess of silanes and subsequently dried in N_2.

Ink preparation. 0.3 % Agarose gel was prepared by dissolving agarose in MilliQ water and heating for 2 min in the microwave. The gel was mixed with the solution of biomolecules in ratio 1:1 (v/v) to a final concentration of 0.15 %.

Dip-pen nanolithography. DPN was carried out on a NScriptor (NanoInk, Chicago, IL, USA) in contact mode, with 512 x 512 data acquisitions, using multipen arrays type E, F, M (NanoInk, Chicago, IL, USA). DPN was conducted at room temperature in air, at 35-60 % relative humidity. Typically the tip was inked by dipping the probes for 5 s into an agarose mixture. The contact time between the tip and aldehyde-functionalized substrate was 7-10 s. After nanolithography the substrates were rinsed thoroughly with water and dried with nitrogen

Fluorescence microscopy. Fluorescence images were acquired with a Carl Zeiss, Axiovert 200M fluorescent microscope.

9.7. References

[1]   D. T. Nguyen, M. Smit, B. Dunn, J. I. Zink, *Chem. Mater.* **2002**, *14*, 4300.

[2]   A. P. McGuigan, M. V. Sefton, *Proc. Natl. Acad. Sci.* **2006**, *103*, 11461.

[3]   H. Uludag, P. De Vos, P. A. Tresco, *Adv. Drug Deliv. Rev.* **2000**, *42*, 29.

[4]   A. S. Hoffman, *Adv. Drug. Deliv. Rev.* **2002**, *54*, 3.

[5]   G. Klock, A. Pfeffermann, C. Ryser, P. Grohn, B. Kuttler, H. J. Hahn, U. Zimmermann, *Biomaterials* **1997**, *18*, 707.

[6]   A. Chenite, C. Chaput, D. Wang, C. Combes, M. Buschmann, C. D. Hoemann, J. C. Leroux, B. L. Atkinson, F. Binete, A. Selmani, *Biomaterials* **2000**, *21*, 2155.

[7]   P. M. Kaufmann, S. Heimrath, B. S. Kim, D. J. Mooney, *Cell Transplant.* **1997**, *6*, 463.

[8]   M. Yamamoto, Y. Tabata, Y. Ikada, *Bioact. Compat. Polym.* **1999**, *14*, 474.

[9]   A. Kinde, J. M. Szabocisk, K. Park, *Biomaterials* **1998**, *19*, 2051.

[10]   R. A. Stile, W. R. Biurghardt, K. E. Healy, *Macromolecules* **1999**, *32*, 7370.

[11]   S. Zalipsky, *Bioconjugate Chem.* **1995**, *6*, 150.

[12]   R. B. Bhatia, C. J. Brinker, *Chem. Mater.* **2000**, *12*, 2434.

[13]   Y. Luo, M. O. Shoichet, *Biomacromolecules* **2004**, *5*, 2315.

[14]   Y. Ling, J. Rubin, Y. Deng, C. Huang, U. Demirci, J. M. Karp, A. Khademhosseini, *Lab Chip* **2007**, *7*, 756.

[15]   V. Normand, D. L. Lootens, E. Amici, K. P. Plucknett, P. Aymard, *Biomacromolecules* **2000**, *1*, 730.

[16]   K. Y. Lee, D. J. Mooney, *Chem. Rev.* **2001**, *101*, 1869.

[17]   C. Rochas, A. Brulet, J. Guenet, *Macromolecules* **1994**, *27*, 3830.

[18]   B. Rahfoth, J. Weisser, F. Sternkopf, T. Aigner, K. von der Mark, R. Brauer, *Osteoarthritis Cartilage* **1998**, *6*, 50.

[19]   L. M. Barrangou, C. R. Daubert, E. A. Foegeding, *Food Hydrocolloids* **2006**, *20*, 184.

[20]   M. Mayer, J. Yang, I. Gitlin, D. H. Gracias, G. M. Whitesides, *Proteomics* **2004**, *4*, 2366.

[21]   K. Salaita, Y. Wang, J. Fragala, R. A. Vega, C. Liu, C. A. Mirkin, *Angew. Chem. Int. Ed.* **2006**, *45*, 7220.

[22]   S.-W. Chung, D. S. Ginger, M. W. Morales, Z. Zhang, V. Chandrasekhar, M. A. Ratner, C. A. Mirkin, *Small* **2005**, *1*, 64.

[23]   D. S. Ginger, H. Zhang, C. A. Mirkin, *Angew. Chem. Int. Ed.* **2004**, *43*, 30.

[24]   K. Salaita, Y. Wang, C. A. Mirkin, *Nature Nanotechnology* **2007**, *2*, 145.

[25]   L. M. Demers, D. S. Ginger, S.-J. Park, Z. Li, S.-W. Chung, C. A. Mirkin, *Science* **2002**, *7*, 1836.

[26]   J.-H. Lim, D. S. Ginger, K.-B. Lee, J. Heo, J.-M. Nam, C. A. Mirkin, *Angew. Chem. Int. Ed.* **2003**, *42*, 2309.

[27]   B. Dugas, N. Paul-Eugène, E. Génot, J. M. Mencia-Huerta, P. Braquet, J. P. Kolb, *Eur. J. Immunol.* **1991**, *21*, 495.

[28]   B. Liedberg, P. Tengvall, *Langmuir* **1995**, *11*, 3821.

[29]   B. Liedberg, M. Wirde, Y. T. Tao, P. Tengvall, U. Gelius, *Langmuir* **1997**, *13*, 5329.

[30]   S. Morgenthaler, S. W. Lee, S. Zurcher, N. D. Spencer, *Langmuir* **2003**, *19*, 10459.

[31]   T. Kraus, R. Stutz, T. E. Balmer, H. Schmid, L. Malaquin, N. D. Spencer, H. Wolf, *Langmuir* **2005**, *21*, 7796.

[32]   P. Bohn, S. Plummer, Q. Wang, B. Coleman, A. Swint, P. Castle, *Abstr. Pap. Am. Chem. Soc.* **2003**, *225*, U687.

[33]   N. Blondiaux, S. Zurcher, M. Liley, N. D. Spencer, *Langmuir* **2007**, *23*, 3489.

Summary

Soft lithography offers great potential for the fabrication of 2D and 3D patterned structures using a variety of materials and patterns. It complements and extends conventional fabrication methods. This thesis is particularly focus on microcontact printing (μCP) as a method to create biological patterns on surfaces and also as a tool used in "in-situ" synthesis. Microcontact printing has unique features that make this technique very attractive: (i) it is simple to introduce in any laboratory, (ii) it is biocompatible, (iii) it can fabricate features below 100 nm, (iv) it is applicable to broad range of materials, (v) it is efficient and not expensive. The important feature is that stamp which is used for printing is flexible and can seal conformally to the surface tolerating the nanoscale roughness. In this thesis the focus is on the application of soft lithography in the fabrication of microsystems useful in studying interactions between biomolecules and cells. The combination of surface chemistry, modification or proper selection of stamp material and μCP of biomolecules has yielded methods for patterning of bioassays (Chapter 2). Despite increasing complexity, the size of the devices has continued to decrease and their surface properties become very important since they can determine the performance of the device. Surface chemistry and the method to immobilize (bio)molecules should be then very carefully chosen. Chapter 2 describes several approaches to tailor the surface of glass, silicon oxide, gold and polymers. Special attention is dedicated to covalent attachment of biomolecules to the substrates since most non-covalent immobilization methods suffer from a lack of complete understanding with respect to the mechanism of binding. Cross-linkers such as homobifunctional and heterobifunctional compounds for direct functionalization of the surface are introduced in order to broaden the scope of covalent chemistries used to immobilize biomolecules. When substrates are patterned for specific attachment of biomolecules, the important issue is to create inert structures which could separate the bioactive pattern. Modifications such as grafting of PEG molecules, BSA, phospholipids SAMs are described. The main focus of Chapter 2 is addressed to microcontact printing of biomolecules, modification of stamp surface to achieve the best printing results, derivation of microcontact printing such as patterning via microwells and microchannels. Scanning probe lithography is also here considered as a valuable technique in fabrication of sub-micrometer patterns.

The ability of creating reversible patterns on the surface by microcontact printing was explored in Chapter 3. The stamp can be used to transfer ink molecules, for instance amines, and react them covalently with aldehyde-functionalized surface via reversible imine bond. These

bonds can be hydrolyzed back to aldehydes and amines. The patterns can be quickly generated, removed and regenerated. The reversibility of the imine bond was further explored in Chapter 4 when dendrimer molecules where patterned onto the surface with gradient of aldehyde functionality. Under certain condition the imine bond could be broken and reformed again causing the movement of these spherical macromolecules. In contrast, the same imine bond can be reduced to the secondary amine and used for irreversible immobilization of biomolecules. Chapter 5 describes microcontact printing of cytophilic proteins which can be used to pattern cells on the surface. When not printed areas are passivated, cells can be positioned and separated in confined domains. This patterning technique can be useful in understanding how spatial or geometric modification of active surfaces can influence cellular behavior such as cell-cell interaction, signaling between cells, and cell motility.

Chapter 6 presents transfer printing of DNA by "dendri-stamps". This method was based on modification of PDMS stamp with PPI dendrimers, which gives a highly positive charge on the surface of the stamp. Dendri-stamps can attract negatively charged DNA in a "layer-by-layer" fashion. These electrostatic interactions between the oligonucleotide and the stamp surface can ensure successful transfer of DNA to the surface. Imine chemistry was applied to bind covalently amino-modified DNA molecules to an aldehyde-terminated substrate. The labile imine bond was further reduced to a stable secondary amine bond forming a robust connection between the DNA strand and the solid support. Moreover, atomic force microscopy tips were modified with dendrimers to introduce a high density of positive charge and attract DNA molecules in order to transfer and deliver them to the surface using dip-pen nanolithography (DPN).

"Click" chemistry in combination with microcontact printing was introduced in Chapter 7. Molecules such as octadecyne or rhodamine lissamine containing acetylene unit in its structure were used as an ink and printed onto azide-terminated silicon and glass substrate to form triazoles without the use of copper(I) catalyst. This subject was further examined in Chapter 8 to immobilize DNA in patterns. Oligonucleotides bearing acetylene unit in the middle and at the terminus of the strand, were printed via dendri-stamp onto azide-terminated glass surface. The immobilized oligonucleotides were subsequently hybridized with complementary strands. The best results for the immobilization and hybridization were achieved using DNA strands, which possess acetylene unit at the termini. These strands presented the largest availability for the hybridization among all tested oligonucleotides. This strategy can be utilized in new immobilization approaches, in DNA studies on the surface, in microarrays and biosensors application.

A new method for the DPN-based direct transfer of biomolecules encapsulated within a matrix was presented in Chapter 9. This technique has shown to be a general method for transfer of molecules since the gel matrix which was used as ink exhibits similar rate of transfer in spite of the type of encapsulated biomolecules. More than 200 spots with uniform size and denisty can be fabricated without re-inking.

This work demonstrates the application and modification of soft lithography, in particular, microcontact printing as a technique for "microcontact" synthesis on the surface and method for the fabrication of patterns in (sub)micrometer scale. The PDMS stamp shows universal properties of a tool for transferring molecules since its surface can be easily adjusted in terms of wettability or functionality. Surface modification of stamp and AFM tip with dendrimers introduces highly dense positive charge to the surface that enhances loading capacities of negatively charged (bio)molecules such as DNA to the surface of the stamp or tip. "Click" chemistry used for the direct microcontact printing shows to be a rigid and straightforward method for the attachment of molecules to the surface. Matrix-assisted dip-pen nanolithography of biomolecules shows the potential to be universal technique to pattern biomolecules on the surface within hundreds of nanometers scale. The wide range of applications presented in this thesis such as: reversible imine patterning, immobilization of proteins for cell guidance, triazole formation by patterning without the use of the catalyst, DNA direct and covalent immobilizations - show the flexibility and the potential of micro- and nano-fabrication techniques such as microcontact printing and dip-pen nanolithography.

Samenvatting

'Soft Lithography' biedt veel mogelijkheden met betrekking tot de fabricatie van 2D en 3D gepatroneerde structuren, waarbij een veelheid aan materialen en structuren toepasbaar zijn. Het vult conventionele fabricage methoden aan en breidt ze uit. Dit proefschrift richt zich met name op 'microcontact printing' (µCP) in haar hoedanigheid van een methode om diverse structuren op oppervlakken aan te brengen, als ook in haar hoedanigheid van een gereedschap dat gebruikt kan worden voor zogenaamde *in-place* synthese. Microcontact printing heeft unieke eigenschappen die deze methode zeer aantrekkelijk maken: (i) het is eenvoudig en gemakkelijk om in elk laboratorium te introduceren, (ii) het is biocompatibel, (iii) er kunnen details kleiner dan 100 nm mee worden gefabriceerd, (iv) het is toepasbaar voor een breed scala aan materialen, (v) het is efficiënt en niet duur. De belangrijkste eigenschap is dat de stempel die voor het printen gebruikt wordt flexibel is en zich nauw voegt naar het oppervlak inclusief de ruwheden op nanoschaal. Deze techniek maakt het vormen van dichtgepakte-monolaagpatronen mogelijk die bijvoorbeeld kunnen dienen als beschermlaag bij etsprocessen voor microelectronica. Het kan gebruikt worden voor het plaatsen van nanodeeltjes, poeders, anorganische materialen, ionen en veel meer. In dit proefschrift ligt de nadruk op het gebruik van *soft lithography* bij de fabricage van microsystemen die nuttig zijn bij het bestuderen van interacties tussen biomoleculen en cellen. De combinatie van oppervlaktechemie, het modificeren van het stempelmateriaal dan wel het maken van een passende keuze hiervoor en het microcontact printen van biomoleculen leverde methoden voor het patroneren van bioassays op (Hoofdstuk 2). Ondanks toenemende complexiteit is de grootte van samengestelde functionele elementen (*devices*) blijven dalen en hun oppervlakte-eigenschappen worden zeer belangrijk omdat zij de prestatie van het device kunnen bepalen. De oppervlaktechemie en de methode waarmee (bio-)moleculen worden geïmmobiliseerd moeten dan zorgvuldig gekozen worden. Hoofdstuk 2 beschrijft enkele benaderingen voor het naar behoefte aan passen van de oppervlakken van glas, siliciumoxide, goud en polymeren. Er wordt speciale aandacht geschonken aan het covalent verbinden van biomoleculen aan deze substraten omdat het bindingsmechanisme van niet-covalent immobilisatie methoden niet volledig begrepen is. Agentia voor kruisverbindingen (*cross-linkers*), zoals homobifunctionele en heterobifunctionele *cross-linkers* en bestanddelen voor de directe functionalisering van het oppervlak werden geïntroduceerd om het bereik van de covalente strategieën ter immobilisering van biomoleculen te vergroten. Wanneer substraten worden gepatroneerd voor de specifieke

binding van biomoleculen, is het belangrijk om inerte structuren te creëren die de bioactieve patronen scheiden. Modificaties, zoals het enten van PEG moleculen, BSA en phospholipede-SAMS zijn algemeen beschreven. Hoofdstuk 2 richt zich hoofdzakelijk op het microcontact printen van biomoleculen, de modificatie van het stempel oppervlak om de beste printresultaten te verkrijgen, als ook op van microcontact printen afgeleide technologieën zoals het patroneren vanuit zogenaamde '*microwells*' en vanuit microkanelen. '*Scanning probe lithography*' wordt hier ook in overweging genomen als zijnde een waardevolle techniek voor de fabricatie van sub-micrometer patronen.

Het vermogen om reversibele patronen middels microcontact printen op een oppervlak te creëren wordt in Hoofdstuk 3 verkend. De stempel kan worden gebruikt voor het overdragen van inkt moleculen, bijvoorbeeld amines en het hen covalent laten reageren met een aldehyde-gefunctionaliseerd oppervlak via een reversibele imine-binding. De patronen kunnen snel worden gegenereerd, verwijderd en geregenereerd. De reversibiliteit van de imine-binding werd verder verkend in Hoofdstuk 4, waarbij een patroon van dendrimeermoleculen werd aangebracht op een oppervlak met een gradiënt van aldehyde-functionaliteiten. Onder bepaalde condities kon de imine-binding worden verbroken en opnieuw gevormd worden, hetgeen verplaatsing van deze sferische macromoleculen veroorzaakt.

In tegenstelling tot het voorgaande kan dezelfde imine binding worden gereduceerd tot een secondaire amine en gebruikt worden voor de irreversibele immobilisatie van biomoleculen. Hoofdstuk 5 beschrijft het microcontact printen van cytofiele proteïnen die kunnen worden gebruik voor het aanbrengen van celpatronen op het oppervlak. Wanneer niet geprinte gebieden worden gepassiveerd kunnen cellen worden gepositioneerd en gescheiden in afgesloten gebieden. Deze methode van patroneren kan nuttig zijn bij het begrip van hoe spatiale of geometrische aanpassing van actieve oppervlakken het cellulaire gedrag, zoals cel-cel interacties, seinen tussen cellen en cel beweegbaarheid kan beïnvloeden.

In Hoofdstuk 6 wordt '*transfer printing*' van DNA met behulp van een zogeheten "dendri-stempel" gepresenteerd. Deze methode was gebaseerd op de modificatie van PDMS stempels met PPI dendrimeren hetgeen resulteert in een hoge positieve lading op het stempeloppervlak. Dendri-stempels kunnen negatief geladen DNA op de zogenaamde '*layer-by-layer*' manier aantrekken. Deze elektrostatische interactie tussen de oligonucleotiden en het stempeloppervlak kan succesvolle overdracht van DNA naar het oppervlak verzekeren. Om amino-gemodificeerd DNA covalent aan een aldehyde getermineert substraat te binden werd de imine chemie toegepast. De labiele iminebinding was verder gereduceerd tot een stabiele

secondaire iminebinding waarmee een robuuste verbinding tussen de DNA-streng en de vaste ondergrond werd gevormd.

In Hoofdstuk 7 werd "Click" chemie in combinatie met microcontact printing geïntroduceerd. Moleculen zoals octadecyne of rhodamine lissamine met acetyleen eenheden in de structuur werden als inkt gebruikt en geprint op azide-getermineerde silicium en glas substraten om triazolen te vormen zonder gebruik te maken van een koper(I) katalysator. Dit onderwerp is verder onderzocht in Hoofdstuk 8 om DNA in patronen te immobiliseren. Oligonucleotides met acetyleen eenheden in het midden en aan het eind van de streng werden via de dendri-stempel op een azide-getermineerd glasoppervlak geprint. De geïmmobiliseerd DNAs werden hieropvolgend gehybridiseerd met complementaire strengen. De beste resultaten voor de immobilisatie en hybridisatie werden bereikt bij gebruik van DNA strengen met de acetyleen eenheden aan het eind van hun streng. Deze strengen toonden de grootste beschikbaarheid voor hybridisatie van alle geteste oligonucleotiden. Deze strategie kan worden gebruikt voor nieuwe benaderingswijzen voor immobilisatie, in DNA studies op oppervlakken en in microarrays en biosensor toepassingen.

Een nieuwe werkwijze voor de directe overdracht, via DPN (dip-pen nanolithography), van biomoleculen ingekapseld in een matrix is weergegeven in Hoofdstuk 9. Deze techniek toont aan, een algemene methode te zijn voor het verplaatsen van moleculen aangezien de gel matrix, welke wordt gebruikt als inkt, dezelfde overdracht vertoont ondanks het type van ingekapselde biomoleculen. Meer dan 200 stipjes met een diameter van 500 nm kunnen in een keer gemaakt worden.

Dit werk toont de toepasbaarheid en aanpasbaarheid van *soft lithography*, met name microcontact printing als techniek voor "microcontact" synthese op oppervlakken en als methode voor de fabricatie van patronen op een (sub)micrometer schaal. De PDMS stempel laat universele eigenschappen van een stuk gereedschap voor de overdracht van moleculen zien en zijn oppervlak kan eenvoudig aangepast worden in termen van bevochtigbaarheid en functionaliteit. Het patroon van deze stempel kan naar specifieke behoeften ontworpen worden met gebruik van grafische computerprogramma's en overdracht naar een lithografisch gefabriceerd cliché of mal. Het brede scala aan toepassingen die in dit proefschrift gepresenteerd werden, zoals: reversibele imine patronering, immobilisatie van proteïnen ten behoeve van celgeleiding, triazol formatie door patronering zonder gebruikmaking van een katalysator, DNA directe en covalente immobilisaties – laten de flexibiliteit en het potentieel van deze techniek zien.

Acknowledgments

Curriculum Vitae

Dorota Idalia Rożkiewicz was born in Gdańsk, Poland. In June 1998 she graduated from The Maria Curie-Sklodowska Technical College of Chemistry in Gdańsk, Poland where she chose analytical chemistry as a major area of research. She obtained her Master and Engineer title in June 2003 at the Technical University of Gdańsk, Poland where she studied biotechnology. During her master project at the Department of Pharmaceutical Technology and Biochemistry under supervision of Prof. Ryszard Andruszkiewicz she was working on synthesis of protected amino acids for the synthesis of peptide antibiotics (Andruszkiewicz, R.; Rożkiewicz, D. *ChemInform* **2004**, *35*, 32). From March to June 2003 she was working in Prof. Julius Vancso group, at the University of Twente under the supervision of Dr. Holger Schönherr. She was working on AFM investigation of lipid vesicles on the surface (Schönherr, H.; Rożkiewicz, D. I.; Vancso, J. G. *Langmuir* **2004**, *20*, 7308-7312). Since October 2003 she had been a PhD student in the group of Prof. Dr. Ir. D. N. Reinhoudt at the University of Twente where she studied microcontact chemistry for the immobilization of biomolecules. From March 2007 she was conducting research at Prof. Chad Mirkin Group at Northwestern University in Evanston, USA. She worked on designing a universal matrix for biomolecule transport by DPN. In January 2008 she will start her postdoctoral studies at Harvard University, Cambridge, USA in the group of Prof. George M. Whitesides.

Publications

1. Rożkiewicz, D. I.; Gierlich, J.; Burley, G. A.; Gutsmiedl, K.; Carell, T.; Ravoo, B. J.; Reinhoudt, D. N. *Transfer Printing of DNA by "Click" Chemistry, ChemBioChem* **2007**, in press.
2. Rożkiewicz, D. I.; Brugman, W.; Kerkhoven, R.; Ravoo, B.J.; Reinhoudt D. N. *Dendrimer-Mediated Transfer Printing of DNA and RNA Microarrays, J. Am. Chem. Soc.* **2007**, in press.
3. Chang, T.; Rożkiewicz, D. I.; Ravoo B. J.; Meijer, E. W.; Reinhoudt D. N. *Directional Movement of Dendritic Macromolecules on Gradient Surfaces, Nano Lett.* **2007**, *7*, 978-980.
4. Cristiano, A.; Lim, C. W.; Rożkiewicz, D. I.; Reinhoudt, D. N.; Ravoo, B. J. *Solid-Supported and Bilayers of Amphiphilic β-Cyclodextrins*, *Langmuir* **2007,** *23*, 8944-8949.

Publications

5.   Sadhu, V.; Perl, A.; Peter, M.; Rożkiewicz, D. I.; Ravoo B. J. Reinhoudt D. N. *Surface Modification of Elastomeric Stamps for Microcontact Printing of Polar Inks*, Langmuir **2007***, 23,* 6850-6855.

6.   Salari, J. W. O.; Speets, E.; Rożkiewicz, D. I.; Ravoo B. J.; Rijnders, G.; Reinhoudt D. N.; Blank, D. H. A. **2007***, Self-Assembled Monolayers of Mono- and Di-alkyl Phosphates on Atomically Flat Strontium Titanate (SrTiO₃),Langmuir, submitted.*

7.   Rożkiewicz, D. I.; Janczewski, D.; Verboom, W.; Ravoo, B. J.; Reinhoudt, D. N. *"Click" Chemistry by Microcontact Printing, Angew. Chem. Int. Ed.* **2006**, *45*, 5292-5296.

8.   Rożkiewicz, D. I.; Kraan, Y.; Subramaniam, V.; Werten, M.W.T; de Wolf, A. F.; Ravoo, B. J.; Reinhoudt, D. N. *Covalent Microcontact Printing of Proteins for Cell Patterning, Chem. Eur. J.* **2006**, *12*, 6290-6297.

9.   Schönherr, H.; Degenhart, G. H.; Dordi, B.; Feng, C. L.; Rozkiewicz, D. I. ; Shovsky, A.; Vancso, G. J. *Adv. Polym. Sci.* **2006**, *200*, 169.

10. Rożkiewicz, D. I.; Ravoo, B. J.; Reinhoudt, D. N. *Reversible and Recyclable Covalent Patterning on Gold and Silicon Oxide Surfaces, Langmuir* **2005**, *21*, 6337-6343.

11. Schönherr, H.; Rożkiewicz, D. I.; Vancso, J. G. *Atomic Force Microscopy Assisted Immobilization of Lipid Vesicles, Langmuir* **2004**, *20*, 7308-7312.

12. Andruszkiewicz, R.; Rożkiewicz, D. I. *An Improved Preparation of N2-tert-Butoxycarbonyl- and N2-Benzyloxycarbonyl-(S)-2,4-diaminobutanoic Acids, ChemInform* **2004**, *35*, 32.

13. Rożkiewicz, D. I.; Korzuch, J. *"Superficial Sorption of Cu^{2+}, Cd^{2+} on Mytillus Trossulus with humusus acids"*, Scientific Paper, **1998** Gdansk, *Polish Academy of Science*.